In-vitro Fatigue Testing Of Thermally Sprayed Hydroxyapatite Coatings

Gledhill, Heather Claire

Award date:
1996

Awarding institution:
University of Bath

In-vitro Fatigue Testing Of Thermally Sprayed Hydroxyapatite Coatings

submitted by Heather Claire Gledhill
for the degree of PhD
of the University of Bath
1997

Heather Claire Gledhill

ProQuest LLC
789 East Eisenhower Parkway
P.O. Box 1346
Ann Arbor, MI 48106-1346

Abstract

Two types of thermally sprayed hydroxyapatite coating, produced by vacuum plasma spraying and a novel detonation gun technique were studied with the aim of investigating their suitability for use in orthopaedic applications. Both coatings were sprayed onto 2 mm thick Ti-6Al-4V coupons for characterisation. Analysis techniques included x-ray diffraction, surface analysis by scanning electron microscopy and Talysurf profileometry and quantative characterisation of polished cross-sections by image analysis. The solubility of the coatings was investigated by analysis before and after ageing in Ringer's salt solution held at 37°C and buffered to either pH 7.2 or pH 4.5. Detonation gun coatings were found to have a lower crystallinity and showed a more rapid dissolution under these *in-vitro* conditions. Both coatings were more dramatically affected by the lower pH regime.

Following characterisation of the coatings in this way, novel research was conducted to document the effects of both static and dynamic loading on the properties of these materials. Coupons were aged under three point static loading and dynamically tested for one or ten million cycles at a rate of 4 Hz. Coatings were fatigued in air, in Ringer's solution and following unloaded ageing in the *in-vitro* tanks prior to testing. This latter test was designed to provide a full simulation of the regime a coating would be expected to experience *in-vivo*. Delaminations were reported for vacuum plasma sprayed coatings fatigue tested with no prior ageing but not for the detonation gun coatings. Delamination following ageing however was not reported for either coating type. Coating behaviour was found to be intimately related to the morphology imposed by the manufacturing technique. It was suggested that if rapid fixation of an hydroxyapatite coated device *in-vivo* is expedited by early dissolution of amorphous material from its surface, detonation gun sprayed coatings may be proposed to be superior.

Acknowledgements

The research presented here would not have been possible without the financial assistance provided jointly by the Engineering and Physical Sciences Research Council and Howmedica International Plc. Grateful acknowledgement of this support is offered, in particular to Dr. Christina Doyle of Howmedica, now a proud advertisement for total hip arthroplasty herself.

I would like to take this opportunity to thank the staff and technicians of the School of Materials Science at the University of Bath, specifically Mr. Mark Deven and Mr. Chris Arnold whose knowledge and skill have proved invaluable. I offer limitless thanks to Dr. Irene Turner for her timely advice; she has shared adversity, be it foreign or home-grown, mechanical or human.

I am extremely grateful for the support and understanding of my family, Hilda, Keith and Neil who have kind hearts and broad shoulders and for the encouragement of my friends in Bath. Finally, I offer special thanks to Mark, who can hold off the end of the world with his bare hands.

It was a puzzling thing. The truth knocks on the door and you say, "Go away, I'm looking for the truth", and so it goes away. Puzzling.

Robert M. Pirsig - *Zen and the Art of Motorcycle Maintenance*

Table of Contents

1. Introduction

Recent developments in the field of orthopaedics have concerned the use of biomedical coatings on total hip replacement devices with the aim of improving the performance of these devices in the body. These coatings consist of novel ceramics and glass ceramics [1] the most widely studied of which is a calcium phosphate material - hydroxyapatite. The significant advantage in the use of these materials is thought to lie in their supposed acceleration of the processes of bony growth in the vicinity of the prosthesis. By encouraging the formation of new bone up to and into the surface of a hip prosthesis the device may be more securely locked in place than can be the case with more conventional surgical techniques. This mechanical interlocking of implant with bone is thought to eliminate problems associated with micro-motion of the device, i.e. loosening. This may in turn recommend coated implants for applications involving younger or more active patients.

It has been suggested that the stimulation of bony ingrowth into the surface of an hydroxyapatite coated implant arises as a result of the dissolution properties of the coating. Upon exposure to aqueous solutions, hydroxyapatite is thought to partially dissolve, releasing Ca^{2+} and PO_4^- ions into the surrounding environment [2, 3]. This ion release creates localised Ca^{2+} supersaturations which are eliminated by reprecipitation of the Ca^{2+} ions along with PO_4^- in the form of new bone. Several authors in the literature have supported this hypothesis by reporting that upon implantation, calcium phosphate ceramics undergo surface transformation into biological apatites [4, 5, 6, 7].

Hydroxyapatite, like many ceramics, however has poor mechanical properties in bulk form which prohibit its use as a sintered device in the load-bearing regions of the body. Therefore, in order to utilise the suggested osteoconductive properties of this material in orthopaedic applications, it is suggested that it be used as a coating on a mechanically strong substrate. For this reason, hydroxyapatite coatings on metallic prostheses have been developed.

Hydroxyapatite coatings on metallic substrates can be manufactured by a variety of different processes. The ceramic is commonly produced as a powder by one of several solution chemistry techniques [8] and is then applied to the substrate. Several methods of applying this powder to the metal have been investigated [9, 10, 11, 12] but the most commonly used are thermal spray techniques. In these processes the ceramic powder is heated in an induced plasma of ionised gases and accelerated towards the substrate upon which it impacts and freezes to form the coating. Thermally sprayed coatings have a characteristic layered or lamellar structure made of individual powder splats oriented parallel to the substrate surface, producing high levels of anisotropy in the coating. Many of the parameters chosen in the control of the thermal spray technique (e.g. powder particle size and morphology, plasma gas mixture, working distance, substrate cooling) will have a dramatic influence on the final structure of the ceramic coating and must be carefully controlled to optimise the final performance of the system in the body.

Thermally sprayed coatings have an inherent propensity to delaminate under the application of stress. Should a bioceramic coating fail in this manner in the body it will have one or more consequences to the patient. Firstly, loss of the coating will remove the effectiveness of the ceramic to perform its role in encouraging early bone ingrowth into the prosthesis. Secondly, the greater exposed surface area of substrate may increase the rate of metal ion release into the patient, thus increasing the probability of patient immune sensitivity and metallosis of surrounding tissues. Finally, most thermally sprayed coatings are applied to substrates which have been roughened by grit blasting to improve the mechanical interlocking of coating to substrate. Should the coating fall away from the substrate in service, residual blasting grit which may be present at the coating / substrate interface will be free to migrate away from the interface and into the body. This grit may cause severe localised tissue inflammation which may ultimately lead to failure of the implant itself and the need for a revision operation. For these reasons, the mechanical stability of thermally sprayed coatings for biomedical applications should be carefully characterised in order to minimise the risks of coating failure.

A particular weakness in the mechanical properties of ceramic coatings lies in their fatigue resistance. All joints in the human body are constantly subjected to fatigue loading during the simple actions of everyday living. In the process of walking a transferred stress equivalent to two and a half times body weight is imposed on the hip joint [13] with a patient being expected to take around one million steps in any one year [14]. Given the damaging consequences of delamination failure of an hydroxyapatite coating and the described regime of cyclic stress such a coating will experience, an understanding of the fatigue properties of such coatings is imperative.

For these reasons, characterisation of the fatigue behaviour of thermally sprayed hydroxyapatite coatings on titanium substrates has been undertaken. This unique study has focused on the examination of hydroxyapatite coatings manufactured by two different techniques. Vacuum plasma sprayed coatings are the most commonly utilised in the field of total hip arthroplasty but have not been investigated under *in-vitro* fatigue situations. In contrast to these coatings, a novel manufacturing technique, detonation gun spraying was also used to produce coatings with a contrasting morphology to the vacuum plasma sprayed materials.

It has been widely discussed in the literature that different phases in hydroxyapatite have different solubilities *in-vitro*. It has been shown that amorphous hydroxyapatite is considerably more soluble in aqueous solutions than crystalline hydroxyapatite [15, 16, 17, 18] . Since it is the dissolution behaviour of the coatings which is thought to be responsible for the early bone forming properties of hydroxyapatite, it may be suggested that the rate of dissolution and hence of bone formation may be controlled. This was done by tailoring the manufacturing technique to produce more or less amorphous hydroxyapatite in the sprayed coating. The higher temperature, higher velocity detonation gun spray process should produce coatings which have a higher amorphous content and therefore higher solubility *in-vitro*. The rapid dissolution of amorphous material from the coating surface may however destabilise the coating lending it a propensity to delaminate under the application of stress. For this reason, the

more crystalline vacuum plasma sprayed coatings may be superior for orthopaedic applications.

Work was carried out with the aim of better understanding the expected behaviour of these two coating types based on the results of extensive characterisation. Coatings were aged with no applied load and under an applied static load in simulated body salt solutions in order to identify their different dissolution behaviours. In conjunction with this work the coatings were subjected to a fatigue trial in the same simulated body environment so that their predicted performance *in-vivo* might be determined. It was hoped that, based on the results of this work, a recommendation regarding the choice of manufacturing technique for producing a superior bioceramic coating for use in total hip arthroplasty may be made.

2. Literature Review

2.1 Biomaterials Science

Developments in modern medicine have lead to such improvements in medical care that life expectancy has increased over the last century. A point has now been reached where instead of dying of disease in middle age a person can expect to live on into their 80s, their body reaching the point of becoming worn out with advancing years. This frailty commonly has associated with it a reduced quality of life which in turn has instigated the development of a new branch of science and engineering. This new area carries the categorisation of *biomaterials* research and covers, amongst other things, the replacing of failing body parts with biological and non-biological, mechanical alternatives. The history of this field now stretches back over one hundred years. It was however, as late as 1982 before the term *biomaterial* was formally defined by the N.I.H. Consensus Development Conference on Clinical Applications of Biomaterials [19] as "a non viable material, used in a medical device, intended to interact with biological systems". The earliest use of biomaterials was in the manufacture of sutures for surgical sewing. The first official record of a biomaterial in the literature however can be accredited to E.J. Greenfield [20] who was granted a patent in 1909 for a design of a metallic cage-like framework for the attachment of an artificial tooth root into the jaw.

The chief design criterion for a biomaterial is that it should be compatible with the body, i.e. it should not promote any adverse reaction such as cell necrosis or tissue inflammation, in its surroundings. The implanted material is expected to withstand any applied physiological force without suffering substantial dimensional change, catastrophic brittle fracture, creep fracture, fatigue failure or stress corrosion. Biomaterials can be found in all classical groups of materials : metals, polymers, ceramics and composites, and are utilised in a wide range of applications. Non biodegradable biomaterials are used in orthopaedic, dental, cardiovascular and ophthalmic applications as well as in *in-vitro* devices such as blood pumps. Certain ceramics and polymers

however, are designed specifically to be degradable and have uses as coated devices and in drug delivery.

The physiological environment, consisting as it does of a warm aqueous solution of anions, cations and biological macromolecules, is extremely hostile to metallic materials. Only metals which are inert such as gold and some platinum group metals, or which can form passive layers in the body such as titanium or chromium can maintain acceptable levels of corrosion when implanted in the body. Surprisingly, it seems that it is not only chlorine ions, which are known to be an extremely aggressive element of saline solutions, but biological macromolecules such as proteins in extracellular fluids which influence corrosion rates most significantly [21]. Usually, in engineering applications the most significant problem with metallic corrosion is its effect on the structural integrity of the component. This not the case in biomedical situations as only in exceptional circumstances will physical corrosive failure of an implant occur. It is, rather, the unresolved effect of the corrosion products on the surrounding tissues which is the principal concern. Even in passive metal implants there is considerable metal ion release into the environment which can result in adverse tissue response such as inflammation and even necrosis.

In theory, polymeric materials should have an advantage over metals as the isotonic saline and protein solution that comprise the extracellular fluid are not normally associated with the degradation of synthetic high molecular weight polymers. The physiological environment does not present the conditions normally required for polymeric degradation such as elevated temperature, electromagnetic radiation or solvent attack. However, certain cells associated with tissue response to trauma could be involved in the acceleration of hydrolytic degradation processes [14]. Polymeric debris may also invoke an adverse tissue response causing irritation and inflammation which, in the example of the surroundings of a hip prostheses, may eventually cause implant loosening. In addition to these problems there are worries associated with polymers cured *in-situ* in the body. Residual monomer from such a reaction can be toxic to the body in many ways, causing cell mutation or death. These problems are discussed below in relation to the use of polymethyl methacrylate as a cement in total hip replacement operations.

Ceramics and glasses can be divided into those which are essentially inert, those which are soluble, and those which display limited or controlled surface reactivity. Inert ceramics are used in applications where permanency is required such as in teeth and as the load bearing surfaces of hip prostheses. Soluble glasses have been used for many years in the controlled delivery of drugs in cattle and have recently begun to be used in humans for slow release contraceptive purposes. Rapidly dissolved ceramics have potential for use as a matrix for new tissue regeneration where the rate of degradation will depend on local conditions and involves both cellular processes and direct solution. Other ceramics which will be discussed in detail later, such as some calcium phosphates partially dissolve, releasing ions into the immediate environment which are thought to positively influence localised tissue responses [22]. These particular materials are often termed *bioactive* materials.

All implanted materials can be considered as sources of irritation or stimuli to surrounding tissues. This stimulus does not promote a response which differs greatly from the body's response to other insults such as trauma, infection or in fact the cellular and humoral response to invading bacteria. This response arises because the reaction is controlled by the same cellular processes and substances in each case. The inflammatory process is aimed at eliminating, or at least containing, the invading agent so that the tissues can be subsequently repaired. This repair process involves the replacement of damaged or dying cells with living cells to repair damaged tissues. If the irritating agent cannot be eliminated or contained which may be the case with an ion-releasing implant the situation becomes more complex and the repair process may never reach completion.

Reaction products such as leached ions or wear debris are often associated with cells typical of both acute and chronic inflammation. The cells try to eliminate the products by a procedure termed phagocytosis. The process is one of the most important functions of cells and is the body's defence against invading microbes and particles. Both neutrophiles and macrophages are phagocytic. The foreign material becomes attached to the surface of the cell after becoming coated by one of the substances (such as immunoglobulin) for which the cell surface has receptors. After attachment the cell engulfs the object which then becomes entrapped in the cell membrane. The cyctoplasmic

granules in the cell then release powerful enzymes to kill bacteria or cause disintegration of the entrapped matter. In the case of particular debris, it is common for the cells to be unable to bring about a complete engulfment which results in the release of the breakdown enzymes into the local environment. These enzymes then contribute to a perpetration of inflammation in the tissues surrounding the implant. Fibroblasts will be active in the environment too, trying to repair the damaged tissues but they may not be able to do this in occasions which provide a continued supply of irritants. This continued trauma will, in the long term, result in a granuloma surrounding the particle which may be associated with swelling and pain to the patient. If the reaction is sufficiently severe the local cells, and indeed tissues, will die, a process which further aggravates the situation. For this reason, the choice of material or combination of materials used in the body must be given careful consideration.

2.2 Orthopaedic Implants

One of the more dramatic developments in orthopaedic surgery has been the total joint prosthesis, which is now frequently used to replace osteoarthritic, (and rheumatic) joints. Osteoarthritis of human joints is an extremely debilitating problem affecting people, both old and young, on a global scale. In the case of osteoarthritis of the hip, disease causes cartilage degeneration and a dramatic distortion of the shape of the femoral head which results in extreme pain and loss of mobility. This disability is due to the breakdown of the normal low-friction cartilage-cartilage contact between the femoral head and the acetabulum in the pelvis. While the problem is associated with the surface of the femoral head, the standard remedy, thought to have been first attempted by Glück in 1891 [23] but pioneered by Sir John Charnley in the late 1950s [24], involves the removal of the femoral head and some of the femoral shaft, in an operation termed a total hip replacement (THR). Following dislocation of the joint and re-section of the femoral head, an alloy stem is secured into the femoral cavity by either cemented or cementless methods. The head of the alloy stem is then located in an ultra-high molecular weight polyethylene acetabular cup fixed in the pelvis.

The introduction of polymethyl methacrylate (PMMA) cements produced a dramatic improvement in the THR operating technique. In the original cemented version of the operation, the alloy stem was secured by bone cement which was polymerised *in-situ.* Surgeons could ensure a tight fit between bone and implant, filling gaps with cement. However, the relatively high exotherm produced during the curing of the PMMA has been found on occasion to produce bone and other tissue necrosis [25]. It is now well known that PMMA has other disadvantages as a bonding agent. The methyl methacrylate monomer is toxic [26]; the insertion of a plug of the polymer as firmly as possible into the medullary cavity tends to force fat into the circulatory system and hypotension and cardiac arrest have occasionally been experienced within a few minutes of insertion of the PMMA cement [27]. Curing of the methacrylate is accompanied by a large volumetric shrinkage of approximately 4% [28]. These concerns, and further worries about the long term durability of cemented implants has led to the development of alternative implantation techniques.

Two alternatives to cemented implantation were proposed in the late 1960s. These were: the use of a metallic implant with a porous surface layer, and the use of an implant with a bioactive surface layer. The first of these approaches involved the modification of the prosthesis stem surface to produce a porous structure made up of a coating of cobalt-chrome [29], titanium alloy [30] or ceramic spheroidal particles [31, 32]. It was demonstrated by Callaghan [33] that cortical bone ingrowth will occur into pores of 200-450 μm in diameter. Consequently, the combination of a direct mechanical contact of the alloy stem with bone and a porous surface would allow for implant fixation by bony ingrowth.

Ingrowth of bony tissue into porous implants or porous implant surfaces with large surface areas is the basis for this biological fixation. There are however several areas of concern which are related to this attachment system, especially if the method is expected to be used for young patients with 20-40 years of post-operative lifetime. L.L. Hench [34] catalogued these as; reduced strength, fatigue resistance and increased notch sensitivity of metal prostheses due to sintering of porous coatings; subsidence of implants and bone resorption due to stress shielding, loss of surface beads and increased surface

area of prosthesis; increased potential for immune hypersensitivity and malignant neoplasms due to increased local levels of metal ions; careful selection of implant size and precise surgical technique required to ensure good loading regime and hence progressive bone ingrowth and implant stabilisation; difficult revision procedure and lack of uniform bony ingrowth into porous implants, especially in elderly or arthritic patients. Obviously these concerns are not always realised but they do demonstrate the difficulties associated with this technique.

The easy ionisation of metal in the body environment results in the release of dissolution products which interfere with the overall health of the patient. In contrast, ceramics are usually in their highest possible oxidation state and therefore do not produce harmful by-products on implantation. Experimentation therefore began into the use of ceramic materials in prostheses. Soon after the introduction of the first alternative to cemented fixation, a second approach became popular. This was to be conceptually opposite to conventional biomaterials philosophy. Rather than producing a biomaterial that would elicit no, or only minimal tissue response, it was suggested that a new range of materials be developed which produced a positive and beneficial response from the body, encouraging normal tissue formation, with, if possible, the production of an intimate bond between the biomaterial and bone.

The new approach to THR aimed to reduce the problem of metal ion release by coating the metallic prosthetic stem with a range of novel ceramics, glasses and glass ceramics [1] which are bioactive. Included in the latter group are the calcium phosphates, notably hydroxyapatite (HA) and tri-calcium phosphate (TCP). The significant advantage of this group of materials is that, by stimulating bone apposition, not only can the implant be secured without cement, but there is the prospect of continuing favourable bone remodelling, rather than bone loss. When implanted, these bioactive materials develop an interface capable of supporting considerable interfacial shear stress. Since the materials with documented bioactive behaviour are glasses and ceramics, it is not possible to use them in most load-bearing situations, especially in the reconstruction of hip and knee joints. It would therefore appear logical to apply these materials as coatings, to metallic, polymeric, or 'inert' ceramic prosthetic substrates.

Composites used in THR have to operate for many years in a hostile environment without planned maintenance. The bones of the skeleton and similarly, a joint prosthesis have to transmit forces and translate motion. They have to sustain forces which originate outside the body due to gravity, and those generated within the body by the muscles. These fluctuating forces are complex at any instant in time in their direction, rate of application and magnitude. Results calculated mathematically using assumptions of the forces transferred by the muscles suggest that the force exerted on the femoral head in a single-leg stance with the pelvis level is approximately 2.7 times body weight [35]. Although much theoretical work has now been done on the mechanics of normal locomotion, only very limited studies measuring the actual forces acting on the THR have been carried out. One such study was conducted by T.A. English and M. Kilvington [13] and involved the *in-vivo* implantation of THR prostheses with telemetric output into two patients. These authors measured forces equivalent to 2.56 time body weight on the joint when patients were walking at 0.46 m/s.

All materials used in THR should be compatible with the body environment, i.e. they should not be seriously degraded in the 37°C, pH 7.25 conditions or produce an adverse tissue reaction. It has been reported [36] that the pericellular environment surrounding osteoclast activity approaches an acid pH of 4.5 to 4.9 which may facilitate dissolution of the organic phases of bone during remodelling. Such acid conditions may of course be extremely damaging to implanted devices. In addition, the materials selected must withstand the normal physiological forces without fracture, either in the short term, associated with overloading, or in the longer term due to fatigue or stress corrosion. The friction and wear characteristics between the alloy stem and the polymeric acetabular cup are also important, both to give the required joint function and to ensure an adequate prosthesis lifetime.

It is now well established that THR failure is not usually associated with mechanical failure of the implant, due to, for example, stem fracture or cup wear, but is commonly associated with effects such as stem or cup loosening [37]. This failure mechanism is usually allied with biological reactions to debris generated by wear of either the metallic part of the implant or the acetabular cup section [38]. Another

mechanism may occur as a result of a specific property of bone which causes it to remodel itself if the natural physiological forces applied to it are sufficiently perturbed [25]. Essentially, the effect of inserting a stiff alloy stem into the naturally hollow tube structure of the femur, is to reduce the forces experienced by the cortical bone itself. As the surrounding bone continually remodels in response to applied physiological forces, the reduced stress being carried by the bone leads to a progressive loss in bone mass and an eventual loosening of the prosthetic implant. A comprehensive summary of the nature of the reaction of tissues to most common total hip replacement materials, both in animals and humans, has been comprehensively reviewed by Boss, Sharjrawi and Mendes [27] in the literature.

2.3 Hydroxyapatite

For more than twenty years, calcium phosphate ceramics have been used in medicine, particularly dentistry, for the replacement of hard tissues [39]. This usage was developed since one of the main compounds forming the mineral component of bones and teeth is apatite. Mature human cortical bone contains ≈ 0.5 volume fraction of crystalline hydroxyapatite dispersed in a matrix of collagen fibres. Using the appropriate fabrication technique it is possible to manufacture synthetic hydroxyapatite, $Ca_5(PO_4)_3OH$ with the same chemical composition as the calcium phosphate in bone (Figure 2-1). It was postulated that devices prepared from this material would elicit a favourable response from the body on implantation. Another apatite, tri-calcium phosphate is also chemically similar to natural hydroxyapatite, having the crystal structure of the mineral β-whitlockite and was considered alongside hydroxyapatite as an implantable material. *In-vitro* and *in-vivo* studies [4, 40] however have shown TCP to have a higher dissolution rate than hydroxyapatite. Pure β-TCP can be between 12 and 22 times more soluble in aqueous solutions than pure hydroxyapatite [41]. Therefore for applications requiring some long term stability such as for hip prostheses, hydroxyapatite is considered superior.

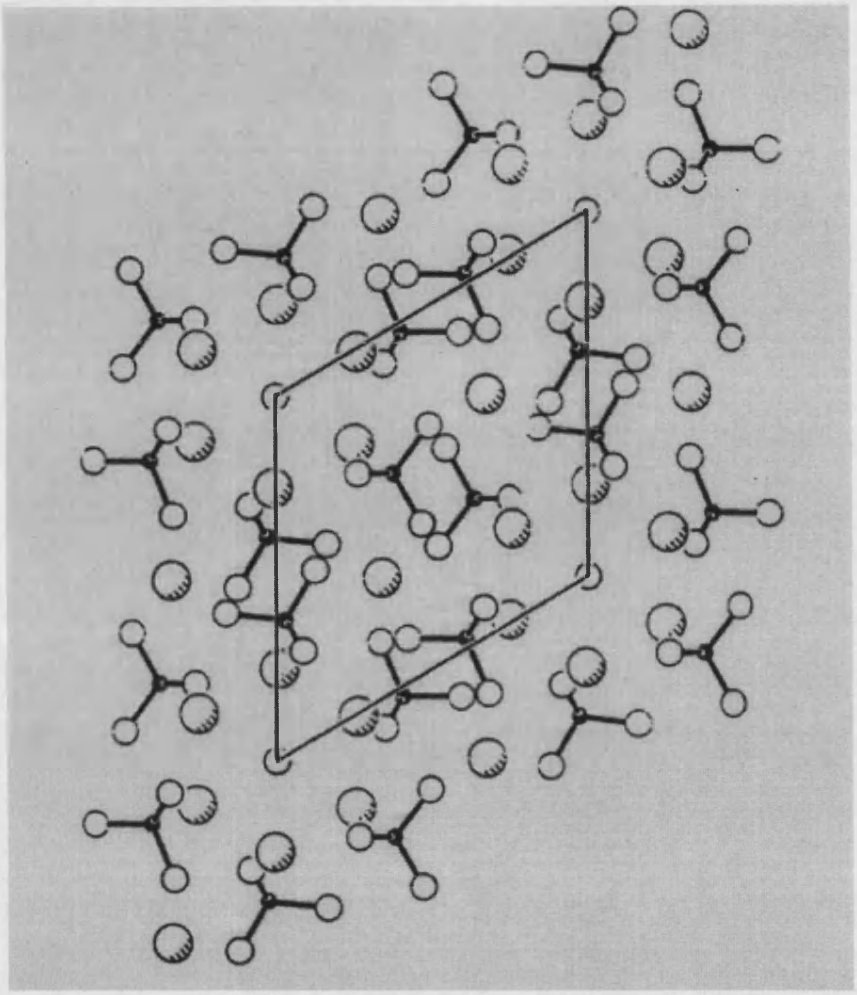

Figure 2-1 :- Projection down c axis of hydroxyapatite showing P (black circles), O (open circles) and Ca (shaded circles) [42]

Osborne [2] concluded that since hydroxyapatite can establish a bond with living bone through free Ca^{2+} and PO_4^- ions at the surface it could be considered to be bioactive. When placed in an aqueous environment, hydroxyapatite releases ions from its surface into solution. The solution pH dictates which ions the surface releases or incorporates as it tries to come into equilibrium with its surroundings. Orly [3] suggested that Ca^{2+} ion release from the surface of implanted materials enhances bone formation on calcium phosphate ceramics. This ion release creates a localised Ca^{2+} concentration which is eliminated by re-precipitation of the Ca^{2+} ions combined with physiological PO_4^{3-} ions from body fluids. Other authors [43, 5, 6] have also reported that upon implantation, calcium phosphate ceramics undergo surface transformation into biological apatites. Apatite crystals have also been observed to form on the surfaces of various

bioactive materials implanted in bone, including synthetic hydroxyapatite [6, 7] bioactive glass [44] and glass ceramics [45].

Radin *et al* [46] exposed various different calcium phosphate ceramics to a calcium and phosphate free solution (0.05 M tris (hydroxy) methylaminomethane and HCl buffer) held at pH 7.3. Analysis of the materials after exposure revealed that the solubilities of the phosphates followed the following trend : hydroxyapatite < calcium deficient hydroxyapatite < dehydroxylated hydroxyapatite < alpha tri-calcium phosphate < beta tri-calcium phosphate. It was also reported that biphase and multiphase mixtures of calcium phosphate ceramics had solubilities governed by the most soluble component.

Best *et al* [47] exposed dense sintered hydroxyapatite discs produced from powders with slightly different chemical compositions and morphologies to a human cell culture medium. After exposure, the surfaces of the discs and the viability of the cells were examined. These authors discovered that, the difference in the original hydroxyapatite powders eventually imposed great enough variations in the final ceramics that cellular groups were viable on one surface and not on the other. It was suggested that this behaviour may have been a result of a negative influence of tri-calcium phosphate, which, although enhancing the dissolution properties of hydroxyapatite ceramics may in fact subdue cellular responses *in-vivo*.

Dissolution of HA implants therefore necessarily affects the rate of formation of new bone in the locality of the material. In the production of these materials an *in-vivo* behavioural strategy has to be determined so that the morphology of the implant can be tailored to produce the desired response. Controlling the ratio of HA to TCP in the material will affect its dissolution rate enormously. The higher the content of TCP the higher the implant dissolution rate due to the preferential dissolution of TCP over HA [48].

Unfortunately the low tensile and impact properties of calcium phosphate ceramics in bulk form prohibit their use in load-bearing regions of the body. In order to utilise their osteoconductive properties, it was therefore suggested that HA ceramics

should be used as thin coatings on metallic implants. This would take advantage of the unique properties of the ceramic while achieving the desired mechanical integrity from the metallic substrate. This concept has currently found widespread application in biomedical prostheses.

2.4 Coated Versus Uncoated Implants

Many investigators have now studied the effect of applying a bioactive coating on the bone bonding properties of prosthetic devices. Cook *et al* [49] implanted bead-blasted commercially pure titanium and HA coated Ti-6Al-4V alloy samples in the femora of dogs and measured the push out strength of each after various implantation times between 5 and 32 weeks. At all evaluation periods they found that the HA coated samples showed a five to eight times higher implant fixation than the uncoated implants. In a later, but very similar study [50], they again reported that, in a direct paired test, when compared to uncoated cobalt chromium implants, hydroxyapatite coated implants enhanced both percent bone ingrowth and interface shear attachment strength. These authors also reported that attachment strength developed much more rapidly with coated implants than with uncoated implants and that osseous tissue proliferation was greater for the coated samples. In contrast to the work of some authors however, Cook *et al* reported that there was no evidence of disruption, mechanical failure, or biologic resoption of the plasma sprayed hydroxyapatite coatings retrieved after any of the time periods used in his research. Oonishi *et al* [51] performed a similar study using HA coated and uncoated titanium implants. These authors found that 4 weeks post implantation, there was better healing of the HA coated implants. However they observed no difference between the two implant types after 12 weeks. They therefore concluded that HA coatings on porous implants were of particular interest in the early postoperative period. Other authors including Hayashi *et al* [52] and Moroni *et al* [53] also reported this effect. They concluded that after an extended period *in-vivo* there was no significant difference in the push out strengths nor appearance of coated and uncoated implants. Shortly after implantation however, they found that the hydroxyapatite coated samples demonstrated considerably improved results over the uncoated samples.

These results suggest that bioactive coatings on implants dramatically improve the early interface strength between bone and implant, which should allow more rapid postoperative load bearing of the prosthesis. The histomorphometric data suggests that bioactive coatings are an effective method of improving bone formation and ingrowth into porous coated prostheses, enhancing stable biological fixation.

2.5 Hydroxyapatite Coatings

The thickness of coatings used by investigators in the literature varies from thin coatings with thickness' in the range of 40-60 μm such as those investigated by Yankee *et al* [54], Maxian *et al* [55] and Klein *et al* [56] to thicker coatings in the range 150 - 200 μm used by, amongst others Wong *et al* [57] and Gross and Berndt [58]. The surface roughness of these coatings varies between 0.4 μm [54] and 14.7 μm [59]. Most thermally sprayed coatings are sprayed onto a grit blasted titanium alloy surface prepared using alumina grit in a manner similar to that described by Yankee *et al* [54].

Geesink *et al* [60] published the first results on loaded HA coated hip implants. They inserted HA coated and non-coated titanium hips in dogs with a follow up period of between 3 weeks and 12 months. Three weeks after implantation, light microscopical evaluation showed that the HA coated hips were already in close contact with surrounding bone. The authors reported a near 100% coverage of bone on the weight-bearing surface of the prosthesis after 6 weeks. The non-coated implants however were surrounded by a fibrous tissue layer between 50 and 500 μm thick after 6 weeks. This led the authors to conclude that HA coatings presented superior fixation for load-bearing implants over non-coated ones. These results were confirmed by similar experiments carried out by Poser *et al* [61] and Thomas *et al* [62].

In addition to their work on coated and uncoated implants, Cook *et al* investigated the effect of small defects in hydroxyapatite coatings on the mechanical and histological properties of coatings implanted in the femora of dogs [63]. The authors

implanted uncoated, HA coated and damaged HA coated implants into dogs and investigated them after 3, 5, 6, 10, 12 and 32 weeks. They found that there were no statistically significant differences between the HA-coated implants with and without defects for either interface shear strength or stiffness; however both HA-coated implant types developed significantly greater interface strength and stiffness when compared to uncoated metallic implants as described above. Histologically, in all areas away from the defect, a progression to near complete mineralisation of osseous tissue directly onto the HA-coated surface was observed with no interpositional fibrous layer. At early time periods (upto six weeks) in the area of the coating defect, bone apposition and mineralisation appeared to stop at the edge of the HA coating. At later time periods (greater than ten weeks) the area of the defect was filled with mineralised osseous tissue in approximately one-half of the specimens. A thin fibrous interpositional layer was observed at the interface of the exposed metal substrate however this appeared to have no effect on the mechanical properties of the implants.

Verheyen *et al* [64] investigated the effect of two different cultures of bacteria on the morphology of HA coatings. They reported substantial damage done to the HA coatings as a result of *in-vitro* experiments with *S aureus* and *S epidermidis*. The coatings showed increased dissolution and calcium ion release when challenged with the bacteria during a 24 hour incubation. The bacteria digested or dissolved the coating, creating irregularly shaped holes. Other authors have monitored the effects of proteins on the dissolution behaviour of bioglasses [65] and bioceramics [66]. Reber [67] *et al* monitored the size of crystallites on the surface of vacuum plasma sprayed coatings exposed to simulated body fluid and to fetal calf serum by x-ray analysis. It was reported that crystallite size reduced considerably on exposure to the simulated body fluid but remained relatively unchanged on exposure to fetal calf serum.

Zyman [68] and co-workers investigated the effect of heat-treatment on the structure of plasma-sprayed HA coatings by XRD and microscopy. They found that after ageing the coatings at 630°C for 30 minutes the diffraction trace for the materials revealed a marked increase in crystallinity and a change in the surface morphology of the coatings viewed by SEM. This result was confirmed by Wang *et al* [59] who measured the

change in crystallinity quantitatively by XRD witnessing a increase in crystallinity from 83% in the as-sprayed state to 95% after heat-treatment at 850°C. Performing the heat treatment at higher temperatures (800-1000°C) Zyman *et al* [69] reported a transformation of the pure HA in the coatings into other calcium phosphate phases such as α-tri-calcium phosphate, β-tri-calcium phosphate and tetra-calcium monoxide diphosphate which led to an increase in the surface roughness of the sample. This transformation was considered to be dependent on the thickness of the hydroxyapatite coatings produced [70]. Transformation of hydroxyapatite into other calcium phosphate phases occurs in the temperature order ; hydroxyapatite (900°C) < beta tri-calcium phosphate (1100°C) < alpha tri-calcium phosphate (1350°C) < tetra calcium monoxide diphosphate (1400°C). As the thickness of the coating increases, so too does the temperature of the surface of the coating, since the thermal diffusivity of the ceramic is low. The higher surface temperature of thicker coatings encourages transformation of the lower temperature phases progressively upto tetra calcium monoxide diphosphate. Therefore thinner coatings show evidence for all the different types of calcium phosphate compositions while in thicker coatings these have transformed leaving little evidence of the lower temperature materials. A phase diagram for calcium oxide showing the transformations of hydroxyapatite with temperature is shown below (Figure 2-2) where C2P is bi-calcium phosphate, C_3P is tri-calcium phosphate, C_4P is tetra-calcium phosphate and Ap is apatite.

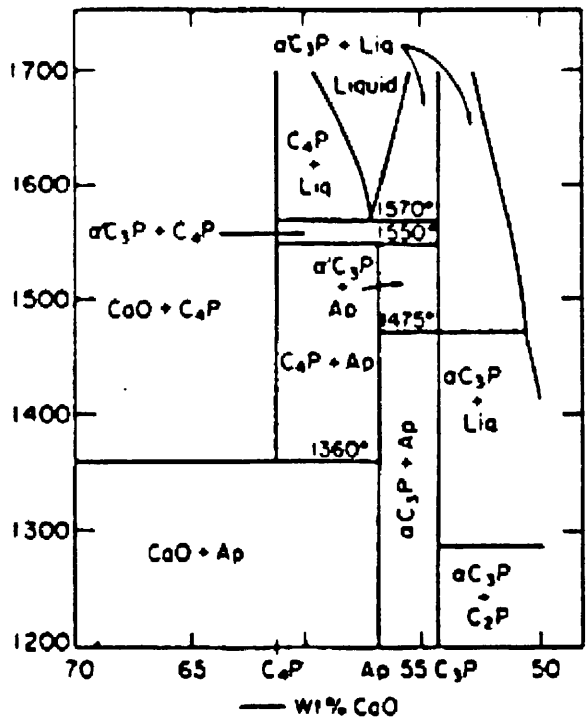

Figure 2-2 :- Phase diagram of CaO/P_2O_5 mixtures, vertical axis = temperature °C, Ap = hydroxyapatite [71]

Other authors have measured the crystallinity of HA coatings using various XRD techniques. Maxian *et al* [55] used coatings with a 60% crystallinity whilst Chen *et al* [72] determined that coatings produced from powders with different particle size distributions had different final crystallinities. Coatings produced from powders with mean particle size of 75 μm had a final crystallinity of only 24 % whilst those produced from powders with a 125 μm mean particle size had crystallinities of around 30 %.

Wong *et al* [57] discussed the importance of the surface topography of HA coated implants on their osseointegration in trabecular bone. Following on from work by Wilke *et al* [73], who had measured the torque removal force for orthopaedic screws and found a general trend of increasing removal torque with increasing surface roughness, Wong *et al* performed a similar experiment which included HA coatings of different surface roughness. It was found that there was an excellent linear correlation between implant

surface roughness and the strength of the bone-implant interface measured by push-out failure load.

Authors have attempted to determine the tensile bond strength and porosity of HA coatings with varying success. One comprehensive paper describing various techniques for measuring the adhesion of thermally sprayed materials and their drawbacks was written by Berndt *et al* [74]. The authors describe not only the formation of thermally sprayed coatings and the rationale for the measurement of coating adhesion but give a detailed examination of several testing morphologies and their associated fractographic analysis. Testing morphologies discussed include shear tests, double torsion tests, double cantilever beam tests, microhardness assessment and failure monitoring using acoustic emission.

Wolke *et al* [75] determined the tensile bond strength for vacuum plasma sprayed HA coatings on Ti-6Al-4V substrates to be 77.4 MPa. In contrast, Iida *et al* [76] determined the effect of substrate surface roughness on the adhesion of particles using an impact separation method and incongruously found that the force of adhesion of a particle to a substrate was less for a rough surface than the adhesion of a particle to a smooth surface. Wang *et al* [59] determined that the porosity levels in plasma sprayed HA produced using different spray parameters lay between 4 and 9 %.

Several investigators have also investigated the effect of an *in-vitro* environment on the properties of hydroxyapatite coatings. Gross and Berndt [8] aged 200 μm thick HA coatings on 316 stainless steel substrates in buffered Ringer's solution held at 37°C and pH 7.35. The coatings were held in the solution for 1 day, 2 days, 4 days, 1 week, 2 weeks, 4 weeks and 12 weeks before being examined. The investigators found that coatings underwent a loss in mass which increased with ageing time *in-vitro*. They also found that heat-treating the coatings at 800°C for 2 hours prevented this mass loss. An increase in crystallinity of the coatings observed as a sharpening of peaks in the XRD trace was reported. Chern Lin [77] and co-workers immersed HA coatings in Hank's solution held at pH 7.2 and 37°C. They observed dissolution of the coating surface and

concurrent deposition of a Ca/P rich layer. They also reported an apparent increase in the crystallinity of the coating. Conversely, Evans and Gregson [78] investigated the effect of an HA coating on the *in-vitro* fatigue properties of Ti-6Al-4V and found that the fatigue endurance of the substrate was reduced by approximately 40% by the coating. This effect of plasma-spray coating on the fatigue life of Ti-6Al-4V was also discussed by Curtiss-Wright [79] who made suggestions for ways of reducing the detrimental effect of plasma coating on the fatigue properties of the substrate.

Reis and Monteiro [80] set up an electrochemical corrosion cell and aged air plasma sprayed HA coatings in Hank's solution and sodium chloride solutions. Coatings were aged under static four point bending and four point fatigue at a fixed imposed stress of 40-80 MPa for one million cycles at a cycle rate of 10 Hz. Open-circuit corrosion potential was recorded with respect to a standard calomel electrode in order to monitor the corrosion behaviour of the material. Metal ion release levels and solution pH as well as coating thickness and microstructure were analysed after the experiment had been concluded. Corrosion potential was seen to initially decrease then stabilise during testing in Hank's solution. This implied that there was no increased tendency of the substrate to corrode in open-circuit testing. It was assumed that coating cracking did not change the metal substrate passive state or at least did not increase its corrosion susceptibility. The 50 μm thick coating was observed under SEM to be smoother and thinner after the corrosion-fatigue test. It was found that coating degradation was not only mechanical in nature (loosening of solid particles from the substrate) but, since dissolution of the coating was observed, also resulted from chemical attack. The authors reported no significant metal ion release levels or surface activation during their experiments.

Most recently, several authors in the literature have been investigating the possibility of improving the stabilisation of HA implants by the incorporation of biologically active agents such as bone morphogenetic protein or growth hormone in the biomaterial coating [81, 82]. It has been shown that growth hormone is a major regulator of skeletal growth and can be used to stimulate longitudinal bone growth when introduced in a controlled manner [83]. Downes and co-workers [84] monitored the release rate of growth hormone from loaded hydroxyapatite, heat-treated hydroxyapatite and

fluoroapatite. They found an increase in the release rate for the heat-treated hydroxyapatite over the as-received hydroxyapatite despite the higher crystallinity of the heat-treated samples. It was suggested that this result could be due to differences in ionic interactions between the oxyapatite of the non-treated coatings and the hydroxyapatite of the heat-treated ones.

The encouraging results of laboratory and animal experiments led to the first human use of a HA coated hip implant in 1986. The follow up to this clinical trial [85] was published a few years later with results which appeared to be extremely good. Tonino *et al* [86] produced one of the most extensive follow up reports on 222 patients who had undergone total hip replacement surgery using an HA coated prosthesis. The authors reported no instances of loosening or other problems which might require revision surgery. This is perhaps the most extensive clinical result published so far and portents an extremely successful future for the HA coated implant.

One histological report of a retrieved hydroxyapatite coated implant has been seen by the author [87]. This report described the results of a histomorphometric analysis of a retrieved ABG implant, removed 3 years and 2 months after insertion. Analysis of the recovered femoral implant showed that the hydroxyapatite coating remained on the majority of the stem on recovery. However, the thickness of the coating depended on its location on the stem and the surrounding tissues in contact with it. The coating remained thick and regular when in contact with bone but highly resorbed with evidence of macrophage activity in soft tissue regions. Where full resorption was observed, no acute inflammatory response, osteolysis or metal ion sensitivity was reported. In some regions, total separation of the hydroxyapatite coating from the metal substrate by new bone growth was observed. The authors concluded that this had occurred in zones where the coating had become fragmented or damaged during the implantation procedure itself. In regions where soft tissue was in contact with the implant no coating was observed, implying that when early bone ingrowth into the coating occurs, no fibrous layer is formed and direct contact between bone and implant is maintained.

D'Antonio *et al* [88] and Geesink [89] reported the results of the follow up of large groups of patients implanted with the same type of proximally covered hydroxyapatite-coated femoral component. These authors reported excellent results for the prostheses with Harris hip-scores around 95, and the rehabilitation of patients comparing favourably with that of patients who had had cemented implants. Radiographic findings revealed the presence of early, rapid remodelling of bone, with bone of increased density at the interface between the hydroxyapatite-coated and uncoated parts of the stem. No radiolucency was reportedly found around the hydroxyapatite-coated regions of the stem.

2.6 Manufacture of Hydroxyapatite Coatings

HA coatings on metallic prostheses can be produced by a variety of different techniques. The HA tends to be applied as a powder, manufactured by one of several solution chemistry techniques [90] . The techniques most commonly reported for the production of HA coatings however are sintering [9], diffusion bonding [10], ion-beam sputter-deposition [91], electrophoretic deposition [11], high velocity oxy fuel deposition [12, 92] and plasma spraying [93]. Of these techniques the thermal spray methods are usually used industrially.

Many thermal spray processes are available for producing coatings suitable for a variety of applications. These processes have one major common characteristic in that they all involve the use of a combusting gaseous medium which simultaneously heats the material to be sprayed and projects it onto the substrate. Among these processes are the commonly used commercial methods of arc metallisation, flame spraying, plasma spraying, vacuum plasma spraying, detonation gun spraying and high velocity oxygen fuel spraying. The velocity and temperature of the heat source are the main differences between the thermal spray processes and it is these parameters that dictate the materials that can be sprayed. Other factors differentiating between spray processes occur with regard to their running cost, i.e. factors such as equipment cost, energy requirements and

feedstock material cost (gases, grit blast media). The technology developed to produce thermally sprayed coatings has now also expanded into the manufacture of net shapes produced by stripping a 'coating' from the 'substrate' or forming tool and using the sprayed material directly in the engineering application.

Thermally sprayed coatings have a characteristic layered or lamella structure made up of individual splats oriented parallel to the substrate surface, producing high levels of anisotropy in the coating. Therefore the properties of a coating will be significantly different from those of the bulk material. Unmelted particles and pores are also embedded in the coating as the splats are laid down. The microstructure of the coating depends on the manner in which individual molten or semi-molten powder particles splat, flatten and solidify on impact with the substrate. The rate of flattening of the particle is an order of magnitude higher than its solidification rate [94] meaning that in the construction of the coating, each particle impact can be considered independently of all the others. If the impact velocity of a molten particle is very high, the flow of molten material during splatting may become unstable and the droplet will disintegrate at its edges giving rise to splashing. The propensity of a droplet to splash in this way can be determined by its Weber number [95]. The Weber number being defined as

$$We = \frac{\rho v^2 d}{\gamma_t}$$

where ρ is the density of the liquid being sprayed, γ_t is the surface tension of the liquid, d is the droplet diameter and v is the droplet velocity. If the Weber number is greater than 80, the droplet will tend to spray on impact. Typical Weber numbers for materials under plasma spraying conditions are around several thousand, for example [96] for Al_2O_3 at its melting point, $\gamma_t = 0.68$ N $m^{-1}$and $\rho = 3.05$ Mg m^{-3}. If d = 20-100 μm and v = 100-400 m s^{-1}, We will be 1000-20000. However, a rough surface can restrict the break up of droplets and may prevent splashing from occurring. The general cross-sectional morphology of a thermally sprayed material is shown below (Figure 2-3). Factors controlled by the thermal spray parameters [97] which may include size and distribution of porosity, micro-cracking, residual stress and oxide content will have a great deal of influence on the eventual performance of the coating system.

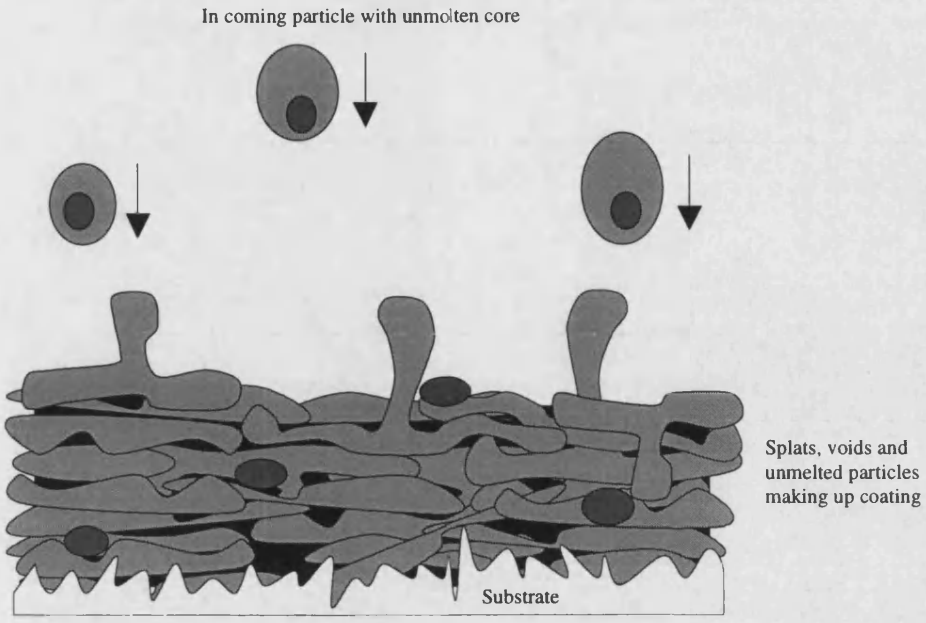

Figure 2-3 :- Schematic view of a cross-section through a thermally sprayed coating

Powder particle size [98] and shape [90, 99, 100] will have a dramatic effect on the structure and adhesion of the coating [101]. To achieve maximum adhesion, powder particles must be completely molten when they impact on the substrate surface. This requires optimising the operating conditions to maximise particle velocity and melting time. The melting time is the time required to ensure that sufficient heat has been transferred from the plasma to the particle core and is obviously dependent on the thermal conductivity properties of the powder. Several mechanisms are involved in the exchange of energy between the plasma and the powder such as radiation, electron bombardment and ion/electron combination on the particle surface, but the dominant heating process has been shown to be thermal conduction through the boundary layer between the plasma and the particle [102]. One author [103] demonstrated mathematically that during plasma spraying of a molybdenum coating onto a steel substrate it was statistically highly improbable that at any one time during coating production, any one impacting powder particle landing on the coating surface would encounter any other molten or semi-molten particle.

Powder particle size also effects its behaviour in the plasma. Small particles melt more rapidly than larger ones but are also prone to evaporation. They also reach

maximum velocity faster than for larger particles but this velocity subsequently decays at a greater rate. Small particles are also easily influenced by the turbulent flow often induced in plasma fields which may give them a large trajectory range when emerging from the plasma [104]. Particle morphology will have a major effect on the flowability of the powder into the plasma. Vardelle *et al* [105] observed that particles which formed agglomerations during flow could partially explode on entering the plasma jet as a result of the high thermal shock they experienced when the gases trapped in the agglomerate pore structure rapidly expanded upon heating. Such effects may cause disruption of the coating morphology and should be taken into account when powders are selected for spraying.

Plasma spray coating of bioactive ceramics onto substrates is the technique most commonly used for the production of coated implants. The plasma spray operation is a refined version of the gas-tungsten-arc welding process (Figure 2-4). In both the air and vacuum techniques a plasma or ionised gas is employed to partially melt and carry the ceramic particulate onto the surface of the substrate. The carrier gas is usually argon, which is ionised as it passes within the high temperature discharge zone which is created as a current arcs across the gap between the anode and the cathode. Adding the carrier gas to the system considerably increases the enthalpy of the plasma, affecting the arc voltage and the plasma "power" which improves the likelihood of particle melting. The nozzle of the plasma gun is kept from melting by water cooling, as temperatures developed in the plasma may exceed 10,000°C.

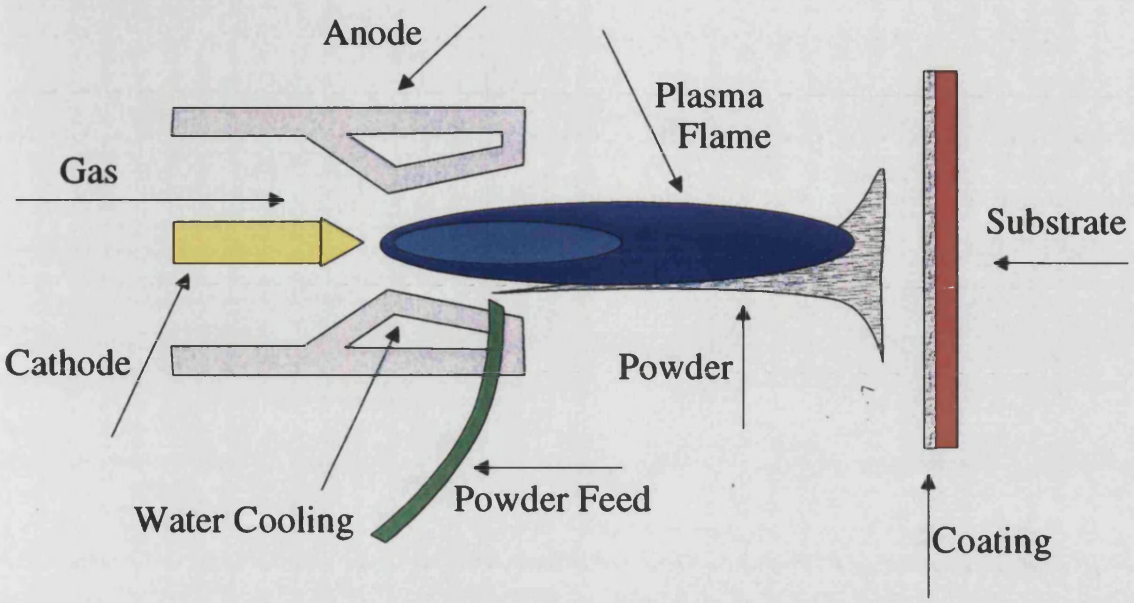

Figure 2-4 :- Schematic diagram showing plasma spray technique

As the ceramic powder remains in the heated plasma zone for only a fraction of a second, only partial melting of the powder usually takes place. Particle melting is a consequence of ionised and dissociated gas recombining on the particle surface releasing considerable energy which is transferred to the powder and causes melting. The distance of the substrate from the plasma is one of the critical factors controlling the degree of melting of the particles and the ability of the particulate to flow into a dense coating. The characteristics of the porous coating are also controlled through variations in particle size and system pressure. One advantage of the plasma spraying process is that during the coating process, the substrate remains at a relatively low temperature (generally less than 300°C) so the mechanical properties of the metallic implant materials are not compromised.

The principal difference between air plasma spraying and vacuum plasma spraying is that the latter is performed at a reduced pressure. Operating the plasma torch in such an environment has three effects: the plasma flame is longer, giving more time for powder particles to melt; powders which are prone to oxidation can be sprayed using this technique avoiding the oxidation effect and the velocity of the particles is increased. These three properties of the vacuum system produce a coating which is more dense and

homogeneous than coatings produced by the air plasma spraying technique, but the cost of the process is considerably increased by the incorporation of a vacuum system.

Plasma spraying will induce a series of changes to the phase composition, structure and *in-vivo* behaviour of the starting materials. The crystalline structure of the coating is determined by the cooling conditions of individual drops at the moment each strikes the substrate and by the temperature of the whole coating during spraying. Naturally, the temperature of the liquid drops is never below that of the melting point of hydroxyapatite powder (1550°C). The fusion droplets can be highly overheated in a plasma, and are very rapidly cooled on impact with the substrate because of the large temperature difference. Two conditions may occur under such a cooling regime [68] . The first of these is the nucleation of a multitude of crystallites in the fused state and their rapid growth yielding a small grained crystalline phase. Secondly, fused droplets may be quenched so rapidly that they will only remain at the crystallisation temperature momentarily and will thus only partially crystallise. Besides, if the diffusion mobility of atoms is inhibited, then this part of the drop will stay non-crystalline for a long time. These parameters can be controlled to produce hydroxyapatite coatings with different relative ratios of amorphous to crystalline phases.

A similar coating can be produced using the detonation gun technique (Figure 2-5). In this process, a controlled mixture of oxygen and acetylene gas is fed into a device rather like a gun barrel. This gas is ignited by spark discharge, the detonation propelling powder fed into the barrel towards the substrate. The energy emitted by the explosion heats the powder to high temperatures and accelerates it to extremely high velocities. The noise of the explosion requires the entire process to be carried out in a soundproof chamber. The operating cycle is automated and repeated many times to produce a continuous deposit.

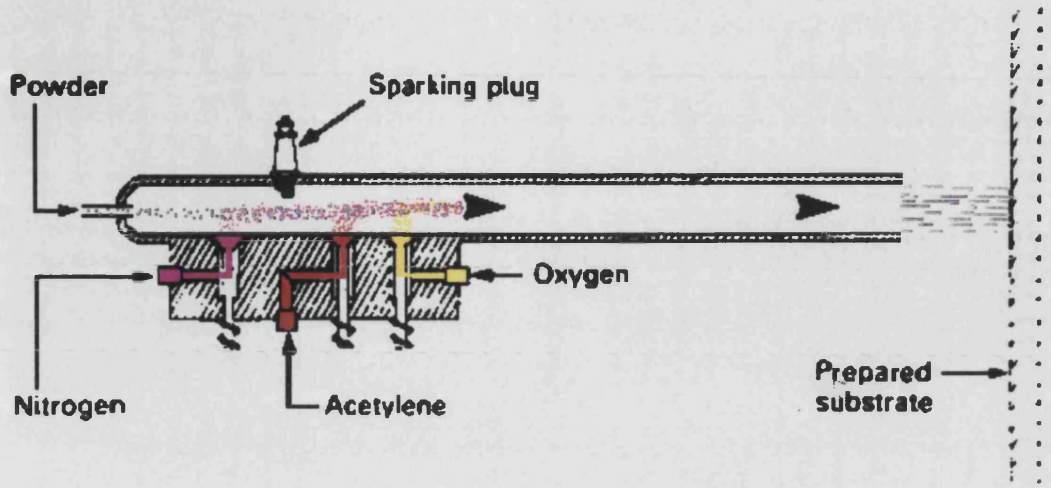

Figure 2-5 :- Schematic representation of the Detonation Gun [106]

It is believed that the higher energy of the detonation gun process will produce coatings which have higher adhesion to the substrate and be of higher density than vacuum plasma sprayed deposits. The detonation gun process induces a particle speed typically around 600 m/s and a gas / particle temperature in excess of 3000°C [107] whereas for the comparable high velocity oxy-fuel process particle speed varies between 150 and 750 m/s, gas / particle temperatures being only around 1700°C. Other potential advantages of this process include the removal of the need to grit blast the substrate surface before spraying and the lower level of heat input to the substrate.

At the molecular or even atomic level, the morphology of the coating will be controlled not only by the cooling rate of molten particles arriving at the sample surface which would affect molecular movement, but also by deposition from the vapour phase present [108].

Adhesion of a sprayed coating to the substrate can be achieved by a number of mechanisms most importantly: mechanical bonding, chemical bonding and physical bonding. Of these three, the dominant mechanism assumed to take place in hydroxyapatite coatings is mechanical bonding. This occurs by mechanical interlocking

between protrusions on the substrate and the coating leading to mechanical adherence. The surface topography therefore greatly influences the adhesion of the coating to the substrate. For this reason, grit blasting is commonly carried out to roughen the substrate surface before the coating is applied. However this process tends to leave a certain amount of residue at the substrate surface which may weaken the bonding between coating and substrate. To overcome this, a bond coat may be applied to the substrate. This bond coat is supposed to further increase the roughness of the substrate before the coating is applied and may reduce some of the residual stresses in the coating [109] arising from the thermal mismatch between coating and substrate. In some cases however, this bond coat is believed to promote chemical bonding by inter-diffusion between the hydroxyapatite coating and the interlayer [110, 111]. Physical bonding through Van der Waals interactions will only occur if the surfaces of particles are in intimate contact, i.e. within 0.5 nm of one another.

The strength of an hydroxyapatite coating will also be directly related to its morphology. The Griffith equation for the fracture strength of a brittle materials such as hydroxyapatite is

$$\sigma_f = \sqrt{\frac{2\gamma E}{\pi a}}$$

where σ_f is the fracture stress, γ is the fracture surface energy, a is the length of a fracture initiating defect such as a crack and E is the Young's modulus. For coatings with defects such as micro-cracks or pores the fracture strength is greatly reduced over that of the bulk material since to initiate failure a crack need only travel from one region of good contact to another.

Residual stresses in hydroxyapatite coatings resulting from the spraying process may also be determinant in the coating's durability. These stresses can cause cracking and spalling off of coatings and will affect their mechanical stability and fatigue resistance. Relaxation of these stresses in service must always be considered as a driving

force for coating debonding. Residual stress levels in coatings can be determined in several ways. Hobbs *et al* [112] measured residual strain levels in ceramic coatings by measuring radii of curvature of coatings after their substrates had been removed by etching. Assuming that an unstressed coating would not deform, this radius of curvature was used to determine the imposed strain which was then converted to a stress. Incongruously these authors found the residual stress in plasma sprayed coatings to be compressive in nature rather than tensile as would be expected. It was assumed that shrinkage cracking considerably reduced tensile stresses formed in the coating. In addition to this it was postulated that a reduction in the cooling rate experienced by the ceramic as a result of the high heating rate imposed by the multi-pass spray technique which would result in a lower contraction strain in the material. This should also reduce the yield stress at which plastic deformation could occur thereby reducing the maximum compressive stress in the coating.

Gill and Clyne [113] monitored the deformation of thin substrates during plasma spraying using video equipment and used this information to determine the residual stress levels in their coatings. They extrapolated their findings to predict the effect of substrate and coating thickness on residual stress. For thicker substrates, they predicted that residual stresses would be very much lower than for thin substrates since the force balancing the stress in the coating would be distributed over a much greater thickness. Also, the thicker substrate would slow the rate of heat flow away from the coating reducing the quenching stress experienced by incoming particles. As the thickness of the coating increased, a stress gradient was found to be formed through the thickness of the coating. It was postulated that this was due to relaxation of stress in lower layers of material held at elevated temperature during later passes of the plasma torch. This relaxation comes about as a result of the following phenomenon. When a splat is quenched and put into tension, there is a small increment in the compressive stress induced in all the underlying material. This builds up and tends to cause a positive gradient of stress in the deposit. The stresses in the existing layers beneath this new deposit are however relaxed by the adoption of the curvature. Therefore multiple effects must be considered when predicting what levels of stress will occur in such coatings. Residual stress determination by x-ray diffraction techniques are described below.

These residual stresses can be generated in several ways during spraying. In the case of hydroxyapatite coatings the most dominant mechanism probably arises due to the high thermal expansion mismatch between the ceramic hydroxyapatite and metallic titanium substrate. The thermal expansion coefficients for bulk hydroxyapatite and Ti-6Al-4V are 13.3 and 8.6 W cm^{-1} K^{-1} at 293 K [101]. This difference results in the substrate contracting more than the ceramic causing the ceramic to become highly stressed. Lesser contraction stresses are also generated in a similar manner when the thermal contraction of a newly arrived particle is inhibited by the underlying cooler particles. This second stress is termed the quenching stress and is always tensile in nature [114].

2.7 Amorphous Versus Semi-Crystalline Hydroxyapatite Coatings

Many authors [15, 16, 17, 18] in the literature, now seem to agree that hydroxyapatite's enhanced bone bonding and osseoconductive behaviour arise from its dissolution properties. These authors suggest that new bone growth onto hydroxyapatite coatings is brought about by partial dissolution of the coating, and subsequent re-precipitation of the calcium phosphate back onto the coating as new natural bone. From these findings, it would seem that the performance of an hydroxyapatite coating will therefore depend on its dissolution behaviour. However, Suzuki *et al* [115] implanted the same hydroxyapatite coated polymeric implants into soft tissues that Nagano *et al* [116] implanted into the tibiae of rabbits. The latter authors reported resorption of the hydroxyapatite coatings while the former reported no detectable coating degradation. This suggests that it is osteoclastic cellular activity rather than simple chemical degradation which brings about dissolution of hydroxyapatite coatings in orthopaedic applications.

The crystallinity of an hydroxyapatite coating is controlled by the processing parameters used during its production as well as any subsequent coating treatment. Post plasma spraying heat treatment for example, causes an increase in the coating crystallinity. Brossa, *et al* [117] found that the shear strengths of hydroxyapatite coatings varied with coating crystallinity and that values reached a maximum for low crystallinity coatings and a minimum for high crystallinity coatings.

Until recently there was much argument in the field as to whether a bioactive coating should dissolve rapidly in the body or remain coherent and intact for far greater durations. It now seems clear however, that since coated and uncoated implants demonstrate the same degree of bonding to bone when removed from the body after extended implantation times, it is the early osseoconductive effects of hydroxyapatite coatings that make them superior to other implant types [53] . In comparison to highly crystalline coatings, amorphous hydroxyapatite shows the high degree of degradation that seems to be favourable for early post operative fixation. In recent studies, de Bruijn *et al* [118] amongst others, have indicated that, to a certain extent, coating stability negatively influences early bone-hydroxyapatite interactions, and that a partial surface degradation may be favourable for early bone formation. Nagano *et al* [116] however implanted both amorphous and crystalline hydroxyapatite coatings on polymeric substrates into the tibiae of rabbits and monitored the bone bonding capabilities of each. They reported that both coating types showed direct apposition to newly forming bone and that even the highly crystalline coating underwent some dissolution with time. The amorphous hydroxyapatite coatings studied by these authors underwent complete dissolution leading to rapid bone ingrowth into the substrate with no intervening fibrous layer. It was therefore concluded that since the hydroxyapatite coating itself is fragile and the bonding strength between the coating and the underlying substrate is usually weak it may be more useful to encourage early formation of ingrowth into the substrate than into the coating. This would encourage mechanical interlocking of the implant and the highest likelihood of success of the prosthesis.

2.8 Titanium As A Substrate Material

Titanium and titanium alloys are now the materials most commonly used as substrates in orthopaedic situations. These alloys can be considered to be superior to [119] and have come to replace stainless steels and cobalt chromium alloys originally utilised as the femoral component of the hip prosthesis. The increasing use of titanium in femoral components has dramatically reduced the reported number of femoral component failures

resulting from mechanical problems [120]. Rotary bending fatigue tests give similar values of approximately 550 M Pa for both wrought cobalt-chromium and Ti-6Al-4V but the titanium alloy has twice the flexural strength of the chromium [121]. Titanium has an elastic modulus of approximately 110 G Pa, approximately half that of stainless steel (200 G Pa) or cobalt chromium (235 G Pa) [122] which is extremely important in consideration of load transfer and the resulting stress shielding which may occur when the material is implanted in the body.

Viceconti *et al* [123] performed rotation bending fatigue testing on four different designs of hip prosthesis: a Cr-Co-Mo alloy anatomical stem; a titanium alloy stem with the same dimensions as the cobalt chrome one; a stem produced from the second with a central anteroposterior hole machined out; a fourth again made from the solid titanium stem but with a porous coating of titanium-sintered beads extending distally to the cylindrical section of the stem. The authors found that the solid titanium stem had a much greater fatigue life than the cobalt chromium device but any machining modifications to the titanium stem reduced its fatigue life considerably. Any machining defects caused critical early failure in the titanium prostheses leading the authors to emphasise the importance of careful device manufacture and design.

Smith [124] investigated the effect of plasma sprayed coatings on the fatigue behaviour of titanium alloy implants. It was found that sinter coating a metal powder onto the surface of a titanium implant caused a significant decrease in the high cycle fatigue strength of the implant from 586 - 620 M Pa down to 172 - 206 M Pa. In orthopaedic situations, high-cycle fatigue is usually taken to be ten million cycles since a patient may take as many as one million steps per year and the implant should last ten years to ensure patient satisfaction. The decrease in endurance limit was not attributed to any phase transformation occurring in the titanium as a result of the high temperatures associated with plasma spraying however, but rather, resulted from the creation of a defect i.e. a micro-notched coating on the surface of the implant. It was thought that the sintered coating disturbed the otherwise smooth implant surface, acting as a stress raiser. Smith found that plasma spraying a coating of titanium onto a titanium prosthesis reduced the fatigue limit of the device, when compared to uncoated samples, by 40 %.

Heat treating of the coated prostheses at 732°C for two hours before fatigue testing reduced the fatigue limit of the devices by a further 18 %. It was again suggested that this reduction in fatigue life resulted from disruption of the smooth prosthesis surface by the intimate and in places metallurgical bond contact between the coating and the substrate.

Kohn, *et al* investigated the fatigue properties of porous coated titanium alloy implants using acoustic emission (AE) testing and examined the failure mode of these materials [125]. Porous titanium bead coated titanium implants were tested in fatigue and acoustic emission was used in conjunction with closed circuit television coverage and scanning electron microscopy (SEM) analysis. Pure titanium beads were sinter coated onto Ti-6Al-4V substrates to a thickness of 750μm. The authors reported that AE can reliably detect incipient fatigue cracks, thereby serving as a sensitive warning to material failure and enabling the differentiation between initiation and propagation. They also reported that fatigue of porous coated Ti-6Al-4V is governed by a sequential multimode fracture process of : transverse fracture in the porous coating ; sphere / sphere and sphere / substrate debonding ; substrate fatigue crack initiation ; slow and rapid substrate fatigue crack propagation. Because of the discontinuity of the porous coating, the first three modes of fracture occur in a discontinuous fashion. Therefore, the AE generated is intermittent and the onset of each mode of failure can be detected by changes in the AE event rate. Although the testing strains used in this experiment were well above those normally experienced *in-vivo* the authors concluded that their work provided a useful guide to the failure mode of porous coated implants.

Another advantage titanium alloys have over other potential substrate materials is their excellent resistant to general corrosion such as pitting corrosion and crevice corrosion [126] - problems which are particularly important in *in-vivo* situations where the substrate could experience attack by the body's fluids.

When thermally sprayed coatings are applied to titanium substrates however, the effect of the imposed environment during spraying may induce microstructural changes which could negatively influence the metal's behaviour in the body. The β-transius for

Ti-6Al-4V occurs at 1040°C, well below temperatures generated by thermal spraying therefore it can be expected that the microstructure of the finished prosthesis substrate will be different from that of the as-received material. If the transition temperature is exceeded, the microstructure of the titanium will be transformed from equiaxed α-Widmanstatten plates and residual β-phase to one consisting of an acicular α-phase interspersed by a stable β-phase [127].

Manero and co-workers [128] heat-treated Ti-6Al-4V alloy cylinders to simulate the effect on microstructure of applying a sintered metallic porous coating at the surface of an implant then compared the mechanical properties of the heat treated materials with those of the as-received titanium under cyclic tension-compression fatigue. Tests were carried out both in air and in Ringer's solution held at 37°C. The authors reported that in all cases, failure in a saline environment always took place both at a lower total number of fatigue cycles and at a lower cumulative plastic strain. This was associated with a change in failure mode for the nucleation of fatigue cracks at slip bands when fatigued in air to the nucleation at the α / β interface when the samples were fatigued in Ringer's solution. From transmission electron microscopy (TEM) and energy dispersive analysis (EDA) investigations, the authors concluded that a high dislocation density at the α / β interfaces promotes precipitation of a titanium hydride when the microstructure of the alloy has been altered by heat treatment. These hydrides promote embrittlement of titanium alloys and their formation would be accelerated by the presence of a saline environment. The effect of phase transformation therefore causes a speeding up of embrittlement of the Ti-6Al-4V alloy and therefore premature fatigue failure.

2.9 Techniques for the Analysis of Hydroxyapatite Coatings

2.9.1 X-Ray Diffraction

X-Ray diffraction is one of the most useful tools available to the materials scientist for the investigation of the fine structure of matter. The use of x-rays for

characterisation of materials dates back to von Laue's discovery in 1912 that crystals diffract x-rays in a manner which allows the determination of their structure. In the same year, W.L. Bragg was able to express the findings of Laue in a simple mathematical formula which described the essential condition which must be met in crystals if diffraction is to occur. The formula is now called the Bragg Law and can be written as follows:

$$n\lambda = 2d\sin\theta$$

where λ is the wavelength of monochromatic x-rays incident on the crystal, θ is the angle of incidence of these x-rays on the crystal whose atoms are spaced at a distance d apart and n is a positive integer.

The x-ray powder diffraction technique is unique in that it is the only analytical method that is capable of providing qualitative and quantitative information about the compounds present in a solid sample. Diffraction patterns are generally obtained with automated instruments similar in design to that shown below (Figure 2-6). The sample is held in the sample holder and rotated in order to increase the randomness of the orientation of the crystals. The diffraction pattern is obtained by automatic scanning in the same way as for an emission or absorption spectrum. The identification of a compound from its diffraction pattern is based upon the position of the lines (in terms of θ or 2θ) and their relative intensities. The diffraction angle 2θ is determined by the spacing between a particular set of planes which in turn is calculated using the Bragg equation from the known wavelength of the x-ray source and the incidence angle.

Identification of compounds is empirical. Powder diffraction file standards are obtained and the d spacings and relative line intensities of the unknown material are compared with these until a positive match is determined.

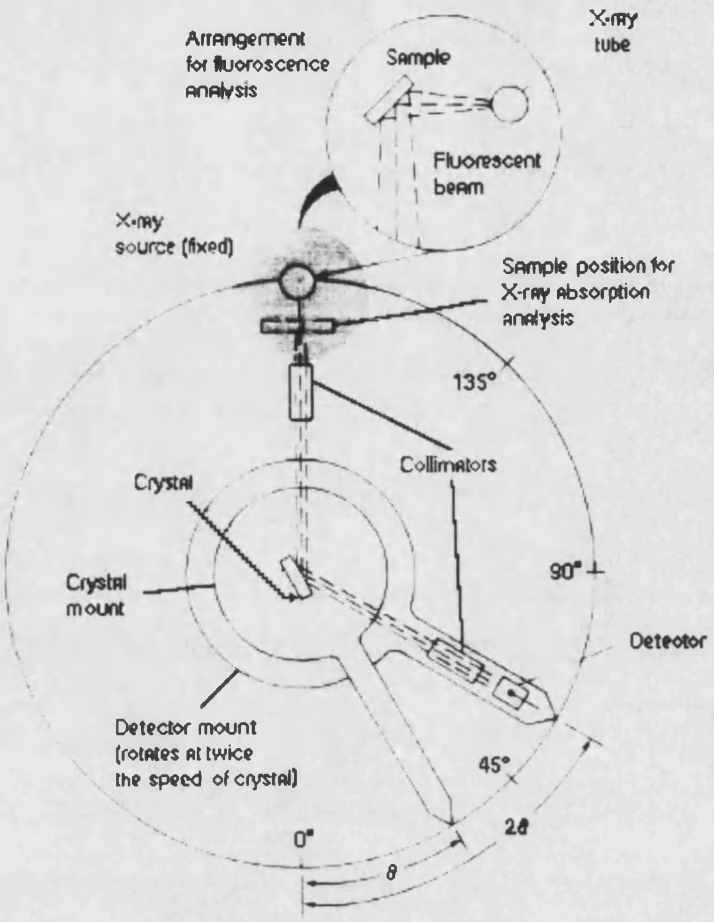

Figure 2-6 :- Schematic diagram showing x-ray diffraction instrument [129]

Materials which are not completely crystalline in nature show diffraction traces which have lines broadened by the amorphous component of the material. Amorphous phases cause a small angular divergence of the diffracted beam, or diffraction scattering at angles near to, but not exactly equal to, the exact Bragg angle for the crystalline material. Various techniques for measuring the degree of crystallinity of a material are based on this broadening effect. Using image analysis of diffraction traces, it is possible to compare the relative ratios of the amorphous broadening with the sharper crystalline peaks and hence determine a percentage of amorphicity.

Strain in the surface layers of a sample is manifest in a distortion of the atomic crystal lattice. This strain can be observed by x-ray diffraction as a shift in diffraction peaks. Measurement of this shift can be related to residual strain which, when combined

with a knowledge of the elastic constant for the material in question, can be used to determine the internal residual stress [130]. Under the condition of plane stress, the in-plane stress σ_{ϖ} can be calculated using

$$\sigma_{\varpi} = \left(\frac{E}{1+\upsilon}\right)_{(hkl)}\left(\frac{1}{d_{\varpi 0}}\right)\left(\frac{\partial d_{\varpi\varphi}}{\partial \sin^2 \varphi}\right)$$

where $\left(\frac{E}{1+\upsilon}\right)_{(hkl)}$ is the elastic constant for the material in the chosen hkl direction and may be different from the bulk material value. For example, Tsui [101] determined the Young's modulus of plasma sprayed hydroxyapatite coatings to be around 5.5 G Pa while the value for bulk sintered hydroxyapatite is usually quoted in the literature to be in the range of 35-90 G Pa [131, 132]. The other parameters are illustrated in the schematic below (Figure 2-7),

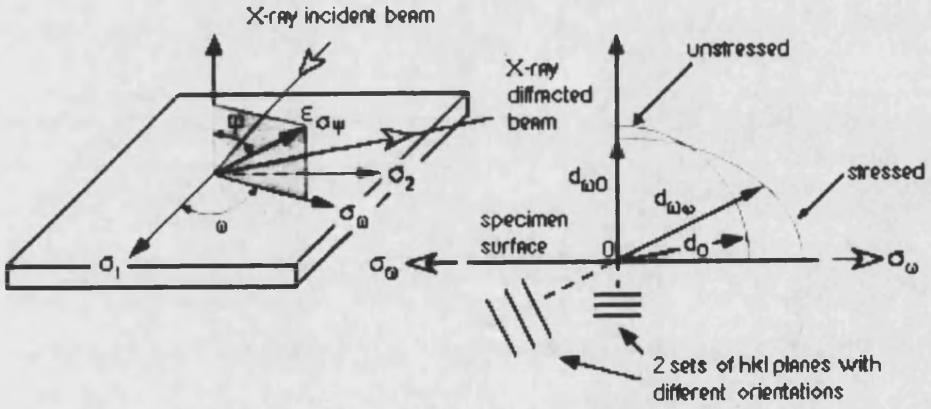

Figure 2-7 :- Schematic showing plane stress elastic model for residual stress determination by an x-ray diffraction technique [133]

where $d_{\varpi 0}$ is the lattice spacing of hkl planes measured at $\varphi = 0$ and is used to estimate d_0, the unstressed lattice spacing with an error of less than 1%. φ is the angle between the normal to the sample surface and the bisector of the incident and diffracted beams. ϖ is the angle between the direction of the measured in-plane stress and the direction of the principal stress σ_1. $d_{\varpi\varphi}$ is the spacing between the lattice planes measured in the direction defined by ϖ and φ. In order to be able to determine these parameters, it is necessary to use an instrument with which φ can be varied since high precision is needed in aligning

the diffraction apparatus or in positioning the sample. However, this technique has been used to determine the residual stress of thermally sprayed coatings [134, 135].

Another method of determining residual stress is to find the residual strain in the surface layers of the material [136], and convert this to a stress value using the known elastic constants for the material in the form of a sprayed coating. Again using the distortion in the atomic lattice as a guide to residual stress this technique involves the determination of this shift and the relation of this quantative measure to a change in residual strain. This is done by measuring the shift of a particular peak in the x-ray diffraction trace for the material [137]. The choice of peak being studied is important since is should have a reasonable relative intensity to the I_{100} hydroxyapatite peak in order to be easily distinguished. The choice of peak can significantly simplify the mathematics associated with calculating the residual strain since the indicies of planes corresponding to the various peaks allow cancellation of terms in the equations. For example, in hydroxyapatite, the choice of the 300 or 004 planes which correspond to major peaks in the x-ray diffraction trace allows such simplification.

Since the structure of the unit cell of hydroxyapatite is hexagonal the lattice parameters can be expressed in the form $a = b \neq c$. The a and c parameters can be calculated from the following relationship

$$\frac{1}{d^2} = \frac{4}{3}\left(\frac{h + hk + l}{a}\right) + \frac{l}{c}$$

when using the 300 plane in hydroxyapatite, this simplifies to

$$a = \sqrt{12d^2} = 2\sqrt{3}d$$

and for the 004 plane in hydroxyapatite, to

$$c = \sqrt{16d^2} = 4d$$

With knowledge of the Young's modulus, E, for the material, which in the case of hydroxyapatite will be different for the coating compared to the bulk material, the change in lattice parameter can be converted to strain, ε, and hence to a stress, σ.

$$\frac{\partial a}{a} = \varepsilon$$

and,

$$\sigma = \varepsilon E$$

This simplified approach often requires the assumption of anisotropy in Young's modulus with lattice direction in the surface layers of the material if the parameter is not easily determined for each direction experimentally.

Sergo *et al* [138] determined residual stress levels in both air and vacuum plasma sprayed hydroxyapatite coatings on titanium substrates using Raman spectroscopy. The authors suggested that the thermal expansion mismatch between the hydroxyapatite and Ti-6Al-4V leads, on cooling from the plasma spraying temperature, to the development of residual stresses given by:

$$\langle\sigma\rangle = \frac{\Delta\alpha \Delta T E(p)}{1-\nu}$$

where $\langle\sigma\rangle$ is the spatial average of the mismatch stress, ν is the Poisson modulus, $\Delta\alpha$ is the difference between the coefficient of thermal expansion of the coating and of the Ti-6Al-4V substrate, E(p) is the Young's modulus which is a strong function of the porosity p, and ΔT is the difference between the stress-free temperature and the ambient temperature, typically the body temperature for biomaterials. The stress-free temperature is the temperature below which stresses cannot be accommodated by some relaxation mechanism, usually plasticity in metals and grain boundary sliding in ceramics. Since the coefficient of thermal expansion of hydroxyapatite ($11.5 \times 10^{-6}K^{-1}$) is higher than that of Ti-6Al-4V ($8.9 \times 10^{-6}K^{-1}$), the value of $\Delta\alpha$ is $2.6 \times 10^{-6}K^{-1}$ and thus, upon cooling, the hydroxyapatite coating will be subject to a residual tension stress. The authors also demonstrated mathematically that a residual tensile stress would thermodynamically encourage dissolution since it would present an additional free energy to the dissolution / re-precipitation equilibrium. Conversely therefore, a residual compressive stress would be assumed to hinder the dissolution of the coating and thus also limit the bioactive nature of the hydroxyapatite. Unfortunately, however, although the authors measured a

tensile stress for air plasma sprayed coatings they determined that, for vacuum plasma sprayed coatings, the residual stress was compressive in nature.

2.9.2 Image Analysis

Digital image analysis is a relatively new technique having its beginnings in 1969 with the introduction of the Quantimet 720 system by the American company Bausch and Lomb. Prior to this, studies of materials have relied on qualitative descriptions of structures with comparison to charts and tables which began to be introduced in the mid 1920s. Such charts gave visual comparisons for measurement of such parameters as grain size [139], inclusions [140] and volume fraction [141]. Despite its manually exhausting procedures, it was proven that quantitative microscopy with the use of overlay grids gave statistically comparable results independent of the analysis technique used [142]. This result gave confidence in the quantitative value of the analysis of microscopical images and led to the development of the modern image analysis system.

The principal stages in image analysis can be considered as : image capture, segmentation, object detection, measuring and analysis. The overall process of analysis is an iterative one which follows a route which is summarised in Figure 2-8 below. Image capture involves the conversion of an image, obtained via for example a video camera attached to an optical microscope, into an electronic signal suitable for digital processing and storage. This dictates that the object under consideration is converted into a pixel based image. Segmentation then describes the process of separating the object or regions of interest from the background. This can be done by several methods, the simplest of which is thresholding in which all tones below a selected level are treated as black and all above, as white. The system is then set-up to recognise white regions as being of interest and black as background for example. The next stage in processing the image involves object detection. This is a data-reduction step which produces a description of each object in a more compact form than as a list of pixel co-ordinates. This process dramatically reduces the amount of data needed to describe the content of an image and hence reduces the power demanded of the computer system. The last two steps,

measuring and analysis are concerned with the gathering of relevant data and its transposition into a form meaningful to the investigation being undertaken, for example, relative porosity levels, coating thickness (measured after calibrating the system with a graticule) or number of grains.

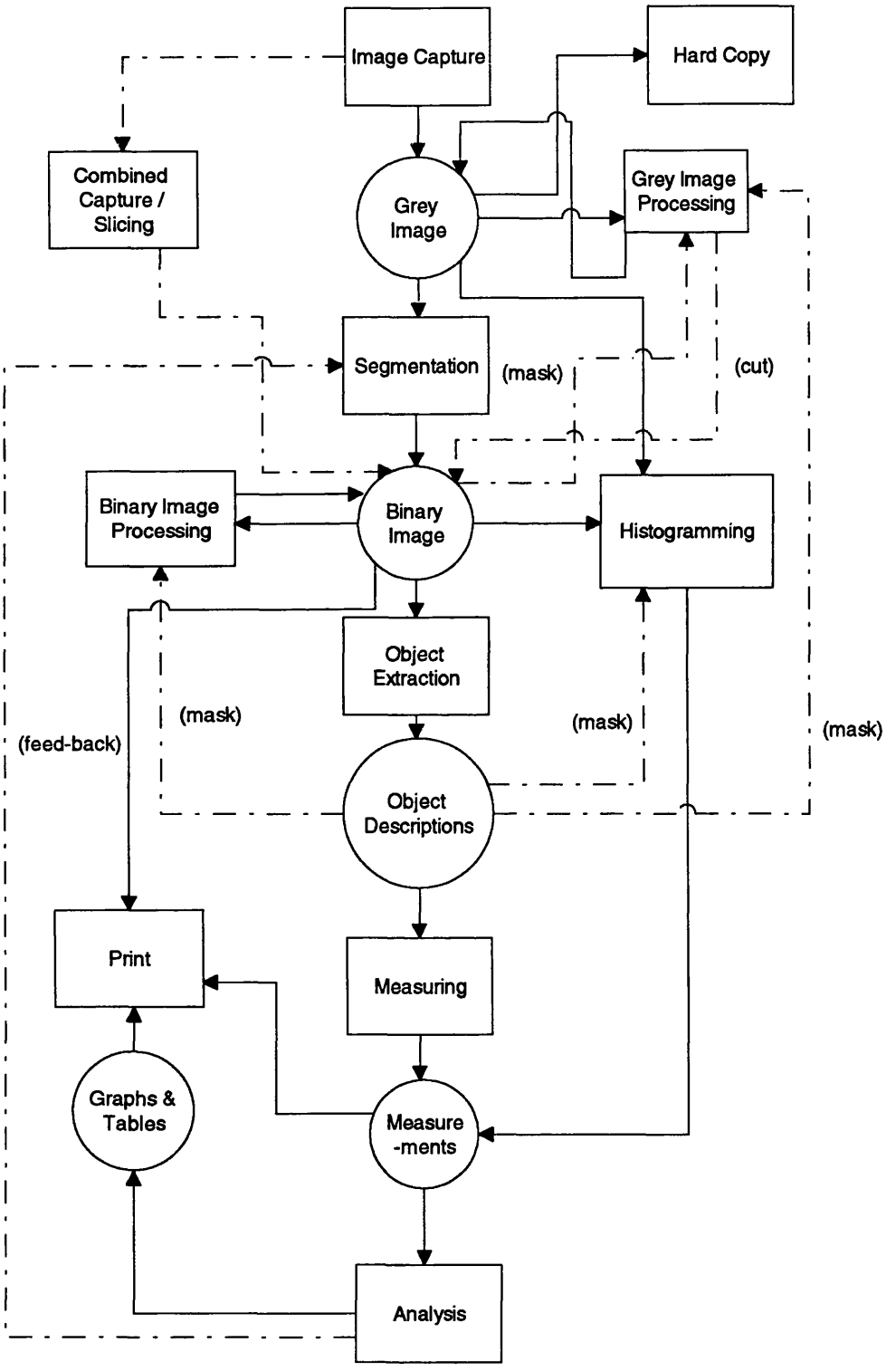

Figure 2-8 :- Schematic diagram showing the processing steps involved in image analysis [143]

2.9.3 Other Techniques

As has already been described above, many other common coating analysis techniques could be used to characterise hydroxyapatite coatings. Since these techniques are widely covered in the literature their operation will not be described here but they include : surface roughness measurement by Talysurf [144], microscopy (SEM [145], TEM [48], atomic force microscopy (AFM) [146] and optical microscopy [48]), spectroscopy [147] (infra-red (IR), fourrier transform infra-red (FTIR), x-ray fluorescence (XRF) and x-ray photoelectron spectroscopy (XPS)), thermo-gravimetric analysis and destructive mechanical testing [148]. Some of the mechanical properties of both hydroxyapatite and medical grade titanium (Ti-6Al-4V) are however listed below [101] (Table 2-1).

Property	*Hydroxyapatite (as VPS coating)*	*Titanium (Ti-6Al-4V)*
Thermal conductivity ($W\ m^{-1}\ K^{-1}$)	0.7 (283 K) 2.2 (1352 K) 2.7 (1770 K)	10.0 (293 - 1000 K)
Specific heat capacity ($J\ kg^{-1}\ K^{-1}$)	766.3 (293 - 1300 K)	650.0 (293 - 1000 K)
Density ($Mg\ m^{-3}$)	variable	4.420
Coefficient of thermal expansion ($M\ K^{-1}$)	13.3 (293 - 1000 K)	8.6 (293 K) 13. 5 (1073 K)
Young's modulus (GPa)	5.5 (298 K)	106.0 (293 K) 62.1 (1073 K)
Poisson's ratio	0.30	0.31
Elastic limit (MPa)	50 (293 - 1000 K)	1100 (293 - 973 K)

Table 2-1 :- Mechanical properties of Hydroxyapatite and Ti-6Al-4V [101]

Pajares, *et al* [149] performed contact damage analysis on air plasma sprayed alumina coatings using a circular indentor. Both thick (350 - 500 μm) and thin (130 - 200 μm) coatings were investigated following single cycles indentation with different

applied loads and for different numbers of cycles. They recorded the morphologies of failure surfaces following indentation and described the types of damage zones occurring as a result of the application of loads to both the ceramic coating and metallic substrates. Damage radiated out from the indentation source with downwards extending cone-like cracks being found in the ceramic coating and upwards extending transverse cracks existing in the substrate. Delamination at the coating / substrate interface was also apparent. The size of the damage zone increased with increasing applied load. It was also reported that the coatings were subject to significant fatigue and that through-thickness cracks developed in coatings predominantly during the loading cycle of fatigue testing, while delamination cracks were formed during the unloading cycle. It was found that damage, once initiated, accumulated with each cycle, indicating a finite lifetime for the coatings.

3. Experimental Techniques

Validation procedure results for some of the techniques described below and a discussion of experimental errors are presented in the appendix.

3.1 Specimen Composition / Morphology

All samples used in this study were in the form of hydroxyapatite coatings on titanium alloy substrates. All substrates were manufactured from the same titanium alloy having a composition of Ti-6Al-4V (BS 3531). The substrates were cut into samples with dimensions 2 mm x 10 mm x 80 mm for static corrosion analysis and 2 mm x 20 mm x 80 mm for all other testing. The titanium was prepared prior to application of the coating by the following method:-

- cleaning operation
- grit blasting with alumina
- cleaning operation
- * pre-coating by plasma-spraying of pure titanium
- * cleaning operation

(* for vacuum plasma sprayed coatings only)

The substrates were then thermally sprayed by BVBA Vanderstraeten, Belgium. Two methodologies of spraying were used, vacuum plasma spraying and detonation gun spraying. Approximate coating thicknesses of 40 μm were requested. Two different spray powders were used to produce the coatings corresponding to the powders usually commercially sprayed by Vanderstraeten.

3.2 Fatigue Test

A three-point bend fatigue testing rig was manufactured with the aim of dynamically testing the HA coatings on the titanium substrates. The jig was designed to impose a fixed deflection (3mm) over a central span of the sample which corresponded to an imposed strain of 1%. This strain was chosen based on average stress values given in the literature for loading on orthopaedic implants during normal walking [13, 35] and was calculated in the manner described below. From bending theory for materials assuming three point bend:

$$\sigma \max = \frac{3F\,d}{2\,b\,t^2}$$

and

$$\delta \max = \frac{F\,d^3}{48\,E\,I}$$

where

$$I = \frac{b\,t^3}{12}$$

and

d	=	length between supports
b	=	width of sample
t	=	thickness of sample
F	=	applied force
E	=	Young's modulus for material
I	=	second moment of area
δ	=	deflection
σ	=	applied stress

For the samples used in this research, d = 0.06 m , b = 0.02 m , t = 0.002 m and E = 1.280 x 10^{11} Pa for Ti-6Al-4V deflections imposed on a sample following the application of various stresses are presented below (Table 3-1).

strain	E (Pa)	σ max (Pa)	F max (N)	load (Kg)	deflection (m)
0.001	1.280×10^{11}	1.280×10^{8}	113.78	11.6	0.003
0.002	1.280×10^{11}	2.560×10^{8}	227.56	23.2	0.006
0.003	1.280×10^{11}	3.840×10^{8}	341.33	34.8	0.009
0.004	1.280×10^{11}	5.120×10^{8}	455.11	46.4	0.012
0.005	1.280×10^{11}	6.400×10^{8}	568.89	58.0	0.015

Table 3-1 :- Deflection calculation results used in the design of the testing fatigue jig

A schematic of the test jig is presented below (Figure 3-1). Samples were mounted in the jig so that the coating was fatigued in tension. Samples were fatigued for either one or ten million cycles [14] at a rate of 4 Hz. This fatigue test was not intended to for use as a basis for statistical fatigue life prediction, but as an indication of coating performance under a simulated physiological environment.

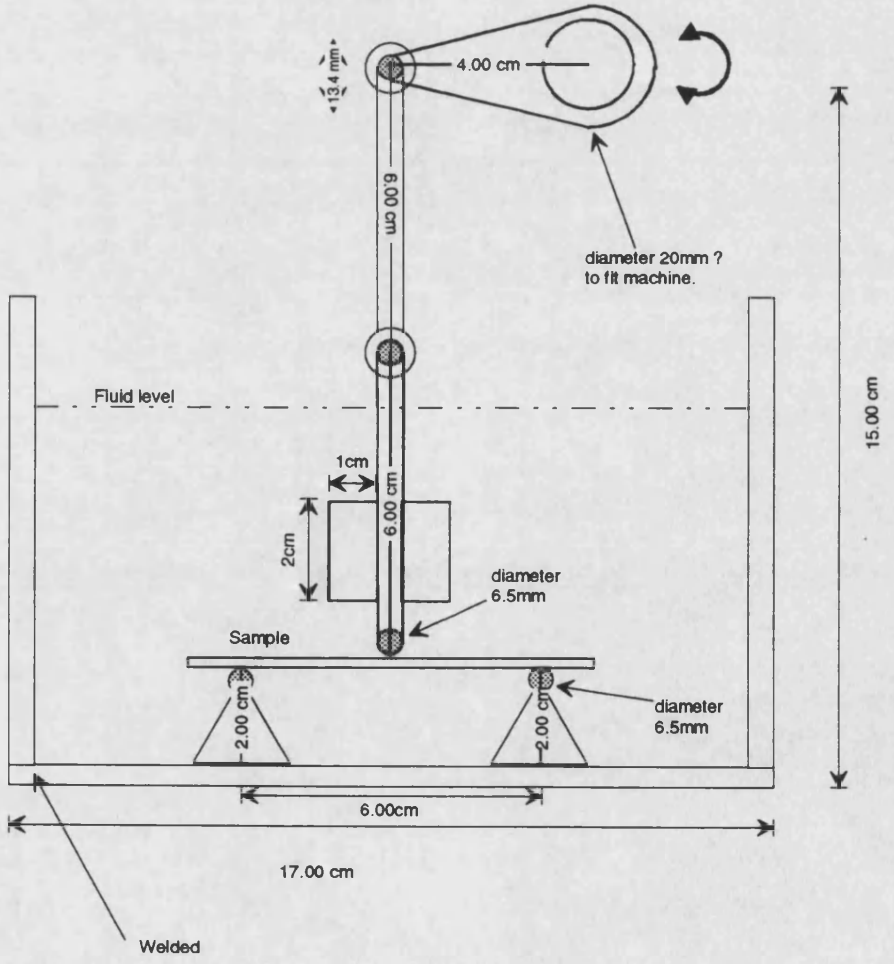

Figure 3-1 - Schematic diagram of in-vitro dynamic fatigue rig (side elevation)

3.3 *In-vitro* Ageing

Two *in-vitro* tanks with pHs of 7.2 and 4.5 were set-up buffered to pHs similar to that of the human body during normal functioning and during trauma or bone remodelling respectively [36]. The two tanks with a volume of 35 litres and 33 litres were filled with a solution made up from dissolved Ringer's salt solution tablets (composition shown in Table 2.1) and distilled water; then were buffered. After testing, samples were washed in distilled water and air dried in an oven held at 60 °C for five hours.

Salt	*Mass (g)*	*mol / litre*
NaCl	80.00	13×10^{-2}
KCl	7.40	4.96×10^{-3}
$MgCl_2.6H_2O$	4.00	9.84×10^{-4}
$NaH_2PO_4.2H_2O$	3.20	1.14×10^{-3}
$CaCl_2$	5.80	2.61×10^{-3}
$NaHCO_3$	40.00	2.38×10^{-3}

Table 3-2 - Composition of Ringer's Salt Solution [8]

The tanks were heated to 37°C corresponding to body temperature using Fisons Haaka DC1 circulatory heaters. Samples to be aged were placed in racks in the tanks with the coating surface facing away from the circulatory jet. The pH of the tanks was measured daily using an ATC Piccolo 2 pH meter before being buffered back to the required pH using 1 molar solutions of hydrochloric acid and tris(hydroxymethyl)aminomethane. Samples were aged in these tanks for the following time periods :-

unloaded samples	static loaded samples	fatigue samples
1, 2, 4, 8 weeks	1, 2, 4, 10, 15 weeks	1, 2, 4, 8, 12 weeks

3.4 *In-vitro* Fatigue Test

The bending table of the fatigue jig was surrounded by a stainless steel tank to allow *in-vitro* sample testing. This tank was heated to 37°C using an Algarde H51/671 100W mini-heater and an Algarde AL-500 (H59-679) electronic thermostat; it was buffered to pH 7.2 as above.

3.5 Static Corrosion Test

Stainless steel jigs designed to hold up to four corrosion samples held at a fixed strain equivalent to that used in dynamic fatigue testing were manufactured. A schematic diagram of the static corrosion jig is presented below (Figure 3-2). Spacers were used in the jigs to ensure correct deflection was imposed all samples. Samples were inserted into the jigs with the coating in tension as in the fatigue test. The jigs were then immersed in the buffered *in-vitro* tanks for the required ageing duration. A further jig was placed in an environment chamber held at 37°C to determine the effect of ageing the samples under loading in air. These air aged samples were statically loaded at 37°C for 1 and 15 weeks. Samples were washed as before in distilled water after testing and air dried in an oven at 60 °C for five hours before further preparation.

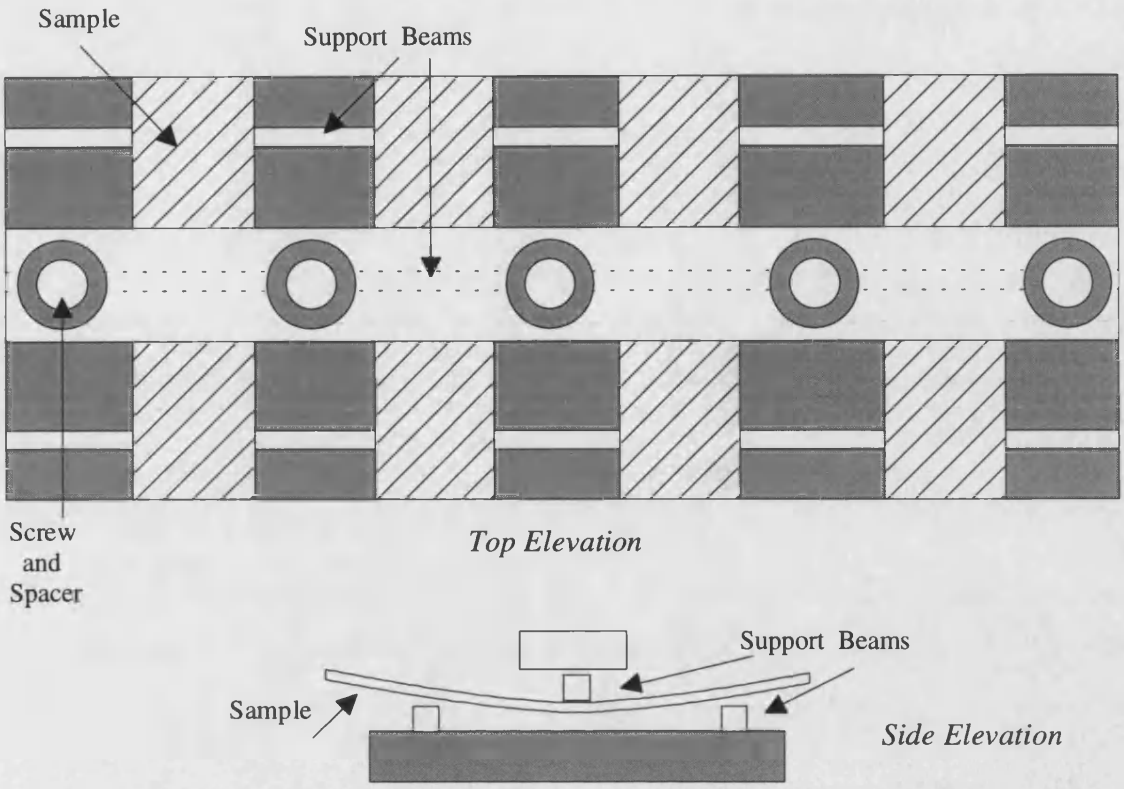

Figure 3-2 :- Schematic diagram of *static corrosion jig*

3.6 X-Ray Diffraction Analysis

After testing, samples were sectioned using a circular saw with distilled water cooling. A sectioned portion of each sample was then oven dried and x-ray diffraction testing carried out. The specimen was scanned between 2θ angles of 20 and 60° using the following equipment whose calibration data is presented in the appendix :

Philips PW 1730 / 00 4 KW X-Ray generator

Philips PW 2273 / 20 long fine focus 2 KW copper target x-ray tube operated at 40 kV and 25 mA

Philips PW 1820 / 00 computer controlled vertical diffractometer goniometer

Philips PW 1711 / 10 xenon proportional counter with PW 1752 / 00 graphite monochromator and PW 1368 / 55 automatic divergence slit assembly

Philips PW 1710 / 00 microprocessor diffractometer control

Philips PW 1877 PC APD, version 3.5 b diffraction software

Powder Diffraction File PDF-2 database sets 1 - 45, International Centre for Diffraction Data (ICDD)

This software detected diffraction peaks with a minimum peak tip width = 0.01(x2i), a maximum peak tip width = 2.00 (x2i), peak base width = 2.00 (x2i) and minimum significance = 0.50. This data was then compared with an hydroxyapatite standard from JCPDS - ICDD CD ROM database to identify diffraction planes from peaks detected by the system. Coating composition was determined by comparison of position and intensity of trace peaks with those of calcium phosphate ceramic standards. The principal phase in the material was thus identified by comparison with standards. Other phases were considered to be 'significant' if five or more peaks with an intensity greater than ten percent were detected for that compound.

From the x-ray data produced, plane spacings, d, for particular planes calculated by the system using Bragg's law and a value of λ = 1.54060 Angstroms for Cu K_α radiation, were used to determine the residual strain levels in the coatings. Choosing a particular HA plane e.g. (300) enabled an expression to be derived for a lattice parameter e.g. a as described previously:

$$a = \sqrt{12d^2} = 2\sqrt{3d}$$

Monitoring the change in this lattice parameter between the HA powder and HA coating allowed the residual strain value, ε, to be determined as follows:

$$\frac{\partial a}{a} = \varepsilon$$

These strain values were then converted to residual stress values using the Young's modulus for HA coatings obtained from the literature.

Diffraction traces derived from the x-ray data were plotted and later used in image analysis determination of crystallinity levels in the coatings.

3.7 Surface Roughness Analysis

Surface profiling was performed on all tested samples after sectioning using a Taylor-Hobson Form Talysurf 50 with a short arm pickup and a spherical sapphire tip stylus. The following measurements were taken from surface traces of the as-received, and tested hydroxyapatite coatings:

R_a - average roughness (also know as centreline average or arithmetic average), defined as the area of the peaks above the centreline plus the area of the valleys below the centreline divided by the assessment length (μm).

R_p - the height of the highest peak over the assessment length (μm)

R_v - the depth of the lowest valley over the assessment length (μm)

R_t - the height from the highest peak to the lowest valley over the assessment length (μm)

3.8 Optical Microscopy

A sectioned portion of the tested samples 15 x 20 mm in size was vacuum mounted in low viscosity epoxy resin. On reaching full hardness, the samples were cut from the resin using a hack saw before being bisected using a Buehler precision diamond sectioning saw. Once re-sectioned the samples were mounted a second time in higher viscosity epoxy resin for grinding and polishing.

The mounted samples were prepared for optical microscopy using the following protocol (Table 3-2):

stage	*cloth*	*table revolution rate (rpm)*	*pressure per sample (lbs)*	*duration (mins)*	*wheel direction*
one	SiC (240 grit)	150	5	3	compliment ary
two	metlap 4 (9μm diamond)	125	5	8	contra
or	texmet (9 μm diamond)	125	5	5	contra
three	ultrapol (3 μm diamond)	160	5	8	compliment ary
or	texmet (3 μm diamond)	160	5	5	compliment ary
four *	texmet one (1μm diamond oil)	200	5	8	compliment ary
five	texmet one (colloidal silica)	125	5	6	compliment ary

* optional

Table 3-3 :- Polishing protocol for VPS HA coatings mounted in epoxy resin

Between each stage, the specimens were thoroughly washed using detergent and cold water then dried with acetone and hot air.

After final polishing, the specimens were examined using a Zeiss optical microscope in both reflective and differential interference contrast (DIC) modes. The specimens were photographed using a camera attached to the microscope.

3.9 Image Analysis

Three different morphological measurements were made on samples using an image analysis technique. The equipment used in this work incorporated an Optimas

image analysis system with Imaging Technology Inc image grabbing software, linked to a Zeiss universal microscope and computer control system. Using this system, crystallinity, porosity and coating thickness were determined.

Crystallinity levels in the coatings were determined by analysis of the x-ray diffraction traces obtained previously. For this work the region of the trace in the range 26 - 36 ° 2θ was used. In order to determine percentage crystallinity, image analysis was used to subtract the area of the amorphous hump portion of the trace from the total trace area to leave the crystalline portion of the trace. The ratio of the crystalline region to the total trace area gives the relative percentage crystallinity in the sample.

Percent porosity can be determined by capturing an image of the coating cross-section and differentiating between porosity and bulk coating by grey level. Grey level manipulation allows different regions of the coating, e.g. dark porosity zones, to be highlighted and their area recorded. The relative area of bulk coating to porosity in a section of the sample can then be used to calculate percentage porosity.

Thickness is also determined from a captured image of the coating cross-section. The image analysis system is calibrated using a graticule then the whole coating cross-section highlighted using grey level adjustment and image processing. Vertical lines are then superimposed over the selected region. The system calculates the length of these lines and by reference to the calibration graticule, gives their real length. The average of all these line lengths then gives the mean coating thickness for that section of sample.

In order to improve grey level contrast in samples prepared for image analysis, sectioned specimens were gold coated before investigation.

3.10 Scanning Electron Microscopy

The sectioned sample surfaces were investigated using a Joel 6310 Scanning Electron Microscope. Accelerating voltages between 12 and 20 kV were used in all cases. Samples were gold sputter coated before analysis and images captured using a camera attached to the microscope.

4. Results - As-Received Hydroxyapatite Coatings

4.1 HA Spray Powders

4.1.1 X-Ray Diffraction Traces

Figure 4-1 shows the x-ray diffraction traces for the vacuum plasma spray and detonation gun spray starting powders.

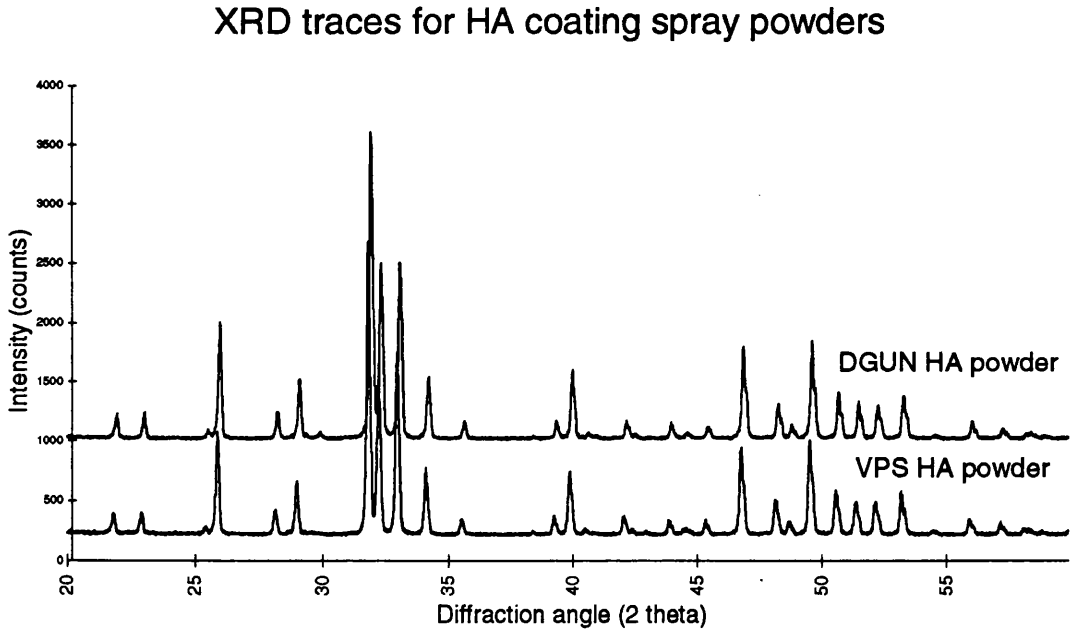

Figure 4-1 :- X-Ray traces for HA spray powders

4.1.2 Crystallinity Results

Table 4-1 presents a summary of the crystallinity data for the vacuum plasma spray and detonation gun spray starting powders

Sample	*No. of tests*	*Mean (%)*	*Standard Deviation*	*Variance*	*95% Confidence Limits*
VPS powder	10	80.4431	3.2129	10.3226	79.799 and 81.087
DGUN powder	10	77.3610	1.3779	1.8986	76.375 and 78.347

Table 4-1 :- Crystallinity results for HA spray powders

4.1.3 X-Ray Plane Analysis

Table 4-2 presents a summary of the x-ray plane analysis results for the vacuum plasma spray and detonation gun spray starting powders.

Sample	*Major Compound*	*Significant Compounds*	*Trace Compounds*
VPS powder	HA	β-TCP	$Ca_4O(PO_4)_2$, $Ca_2P_2O_7$
DGUN powder	HA	$Ca_4O(PO_4)_2$	β-TCP

Table 4-2 :- X-Ray plane analysis results for HA spray powders

4.1.4 Scanning Electron Microscopy

The VPS HA spray powder (Figure 4-2) consists of discrete particles with an angular appearance. The particles vary in dimensions and can be either regularly sided with an average particle size of 100 μm or planar, with sizes reaching over 200 μm in one dimension. The particles appear to be porous and although found to be highly crystalline by X-ray analysis, have a significant area of smooth, glassy material on the surface similar to the amorphous regions in the sprayed coatings. Small regular crystallites can also be observed on the powder surface at higher magnification. The angular nature of the particles and their irregular edges suggest they have been manufactured via a cleavage process.

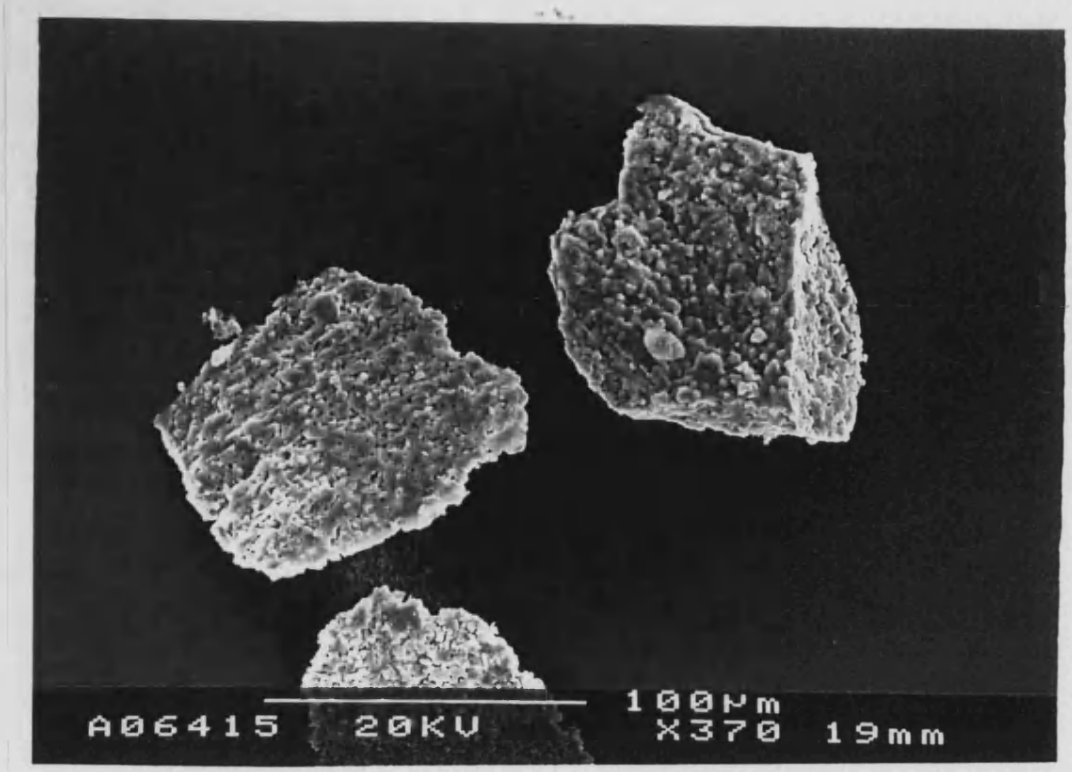

Figure 4-2 :- Scanning electron micrograph showing VPS HA spray powder

The DGUN HA spray powder (Figure 4-3) has a very different morphology to that of the VPS powder. These particles, although again apparently highly porous are much more spherical in nature and were probably manufactured by a spray drying route. Again, although X-ray diffraction studies reveal the particles to be highly crystalline in nature, their surfaces, like the VPS particles, show significant areas of smooth, glassy material. These powder spheres appear to be composed of agglomerates of smaller particles fused into single discrete balls. The particles are also much smaller in size than the material used in the manufacture of VPS coatings, being on average approximately 50 µm in diameter.

Figure 4-3 :- Scanning electron micrograph showing DGUN HA spray powder

4.2 VPS HA Coating As-received

4.2.1 X-Ray Diffraction Trace

Figure 4-4 shows the x-ray diffraction trace for the vacuum plasma sprayed hydroxyapatite coating in its as-received form.

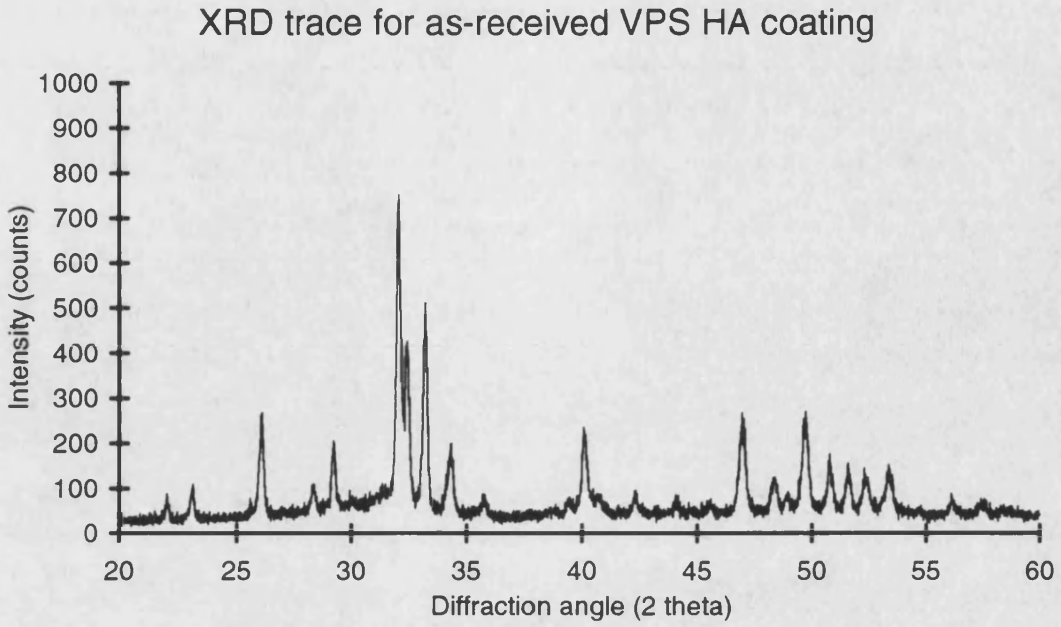

Figure 4-4 :- X-Ray diffraction trace for as-received VPS HA coating

4.2.2 Crystallinity Result

Table 4-3 presents a summary of the crystallinity results for the as-received vacuum plasma sprayed hydroxyapatite coating.

Sample	*No. of tests*	*Mean (%)*	*Standard Deviation*	*Variance*	*95% Confidence Limits*
as-received	10	60.3542	2.1942	4.8145	59.738 and 61.053

Table 4-3 :- Crystallinity results for as-received VPS HA Coating

4.2.3 X-Ray Plane Analysis

Table 4-4 presents a summary of the x-ray plane analysis for the as-received vacuum plasma sprayed hydroxyapatite coatings.

Sample	Major Compound	Significant Compounds	Trace Compounds
as-received	HA	-	α-TCP, β-TCP, $Ca_4O(PO_4)_2$, $Ca_2P_2O_7$

Table 4-4 :- X-Ray plane analysis results for as-received VPS HA coating

4.2.4 Optical Microscopy

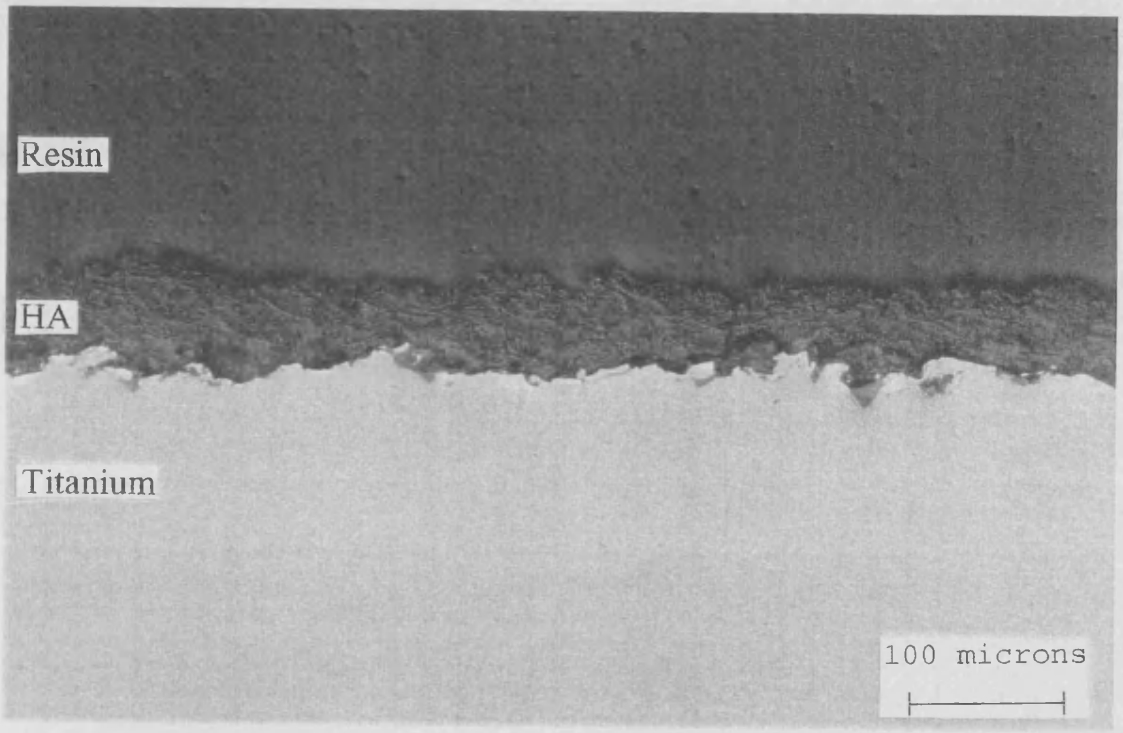

Figure 4-5 :- Optical micrograph showing cross-section through as-received VPS HA coating (DIC)

The polished cross-section through the as-received VPS HA coating (Figure 4-5) clearly reveals its lamella morphology. Each layer in the coating cross-section would correspond to one pass of the plasma torch over the substrate during manufacture of the coating. The polishing procedure imposes relief in the image probably differentiating between amorphous and crystalline phases. The coating appears to be dense, with good adherence to the substrate. The irregular cross-sectional thickness determined by image analysis is apparent and can be seen to reflect the irregular nature of the titanium substrate surface. The surface of the coating also seems to be irregular, an observation supported by surface roughness measurements. There is no evidence of cracking in the coating cross-section either between coating layers or through its thickness.

The substrate can be seen to consist of two phases, the bulk Ti-6Al-4V alloy and a fine pure titanium inter-layer, between 5 and 10 μm in thickness, lying directly between the coating and the substrate probably supplied as a bond layer. There are large amounts of alumina grit at the interface between the coating and the substrate, these particles being extremely angular in nature and approximately 10 μm in size. The alumina is a residue of the grit blasting stage of coating preparation and clearly indicates that the subsequent cleaning stages after grit blasting were inadequate to remove all the alumina.

4.2.5 Scanning Electron Microscopy

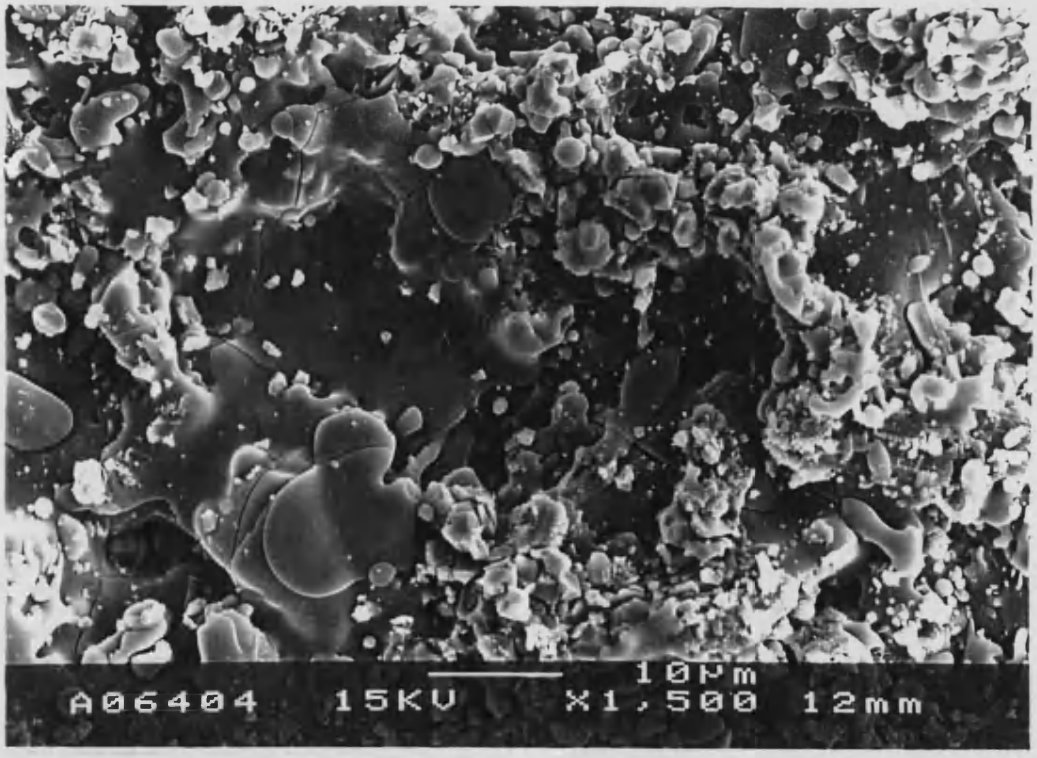

Figure 4-6 :- Scanning electron micrograph showing surface of as-received VPS HA coating

Scanning electron microscopy of the surface of the as-received VPS HA coating (Figure 4-6) again shows the irregular construction of the coating. The surface consists of flat glassy regions attributed to amorphous material and irregular regions considered to be composed of residual crystallites from the spray powder and agglomerated splat debris. Several large splats can be seen often over 50 μm in width indicating the large

extent to which the molten material disperses across the surface of the coating on impact during spraying. Several micro-cracks can also be seen on the sample surface. Such cracks are formed by the relief of residual stresses set up in the coating as a result of the difference in thermal expansion coefficients between the metallic substrate and the ceramic.

4.2.6 Coating Thickness Result

Table 4-5 presents a summary of the cross-sectional thickness results for the as-received vacuum plasma sprayed hydroxyapatite coating.

Sample	*No. of tests*	*Mean (μm)*	*Standard Deviation*	*Variance*	*95% Confidence Limits*
as-received	10	42.4840	11.6308	135.2751	41.501 and 42.484

Table 4-5 :- Cross-sectional thickness results for as-received VPS HA coating

4.2.7 Coating Porosity Result

Table 4-6 presents a summary of the cross-sectional porosity results for the as-received vacuum plasma sprayed hydroxyapatite coating.

Sample	*No. of tests*	*Mean (%)*	*Standard Deviation*	*Variance*	*95% Confidence Limits*
as-received	10	5.7490	1.4642	2.1440	4.702 and 6.797

Table 4-6 :- Cross-sectional porosity results for as-received VPS HA coating

4.2.8 Surface Roughness (Ra) Result

Table 4-7 presents the result of surface roughness analysis of the as-received vacuum plasma sprayed hydroxyapatite coating.

Sample	Scan Length (mm)	Ra (μm)	Rp (μm)	Rv (μm)	Rt (μm)
as-received	5.4904	5.1683	23.1762	15.9535	39.1297

Table 4-7 :- Surface roughness results for as-received VPS HA coating

4.2.9 Residual Stress Result

Table 4-8 presents the result of residual stress analysis of the as-received vacuum plasma sprayed hydroxyapatite coating.

Sample	d(c)	strain (c) %	E (Pa)	residual stress (MPa)
VPS HA powder	1.7209	0.003777	5.5^{09}	-
as-received	1.7144	0.004068	5.5^{09}	20.7740

Table 4-8 :- Residual stress results in 004 plane for as-received VPS HA coating

4.3 DGUN HA Coating As-received

4.3.1 X-Ray Diffraction Trace

Figure 4-7 presents a section from the x-ray diffraction trace for the as-received detonation gun sprayed hydroxyapatite coatings.

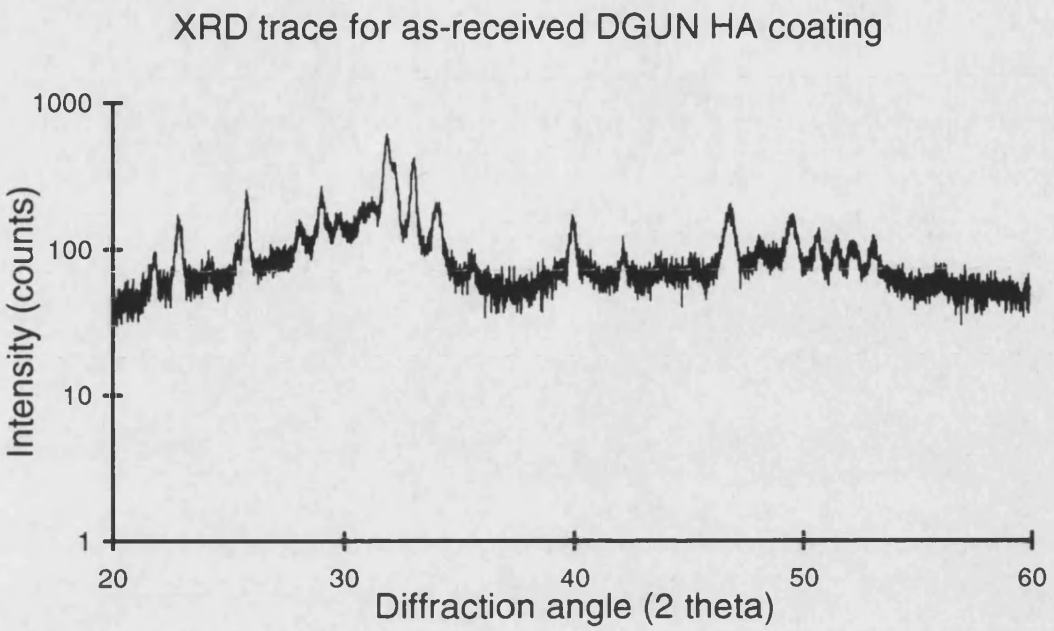

Figure 4-7 :- X-Ray diffraction trace for as-received DGUN HA coating

4.3.2 Crystallinity Result

Table 4-9 presents a summary of the crystallinity results for the as-received detonation gun sprayed hydroxyapatite coating.

Sample	*No. of tests*	*Mean (%)*	*Standard Deviation*	*Variance*	*95% Confidence Limits*
as-received	10	34.4223	0.9046	0.8183	33.775 and 35.069

Table 4-9 :- Crystallinity results for as-received DGUN HA Coating

4.3.3 X-Ray Plane Analysis

Table 4-10 presents a summary of the x-ray plane analysis for the as-received detonation gun sprayed hydroxyapatite coating.

Sample	*Major Compound*	*Significant Compounds*	*Trace Compounds*
as-received	HA	β-TCP, $Ca_4O(PO_4)_2$	α-TCP

Table 4-10 :- X-Ray plane analysis results for as-received DGUN HA coating

4.3.4 Optical Microscopy

The polished cross-section through the as-received DGUN HA coating (Figure 4-8) reveals it to have a features on a finer morphological scale to the VPS HA coating. The polishing procedure has again imposed relief on the different phases in the cross-section but in this material, the phases are not as discrete as in the VPS coating. This coating also does not appear to be as well bonded to the substrate as the VPS coating, a dark line between the substrate and coating suggesting that even in its as-received state there is some delamination. There are still large amounts of alumina grit at the interface between the substrate and the coating which, as before suggests inadequate cleaning after the grit blasting stage. In this material there is no evidence for a pure titanium bond layer between the titanium alloy and the alloy substrate itself.

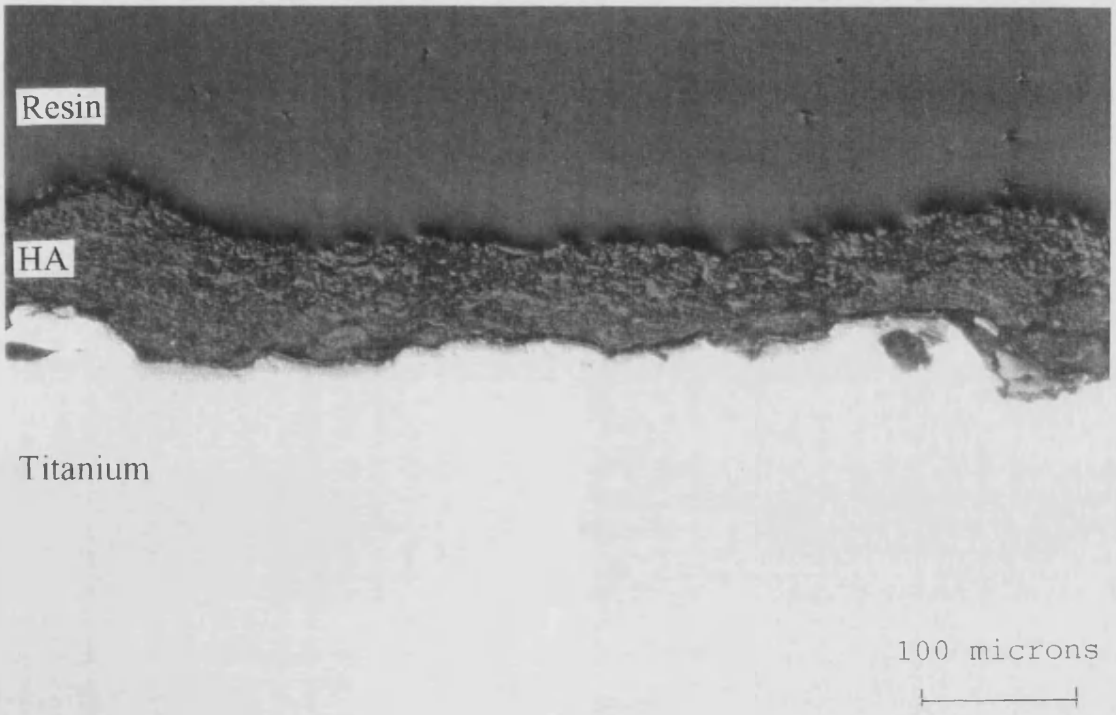

Figure 4-8 :- Optical micrograph showing cross-section through as-received DGUN HA coating (DIC)

Although the variation in cross-sectional thickness is the same for both the VPS and DGUN coatings, the DGUN material seems to have a much more regular thickness. The change in cross-section is much more gradual in these coatings rather than the more dramatic changes observed in VPS coatings. The titanium substrate for the DGUN coatings also has a much smoother appearance which has probably been carried through to the coating giving it a less irregular morphology.

4.3.5 Scanning Electron Microscopy

The surface of the DGUN HA coating (Figure 4-9) was again extremely irregular in nature but distinctly different from that of the VPS coating. Again the surface showed flat glassy regions and rougher agglomerated zones but the surface of the amorphous material was pitted and marked in a way not seen in the VPS HA. These glassy regions had the appearance of etched glass in some areas and large spherical holes in others approaching 10 μm in diameter. It is possible that these marks were caused by the surface tension of the amorphous material being insufficient to hold the phase together as it was smeared across the coating surface during spraying. These small pockets may also be a feature of the explosive nature of the detonation spraying process causing fragmentation of molten droplets. Again several micro-cracks can also be seen on the sample surface indicative of the relief of stresses in the coating.

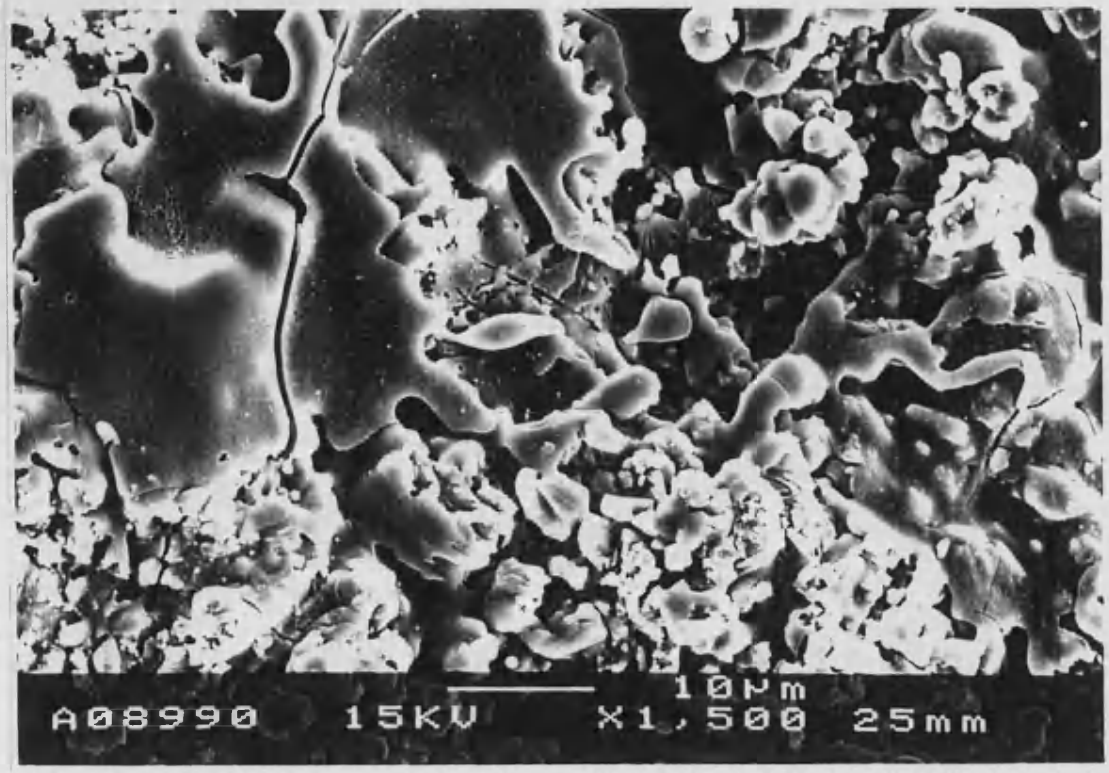

Figure 4-9 :- Scanning electron micrograph showing surface of as-received DGUN HA coating

4.3.6 Coating Thickness Result

Table 4-11 presents a summary of the cross-sectional thickness results for the as-received detonation gun sprayed hydroxyapatite coating.

Sample	*No. of tests*	*Mean (µm)*	*Standard Deviation*	*Variance*	*95% Confidence Limits*
as-received	10	70.0840	9.5690	91.5653	69.275 and 70.893

Table 4-11 :- Cross-sectional thickness results for as-received DGUN HA coating

4.3.7 Coating Porosity Result

Table 4-12 presents a summary of the cross-sectional porosity results for the as-received detonation gun sprayed hydroxyapatite coating.

Sample	No. of tests	Mean (%)	Standard Deviation	Variance	95% Confidence Limits
as-received	10	1.4485	0.7381	0.5448	1.103 and 1.794

Table 4-12 :- Cross-sectional porosity results for as-received DGUN HA coating

4.3.8 Surface Roughness (Ra) Result

Table 4-13 presents the result of surface roughness analysis of the as-received detonation gun sprayed hydroxyapatite coating.

Sample	Scan Length (mm)	Ra (μm)	Rp (μm)	Rv (μm)	Rt (μm)
as-received	11.3739	5.5294	27.5104	19.4195	46.9298

Table 4-13 :- Surface roughness results for as-received DGUN HA coating

4.3.9 Residual Stress Result

Table 4-14 presents the result of residual stress analysis of the as-received detonation gun sprayed hydroxyapatite coating.

Sample	d(c)	strain (c) %	E (Pa)	residual stress (MPa)
DGUN HA powder	1.7172	0.003203	5.5^{09}	-
as-received	1.7262	0.005241	5.5^{09}	28.8260

Table 4-14 :- Residual stress results in 004 plane for as-received DGUN HA coatings

5. Results - Unloaded Aged Hydroxyapatite Coatings

5.1 VPS HA Coatings Aged Unloaded pH 7.2

5.1.1 X-Ray Diffraction Traces

Figure 5-1 presents sections from the x-ray diffraction traces for the vacuum plasma sprayed hydroxyapatite coatings aged for various time periods in Ringer's solution buffered to pH 7.2.

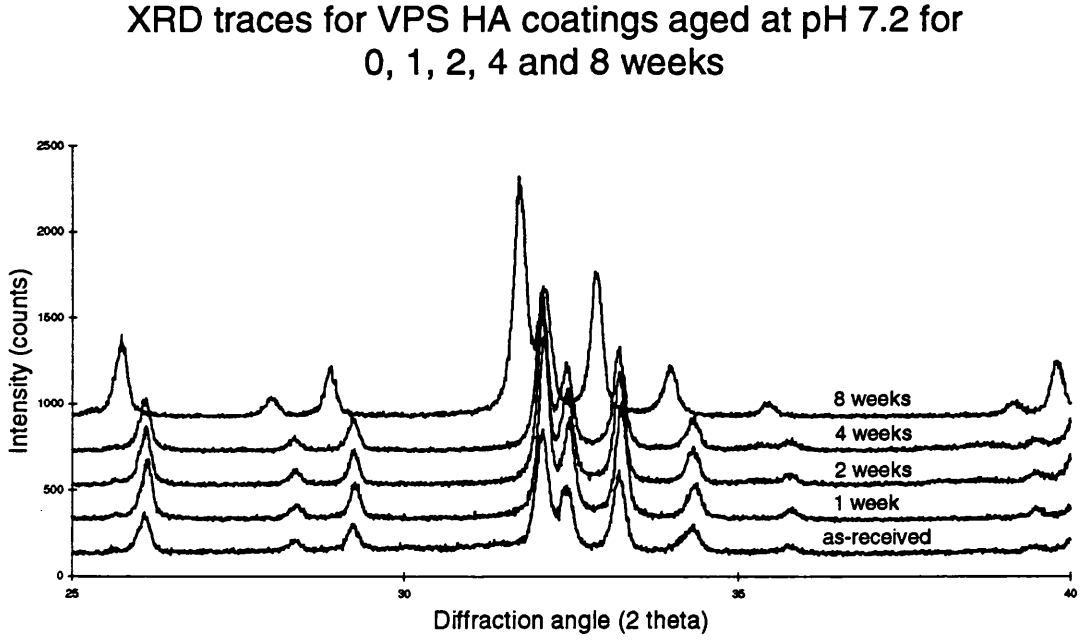

Figure 5-1 :- Amorphous hump region from X-Ray diffraction traces of VPS HA coatings aged unloaded at pH 7.2

5.1.2 Crystallinity Results

Table 5-1 presents a summary of the crystallinity results for vacuum plasma sprayed hydroxyapatite coatings aged for various time periods in Ringer's solution buffered to pH 7.2.

Sample	*No. of tests*	*Mean (%)*	*Standard Deviation*	*Variance*	*95% Confidence Limits*
as-received	10	60.3542	2.1942	4.8145	59.738 and 61.053
pH 7.2 x 1	10	66.4980	3.7892	14.3581	65.857 and 67.139
pH 7.2 x 2	10	67.6779	4.4999	20.2499	67.041 and 68.315
pH 7.2 x 4	10	65.8775	4.3186	18.6502	65.240 and 66.515
pH 7.2 x 8	10	60.5611	3.0629	9.3815	59.915 and 61.207

Table 5-1 :- Crystallinity results for VPS HA coatings aged unloaded pH 7.2

Table 5-2 presents the significance test results for the crystallinity data from vacuum plasma sprayed coatings aged in Ringer's solution buffered to pH 7.2. The data was tested using a Student T-test at the 5 % significance level.

crystallinity	*as-received*	*1 week*	*2 weeks*	*4 weeks*	*8 weeks*
as-received		✓	✓	✓	✖
1 week	✓		✖		
2 weeks	✓	✖		✖	
4 weeks	✓		✖		✓
8 weeks	✖			✓	

Table 5-2 :- Significant test results for VPS HA coatings aged unloaded pH 7.2

✓ = significantly different

✖ = not significantly different

= not tested

Therefore, a significant change in crystallinity was found between the as-received coating and the aged coatings, except in the case of the coating aged for eight weeks.

With this same exception, there was found to no significant change in crystallinity between ageing times.

5.1.3 X-Ray Plane Analysis

Table 5-3 presents a summary of the x-ray plane analysis results for the vacuum plasma sprayed hydroxyapatite coatings aged for various time periods in Ringer's solution buffered to pH 7.2.

Sample	*Major Compound*	*Significant Compounds*	*Trace Compounds*
as-received	HA	-	α-TCP, β-TCP, $Ca_4O(PO_4)_2$, $Ca_2P_2O_7$
pH 7.2 x 1	HA	-	β-TCP, $Ca_4O(PO_4)_2$, $Ca_2P_2O_7$
pH 7.2 x 2	HA	-	α-TCP, β-TCP, $Ca_4O(PO_4)_2$, $Ca_2P_2O_7$
pH 7.2 x 4	HA	-	α-TCP, β-TCP, $Ca_4O(PO_4)_2$, $Ca_2P_2O_7$
pH 7.2 x 8	HA	β-TCP	α-TCP, $Ca_4O(PO_4)_2$,

Table 5-3 :- X-Ray plane analysis results for VPS HA coatings aged unloaded pH 7.2

5.1.4 Optical Microscopy

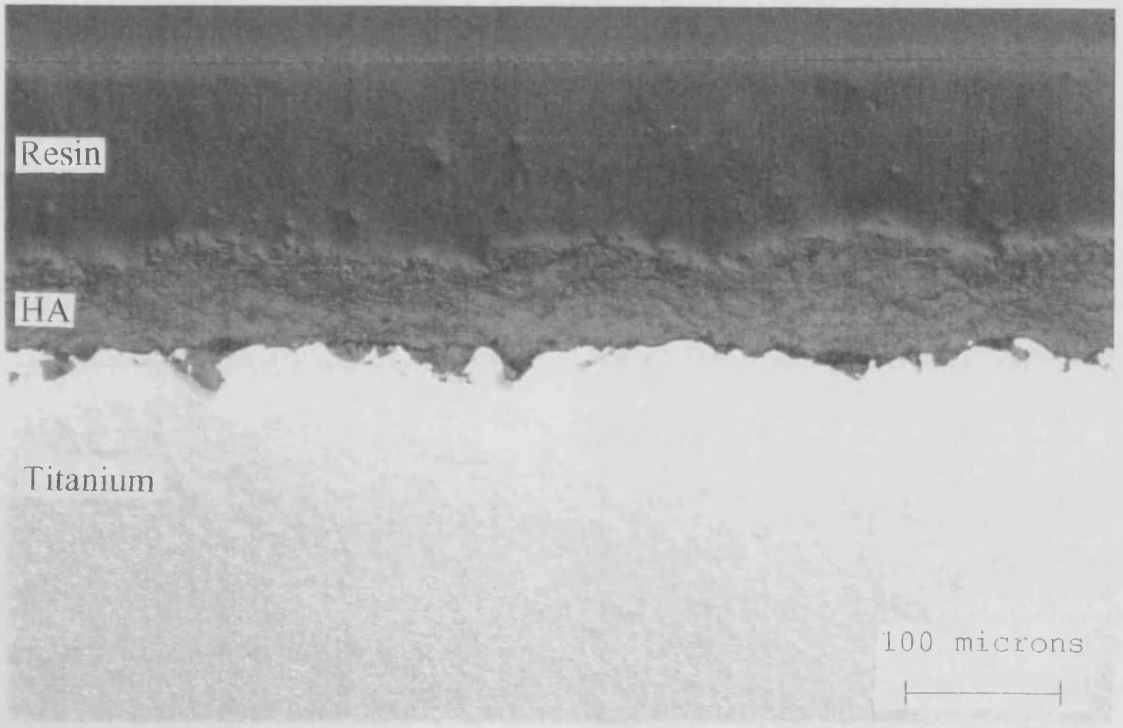

Figure 5-2 :- Optical micrograph showing cross-section through VPS HA coating aged unloaded pH 7.2 x 1 week

The polished cross-section through the coating aged for one week in Ringer's solution at pH 7.2 appears to be fairly similar to the as-received coating (Figure 5-2). The distinctive difference between phases resulting from differential polishing rates is less marked in this coating although this may be an artefact of polishing. The lamella structure to the coating is still visible as is the interfacial pure titanium layer in the substrate. Again there is no evidence of cracking through the thickness of the coating nor between layers but there is a darker layer between the coating and the substrate which may be an early indication of delamination. The coating's general adherence to the substrate however still appears to be good. Overall there is little or no discernible difference between this coating and the as-received coating.

Coatings aged for two and four weeks (not shown here) have a very similar appearance. There is no evidence for a change in the cross-sectional structure of the coatings resulting from their *in-vitro* ageing. If any dissolution of the coating is occurring it is not discernible in the cross-sectional view.

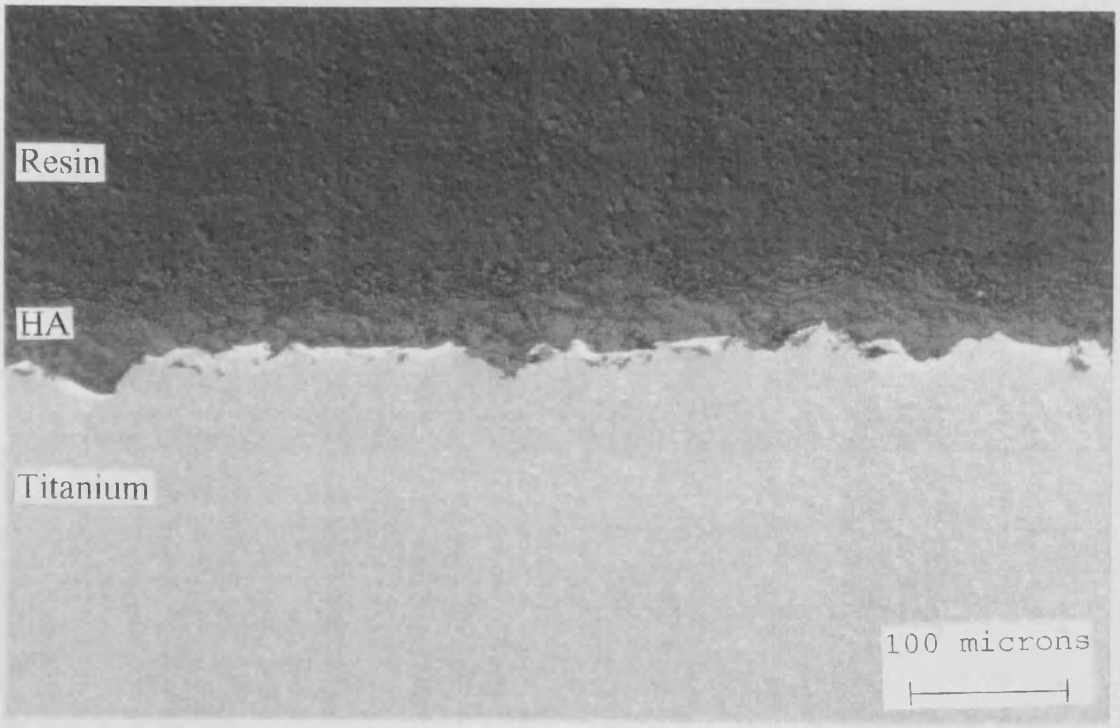

Figure 5-3 :- Optical micrograph showing cross-section through VPS HA coating aged unloaded pH 7.2 x 8 weeks

Again, the morphology of the polished cross-section through this sample aged for eight weeks at pH 7.2 (Figure 5-3) seems to be very similar to that of the as-received sample. The sprayed layers are still discernible. There is no visible change in the coating surface roughness when viewed in this way and adherence to the substrate still appears to be good despite possible indications of the early signs of delamination in coatings aged for shorter durations. There are still no signs of cracking either along the coating / substrate interface or through the coating thickness.

The effect of the ageing medium on the cross-sectional appearance of the VPS HA coatings therefore appears to be negligible, even after a duration of eight weeks. This implies that the coatings on the whole remain stable under these imposed conditions.

5.1.5 Scanning Electron Microscopy

Figure 5-4 :- Scanning electron micrograph showing surface of VPS HA coating aged unloaded pH 7.2 x 1 week

After ageing in Ringer's solution for one week at pH 7.2, the appearance of the surface of the VPS HA coating has changed (Figure 5-4). There appears to be have been an etching of the amorphous glassy phase on the surface which has left it pitted. This etching leaves the coating surface looking much rougher on a microscopic level. There seems to be a finer structure now visible in the coating surface which may have been revealed by dissolution of the smoother amorphous material previously surrounding it. There is a higher proportion of angular debris. Where the glassy material remains it is possible to discern undulations below its surface, giving the appearance of a thinning of the layer to reveal the shape of the material below. There are still micro-cracks crossing the sample surface although these do not appear to have altered in shape or frequency.

The surfaces of samples aged for two and four weeks (not shown here) also show signs of this same alteration in appearance over the as-received surface. Still there is a large amount of pitting of the smoother phase in the surface and much greater evidence of regular crystalline particles on the surface. These particles are discrete and apparently not well adhered to each other suggesting that they have been left behind after the dissolution of amorphous material from around them. Again the surface appears to be much rougher on a micro-scale and there is some evidence to suggest that the surface modification process is accelerated with prolonged exposure to the *in-vitro* medium.

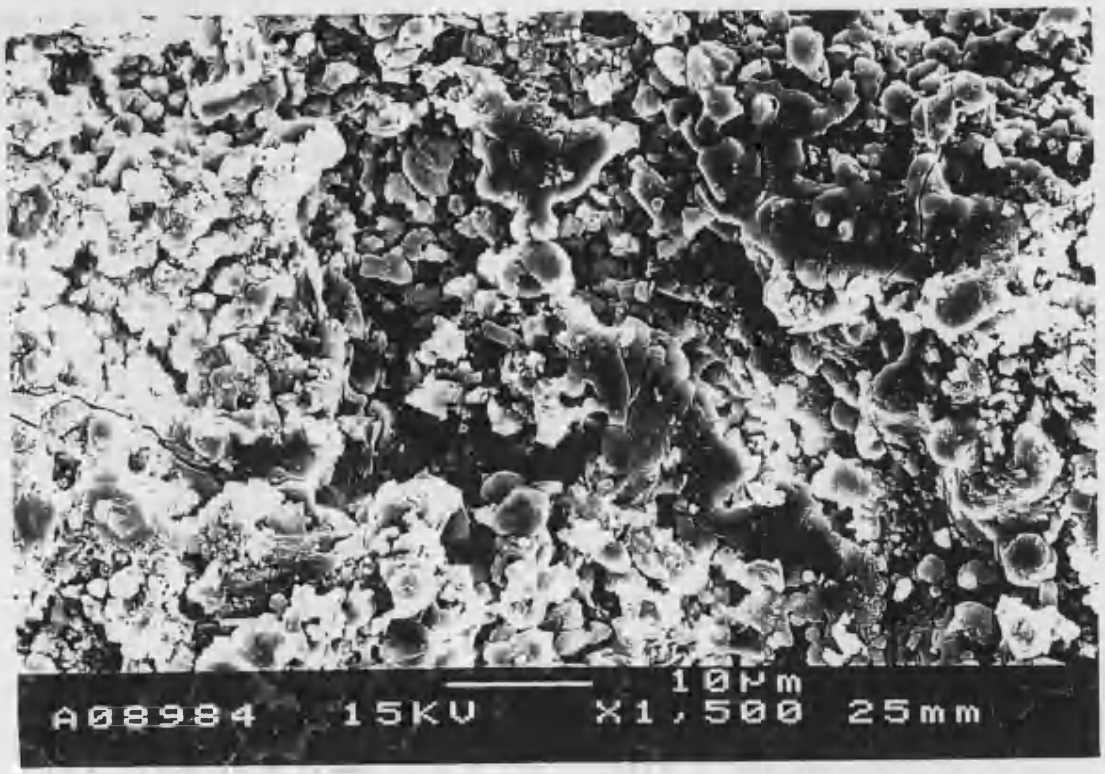

Figure 5-5 :- Scanning electron micrograph showing surface of VPS HA coating aged unloaded pH 7.2 x 8 weeks

The surface of the sample aged for eight weeks at pH 7.2 again is markedly different from that of the as-received sample (Figure 5-5). It is not however considerably different from the coatings which have been aged for shorter durations. The glassy material has in great proportion been removed from the surface by dissolution again leading to an apparent increase in roughness. Any remaining amorphous material is badly damaged and has a lace-like appearance in some areas or an obvious thinning in others. Looking at the overall appearance of the surface the dissolution effect seems to have been most severe in the case of the coatings aged for the longest durations.

5.1.6 Coating Thickness Results

Table 5-4 presents a summary of the cross-sectional thickness results for the vacuum plasma sprayed hydroxyapatite coatings aged for various time periods in Ringer's solution buffered to pH 7.2.

Sample	*No. of tests*	*Mean (μm)*	*Standard Deviation*	*Variance*	*95% Confidence Limits*
as-received	10	42.4840	11.6308	135.2751	41.501 and 42.484
pH 7.2 x 1	10	64.3384	10.3595	107.3197	63.663 and 64.538
pH 7.2 x 2	10	37.4081	10.4224	108.6256	36.527 and 37.408
pH 7.2 x 4	10	34.5115	10.3665	107.4652	33.627 and 34.512
pH 7.2 x 8	10	44.0419	10.3800	107.7446	43.129 and 44.015

Table 5-4 :- Cross-sectional thickness results for VPS HA coatings aged unloaded pH 7.2

Table 5-5 presents the significance test results for the cross-sectional thickness data from vacuum plasma sprayed coatings aged in Ringer's solution buffered to pH 7.2. The data was tested using a Student T-test at the 5 % significance level.

thickness	*as-received*	*1 week*	*2 weeks*	*4 weeks*	*8 weeks*
as-received		✓	✖	✖	✖
1 week	✓		✖		
2 weeks	✖	✖		✖	
4 weeks	✖		✖		✖
8 weeks	✖			✖	

Table 5-5 :- Significant test results for VPS HA coatings aged unloaded pH 7.2

✓ = significantly different

✖ = not significantly different

= not tested

Therefore, there was only found to be a significant difference in cross-sectional coating thickness in the case of the coating aged at pH 7.2 for one week. At all other times there was found to be no significant difference between the as-received coating and the coatings aged at pH 7.2 nor between ageing times.

5.1.7 Coating Porosity Results

Table 5-6 presents a summary of the cross-sectional porosity results for the vacuum plasma sprayed hydroxyapatite coatings aged for various time periods in Ringer's solution buffered to pH 7.2.

Sample	*No. of tests*	*Mean (%)*	*Standard Deviation*	*Variance*	*95% Confidence Limits*
as-received	10	5.749	1.464	2.144	4.702 and 6.797
pH 7.2 x 1	10	1.345	0.669	0.447	0.869 and 1.853
pH 7.2 x 2	10	0.527	0.478	0.229	0.185 and 0.869
pH 7.2 x 4	10	1.712	0.630	0.397	1.261 and 2.163
pH 7.2 x 8	10	1.151	0.488	0.238	0.802 and 1.500

Table 5-6 :- Cross-sectional porosity results for VPS HA coatings aged unloaded pH 7.2

Table 5-7 presents the significance test results for the cross-sectional porosity data from vacuum plasma sprayed coatings aged in Ringer's solution buffered to pH 7.2. The data was tested using a Student T-test at the 5 % significance level.

porosity	*as-received*	*1 week*	*2 weeks*	*4 weeks*	*8 weeks*
as-received		✓	✓	✓	✓
1 week	✓		✓		
2 weeks	✓	✓		✓	
4 weeks	✓		✓		✓
8 weeks	✓			✓	

Table 5-7 :- Significant test results for VPS HA coatings aged unloaded pH 7.2

✓ = significantly different

✖ = not significantly different

= not tested

Therefore, there was found to be a significant difference between the porosities of the aged coatings and the as-received coating, and also between coatings aged for different time periods.

5.1.8 Surface Roughness (Ra) Results

Table 5-8 presents a summary of the surface roughness analysis for vacuum plasma sprayed hydroxyapatite coatings aged for various time periods in Ringer's solution buffered to pH 7.2.

Sample	*Scan Length (mm)*	*Ra (μm)*	*Rp (μm)*	*Rv (μm)*	*Rt (μm)*
as-received	5.4904	5.1683	23.1762	15.9535	39.1297
pH 7.2 x 1	5.4883	5.8814	17.7633	18.2286	35.9918
pH 7.2 x 2	5.4836	6.9490	22.9282	24.3110	47.2391
pH 7.2 x 4	5.4284	7.3086	28.1818	19.7131	47.8949
pH 7.2 x 8	5.5622	7.0368	23.9010	22.1417	46.0427

Table 5-8 :- Surface roughness results for VPS HA coatings aged unloaded pH 7.2

5.1.9 Residual Stress Results

Table 5-9 presents a summary of the residual stress analysis of the vacuum plasma sprayed hydroxyapatite coatings aged for various time periods in Ringer's solution buffered to pH 7.2.

Sample	*d(c)*	*strain (c) %*	*E (Pa)*	*residual stress (MPa)*
VPS HA powder	1.7209	0.003777	5.5^{09}	-
as-received	1.7144	0.004068	5.5^{09}	20.7740
pH 7.2 x 1	1.7139	0.004068	5.5^{09}	22.3720
pH 7.2 x 2	1.7139	0.004068	5.5^{09}	22.3720
pH 7.2 x 4	1.7144	0.003777	5.5^{09}	20.7740
pH 7.2 x 8	1.7235	0.001511	5.5^{09}	8.3096

Table 5-9 :- Residual stress results in 004 plane for VPS HA coatings aged unloaded pH 7.2

5.2 DGUN HA Coatings Aged Unloaded pH 7.2

5.2.1 X-Ray Diffraction Traces

Figure 5-6 presents sections from the x-ray diffraction traces for the detonation gun sprayed hydroxyapatite coatings aged for various time periods in Ringer's solution buffered to pH 7.2.

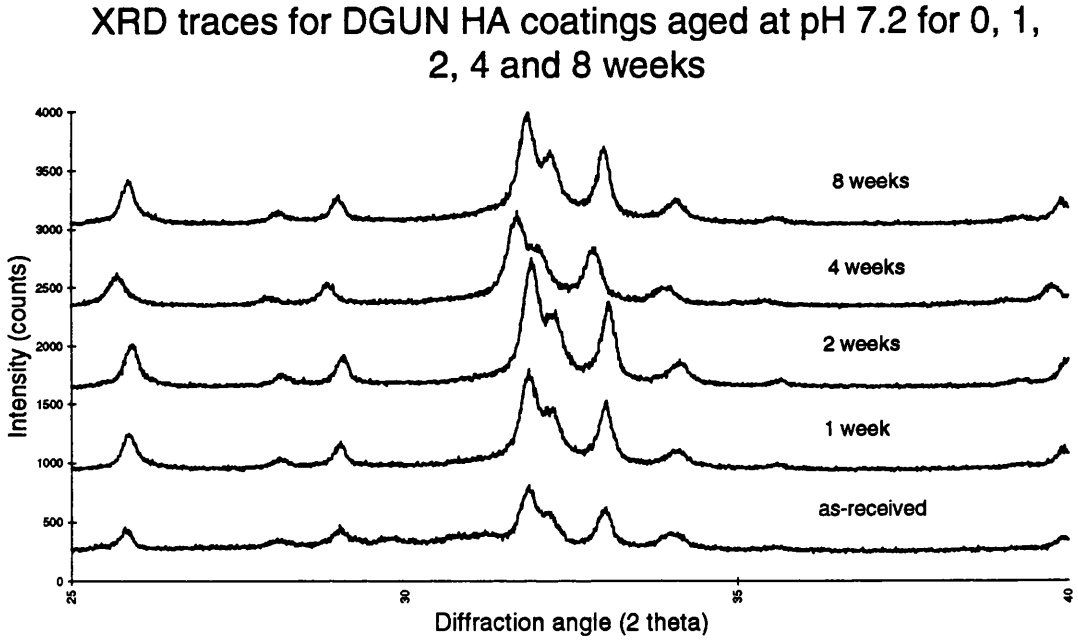

Figure 5-6 :- Amorphous hump region from X-Ray diffraction traces of DGUN HA coatings aged unloaded at pH 7.2

5.2.2 Crystallinity Results

Table 5-10 presents a summary of the crystallinity results for the detonation gun sprayed hydroxyapatite coatings aged for various time periods in Ringer's solution buffered to pH 7.2.

Sample	*No. of tests*	*Mean (%)*	*Standard Deviation*	*Variance*	*95% Confidence Limits*
as-received	10	34.4223	0.9043	0.8183	33.7752 and 35.0694
pH 7.2 x 1	10	43.7842	1.3445	1.8076	42.8224 and 44.7460
pH 7.2 x 2	10	48.8118	1.2642	1.5983	47.9074 and 49.7162
pH 7.2 x 4	10	44.3443	1.3181	1.7374	43.4014 and 45.2872
pH 7.2 x 8	10	44.2908	1.1208	1.2562	43.4890 and 45.0926

Table 5-10 :- Crystallinity results for DGUN HA coatings aged unloaded pH 7.2

Table 5-11 presents the significance test results for the crystallinity data from detonation gun sprayed coatings aged in Ringer's solution buffered to pH 7.2. The data was tested using a Student T-test at the 5 % significance level.

crystallinity	*as-received*	*1 week*	*2 weeks*	*4 weeks*	*8 weeks*
as-received		✓	✓	✓	✓
1 week	✓		✓		
2 weeks	✓	✓		✓	
4 weeks	✓		✓		✖
8 weeks	✓			✖	

Table 5-11 :- Significant test results for DGUN HA coatings aged unloaded pH 7.2

✓ = significantly different

✖ = not significantly different

= not tested

Therefore, it was found that there was a significant change in crystallinity between the as-received coating and the aged coatings. There was also found to be a significant difference between the crystallinities of coatings aged at different time periods except between coatings aged for four and eight weeks.

5.2.3 X-Ray Plane Analysis

Table 5-12 presents a summary of the x-ray plane analysis for the detonation gun sprayed hydroxyapatite coatings aged for various time periods in Ringer's solution buffered to pH 7.2.

Sample	*Major Compound*	*Significant Compounds*	*Trace Compounds*
as-received	HA	β-TCP, $Ca_4O(PO_4)_2$	α-TCP
pH 7.2 x 1	HA	-	β-TCP
pH 7.2 x 2	HA	-	β-TCP, α-TCP, $Ca_4O(PO_4)_2$
pH 7.2 x 4	HA	-	β-TCP, α-TCP, $Ca_4O(PO_4)_2$
pH 7.2 x 8	HA	-	β-TCP, α-TCP, $Ca_4O(PO_4)_2$

Table 5-12 :- X-Ray plane analysis results for DGUN HA coatings aged unloaded pH 7.2

5.2.4 Optical Microscopy

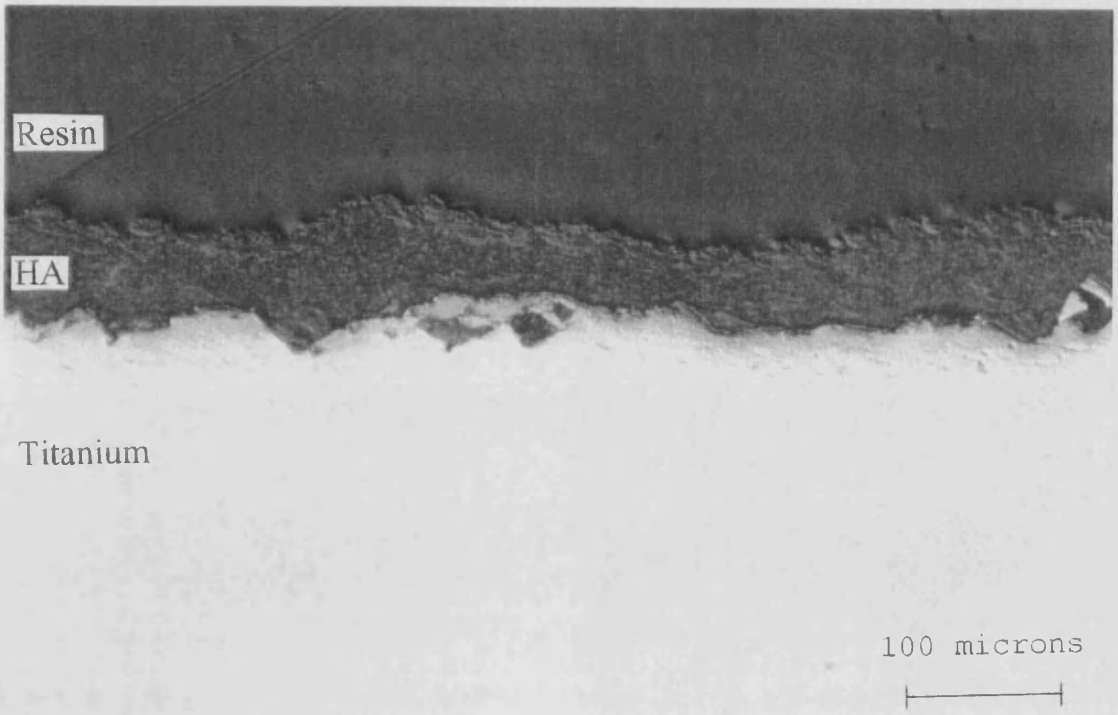

Figure 5-7 :- Optical micrograph showing cross-section through DGUN HA coating aged unloaded pH 7.2 x 1 week

The DGUN HA coating aged in Ringer's solution for one week (Figure 5-7) appears identical to the as-received coating when viewed by optical microscopy in all respects except one. There appears to be a modified layer, approximately 10 μm thick running along the surface of the coating. The other parts of the coating appear to be unaffected by the ageing medium. The coating showing no apparent change in thickness or porosity and still seeming to be well adhered to the substrate although a dark line is apparent across the whole coating cross-section. There is no evidence of micro-cracking either between lamella layers in the body of the coating or through its thickness.

DGUN HA coating aged in Ringer's solution for two weeks (not shown) appears to be very dense and shows no evidence for the dark line at the interface between the coating and the substrate. There is also no evidence for a surface modified layer in this coating. However, the coating aged for four weeks (not shown) again shows evidence of this surface layer as well as the dark region at the interface and in fact has an appearance much more closely resembling that of the one week aged sample that the two week aged one. Both coatings however show no apparent increase in porosity or change in thickness as a result of ageing *in-vitro*.

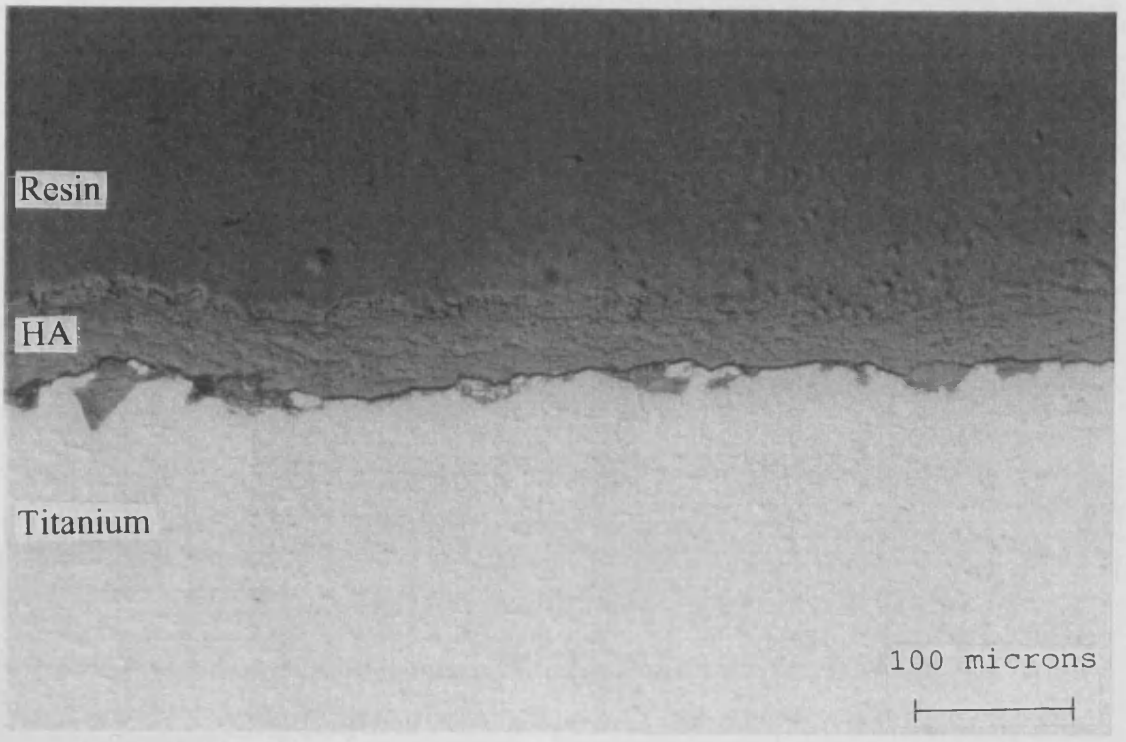

Figure 5-8 :- Optical micrograph showing cross-section through DGUN HA coating aged unloaded pH 7.2 x 8 weeks

The modified surface layer is again no longer visible in DGUN coatings aged in Ringer's solution for eight weeks (Figure 5-8). The dark region at the interface between the coating and the substrate also appears to be more apparent and seems to be more like a delamination zone than in coatings aged for shorter durations. Despite this region however the coating still seems to be well adhered to the substrate although this possible delamination seems to be fairly continuous along the entire cross-section of the sample.

5.2.5 Scanning Electron Microscopy

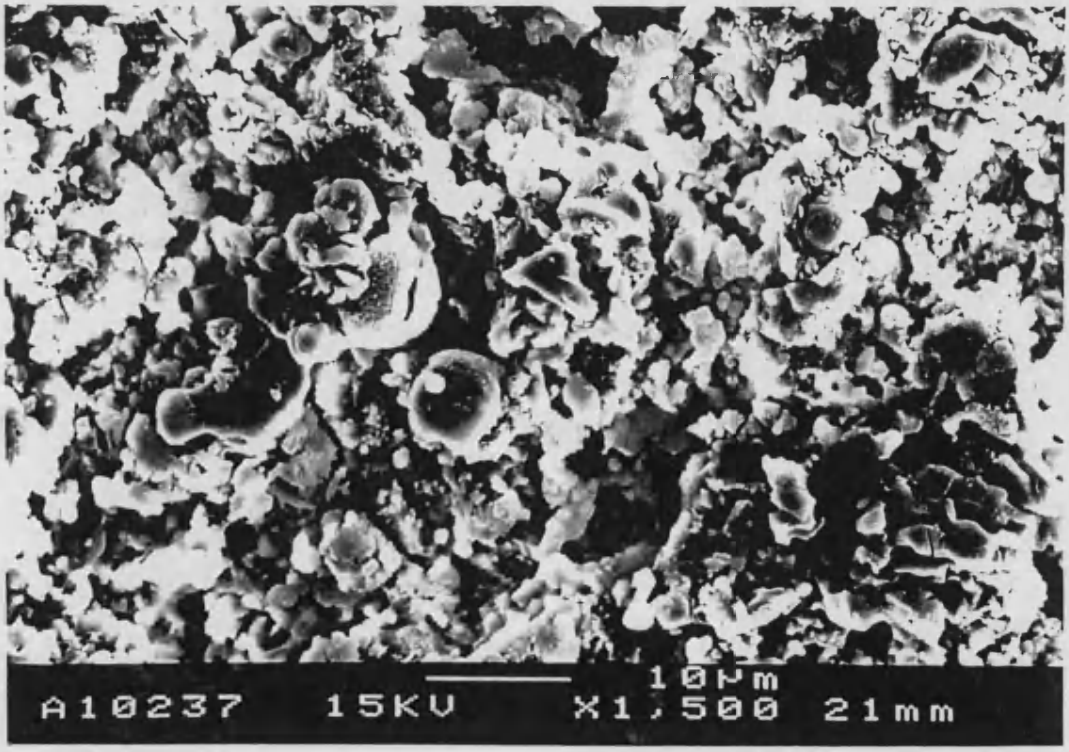

Figure 5-9 :- Scanning electron micrograph showing surface of DGUN HA coating aged unloaded pH 7.2 x 1 week

Even after ageing for only one week at pH 7.2, the DGUN HA coating has a surface which is considerably different from that of the as-received coating (Figure 5-9). There is little remaining evidence of the smooth glassy splats clearly visible in the as-received surface, any remaining amorphous material appearing to be pocket or etched by the ageing medium. It seems that most of the glassy phase in the surface layers of the coating has been dissolved *in-vitro* to reveal the agglomerated layers below. It is possible

to look further into the coating itself, there is apparently greater depth to visible porosity in the surface and the whole coating seems to have a much higher surface roughness. Micro-cracks running across the sample surface are far less visible in the sample aged for one week but can still be observed although their path is less clear.

A similar morphology can be seen in coatings aged for two and four weeks at pH 7.2 (not shown).There does not seem to have been an exacerbation of effects produced in the first week of exposure to the *in-vitro* medium. There is still little evidence of the original amorphous material visible in the as-received coating, any remaining flat regions having an etched or lace-like morphology over their surfaces. Again, in these coatings, micro-cracks can still be seen running over the surface although, as before, their path is not as well defined as in the as-received coating.

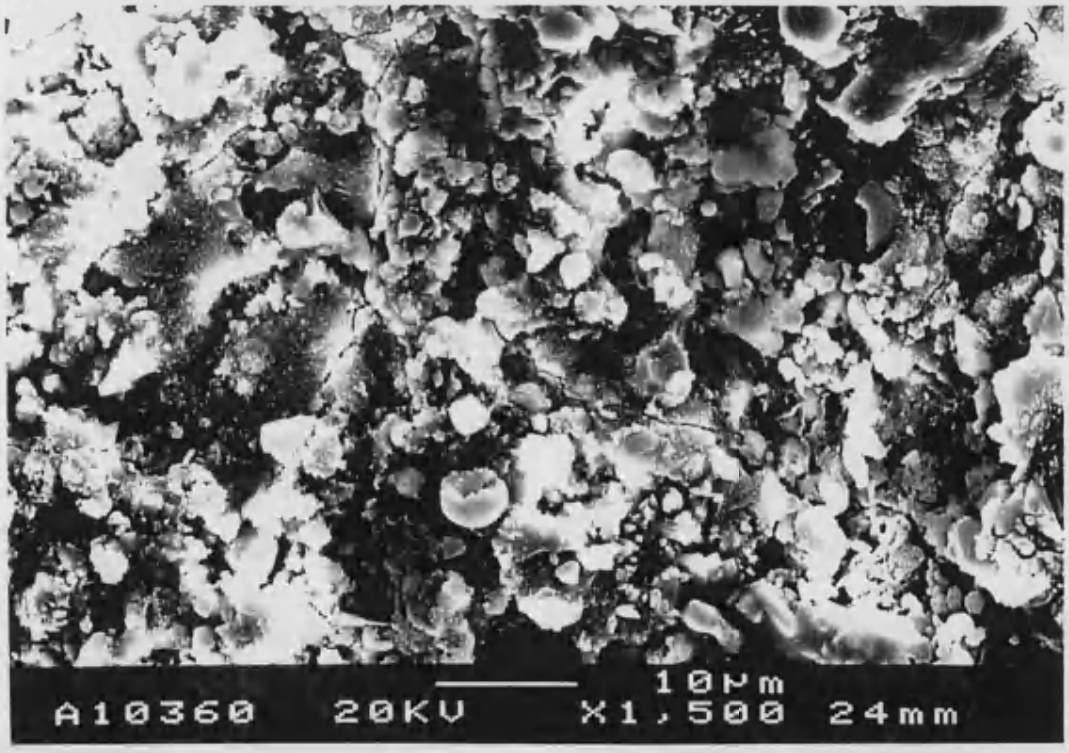

Figure 5-10 :- Scanning electron micrograph showing surface of DGUN HA coating aged unloaded pH 7.2 x8 weeks

The DGUN HA coatings aged for 8 weeks at pH 7.2 again show the dramatic influence of the ageing medium on the morphology of the coating surface (Figure 5-10).

These coatings however have an apparently less rough surface when compared to the samples aged for lesser periods. There is more evidence of amorphous regions in these surfaces although these are extremely pitted, showing signs of the effects of dissolution. It is suggested that in these coatings which have been aged for the longer duration, the layers observed in other coatings have become so fragile due to loss of the amorphous phase that they have broken away from the surface revealing fresh layers below. It is this newly exposed layer that is seen in the coatings aged for eight weeks. It can be suggested that the amorphous material acts as a binder phase holding the agglomerated, crystalline particles in place.

5.2.6 Coating Thickness Results

Table 5-13 presents a summary of the cross-sectional thickness results for the detonation gun sprayed hydroxyapatite coatings aged for various time periods in Ringer's solution buffered to pH 7.2.

Sample	*No. of tests*	*Mean (μm)*	*Standard Deviation*	*Variance*	*95% Confidence Limits*
as-received	10	70.0840	9.5690	91.5653	69.275 and 70.893
pH 7.2 x 1	10	54.3889	11.3551	128.9372	53.429 and 55.349
pH 7.2 x 2	10	67.3853	10.0552	101.1064	66.535 and 68.235
pH 7.2 x 4	10	51.1031	8.7133	75.9223	50.367 and 51.840
pH 7.2 x 8	10	51.1856	8.2468	68.0098	50.489 and 51.883

Table 5-13 :- Cross-sectional thickness results for DGUN HA coatings aged unloaded pH 7.2

Table 5-14 presents the significance test results for the cross-sectional thickness data from detonation gun sprayed coatings aged in Ringer's solution buffered to pH 7.2. The data was tested using a Student T-test at the 5 % significance level.

thickness	as-received	1 week	2 weeks	4 weeks	8 weeks
as-received		✓	✖	✓	✓
1 week	✓		✓		
2 weeks	✖	✓		✓	
4 weeks	✓		✓		✖
8 weeks	✓			✖	

Table 5-14 :- Significant test results for DGUN HA coatings aged unloaded pH 7.2

✓ = significantly different

✖ = not significantly different

= not tested

Therefore, there was found to be a variability in the significance of changes in thickness found for DGUN coatings aged under no load at pH 7.2. This result was not unexpected since the standard deviation in individual thickness results was so high.

5.2.7 Coating Porosity Results

Table 5-15 presents a summary of the cross-sectional porosity results for the detonation gun sprayed hydroxyapatite coatings aged for various time periods in Ringer's solution buffered to pH 7.2.

Sample	No. of tests	Mean (%)	Standard Deviation	Variance	95% Confidence Limits
as-received	10	1.4485	0.7381	0.5448	1.103 and 1.794
pH 7.2 x 1	10	2.9865	0.9681	0.9371	2.533 and 3.496
pH 7.2 x 2	10	3.0422	2.5329	6.4158	1.857 and 4.228
pH 7.2 x 4	10	2.0629	1.0608	1.1254	1.566 and 2.559
pH 7.2 x 8	10	5.3061	1.4931	2.2293	4.607 and 6.005

Table 5-15 :- Cross-sectional porosity results for DGUN HA coatings aged unloaded pH 7.2

Table 5-16 presents the significance test results for the cross-sectional porosity data from detonation gun sprayed coatings aged in Ringer's solution buffered to pH 7.2. The data was tested using a Student T-test at the 5 % significance level.

porosity	*as-received*	*1 week*	*2 weeks*	*4 weeks*	*8 weeks*
as-received		✓	✓	✖	✓
1 week	✓		✖		
2 weeks	✓	✖		✖	
4 weeks	✖		✖		✓
8 weeks	✓			✓	

Table 5-16 :- Significant test results for DGUN HA coatings aged unloaded pH 7.2

✓ = significantly different

✖ = not significantly different

= not tested

Therefore, there was found to a significant difference between the porosity of the as-received coating and the aged coatings except in the case of the coating aged for four weeks. There was found to be no significant difference in the porosities of coatings aged for different time periods except in the case of coatings aged for four and eight weeks.

5.2.8 Surface Roughness (Ra) Results

Table 5-17 presents a summary of the surface roughness results for the detonation gun sprayed hydroxyapatite coatings aged for various time periods in Ringer's solution buffered to pH 7.2.

Sample	Scan Length (mm)	Ra (μm)	Rp (μm)	Rv (μm)	Rt (μm)
as-received	11.3739	5.5294	27.5104	19.4195	46.9298
pH 7.2 x 1	11.2502	6.0100	35.5934	16.2137	51.8071
pH 7.2 x 2	11.3924	6.6902	36.7447	19.9817	56.7264
pH 7.2 x 4	11.4004	4.9018	33.9557	21.0785	55.0342
pH 7.2 x 8	11.3468	5.3168	26.1848	19.7214	45.9063

Table 5-17 :- Surface roughness results for DGUN HA coatings aged unloaded pH 7.2

5.2.9 Residual Stress Results

Table 5-18 presents a summary of the residual stress analysis for the detonation gun sprayed hydroxyapatite coatings aged for various time periods in Ringer's solution buffered to pH 7.2.

Sample	d(c)	strain (c) %	E (Pa)	residual stress (MPa)
DGUN HA powder	1.7172	0.003203	5.5^{09}	-
as-received	1.7262	0.005241	5.5^{09}	28.8260
pH 7.2 x 1	1.7229	0.003319	5.5^{09}	18.2565
pH 7.2 x 2	1.7209	0.002155	5.5^{09}	11.8507
pH 7.2 x 4	1.7314	0.008269	5.5^{09}	45.4810
pH 7.2 x 8	1.7240	0.003960	5.5^{09}	21.7796

Table 5-18 :- Residual stress results in 004 plane for DGUN HA coatings aged unloaded pH 7.2

5.3 VPS HA Coatings Aged Unloaded pH 4.5

5.3.1 X-Ray Diffraction Traces

Figure 5-11 presents sections from the x-ray diffraction traces for the vacuum plasma sprayed hydroxyapatite coatings aged for various time periods in Ringer's solution buffered to pH 4.5.

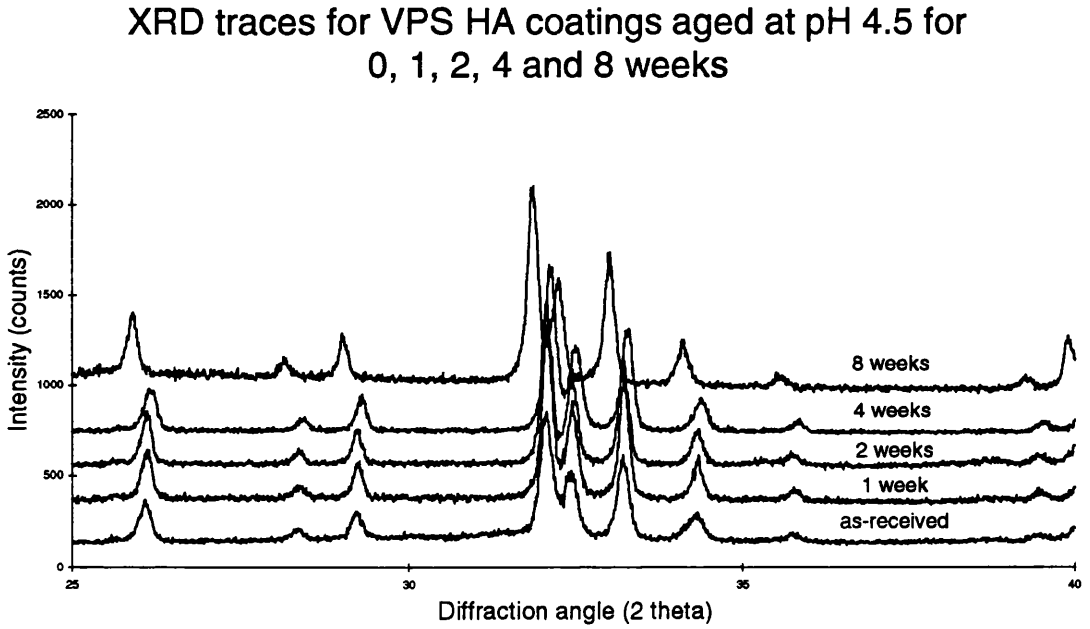

Figure 5-11 :- Amorphous hump region from X-Ray diffraction traces of VPS HA coatings aged unloaded at pH 4.5

5.3.2 Crystallinity Results

Table 5-19 presents a summary of the crystallinity results for the vacuum plasma sprayed hydroxyapatite coatings aged for various time periods in Ringer's solution buffered to pH 4.5.

Sample	*No. of tests*	*Mean (%)*	*Standard Deviation*	*Variance*	*95% Confidence Limits*
as-received	10	60.3542	2.1942	4.8145	59.738 and 61.053
pH 4.5 x 1	10	59.1225	4.1489	17.2136	58.484 and 59.761
pH 4.5 x 2	10	58.9098	5.4013	29.1744	58.276 and 59.544
pH 4.5 x 4	10	64.8969	3.6290	13.1693	64.256 and 65.538
pH 4.5 x 8	10	40.9170	5.2331	27.3854	40.282 and 41.552

Table 5-19 :- Crystallinity results for VPS HA coatings aged unloaded pH 4.5

Table 5-20 presents the significance test results for the crystallinity data from vacuum plasma sprayed coatings aged in Ringer's solution buffered to pH 4.5. The data was tested using a Student T-test at the 5 % significance level.

crystallinity	*as-received*	*1 week*	*2 weeks*	*4 weeks*	*8 weeks*
as-received		✖	✖	✓	✓
1 week	✖		✖		
2 weeks	✖	✖		✓	
4 weeks	✓		✓		✓
8 weeks	✓			✓	

Table 5-20 :- Significant test results for VPS HA coatings aged unloaded pH 4.5

✓ = significantly different

✖ = not significantly different

= not tested

Therefore, there was found to be a variability in the significance of changes in crystallinity between the as-received coating and the aged coatings and between ageing times.

5.3.3 X-Ray Plane Analysis

Table 5-21 presents a summary of the x-ray plane analysis for the vacuum plasma sprayed hydroxyapatite coatings aged for various time periods in Ringer's solution buffered to pH 4.5.

Sample	*Major Compound*	*Significant Compounds*	*Trace Compounds*
as-received	HA	-	α-TCP, β-TCP, $Ca_4O(PO_4)_2$, $Ca_2P_2O_7$
pH 4.5 x 1	HA	-	α-TCP, β-TCP, $Ca_4O(PO_4)_2$, $Ca_2P_2O_7$
pH 4.5 x 2	HA	-	α-TCP, β-TCP, $Ca_4O(PO_4)_2$, $Ca_2P_2O_7$
pH 4.5 x 4	HA	β-TCP	α-TCP, $Ca_4O(PO_4)_2$, $Ca_2P_2O_7$
pH 4.5 x 8	HA	-	α-TCP, β-TCP, $Ca_4O(PO_4)_2$, $Ca_2P_2O_7$

Table 5-21 :- X-Ray plane analysis results for VPS HA coatings aged unloaded pH 4.5

5.3.4 Optical Microscopy

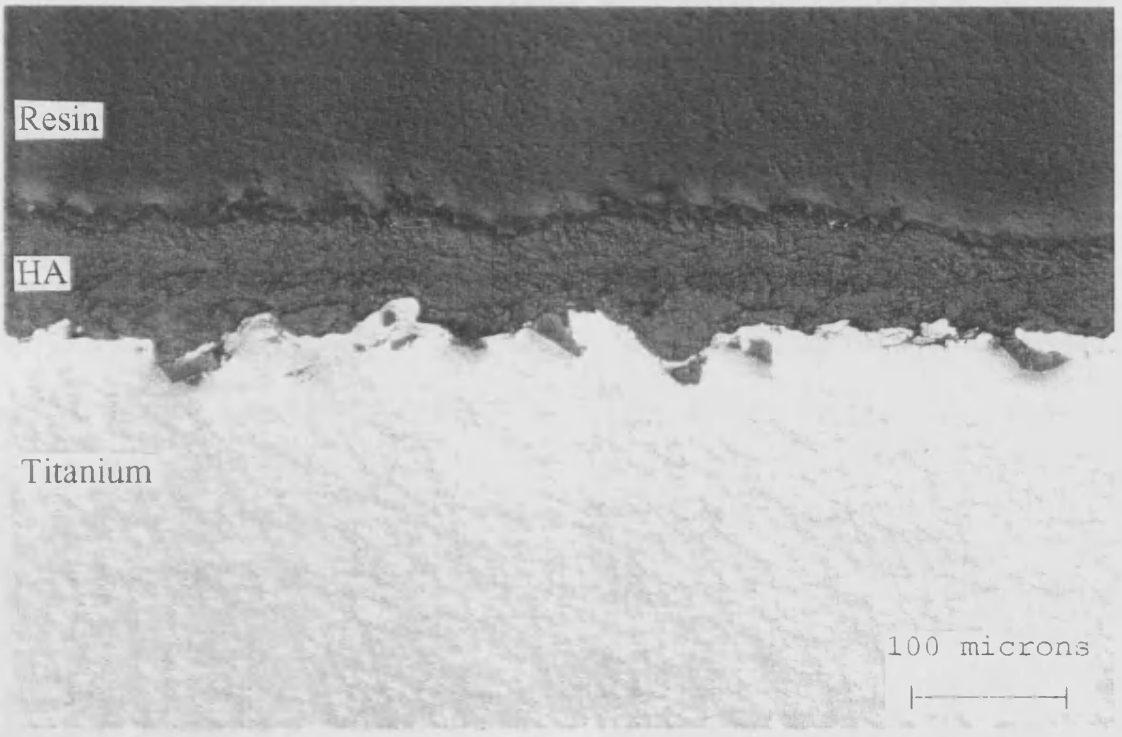

Figure 5-12 :- Optical micrograph showing cross-section through VPS HA coating aged unloaded pH 4.5 x 1 week

The polished cross-section through the VPS HA coatings aged at pH 4.5 for one week (Figure 5-12) looks very similar to the as-received coating cross-section. The only discernible change between the as-received coating and this one has occurred at the surface of the cross-section. Here there appears to be a modified layer which had polished slightly differently from the rest of the coating implying that it has a different structure.

This layer seems to be more defined in the coating aged for two weeks at pH 4.5 (not shown) but again, in all other respects the cross-section appears to be very similar to that of the as-received coating.

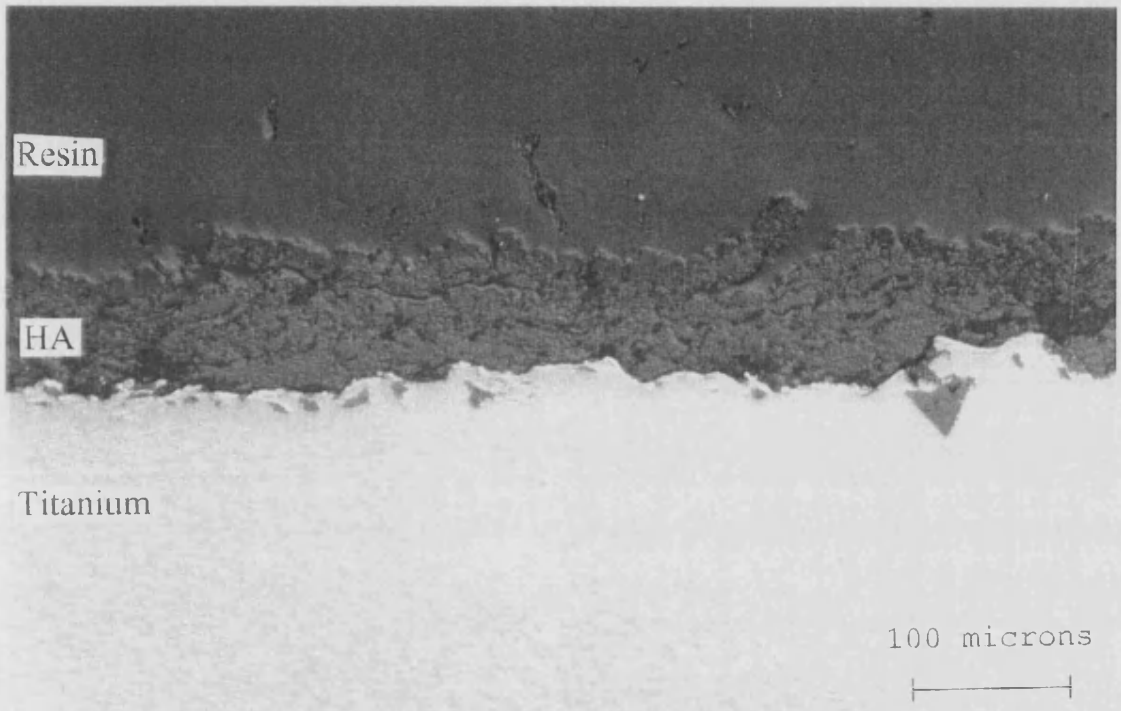

Figure 5-13 :- Optical micrograph showing cross-section through VPS HA coating aged unloaded pH 4.5 x4 weeks

The coating aged for four weeks at pH 4.5 (Figure 5-13) shows a disintegration of the surface layers which have begun spalling off in areas or have been lost completely in others. There are delamination cracks further down in the coating also, although the coating still seems to be well adhered to the substrate The surface delamination in these coatings appears to have taken place just below the modified layer.

Coatings aged for eight weeks at pH 4.5 (not shown) disintegrated completely on removal from the *in-vitro* tank preventing sectioning and polishing of these samples. It is assumed that the effect observed in coatings aged for shorter times had become so accentuated in these coatings that complete delamination of the coating from the substrate had occurred.

5.3.5 Scanning Electron Microscopy

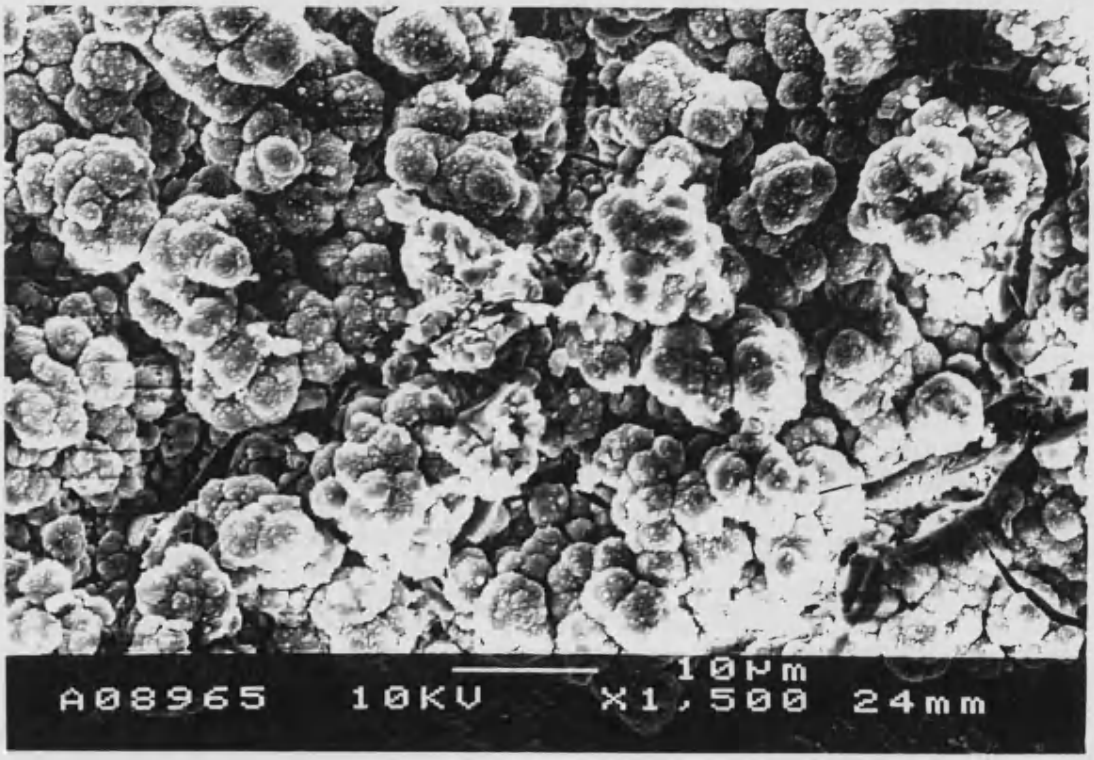

Figure 5-14 :- Scanning electron micrograph showing surface of VPS HA coating aged unloaded pH 4.5 x 1 week

The surface of the coatings aged at pH 4.5 for one week (Figure 5-14) have a dramatically different appearance to the as-received coatings. Here the surface shows an abundance of cauliflower like protuberances which seem to cover the surface of the coating. These protuberances are spherical in morphology and are composed of what appear to be tiny crystallites. These crystallites vary considerably in size the largest being approximately 4 µm in diameter. Below the level of this structure the micro-cracks

visible in the as-received coating can still be seen implying that this structure has grown on the original surface of the coating. It is possible that this material is in the form of re-deposited calcium phosphate which comes from previously dissolved amorphous material from the coating surface.

Coatings aged for two weeks at pH 4.5 (not shown here) show the same cauliflower like morphology on their surfaces. However in this material the deposits are not continuous over the entire coating surface and the material below is once again visible. It is as if the deposited layer has broken off the substrate in areas revealing the original coating. As can be seen through the lost regions, the coating remaining below shows no evidence of the glassy, amorphous material so evident in the as-received coating. It is suggested that this material has initially been dissolved by the *in-vitro* medium only to be re-deposited in the form of crystalline cauliflower-like growths which then later became detached from the coating once again.

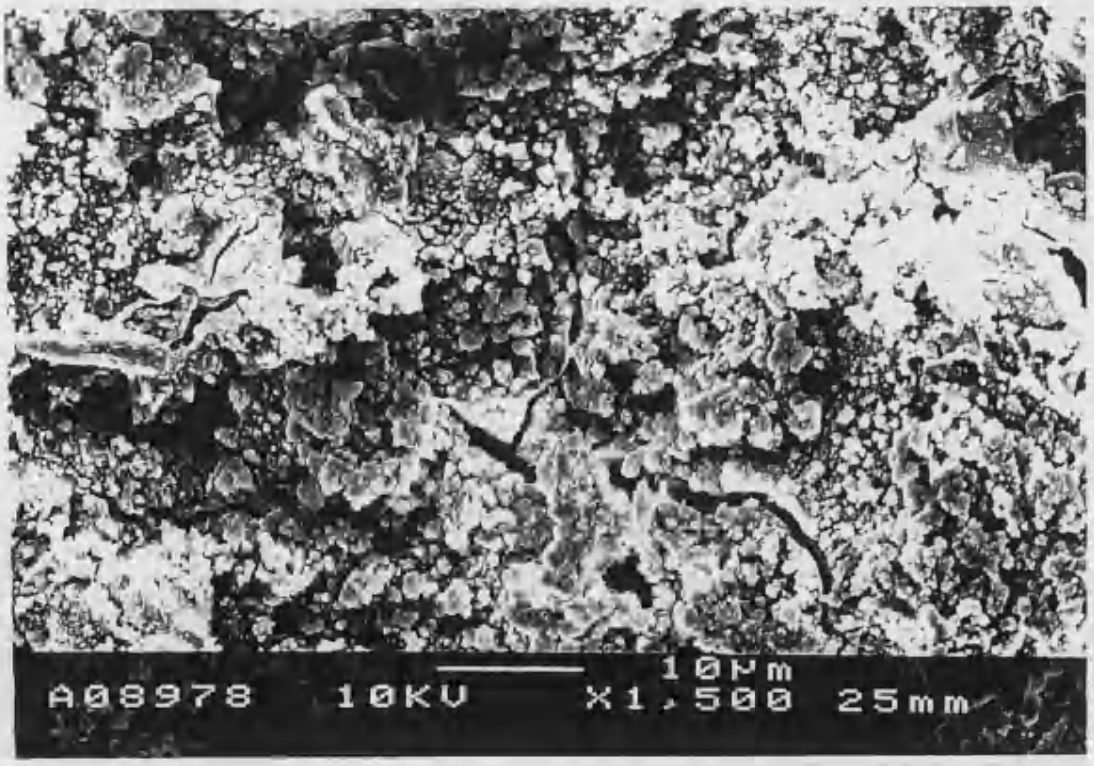

Figure 5-15 :- Scanning electron micrograph showing surface of VPS HA coating aged unloaded pH 4.5 x 4 weeks

In contrast to the two coatings which were aged for shorter durations, the coating aged for four weeks (Figure 5-15) shows no evidence for the cauliflower-like growths. All evidence of their formation has been lost in this surface. The coating shows signs of complete dissolution of the glassy amorphous material but no sign of its re-desposition. If the process suggested above has continued in this case, then the re-deposited material has completely detached from the coating surface leaving only the etched material behind.

Coatings aged for eight weeks at pH 4.5 (not shown) disintegrated completely on removal from the *in-vitro* tank preventing sectioning of these samples for microscopy. It is assumed that the effect observed in coatings aged for shorter times had become so accentuated in these coatings that complete loss of the coating from the substrate had occurred.

5.3.6 Coating Thickness Results

Table 5-22 presents a summary of the cross-sectional thickness results for the vacuum plasma sprayed hydroxyapatite coatings aged for various time periods in Ringer's solution buffered to pH 4.5.

Sample	*No. of tests*	*Mean (μm)*	*Standard Deviation*	*Variance*	*95% Confidence Limits*
as-received	10	42.4840	11.6308	135.2751	41.501 and 42.484
pH 4.5 x 1	10	88.4262	13.8336	191.3683	87.257 and 88.426
pH 4.5 x 2	10	46.5020	11.8170	139.6425	55.503 and 56.502
pH 4.5 x 4	10	68.5286	13.2055	174.3860	67.402 and 68.529
pH 4.5 x 8	10	n / a *	n / a	n / a	n / a

Table 5-22 :- Cross-sectional thickness results for VPS HA coatings aged unloaded pH 4.5

* The coating aged at pH 4.5 for eight weeks disintegrated on removal from the tank and thus could not be analysed.

Table 5-23 presents the significance test results for the cross-sectional thickness data from vacuum plasma sprayed coatings aged in Ringer's solution buffered to pH 4.5. The data was tested using a Student T-test at the 5 % significance level.

thickness	*as-received*	*1 week*	*2 weeks*	*4 weeks*	*8 weeks*
as-received		✓	✖	✓	
1 week	✓		✓		
2 weeks	✖	✓		✓	
4 weeks	✓		✓		
8 weeks					

Table 5-23 :- Significant test results for VPS HA coatings aged unloaded pH 4.5

✓ = significantly different
✖ = not significantly different
= not tested

Therefore, there was found to be a significant difference in the coating thickness from the as-received coating in the case of the coatings aged at pH 4.5 for one and four weeks. There was also found to be a significant change in coating thickness between ageing periods.

5.3.7 Coating Porosity Results

Table 5-24 presents a summary of the cross-sectional porosity results for the vacuum plasma sprayed hydroxyapatite coatings aged for various time periods in Ringer's solution buffered to pH 4.5.

Sample	No. of tests	Mean (%)	Standard Deviation	Variance	95% Confidence Limits
as-received	10	5.749	1.464	2.144	4.702 and 6.797
pH 4.5 x 1	10	3.407	1.0332	1.0674	2.668 and 4.146
pH 4.5 x 2	10	0.965	0.6620	0.4383	0.491 and 1.439
pH 4.5 x 4	10	4.936	1.7317	2.9989	3.697 and 6.175
pH 4.5 x 8	10	n / a*	n / a	n / a	n / a

Table 5-24 :- Cross-sectional porosity results for VPS HA coatings aged unloaded pH 4.5

* The coating aged at pH 4.5 for eight weeks disintegrated on removal from the tank and thus could not be analysed.

Table 5-25 presents the significance test results for the cross-sectional porosity data from vacuum plasma sprayed coatings aged in Ringer's solution buffered to pH 4.5. The data was tested using a Student T-test at the 5 % significance level.

porosity	as-received	1 week	2 weeks	4 weeks	8 weeks
as-received		✓	✓	✖	
1 week	✓		✓		
2 weeks	✓	✓		✓	
4 weeks	✖		✓		
8 weeks					

Table 5-25 :- Significant test results for VPS HA coatings aged unloaded pH4.5

✓ = significantly different

✖ = not significantly different

= not tested

Therefore it was found that there was a variable significance in the differences in porosity between the aged coatings and the as-received coating. However a significant difference was found in the porosities of coatings aged for different time periods.

5.3.8 Surface Roughness (Ra) Results

Table 5-26 presents a summary of the surface roughness results for the vacuum plasma sprayed hydroxyapatite coatings aged for various time periods in Ringer's solution buffered to pH 4.5.

Sample	*Scan Length (mm)*	*Ra (μm)*	*Rp (μm)*	*Rv (μm)*	*Rt (μm)*
as-received	5.4904	5.1683	23.1762	15.9535	39.1297
pH 4.5 x 1	5.7740	8.0235	25.8564	23.7931	49.6495
pH 4.5 x 2	5.6578	8.0351	31.8698	23.8024	55.6722
pH 4.5 x 4	5.7047	6.8118	29.0474	23.6127	52.6601
pH 4.5 x 8	n / a*	n / a	n / a	n / a	n / a

Table 5-26 :- Surface roughness results for VPS HA coatings aged unloaded pH 4.5

* The coating aged at pH 4.5 for eight weeks disintegrated on removal from the tank and thus could not be analysed.

5.3.9 Residual Stress Results

Table 5-27 presents a summary of the residual stress analysis results for the vacuum plasma sprayed hydroxyapatite coatings aged for various time periods in Ringer's solution buffered to pH 4.5.

Sample	*d(c)*	*strain (c) %*	*E (Pa)*	*residual stress (MPa)*
VPS HA powder	1.7209	0.003777	5.5^{09}	-
as-received	1.7144	0.004068	5.5^{09}	20.7740
pH 4.5 x 1	1.7138	0.004126	5.5^{09}	22.6916
pH 4.5 x 2	1.7150	0.003428	5.5^{09}	18.8564
pH 4.5 x 4	1.7110	0.005753	5.5^{09}	31.6404
pH 4.5 x 8	1.7203	0.000349	5.5^{09}	1.9176

Table 5-27 :- Residual stress results in 004 plane for VPS HA coatings aged unloaded pH 4.5

5.4 DGUN HA Coatings Aged Unloaded pH 4.5

5.4.1 X-Ray Diffraction Traces

Figure 5-16 presents sections from the x-ray diffraction traces for the detonation gun sprayed hydroxyapatite coatings aged for various time periods in Ringer's solution buffered to pH 4.5.

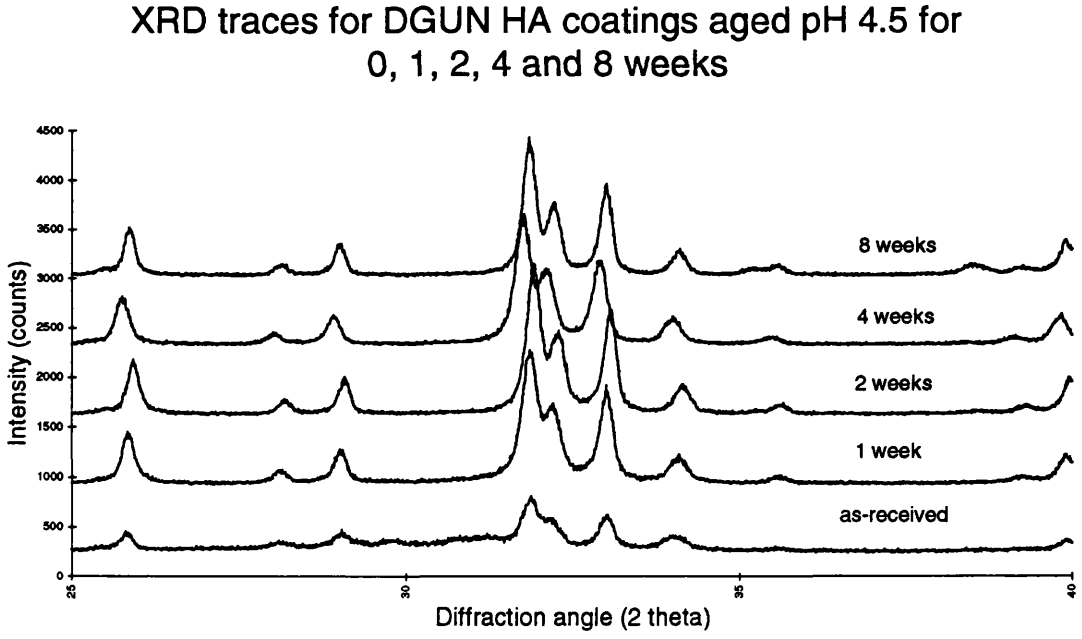

Figure 5-16 :- Amorphous hump region from X-Ray diffraction traces of DGUN HA coatings aged unloaded at pH 4.5

5.4.2 Crystallinity Results

Table 5-28 presents a summary of the crystallinity results for the detonation gun sprayed hydroxyapatite coatings aged for various time periods in Ringer's solution buffered to pH 4.5.

Sample	*No. of tests*	*Mean (%)*	*Standard Deviation*	*Variance*	*95% Confidence Limits*
as-received	10	34.4223	0.9043	0.8183	33.7752 and 35.0694
pH 4.5 x 1	10	58.4416	1.3073	1.7089	57.5064 and 59.3767
pH 4.5 x 2	10	64.7942	1.5489	2.3991	63.6862 and 65.9022
pH 4.5 x 4	10	60.9710	1.4135	1.9980	60.9710 and 61.9821
pH 4.5 x 8	10	67.7541	1.7632	3.1090	66.4928 and 69.1055

Table 5-28 :- Crystallinity results for DGUN HA coatings aged unloaded pH 4.5

Table 5-29 presents the significance test results for the crystallinity data from detonation gun sprayed coatings aged in Ringer's solution buffered to pH 4.5. The data was tested using a Student T-test at the 5 % significance level.

crystallinity	*as-received*	*1 week*	*2 weeks*	*4 weeks*	*8 weeks*
as-received		✓	✓	✓	✓
1 week	✓		✓		
2 weeks	✓	✓		✓	
4 weeks	✓		✓		✓
8 weeks	✓			✓	

Table 5-29 :- Significant test results for DGUN HA coatings aged unloaded pH 4.5

✓ = significantly different

✖ = not significantly different

= not tested

Therefore, there was found to be a significant change in crystallinity between the as-received coating and the aged coatings. There was also found to be a significant difference between the crystallinities of coatings aged at different time periods.

5.4.3 X-Ray Plane Analysis

Table 5-30 presents a summary of the x-ray plane analysis results for the detonation gun sprayed hydroxyapatite coatings aged for various time periods in Ringer's solution buffered to pH 4.5.

Sample	*Major Compound*	*Significant Compounds*	*Trace Compounds*
as-received	HA	β-TCP, $Ca_4O(PO_4)_2$	α-TCP
pH 4.5 x 1	HA	-	β-TCP, α-TCP, $Ca_4O(PO_4)_2$
pH 4.5 x 2	HA	-	β-TCP, α-TCP, $Ca_4O(PO_4)_2$
pH 4.5 x 4	HA	α-TCP, $Ca_4O(PO_4)_2$	β-TCP
pH 4.5 x 8	HA	-	β-TCP, α-TCP, $Ca_4O(PO_4)_2$

Table 5-30 :- X-Ray plane analysis results for DGUN HA coatings aged unloaded pH 4.5

5.4.4 Optical Microscopy

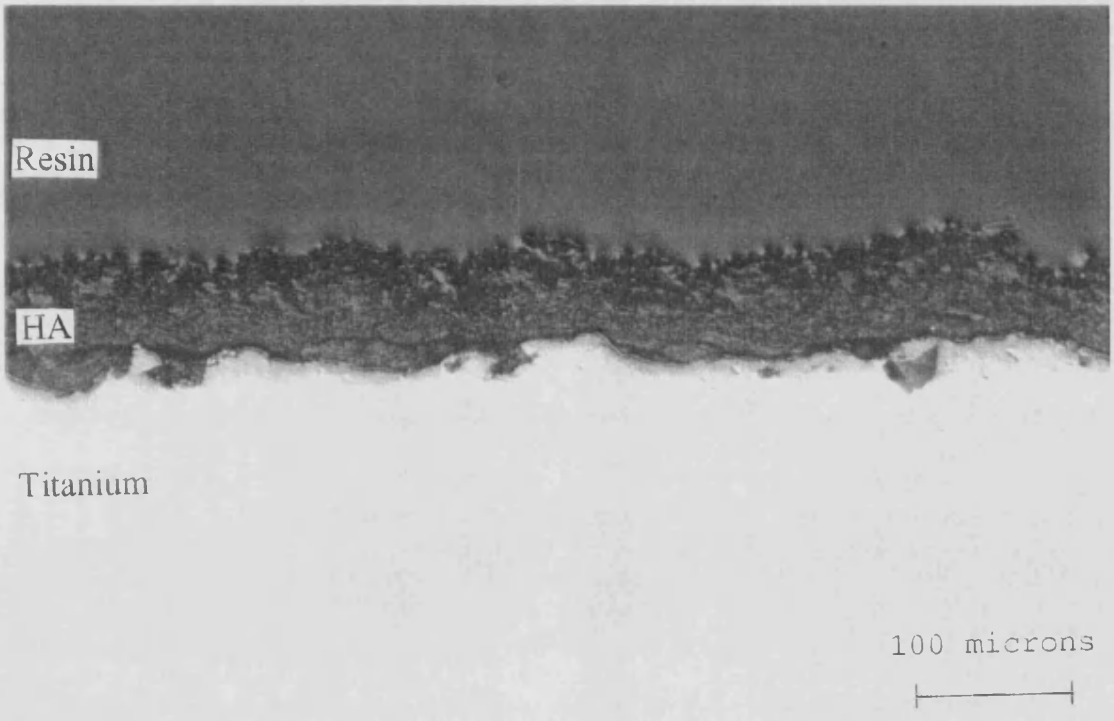

Figure 5-17 :- Optical micrograph showing cross-section through DGUN HA coating aged unloaded pH 4.5 x 1 week

The DGUN HA coating aged for one week at pH 4.5 (Figure 5-17) shows a considerably altered morphology over that of the as-received DGUN coating. The coating appears to have been most dramatically altered by the *in-vitro* medium in the top third of the coating, nearest the surface of the hydroxyapatite. In this damaged layer the coating appears to be extremely porous and poorly consolidated. Further into the bulk of the coating however, the material resumes an appearance more like that of the as-received material. This unaltered material seems to have a similar porosity and overall morphology similar to the original coating. There is still evidence for a dark layer, possibly a delamination layer between the coating and titanium but despite this, the material seems to be well adhered to the substrate.

The DGUN HA coatings aged for two and four weeks at pH 4.5 (not shown) again appear to have been considerably altered by *in-vitro* ageing. The modified layer first seen in the coating aged for one week has now progressed through the entire thickness of the coating and reached the substrate. Both these coatings appear to be highly porous in nature, this porosity taking the form of large pores lying horizontally through the coating. The coatings are still apparently well adhered to the substrate but have a morphology which would appear to be extremely friable in nature.

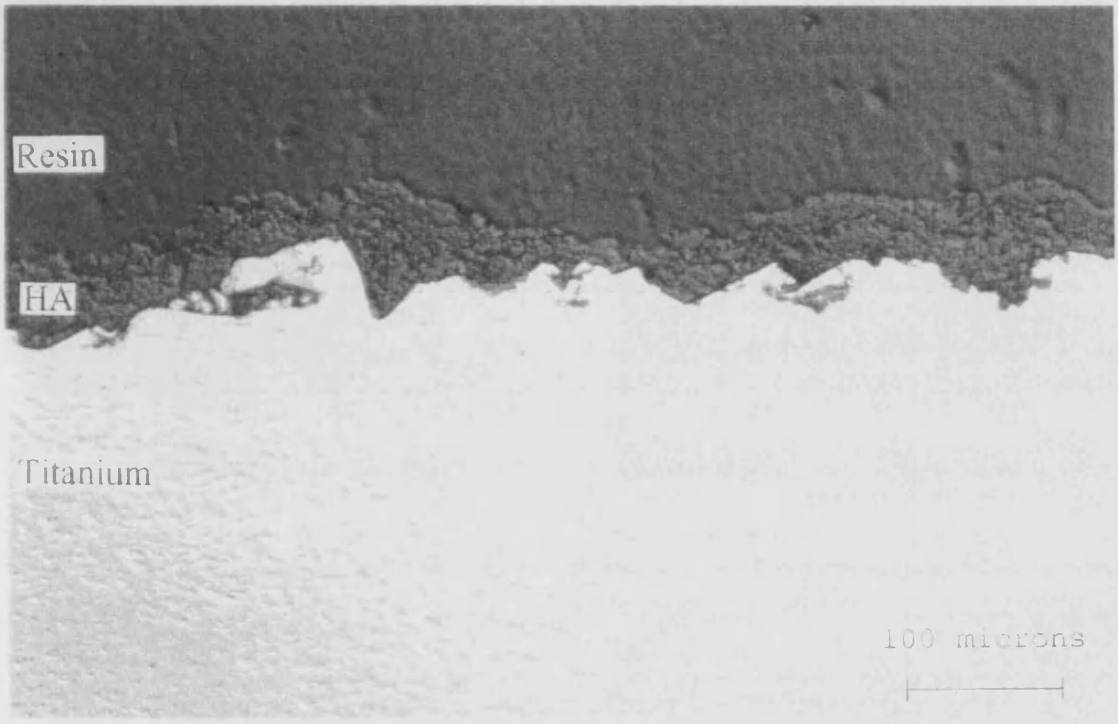

Figure 5-18 :- Optical micrograph showing cross-section through DGUN HA coating aged unloaded pH 4.5 x 8 weeks

The DGUN HA coating aged for eight weeks at pH 4.5 (Figure 5-18) again has a through thickness modified morphology similar to that of the modified areas of coatings aged for shorter durations. In addition to this alteration in the structure of the material in this coating, it appears that large areas of the coating have become thinner; in some areas no coating remains on the substrate at all. It is entirely possible that observations about the fragile appearance of the coatings aged for shorter time periods have been substantiated here and that damaged material has broken away from the bulk of the coating.

5.4.5 Scanning Electron Microscopy

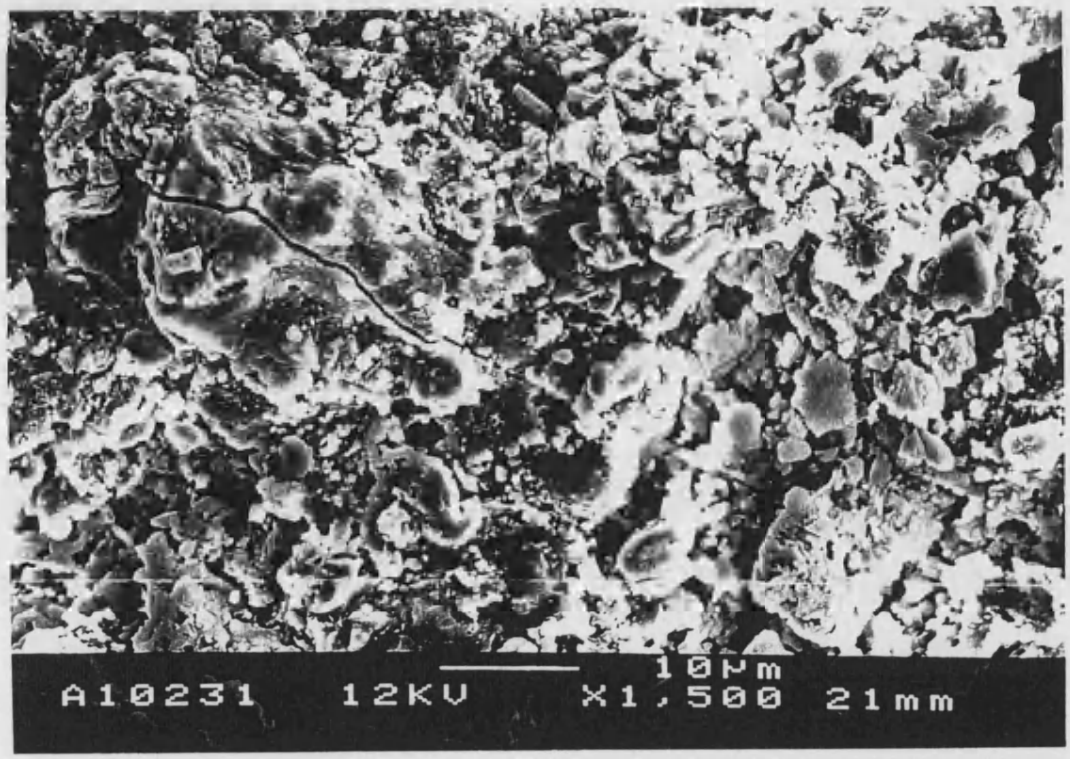

Figure 5-19 :- Scanning electron micrograph showing surface of DGUN HA coating aged unloaded pH 4.5 x 1 week

DGUN HA coatings aged for one week at pH 4.5 (Figure 5-19) have a similar appearance to that of the coatings aged at pH 7.2. Again the morphology of the surface has been considerably altered over that of the as-received coating. The large regions of glassy amorphous material seen in splats over the surface of the as-received coating have all but disappeared from the aged surface, the remaining smooth areas being pitted and marked by the process of dissolution. As in the case of the coatings aged at pH 7.2, the surface of these coatings appears to be considerably rougher than that of the as-received material since the flat phase has been removed. Again in a similar manner to the other aged coatings, it is still possible to see micro-cracks running across the coating surface, in this case however, the cracks are well defined and their paths through the remains of amorphous splats are very clear.

The coatings aged at pH 4.5 for two and four weeks (not shown) have an appearance more like that of the coating aged at pH 7.2 for eight weeks that of the coatings aged for a shorter duration. There seems to be more evidence for the existence of the flatter, glassy regions in these coatings although their surfaces, again, are greatly pitted. Again it is suggested that dissolution of the amorphous phase leads to instability in the coating surface and the loss of the outermost layer to reveal fresh coating below which is seen under SEM examination. The principal difference between coatings aged at pH 4.5 and those aged at pH 7.2 lies in the appearance of the micro-cracks running along the coating surface. In the coatings exposed to the lower pH medium, the cracks are clean and sharp rather than more diffuse as in the latter case. It is possible that these cracks are newly formed rather than being original cracks which have been attacked by the ageing medium.

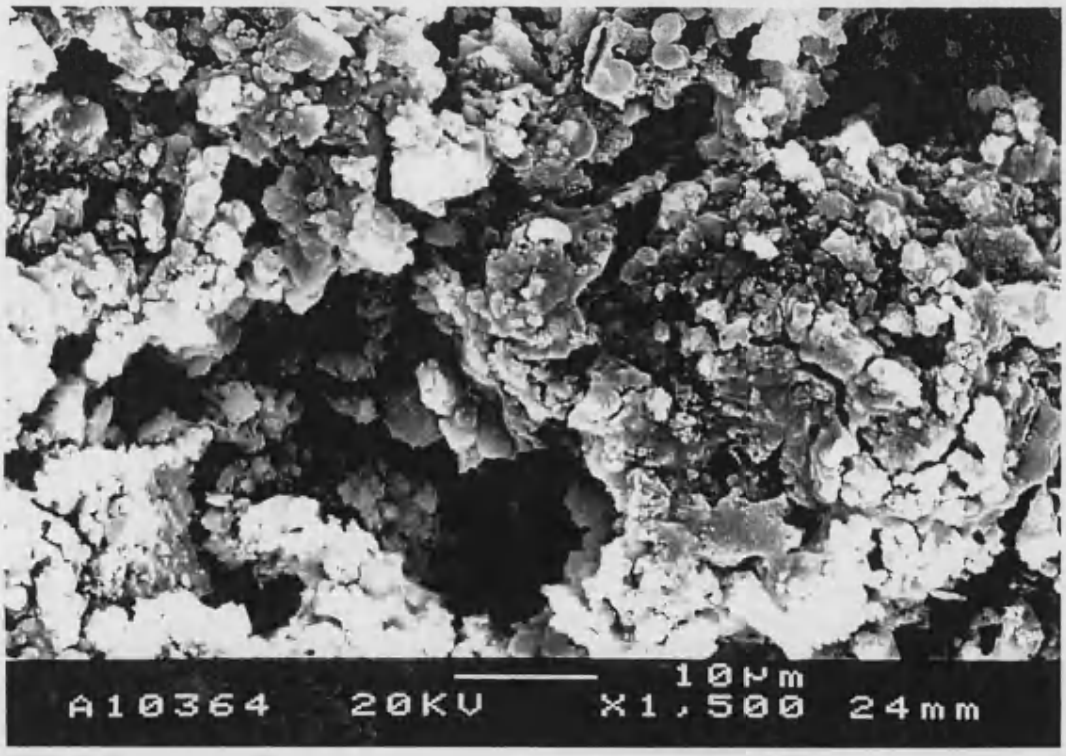

Figure 5-20 :- Scanning electron micrograph showing surface of DGUN HA coating aged unloaded pH 4.5 x8 weeks

The coating aged for 8 weeks at pH 4.5 (Figure 5-20) presents strong evidence for the supposition that parts of the coating surface become detached during *in-vitro* ageing. In these coatings the surface layers have a similar appearance to that of the

coatings aged for one week but there are deep fissures in the surface that give the appearance of the loss of sizeable amounts of material. The coating has a much greater surface roughness lent to it by these fissures and although lower layers in the coatings cannot be seen in these pores it can be envisaged that the loss of material from these holes allows the exposure of new layers to the medium. Again, sharp, well defined micro-cracks are visible on the coating surface, running through the highest levels of the exposed surface.

5.4.6 Coating Thickness Results

Table 5-31 presents a summary of the cross-sectional thickness results for the detonation gun hydroxyapatite coatings aged for various time periods in Ringer's solution buffered to pH 4.5.

Sample	*No. of tests*	*Mean (μm)*	*Standard Deviation*	*Variance*	*95% Confidence Limits*
as-received	10	70.0840	9.5690	91.5653	69.275 and 70.893
pH 4.5 x 1	10	58.1791	8.7504	76.5694	57.4394 and 58.9188
pH 4.5 x 2	10	52.7996	8.5934	73.8466	52.0731 and 53.5260
pH 4.5 x 4	10	56.9280	9.6801	93.7047	56.1097 and 57.7463
pH 4.5 x 8	10	38.4482	11.4079	130.1409	37.4838 and 39.4125

Table 5-31 :- Cross-sectional thickness results for DGUN HA coatings aged unloaded pH 4.5

Table 5-32 presents the significance test results for the cross-sectional thickness data from detonation gun sprayed coatings aged in Ringer's solution buffered to pH 4.5. The data was tested using a Student T-test at the 5 % significance level.

thickness	as-received	1 week	2 weeks	4 weeks	8 weeks
as-received		✓	✓	✓	✓
1 week	✓		✖		
2 weeks	✓	✖		✖	
4 weeks	✓		✖		✓
8 weeks	✓			✓	

Table 5-32 :- Significant test results for DGUN HA coatings aged unloaded pH 4.5

✓ = significantly different

✖ = not significantly different

= not tested

Therefore, it was found that the thicknesses of all aged DGUN coatings were significantly different from the as-received coating thickness. There was however little significant change in coating thickness between coatings aged for different durations.

5.4.7 Coating Porosity Results

Table 5-33 presents a summary of the cross-sectional porosity results for the detonation gun hydroxyapatite coatings aged for various time periods in Ringer's solution buffered to pH 4.5.

Sample	No. of tests	Mean (%)	Standard Deviation	Variance	95% Confidence Limits
as-received	10	1.4485	0.7381	0.5448	1.103 and 1.794
pH 4.5 x 1	10	12.7050	5.2046	27.0874	10.269 and 15.141
pH 4.5 x 2	10	10.2140	4.0263	16.2113	8.330 and 12.098
pH 4.5 x 4	10	9.3524	3.6382	13.2365	7.650 and 11.055
pH 4.5 x 8	10	6.8916	2.4108	5.8117	5.763 and 8.020

Table 5-33 :- Cross-sectional porosity results for DGUN HA coatings aged unloaded pH 4.5

Table 5-34 presents the significance test results for the crystallinity data from detonation gun sprayed coatings aged in Ringer's solution buffered to pH 4.5. The data was tested using a Student T-test at the 5 % significance level.

porosity	*as-received*	*1 week*	*2 weeks*	*4 weeks*	*8 weeks*
as-received		✓	✓	✓	✓
1 week	✓		✖		
2 weeks	✓	✖		✖	
4 weeks	✓		✖		✓
8 weeks	✓			✓	

Table 5-34 :- Significant test results for DGUN HA coatings aged unloaded pH 4.5

✓ = significantly different

✖ = not significantly different

= not tested

Therefore, it was found that there was a significant difference between the porosity of the as-received coating and the aged coatings. There was found to be no significant difference in the porosities of coatings aged for different time periods except in the case of coatings aged between four and eight weeks.

5.4.8 Surface Roughness (Ra) Results

Table 5-35 presents a summary of the surface roughness results for the detonation gun hydroxyapatite coatings aged for various time periods in Ringer's solution buffered to pH 4.5.

Sample	Scan Length (mm)	Ra (μm)	Rp (μm)	Rv (μm)	Rt (μm)
as-received	11.3739	5.5294	27.5104	19.4195	46.9298
pH 4.5 x 1	11.0802	6.4558	26.5579	21.2120	47.7699
pH 4.5 x 2	11.1815	6.0744	51.5508	23.0426	74.5933
pH 4.5 x 4	10.9431	6.0581	25.7882	21.3694	47.1576
pH 4.5 x 8	10.8639	6.2296	28.5386	22.3760	50.9145

Table 5-35 :- Surface roughness results for DGUN HA coatings aged unloaded pH 4.5

5.4.9 Residual Stress Results

Table 5-36 presents a summary of the residual stress analysis results for the detonation gun hydroxyapatite coatings aged for various time periods in Ringer's solution buffered to pH 4.5.

Sample	d(c)	strain (c) %	E (Pa)	residual stress (MPa)
DGUN HA powder	1.7172	0.003203	5.5^{09}	-
as-received	1.7262	0.005241	5.5^{09}	28.8260
pH 4.5 x 1	1.7247	0.004368	5.5^{09}	24.0217
pH 4.5 x 2	1.7206	0.001980	5.5^{09}	10.8898
pH 4.5 x 4	1.7258	0.005008	5.5^{09}	27.5448
pH 4.5 x 8	1.7214	0.002446	5.5^{09}	13.4521

Table 5-36 :- Residual stress results in 004 plane for DGUN HA coatings aged unloaded pH 4.5

6. Results - Statically Loaded HA Coatings

6.1 VPS HA Coatings Aged Under Static Loading in Air at 37°C

6.1.1 X-Ray Diffraction Traces

Figure 6-1 presents sections from the x-ray diffraction traces for the vacuum plasma sprayed hydroxyapatite coatings aged for various time periods under static loading in air held at 37°C.

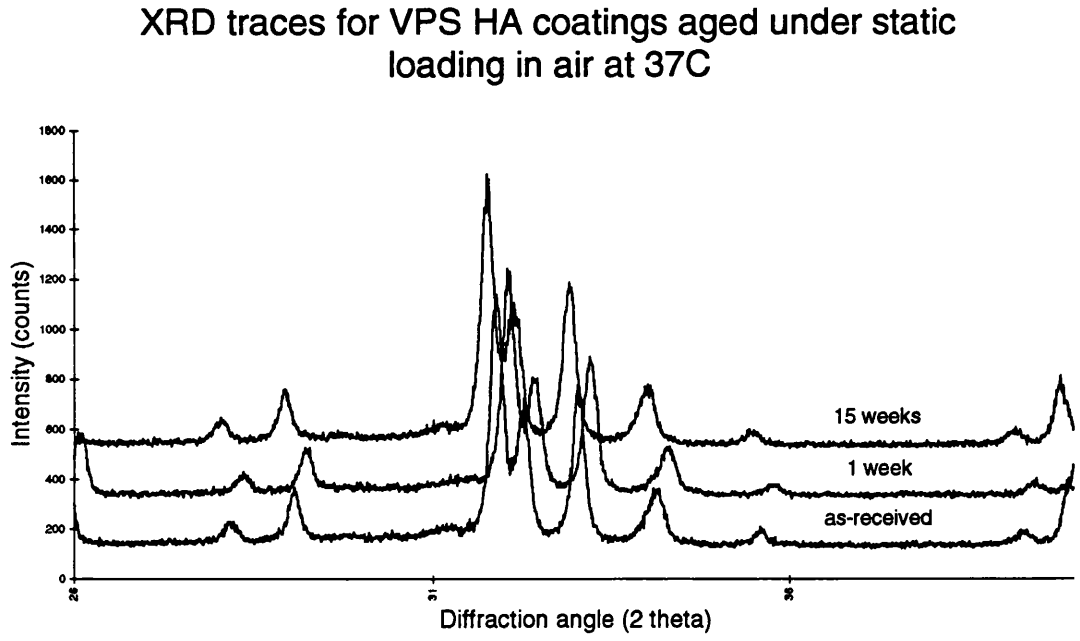

Figure 6-1 :- X-Ray diffraction traces for VPS HA coatings aged under static loading in air at 37°C

6.1.2 Crystallinity Results

Table 6-1 presents a summary of the crystallinity results for the vacuum plasma sprayed hydroxyapatite coatings aged for various time periods under static loading in air held at 37°C.

Sample	*No. of tests*	*Mean (%)*	*Standard Deviation*	*Variance*	*95% Confidence Limits*
as-received	10	60.9231	5.8287	33.9742	60.290 and 61.556
air x 1	10	62.2257	4.9159	24.1658	61.590 and 62.861
air x 15	10	54.4772	4.3857	19.2344	53.840 and 55.120

Table 6-1 :- Crystallinity results for VPS HA coatings aged under static loading in air at 37°C

Using a 2-tailed Student T-test the significance of these results was determined at the 5% level, revealing that :

The coating aged in air for one week did not have a significantly different crystallinity to that of the as-received coating.

The coating aged in air for fifteen weeks had a significantly different crystallinity to that of the as-received coating and also from that of the coating aged in air for one week.

6.1.3 X-Ray Plane Analysis

Table 6-2 presents a summary of the x-ray plane analysis results for the vacuum plasma sprayed hydroxyapatite coatings aged for various time periods under static loading in air held at 37°C.

Sample	*Major Compound*	*Significant Compounds*	*Trace Compounds*
as-received	HA	β-TCP	α-TCP, $Ca_4O(PO_4)_2$, $Ca_2P_2O_7$
air x 1	HA	β-TCP	α-TCP, $Ca_4O(PO_4)_2$, $Ca_2P_2O_7$
air x 15	HA	β-TCP	α-TCP, $Ca_4O(PO_4)_2$, $Ca_2P_2O_7$

Table 6-2 :- X-Ray plane analysis results for VPS HA coatings aged under static loading in air at 37°C

6.1.4 Optical Microscopy

The polished cross-sections through VPS HA coatings aged under static loading in air at 37°C for one week (not shown) and fifteen weeks (Figure 6-2) show no change in morphology over the as-received sample. The coatings still demonstrate their layered nature and show no change in structure at the coating surface. The coating aged for fifteen weeks at 37°C does have some fairly large pores in the lower half of the coating but the material still seems to be well adhered to the substrate. No overall change in thickness is apparent in either the week aged or fifteen week aged coatings.

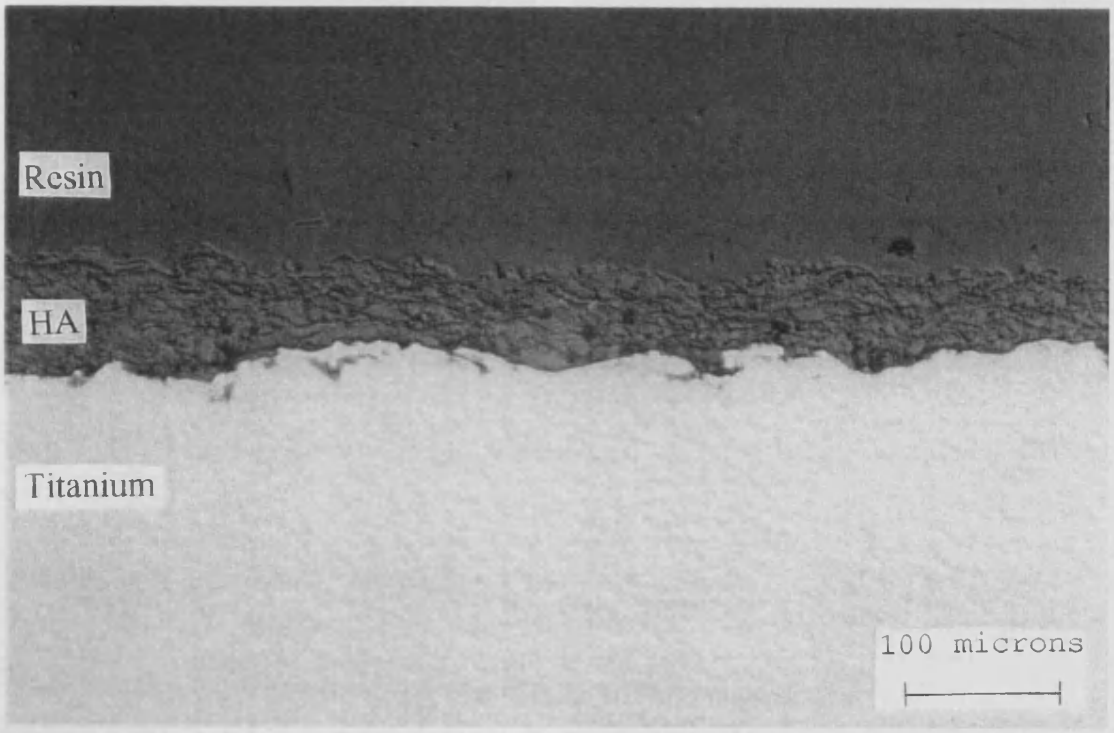

Figure 6-2 :- Optical micrograph showing cross-section through VPS HA coating aged under static loading in air at 37°C for fifteen weeks

6.1.5 Scanning Electron Microscopy

The surface of the VPS HA coatings aged under static loading in air at 37°C shows very little change in morphology over the as-received coating. There is no evidence for loss of amorphous material in the coating aged for one week (not shown) nor for any increase in surface cracking. There does not seem to have been any loss of material from the coating surface nor increase in the volume of crystallites on the surface. There is again very little, if any discernible change in the coatings aged for fifteen weeks in air at 37°C (Figure 6-3). The only possible difference between this coating surface and that of the coating aged for one week can be found in small areas of altered material lying on the extreme edges of amorphous splats. These regions seem to indicate small amounts of etching occurring to the glassy phase but these zones are extremely small in size and irregular in occurrence. Overall therefore it can be said that there is very little noticeable change in the surface of the coatings even after fifteen weeks ageing in air.

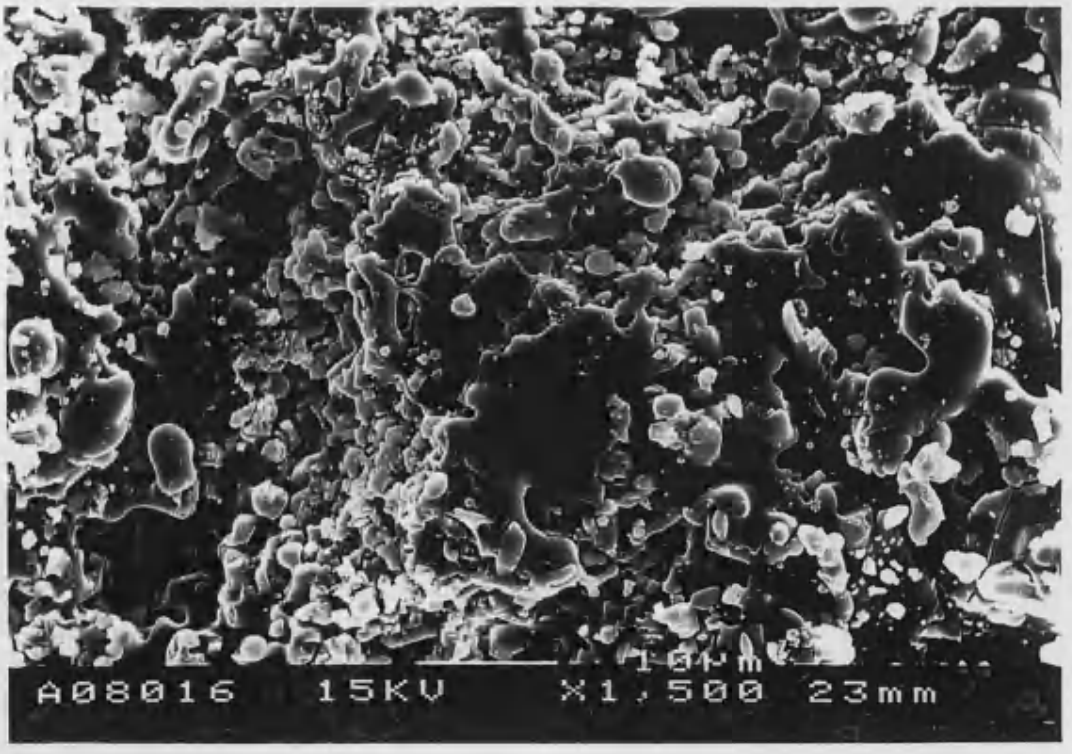

Figure 6-3 :- Scanning electron micrograph showing surface of VPS HA coating aged under static loading in air at 37°C for fifteen weeks

6.1.6 Coating Thickness Results

Table 6-3 presents a summary of the cross-sectional thickness results for the vacuum plasma sprayed hydroxyapatite coatings aged for various time periods under static loading in air held at 37°C.

Sample	*No. of tests*	*Mean (μm)*	*Standard Deviation*	*Variance*	*95% Confidence Limits*
as-received	10	57.443	10.621	112.813	56.545 and 58.341
air x 1	10	60.157	11.822	139.755	59.158 and 61.156
air x 15	10	54.038	8.662	75.030	53.306 and 54.771

Table 6-3 :- Cross-sectional thickness results for VPS HA coatings aged under static loading in air at 37°C

Using a 2-tailed Student T-test the significance of these results was determined at the 5% level, revealing that :

The coating aged in air at 37°C for one week did not have a significantly different thickness to that of the as-received coating.

The coating aged in air at 37°C for fifteen weeks did not have a significantly different thickness to that of the as-received coating nor from the coating aged in air at 37°C for one week.

Therefore, there was found to be no significant differences between the thicknesses of coatings aged either not at all or in air at 37°C for various time periods.

6.1.7 Coating Porosity Results

Table 6-4 presents a summary of the cross-sectional porosity results for the vacuum plasma sprayed hydroxyapatite coatings aged for various time periods under static loading in air held at 37°C.

Sample	No. of tests	Mean (%)	Standard Deviation	Variance	95% Confidence Limits
as-received	10	4.680	1.817	3.301	3.830 and 5.530
air x 1	10	9.821	2.904	8.432	8.462 and 11.180
air x 15	10	18.292	4.375	19.144	16.183 and 20.400

Table 6-4 :- Cross-sectional porosity results for VPS HA coatings aged under static loading in air at 37°C

Using a 2-tailed Student T-test the significance of these results was determined at the 5% level, revealing that :

The coating aged in air at 37°C for one week had a significantly different porosity to that of the as-received coating.

The coating aged in air at 37°C for fifteen weeks had a porosity that was both significantly different from that of the as-received coating and from that of the coating aged in air at 37°C for one week.

Therefore it was found that there was a significant difference in the porosities both between the as-received coating and the aged coatings and between the coatings aged for different time periods.

6.1.8 Surface Roughness (Ra) Results

Table 6-5 presents a summary of the surface roughness results for the vacuum plasma sprayed hydroxyapatite coatings aged for various time periods under static loading in air held at 37°C.

Sample	Scan Length (mm)	Ra (μm)	Rp (μm)	Rv (μm)	Rt (μm)
as-received	5.7931	5.5727	18.6202	22.0552	40.6753
air x 1	5.6905	5.4698	21.0322	16.8425	37.8747
air x 15	5.6949	5.8014	18.4224	19.7118	38.1343

Table 6-5 :- Surface roughness results for VPS HA coatings aged under static loading in air at 37°C

6.1.9 Residual Stress Results

Table 6-6 presents a summary of the residual stress analysis results for the vacuum plasma sprayed hydroxyapatite coatings aged for various time periods under static loading in air held at 37°C.

Sample	*d(c)*	*strain (c) %*	*E (Pa)*	*residual stress (MPa)*
VPS HA powder	1.7209	0.003777	5.5^{09}	-
as-received	1.7200	0.000523	5.5^{09}	2.8764
air x 1	1.7150	0.003428	5.5^{09}	18.8564
air x 15	1.7235	0.001511	5.5^{09}	8.3096

Table 6-6 :- Residual stress results in 004 plane for VPS HA coatings aged under static loading in air at 37°C

6.2 DGUN HA Coatings Aged Under Static Loading in Air at 37°C

6.2.1 X-Ray Diffraction Traces

Figure 6-4 presents sections from the x-ray diffraction traces for the detonation gun sprayed hydroxyapatite coatings aged for various time periods under static loading in air held at 37°C.

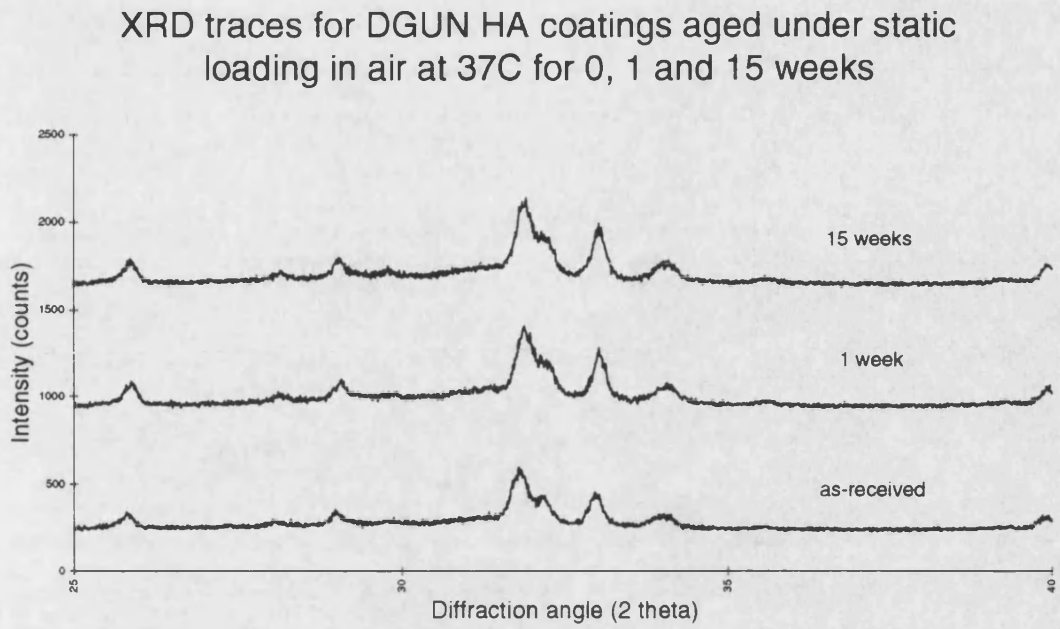

Figure 6-4 :- X-Ray diffraction traces for DGUN HA coatings aged under static loading in air at 37°C

6.2.2 Crystallinity Results

Table 6-7 presents a summary of the crystallinity results for the detonation gun sprayed hydroxyapatite coatings aged for various time periods under static loading in air held at 37°C.

Sample	*No. of tests*	*Mean (%)*	*Standard Deviation*	*Variance*	*95% Confidence Limits*
as-received	10	38.8604	1.2085	1.4604	37..996 and 39.725
air x 1	10	38.7780	1.4660	2.1491	37.729 and 39.827
air x 15	10	39.2296	1.5867	2.5177	38.095 and 40.345

Table 6-7 :- Crystallinity results for DGUN HA coatings aged under static loading in air at 37°C

Using a 2-tailed Student T-test the significance of these results was determined at the 5% level, revealing that :

The coating aged in air for one week did not have a significantly different crystallinity to that of the as-received coating.

The coating aged in air for fifteen weeks did not have a significantly different crystallinity to that of the as-received coating and also did not have a crystallinity that differed significantly from the coating aged in air for one week.

6.2.3 X-Ray Plane Analysis

Table 6-8 presents a summary of the x-ray plane analysis results for the detonation gun sprayed hydroxyapatite coatings aged for various time periods under static loading in air held at 37°C.

Sample	*Major Compound*	*Significant Compounds*	*Trace Compounds*
as-received	HA	β-TCP	α-TCP
air x 1	HA	β-TCP	$Ca_4O(PO_4)_2$
air x 15	HA	α-TCP	β-TCP, $Ca_4O(PO_4)_2$

Table 6-8 :- X-Ray plane analysis results for DGUN HA coatings aged under static loading in air at 37°C

6.2.4 Optical Microscopy

DGUN HA coatings aged under static loading in air for one (not shown) and fifteen weeks show no dramatic change in bulk morphology in comparison with the as-received coating. Both coatings still demonstrate the layer morphology of the as-received sample and seem to be well adhered to the substrate although there is a dark line between coating and substrate in the case of the coating aged for one week in air. This apparent crack moves virtually continuously along the entire length of the cross-section, occasionally deviating from the interface approximately 5 μm into the coating itself. The

crack moves along the interface and over residual alumina grit separating it from the coating. This dark line is not visible in the coating aged for fifteen weeks in air at 37°C (Figure 6-5). There is no sign of any form of separation between coating and substrate in this sample. The surface layers of this coating appear to have a slightly modified morphology however, showing an apparent increase in surface roughness on a microscopic scale. This surface layer which is less than 5 μm in thickness is also much darker than the bulk of the coating and seems to be much more porous in nature than the bulk of the coating. It is possible that in the case of this coating aged for fifteen weeks in air, the amorphous phase at the coating surface has been attacked and etched away during ageing.

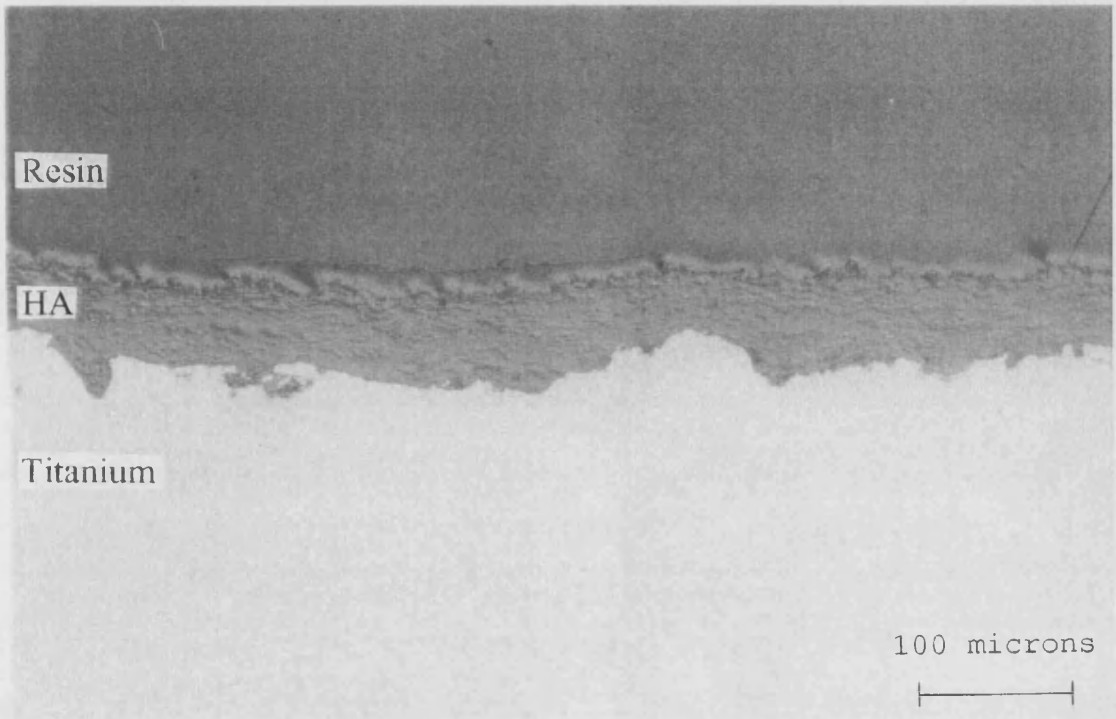

Figure 6-5 :- Optical micrograph showing cross-section through DGUN HA coating aged under static loading in air at 37°C for fifteen weeks

6.2.5 Scanning Electron Microscopy

Looking at the surface of the DGUN HA coating which had been held under static loading in air at 37°C for one week (Figure 6-6) we can see virtually no difference in the appearance of this sample from that of the as-received sample. There is no evidence for surface degradation nor any signs of an increase in surface micro-cracking. Micro-cracks are however still visible in small numbers, the sharpness of their edges again indicating that little or no attack of the surface of the coating has occurred. There appears to have been no loss of material from the coating surface.

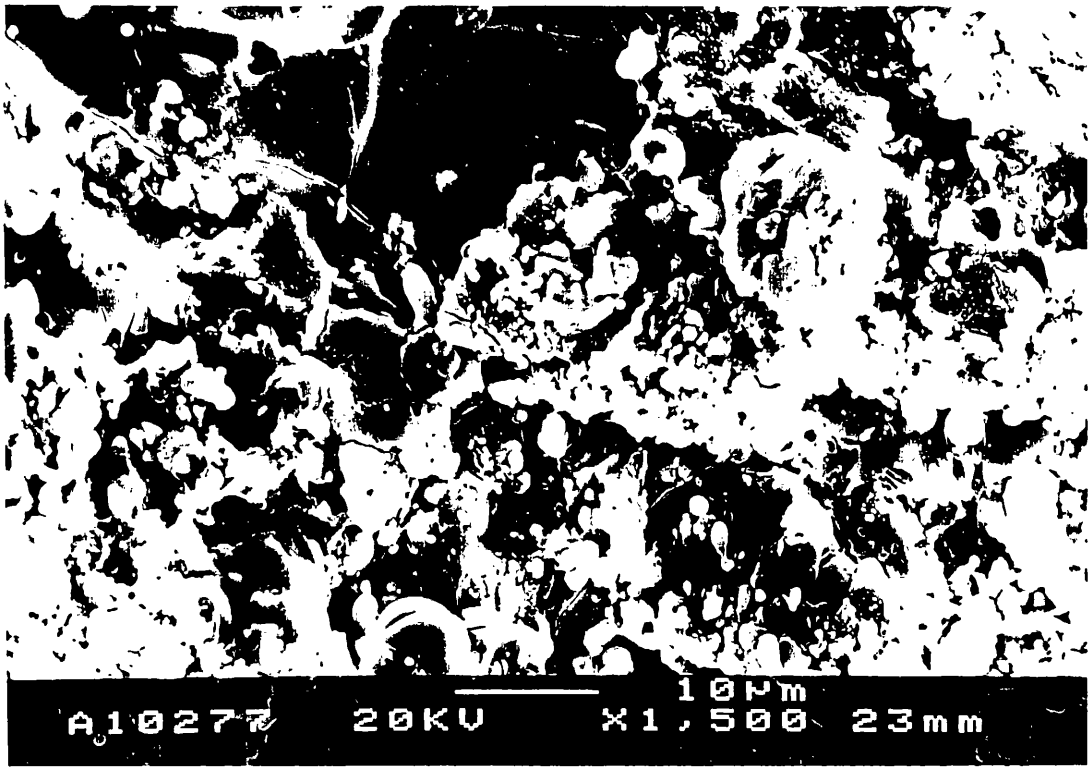

Figure 6-6:- Scanning electron micrograph showing surface of DGUN HA coating aged under static loading in air at 37°C for one week

Looking at the surface of the coating aged for fifteen weeks under static loading in air at 37°C (Figure 6-7) little difference can again be seen in the material's appearance over that of the as-received coating. There are no signs of degradation of the amorphous material on the coating surface and no evidence of an increase in micro-cracking as a result of the applied static load. Again, the sharpness of existing micro-cracks indicates

that no surface dissolution or etching has occurred with ageing in air even after extended periods of exposure.

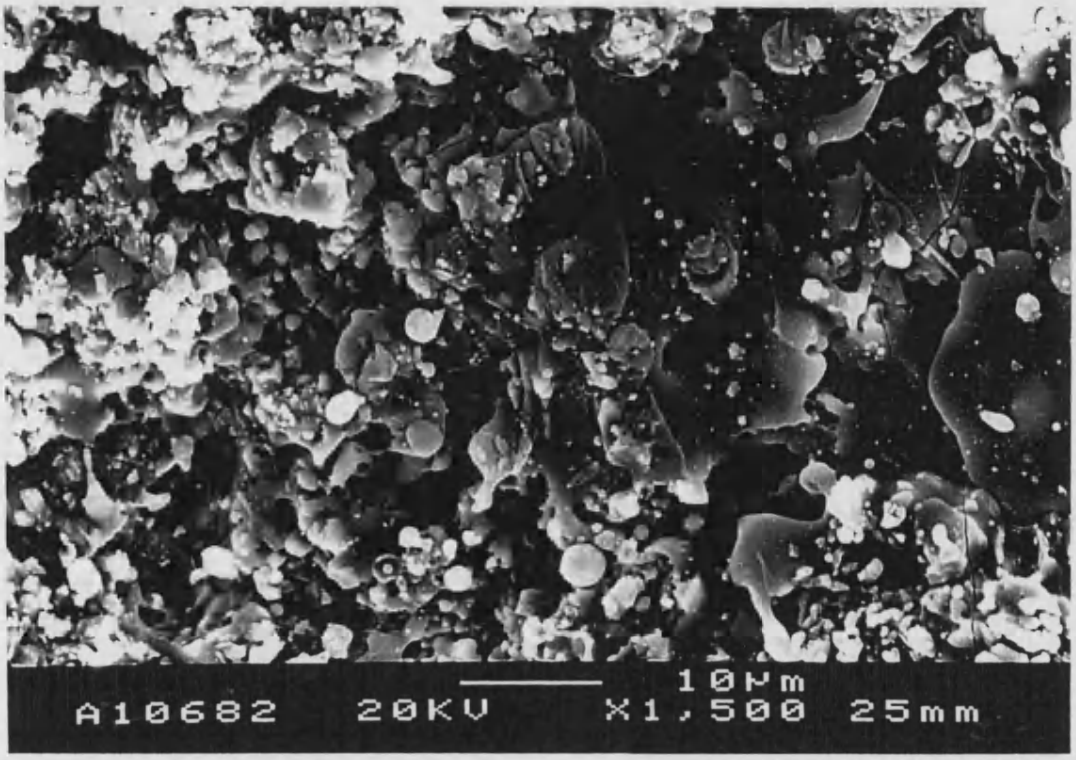

Figure 6-7 :- Scanning electron micrograph showing surface of DGUN HA coating aged under static loading in air at 37°C for fifteen weeks

6.2.6 Coating Thickness Results

Table 6-9 presents a summary of the cross-sectional thickness results for the detonation gun sprayed hydroxyapatite coatings aged for various time periods under static loading in air held at 37°C.

Sample	*No. of tests*	*Mean (μm)*	*Standard Deviation*	*Variance*	*95% Confidence Limits*
as-received	10	71.2908	8.4365	71.1752	70.578 and 72.004
air x 1	10	49.9272	7.7198	59.5959	49.275 and 50.580
air x 15	10	57.3678	12.0771	145.8550	56.347 and 58.389

Table 6-9 :- Cross-sectional thickness results for DGUN HA coatings aged under static loading in air at 37°C

Using a 2-tailed Student T-test the significance of these results was determined at the 5% level, revealing that :

The coating aged in air at 37°C for one week had a significantly different thickness to that of the as-received coating.

The coating aged in air at 37°C for fifteen weeks also had a significantly different thickness to that of the as-received coating but was not significantly different from the coating aged in air at 37°C for one week.

Therefore, there was found to be a significant difference between the thicknesses of the as-received coating and those which had been aged in air but not between coatings aged in air at 37°C for different time periods.

6.2.7 Coating Porosity Results

Table 6-10 presents a summary of the cross-sectional porosity results for the detonation gun spray hydroxyapatite coatings aged for various time periods under static loading in air held at 37°C.

Sample	*No. of tests*	*Mean (%)*	*Standard Deviation*	*Variance*	*95% Confidence Limits*
as-received	10	1.2605	0.7242	0.5245	0.922 and 1.600
air x 1	10	1.9222	0.5581	0.3115	1.661 and 2.183
air x 15	10	5.8335	1.9150	3.6672	4.937 and 6.730

Table 6-10 :- Cross-sectional porosity results for DGUN HA coatings aged under static loading in air at 37°C

Using a 2-tailed Student T-test the significance of these results was determined at the 5% level, revealing that :

The coating aged in air at 37°C for one week had a significantly different porosity to that of the as-received coating.

The coating aged in air at 37°C for fifteen weeks had a porosity that was both significantly different from that of the as-received coating and from that of the coating aged in air at 37°C for one week.

Therefore it was found that there was a significant difference between the porosities of the as-received coating and the aged coatings and also between the coatings aged for different time periods.

6.2.8 Surface Roughness (Ra) Results

Table 6-11 presents a summary of the surface roughness results for the detonation gun sprayed hydroxyapatite coatings aged for various time periods under static loading in air held at 37°C.

Sample	*Scan Length (mm)*	*Ra (μm)*	*Rp (μm)*	*Rv (μm)*	*Rt (μm)*
as-received	11.4025	5.9837	30.1268	19.2205	49.3472
air x 1	11.2633	5.5949	27.8992	23.0030	50.9023
air x 15	11.3906	5.6261	34.9283	16.8339	51.7622

Table 6-11 :- Surface roughness results for DGUN HA coatings aged under static loading in air at 37°C

6.2.9 Residual Stress Results

Table 6-12 presents a summary of the residual stress analysis results for the detonation gun sprayed hydroxyapatite coatings aged for various time periods under static loading in air held at 37°C.

Sample	*d(c)*	*strain (c) %*	*E (Pa)*	*residual stress (MPa)*
DGUN HA powder	1.7172	0.003203	5.5^{09}	-
as-received	1..7220	0.002795	5.5^{09}	15.3739
air x 1	1.7226	0.003145	5.5^{09}	17.2956
air x 15	1.7226	0.003145	5.5^{09}	17.2956

Table 6-12 :- Residual stress results in 004 plane for DGUN HA coatings aged under static loading in air at 37°C

6.3 VPS HA Coatings Aged Under Static Loading at pH 7.2

6.3.1 X-Ray Diffraction Traces

Figure 6-8 presents sections from the x-ray diffraction traces for the vacuum plasma sprayed hydroxyapatite coatings aged for various time periods under static loading in Ringer's solution buffered to pH 7.2.

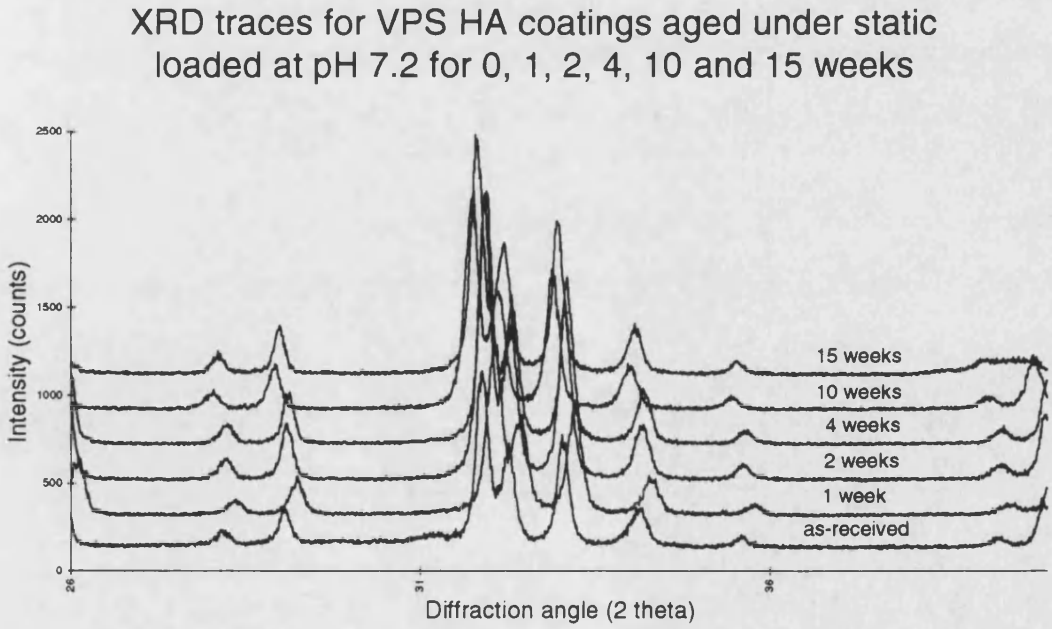

Figure 6-8 :- X-Ray diffraction traces for VPS HA coatings aged under static loading at pH 7.2

6.3.2 Crystallinity Results

Table 6-13 presents a summary of the crystallinity results for the vacuum plasma sprayed hydroxyapatite coatings aged for various time periods under static loading in Ringer's solution buffered to pH 7.2.

Sample	*No. of tests*	*Mean (%)*	*Standard Deviation*	*Variance*	*95% Confidence Limits*
as-received	10	60.9231	5.8287	33.9742	60.290 and 61.556
pH 7.2 x 1	10	67.3468	5.6089	61.4600	66.713 and 67.980
pH 7.2 x 2	10	75.5181	5.7028	32.5220	74.855 and 76.151
pH 7.2 x 4	10	74.0278	3.9788	15.8232	73.388 and 74.668
pH 7.2 x 10	10	73.2593	5.4048	29.2121	72.625 and 73.893
pH 7.2 x 15	10	54.7575	17.0072	289.2437	54.133 and 55.382

Table 6-13 :- Crystallinity results for VPS HA coatings aged under static loading at pH 7.2

Table 6-14 presents the significant test results from crystallinity data for the vacuum plasma sprayed coatings aged under static loading at pH 7.2, tested using a Student T-test at the 5 % significance level.

crystallinity	*as-received*	*1 week*	*2 weeks*	*4 weeks*	*10 weeks*	*15 weeks*
as-received		✓	✓	✓	✓	✖
1 week	✓		✓			
2 weeks	✓	✓		✖		
4 weeks	✓		✖		✖	
10 weeks	✓			✖		✓
15 weeks	✖				✓	

Table 6-14 :- Significant test results for VPS HA coatings aged under static loading at pH 7.2

✓ = significantly different

✖ = not significantly different

= not tested

Therefore it was found that all the aged coatings except that aged for fifteen weeks had significantly different crystallinities from that of the as-received coating. There was however no significant change in crystallinity between ageing times except between ten and fifteen weeks ageing.

6.3.3 X-Ray Plane Analysis

Table 6-15 presents a summary of the x-ray plane analysis results for the vacuum plasma sprayed hydroxyapatite coatings aged for various time periods under static loading in Ringer's solution buffered to pH 7.2.

Sample	*Major Compound*	*Significant Compounds*	*Trace Compounds*
as-received	HA	β-TCP	α-TCP, $Ca_4O(PO_4)_2$, $Ca_2P_2O_7$
pH 7.2 x 1	HA	$Ca_4O(PO_4)_2$	β-TCP
pH 7.2 x 2	HA	$Ca_4O(PO_4)_2$	β-TCP, α-TCP, $Ca_2P_2O_7$
pH 7.2 x 4	HA	-	β-TCP , $Ca_4O(PO_4)_2$
pH 7.2 x 10	HA	$Ca_4O(PO_4)_2$	β-TCP, $Ca_2P_2O_7$
pH 7.2 x 15	HA	β-TCP , $Ca_4O(PO_4)_2$	-

Table 6-15 :- X-Ray plane analysis results for VPS HA coatings aged under static loading at pH 7.2

6.3.4 Optical Microscopy

Static loading of VPS HA samples at pH 7.2 appears to have very little effect on the morphology of the coatings. The coatings aged for all time periods (1, 2, 4 and 10 weeks not shown) appeared to have a similar thickness and porosity to the as-received coating. Coatings aged for one week at pH 7.2 still showed the distinct layered structure associated with VPS coatings, were apparently strongly adhered to the substrate and showed no surface modified layer associated with *in-vitro* dissolution. The coating surface showed no obvious increase in roughness and the pure titanium bond layer between the Ti-6Al-4V and the coating itself was still clearly visible. The same general

appearance was observed in coatings aged under static loading for two weeks *in-vitro*. There was again no obvious change in thickness, perhaps a slight increase in porosity, and the coating was still apparently well adhered to the substrate. In this case however a fine black line could be seen running along the cross-section of the coating and occasionally intruding into the coating itself.

This black line could again be seen in some parts of the coating aged for four weeks at pH 7.2 but did not run continuously along the cross-section. In all other respects, the coating aged for four weeks appeared identical in morphology to those aged for one and two weeks. The coating aged for ten weeks at pH 7.2 under static loading still appeared unchanged when compared to the other coatings. There was again no obvious alteration in the morphology of the coating; no change in thickness or porosity and no modified surface layer. Again the fine black line was present running along some regions of the interface between coating and titanium substrate, but this line was not continuous and the coating appeared to be well adhered to the metal.

The coating aged for fifteen weeks is shown here (Figure 6-9) as being representative of the morphology of all the above coatings. Even after this amount of time under static loading at pH 7.2 there seems to be virtually no modification to the cross-sectional appearance of the coating. There is no evidence for alteration of the coating surface, nor any increase in porosity or decrease in coating thickness. The layered structure of the coating is still highly visible and the coating seems to be adhered well to the substrate. The fine black line seen in earlier coatings is again present here, this time running continuously along the length of the coating, as it was in the coating aged for two weeks *in-vitro*.

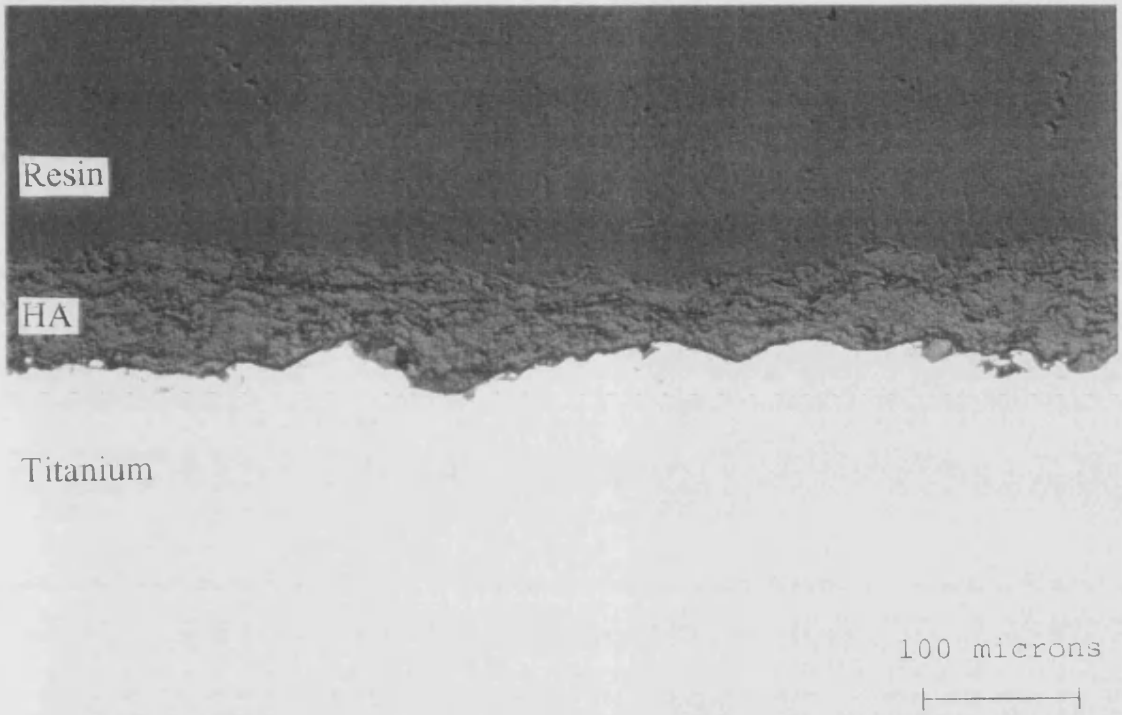

Figure 6-9 :- Optical micrograph showing cross-section through VPS HA coating aged under static loading at pH 7.2 for fifteen weeks

Looking at all the optical micrographs for coatings aged under static loading at pH 7.2 there appears to be no obvious modification to the morphology of the hydroxyapatite coatings, except for a small increase in porosity, even after fifteen weeks in simulated body salt solution.

6.3.5 Scanning Electron Microscopy

The coating aged for one week at pH 7.2 under static loading (Figure 6-10) had a surface morphology similar to that observed in the as-received sample. The surface still supported micro-cracks and a mixture of agglomerated or crystal-like debris and flatter amorphous regions. The coating also seemed to have a lesser amount of this amorphous material on its surface, probably due to the preferential dissolution of this material. The major difference between the two micrographs lay in the appearance of the glassy amorphous regions of the coating. In the aged sample, this amorphous material appeared to have been slightly etched by the *in-vitro* medium and had lost its smooth appearance.

This effect was again observed in the surface of the coating aged for two weeks under static loading at pH 7.2 (not shown). Again the coating had the characteristic two phase morphology, again micro-cracks were seen running along the surface but again the glassy regions were etched, loosing some of their smooth appearance.

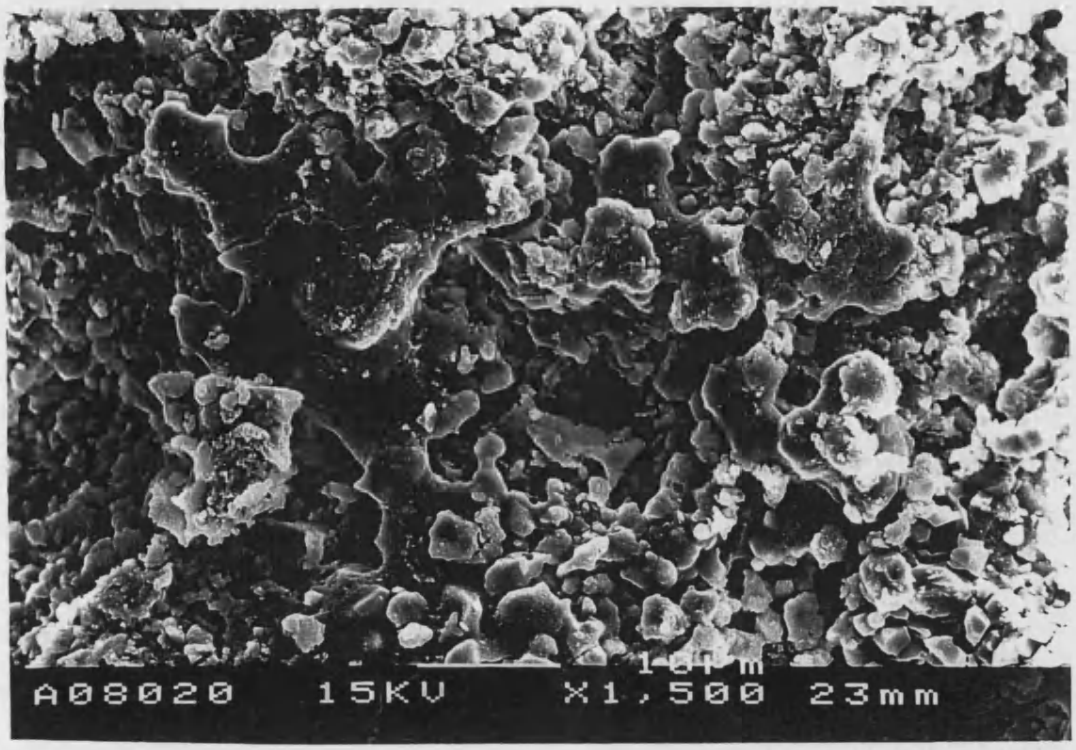

Figure 6-10 :- Scanning electron micrograph showing surface of VPS HA coating aged under static loading at pH 7.2 for one week

This apparent partial dissolution of the amorphous material continued to be observed on the surface of coatings aged for four weeks under static loading at pH 7.2 (not shown). The coating still showed evidence of the two phase morphology associated with VPS coatings but the etching of the glassy regions was even more pronounced that before, leading to the appearance of large pits in the amorphous material. The structure of the amorphous splats seemed to be badly broken down, regions of their surface having been broken up and assuming a lace-like morphology. What remained of the amorphous zones however, still carried micro-cracks whose edges and paths were well defined. The coating aged for ten weeks (not shown) had an appearance very similar to that of the coating aged for four weeks, except for a progression of the apparent dissolution of the

amorphous material. This etching of the amorphous phase greatly increased the roughness of the surface of the coating on a micro-scale. Sharp cracks could again be seen crossing the coating surface but no pull out or loss of coherence in the remaining agglomerated material was apparent.

The surface of the coating aged for fifteen weeks under static loading at pH 7.2 (Figure 6-11) had a different appearance to that of the coatings aged for shorter durations. The dissolved morphology seemed to have taken on a new progression. The pocked amorphous material now appeared to be covered in a three-dimensional deposit giving these zones a coral-like appearance rather than the etched morphology seen previously. The amorphous material did not seem to have been removed completely but rather, after the initial dissolution, a new material had been deposited on the surface. The evidence for this material being deposited after earlier dissolution lay in examination of the appearance of the micro-cracks running across the coating surface. In coatings aged for shorter periods these cracks still appeared to be sharp but in the coating aged for fifteen weeks, the cracks were bridged by the new deposit showing that it had occurred later in the life of the surface.

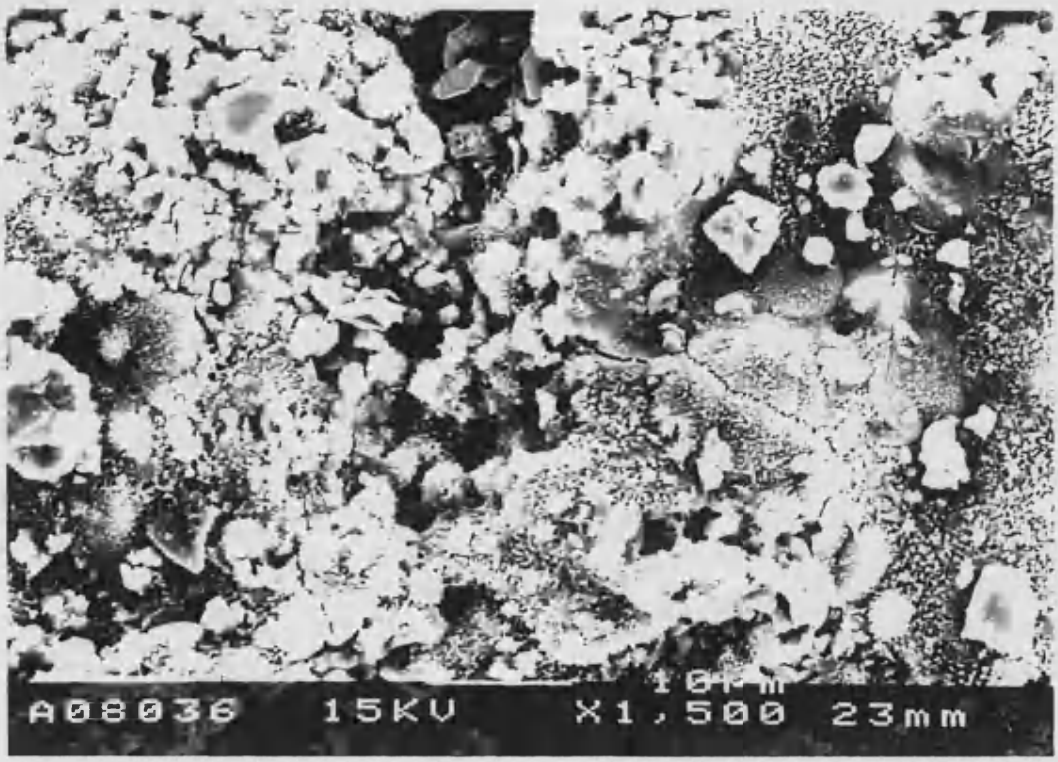

Figure 6-11 :- Scanning electron micrograph showing surface of VPS HA coating aged under static loading at pH 7.2 for fifteen weeks

Observing the degree of modification the surface of the coatings as a whole have undergone, even after fifteen weeks ageing at pH 7.2 it is not surprising that no discernible difference between the appearance of the samples was detectable by optical microscopy. Even the coatings aged for fifteen weeks still showed the flat, glassy amorphous material present, if etched, on its surface, showing the small degree the combination of *in-vitro* medium and static loading affected the coatings.

6.3.6 Coating Thickness Results

Table 6-16 presents a summary of the cross-sectional thickness results for the vacuum plasma sprayed hydroxyapatite coatings aged for various time periods under static loading in Ringer's solution buffered to pH 7.2.

Sample	*No. of tests*	*Mean (μm)*	*Standard Deviation*	*Variance*	*95% Confidence Limits*
as-received	10	57.443	10.621	112.813	56.545 and 58.341
pH 7.2 x 1	10	46.302	13.379	119.002	45.171 and 47.433
pH 7.2 x 2	10	54.299	11.922	142.140	53.282 and 55.297
pH 7.2 x 4	10	58.437	8.886	78.955	57.686 and 59.189
pH 7.2 x 10	10	44.402	12.512	156.557	43.345 and 45.460
pH 7.2 x 15	10	59.545	10.263	105.320	58.678 and 60.413

Table 6-16 :- Cross-sectional thickness results for VPS HA coatings aged under static loading at pH 7.2

Table 6-17 presents the significant test results from thickness data for the vacuum plasma sprayed coatings aged under static loading at pH 7.2, tested using a Student T-test at the 5 % significance level.

thickness	*as-received*	*1 week*	*2 weeks*	*4 weeks*	*10 weeks*	*15 weeks*
as-received		✓	✖	✖	✓	✖
1 week	✓		✖			
2 weeks	✖	✖		✖		
4 weeks	✖		✖		✖	
10 weeks	✓			✖		✓
15 weeks	✖				✓	

Table 6-17 :- Significant test results for VPS HA coatings aged under static loading at pH 7.2

✓ = significantly different

✖ = not significantly different

= not tested

Therefore, it was found that the aged coatings did not have a significantly different thickness to that of the as-received coating except in the case of the coatings aged at pH 7.2 for one week and ten weeks. The was a variable significance in the change in thickness between ageing periods.

6.3.7 Coating Porosity Results

Table 6-18 presents a summary of the cross-sectional porosity results for the vacuum plasma sprayed hydroxyapatite coatings aged for various time periods under static loading in Ringer's solution buffered to pH 7.2.

Sample	*No. of tests*	*Mean (%)*	*Standard Deviation*	*Variance*	*95% Confidence Limits*
as-received	10	4.680	1.817	3.301	3.830 and 5.530
pH 7.2 x 1	10	11.462	3.181	10.121	9.973 and 12.950
pH 7.2 x 2	10	14.413	4.046	16.370	12.519 and 16.306
pH 7.2 x 4	10	15.028	5.518	30.445	12.369 and 17.688
pH 7.2 x 10	10	17.277	5.127	26.283	14.806 and 19.748
pH 7.2 x 15	10	12.758	2.493	6.215	11.556 and 13.960

Table 6-18 :- Cross-sectional porosity results for VPS HA coatings aged under static loading at pH 7.2

Table 6-19 presents the significant test results from porosity data for the vacuum plasma sprayed coatings aged under static loading at pH 7.2, tested using a Student T-test at the 5 % significance level.

porosity	*as-received*	*1 week*	*2 weeks*	*4 weeks*	*10 weeks*	*15 weeks*
as-received		✓	✓	✓	✓	✓
1 week	✓		✓			
2 weeks	✓	✓		✖		
4 weeks	✓		✖		✖	
10 weeks	✓			✖		✓
15 weeks	✓				✓	

Table 6-19 :- Significant test results for VPS HA coatings aged under static loading at pH 7.2

✓ = significantly different

✖ = not significantly different

= not tested

Therefore it was found that there was a significant difference in the porosities between the as-received coating and the aged coatings. There was however found to be a variable significance in the differences in porosity between coatings aged for different time periods.

6.3.8 Surface Roughness (Ra) Results

Table 6-20 presents a summary of the surface roughness results for the vacuum plasma sprayed hydroxyapatite coatings aged for various time periods under static loading in Ringer's solution buffered to pH 7.2.

Sample	*Scan Length (mm)*	*Ra (μm)*	*Rp (μm)*	*Rv (μm)*	*Rt (μm)*
as-received	5.7931	5.5727	18.6202	22.0552	40.6753
pH 7.2 x 1	5.6624	5.3149	19.8147	19.2693	39.0840
pH 7.2 x 2	5.7190	5.8206	21.8111	28.0935	49.9046
pH 7.2 x 4	5.7342	6.1338	21.5537	18.7488	40.3026
pH 7.2 x 10	5.7154	5.0917	14.9056	20.7757	35.6813
pH 7.2 x 15	5.5714	5.2190	19.7435	16.5591	36.3026

Table 6-20 :- Surface roughness results for VPS HA coatings aged under static loading at pH 7.2

6.3.9 Residual Stress Results

Table 6-21 presents a summary of the residual stress analysis results for the vacuum plasma sprayed hydroxyapatite coatings aged for various time periods under static loading in Ringer's solution buffered to pH 7.2.

Sample	*d(c)*	*strain (c) %*	*E (Pa)*	*residual stress (MPa)*
VPS HA powder	1.7209	0.003777	5.5^{09}	-
as-received	1.7200	0.000523	5.5^{09}	2.8764
pH 7.2 x 1	1.7151	0.003370	5.5^{09}	18.5368
pH 7.2 x 2	1.7184	0.001453	5.5^{09}	7.9900
pH 7.2 x 4	1.7169	0.002324	5.5^{09}	12.7840
pH 7.2 x 10	1.7328	0.001655	5.5^{09}	9.2684
pH 7.2 x 15	1.7214	0.000291	5.5^{09}	1.5980

Table 6-21 :- Residual stress results in 004 plane for VPS HA coatings aged under static loading at pH 7.2

6.4 DGUN HA Coatings Aged Under Static Loading at pH 7.2

6.4.1 X-Ray Diffraction Traces

Figure 6-12 presents sections from the x-ray diffraction traces for the detonation gun sprayed hydroxyapatite coatings aged for various time periods under static loading in Ringer's solution buffered to pH 7.2.

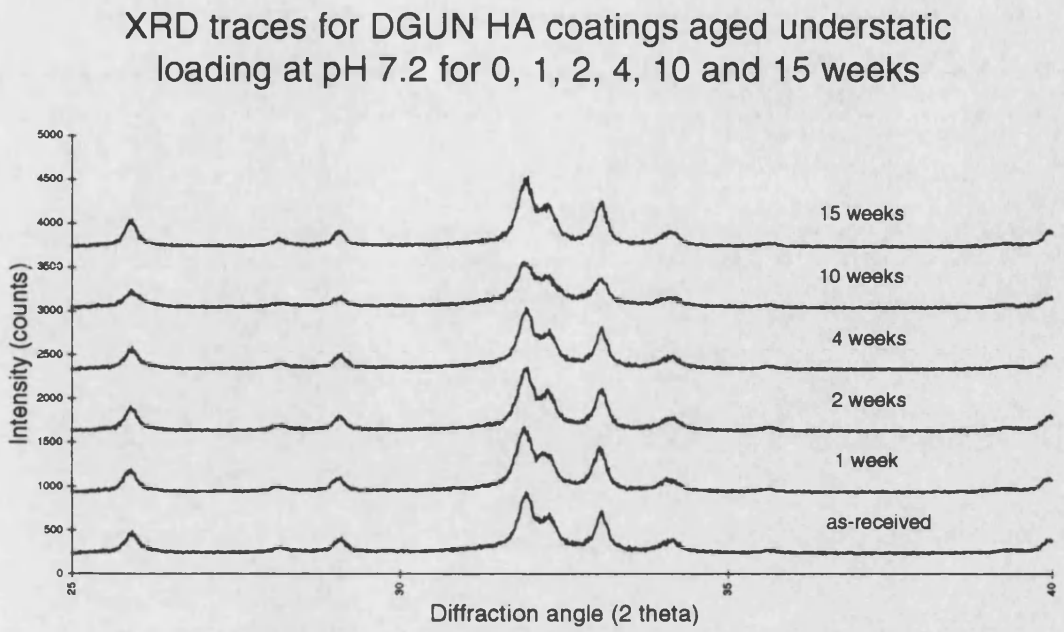

Figure 6-12 :- X-Ray diffraction traces for DGUN HA coatings aged under static loading at pH 7.2

6.4.2 Crystallinity Results

Table 6-22 presents a summary of the crystallinity results for the detonation gun sprayed hydroxyapatite coatings aged for various time periods under static loading in Ringer's solution buffered to pH 7.2.

Sample	*No. of tests*	*Mean (%)*	*Standard Deviation*	*Variance*	*95% Confidence Limits*
as-received	10	38.8604	1.2085	1.4604	37.996 and 39.725
pH 7.2 x 1	10	51.4134	2.0485	4.1965	49.948 and 52.879
pH 7.2 x 2	10	51.4760	0.8567	0.7339	50.863 and 52.089
pH 7.2 x 4	10	48.7117	1.2135	1.4726	47.844 and 49.580
pH 7.2 x 10	10	40.3808	0.5300	0.2809	40.002 and 40.760
pH 7.2 x 15	10	53.5389	1.5939	2.5405	52.399 and 54.679

Table 6-22 :- Crystallinity results for DGUN HA coatings aged under static loading at pH 7.2

Table 6-23 presents the significant test results from crystallinity data for the detonation gun sprayed coatings aged under static loading at pH 7.2, tested using a Student T-test at the 5 % significance level.

crystallinity	*as-received*	*1 week*	*2 weeks*	*4 weeks*	*10 weeks*	*15 weeks*
as-received		✓	✓	✓	✓	✓
1 week	✓		✖			
2 weeks	✓	✖		✓		
4 weeks	✓		✓		✓	
10 weeks	✓			✓		✓
15 weeks	✓				✓	

Table 6-23 :- Significant test results for DGUN HA coatings aged under static loading at pH 7.2

✓ = significantly different

✖ = not significantly different

= not tested

Therefore it was found that all the aged coatings had significantly different crystallinities from that of the as-received coating. All the coatings also had crystallinities which varied significantly from ageing period to ageing period except in the case of the coatings aged for one and two weeks.

6.4.3 X-Ray Plane Analysis

Table 6-24 presents a summary of the x-ray plane analysis results for the detonation gun sprayed hydroxyapatite coatings aged for various time periods under static loading in Ringer's solution buffered to pH 7.2.

Sample	*Major Compound*	*Significant Compounds*	*Trace Compounds*
as-received	HA	β-TCP	α-TCP
pH 7.2 x 1	HA	β-TCP	α-TCP, $Ca_4O(PO_4)_2$
pH 7.2 x 2	HA	-	β-TCP, α-TCP, $Ca_4O(PO_4)_2$
pH 7.2 x 4	HA	-	β-TCP, α-TCP, $Ca_4O(PO_4)_2$
pH 7.2 x 10	HA	-	β-TCP, α-TCP, $Ca_4O(PO_4)_2$
pH 7.2 x 15	HA	β-TCP	α-TCP, $Ca_4O(PO_4)_2$

Table 6-24 :- X-Ray plane analysis results for DGUN HA coatings aged under static loading at pH 7.2

6.4.4 Optical Microscopy

The coating aged for just one week under static loading at pH 7.2 (Figure 6-13) shows some modification in morphology over that of the as-received coating. Although the bulk of the coating appears to be unchanged, i.e. shows no apparent change in thickness or porosity, there has been an obvious modification to the surface layers of the coating. This modified surface layer extends approximately 5 μm into the surface of the coating and has a much more uniform appearance than the bulk of the coating. The coating is still attached to the substrate but there is evidence for delamination at this interface, observed as a black line running virtually continuously along the length of the cross-section. The bulk of the coating still demonstrates the fine lamella structure of the as-received coating and there is no evidence for major coating cracking although two cracks were observed running from the surface of the coating through to the substrate.

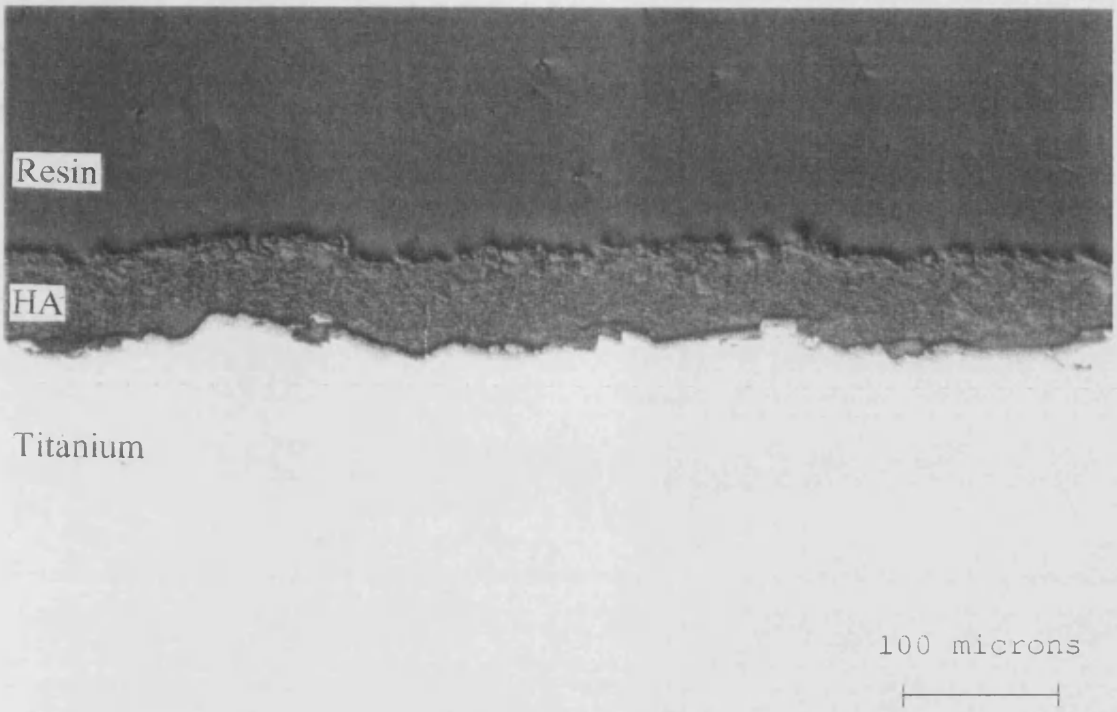

Figure 6-13 :- Optical micrograph showing cross-section through DGUN HA coating aged under static loading at pH 7.2 for one week

The coating aged for two weeks at pH 7.2 under static loading (not shown) again shows this delamination line running continuously along the length of the coating cross-section. However, in this case, no surface modified layer can be discerned. The appearance of this coating is very similar to that of the as-received coating, showing no apparent change in thickness or porosity. Again two surface to substrate cracks were observed but these didn't appear to affect the cohesion of the coating to the substrate. The modified layer however appeared to have returned in the coating aged for four weeks at pH 7.2 under static loading (not shown). Here the layer appeared to be thicker than in the coating aged for two weeks, being approximately 10 μm in thickness. Again, as in the coating aged for one week the remainder of the coating appeared to be unaffected by the ageing medium and overall the coating had a similar thickness and porosity to that of the as-received coating. This coating also demonstrated the thin black interface layer observed in all the other aged coatings but in this case no through thickness micro-cracks were detected.

The coating aged for ten weeks under static loading (not shown) did not show evidence for this dark interface layer and again still appeared to be well adhered to the substrate. As in the case of the coating aged for two weeks, there was no evidence for a surface modified layer and the coating seemed to have a similar thickness to the other aged coatings, a few large pores were however observed. The bulk of the coating again had a similar appearance to that of the other aged coatings and indeed of the as-received coating. The coating aged for fifteen weeks under static loading (Figure 6-14) again showed no evidence for a large modified surface layer. The extreme outer coating surface however did seem to have an increased microscopic roughness however which might be indicative of surface dissolution. There was again no real evidence of a dark interlayer between the substrate and the coating, the coating again appearing to be well adhered to the substrate. Again the bulk of the coating appeared to be very little altered in comparison both to the other aged coatings and the as-received coating.

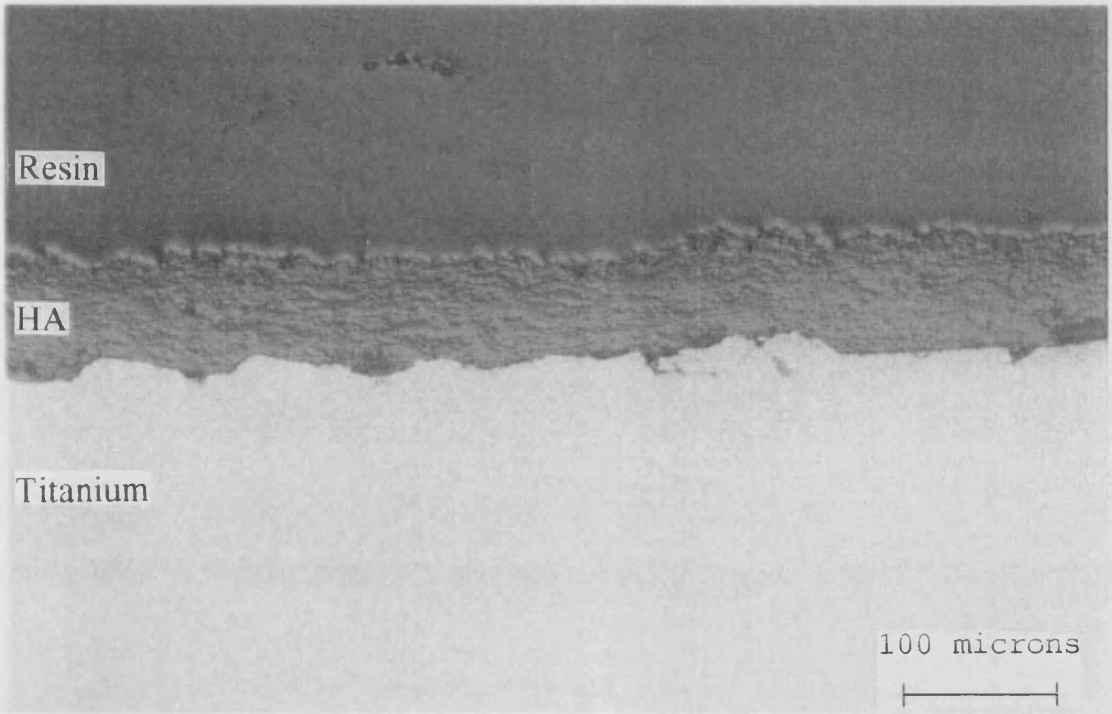

Figure 6-14 :- Optical micrograph showing cross-section through DGUN HA coating aged under static loading at pH 7.2 for fifteen weeks

Overall, the effect of both ageing medium and static loading appeared to have a minimal impact on the cross-sectional morphology of the DGUN coatings. There was some evidence for a small increase in porosity levels in the coatings but no change in thickness was observed. In some cases there appeared to be a modified layer descending for 5 - 10 μm into the surface of the coating but this effect might be an artefact of the polishing procedure.

6.4.5 Scanning Electron Microscopy

The surface of the coating aged under static loading at pH 7.2 for one week (Figure 6-15) shows a considerable change in morphology over the as-received coating. The principal difference between this coating and the control sample lies in the reduction in the total surface area covered by the glassy, amorphous material. It appears that this material has been etched away from the surface of the coating leaving more of the agglomerated and crystalline material exposed. Large micro-cracks are visible in the sample surface, the edges of these cracks being smoothed by the dissolution process. Deep pores can be seen in the surface revealing material in lower coating levels exposed to the medium.

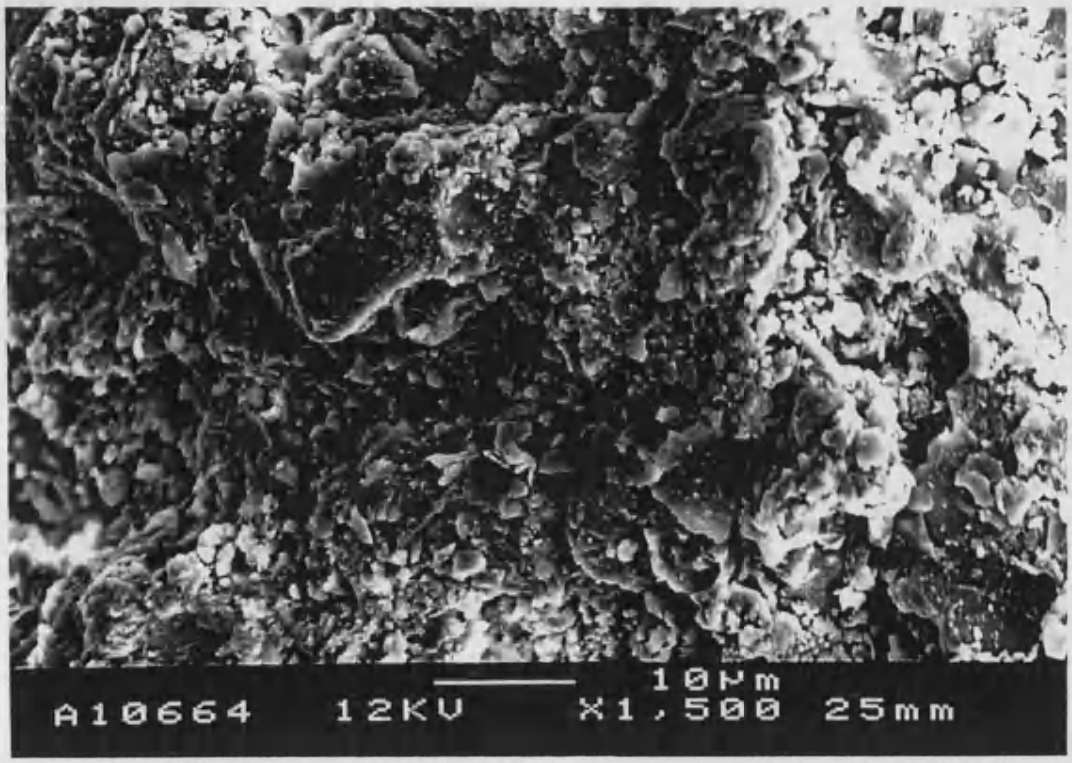

Figure 6-15 :- Scanning electron micrograph showing surface of DGUN HA coating aged under static loading at pH 7.2 for one week

Looking at the surface of the coating aged for two weeks at pH 7.2 under static load (not shown) we can see another change in surface morphology. Here the surface seems to be rougher in nature, possibly as a result of the loss of agglomerates from regions on the coating surface. There are however regions of glassy material visible in the pits in the coating surface although these regions are starting to show signs of etching by the in-vitro medium. Micro-cracks are still visible, running through the amorphous regions of the coating. Yet again, we see a change in morphology for the coating aged for four weeks (not shown). Here we can see only very small amounts of smooth hydroxyapatite, rather, regions which appeared to have once been amorphous in nature are now covered with small, nodular, cauliflower-like protuberances. These protuberances have the appearance of crystalline hydroxyapatite. The edges of some of these crystallites can be seen to be overlying micro-cracks on the surface of the coating which is evidence that the crystallites were deposited at a later time and were not present initially after spraying. The coating surface again appears to be rough, having large height differences between the surface of agglomerated material and the crystalline

nodules below. On the surface of the sample aged for ten weeks under static loading at pH 7.2 (not shown) the morphology of the coating seems to have reverted to that of the coating aged for just one week. Here again we see little evidence for the amorphous material, only rough agglomerated regions remaining. There is also no evidence for the cauliflower-like deposits on the coating surface. It seems that the re-precipitated nodular material has been lost from the surface leaving only the etched material below.

The coating aged for fifteen weeks (Figure 6-16) again has the appearance of the coating aged for four weeks in the *in-vitro* ageing medium. Here again glassy, amorphous regions are visible on the coating surface although again, they are slightly etched. Sharp edged micro-cracks are again visible running through the amorphous regions. It is almost as if the effect of the ageing medium is cyclic in nature. There is again evidence of the loss of material from the surface of the coating and deep pores are clearly visibly suggesting the loss of regions of the coating.

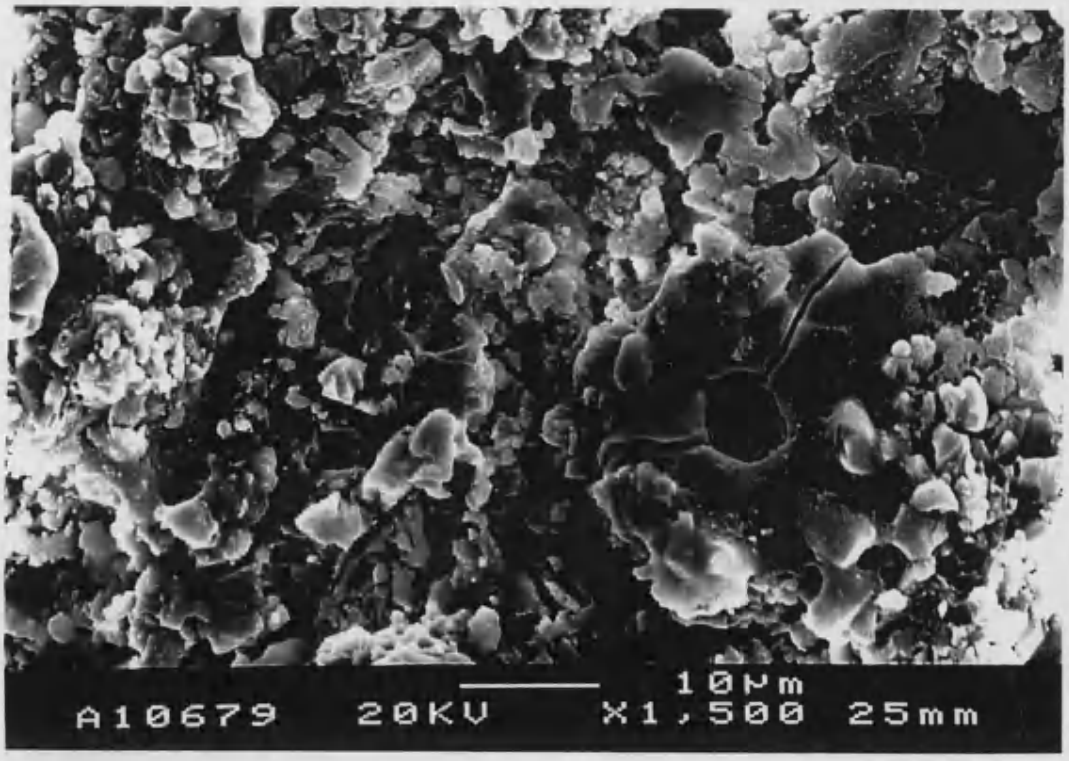

Figure 6-16 :- Scanning electron micrograph showing surface of DGUN HA coating aged under static loading at pH 7.2 for fifteen weeks

It appears that the effect of the ageing medium is cyclic in nature. The amorphous regions on the coating surface are etched by the *in-vitro* medium, crystalline hydroxyapatite is re-deposited on the coating surface, this new layer then breaks away from the surface and a fresh layer of coating is exposed to the environment.

6.4.6 Coating Thickness Results

Table 6-25 presents a summary of the cross-sectional thickness results for the detonation gun sprayed hydroxyapatite coatings aged for various time periods under static loading in Ringer's solution buffered to pH 7.2.

Sample	*No. of tests*	*Mean (μm)*	*Standard Deviation*	*Variance*	*95% Confidence Limits*
as-received	10	71.2908	8.4365	71.1752	70.578 and 72.004
pH 7.2 x 1	10	44.9667	7.0955	50.3458	44.367 and 45.567
pH 7.2 x 2	10	68.7076	8.5169	72.5375	67.988 and 69.428
pH 7.2 x 4	10	54.5449	8.6923	75.553	53.810 and 55.280
pH 7.2 x 10	10	63.2346	10.9232	119.3152	62.311 and 64.158
pH 7.2 x 15	10	65.6057	11.1131	123.5013	64.666 and 66.545

Table 6-25 :- Cross-sectional thickness results for DGUN HA coatings aged under static loading at pH 7.2

Table 6-26 presents the significant test results from thickness data for the detonation gun sprayed coatings aged under static loading at pH 7.2, tested using a Student T-test at the 5 % significance level.

thickness	*as-received*	*1 week*	*2 weeks*	*4 weeks*	*10 weeks*	*15 weeks*
as-received		✓	✖	✓	✓	✖
1 week	✓		✓			
2 weeks	✖	✓		✓		
4 weeks	✓		✓		✓	
10 weeks	✓			✓		✖
15 weeks	✖				✖	

Table 6-26 :- Significant test results for DGUN HA coatings aged under static loading at pH 7.2

✓ = significantly different

✖ = not significantly different

= not tested

Therefore, it was found that the aged coatings had significantly different thicknesses to that of the as-received coating except in the case of the coating aged at pH 7.2 for fifteen weeks. The coatings were also significantly different from each other between time periods except in the case of coatings aged between ten and fifteen weeks.

6.4.7 Coating Porosity Results

Table 6-27 presents a summary of the cross-sectional porosity results for the detonation gun sprayed hydroxyapatite coatings aged for various time periods under static loading in Ringer's solution buffered to pH 7.2.

Sample	*No. of tests*	*Mean (%)*	*Standard Deviation*	*Variance*	*95% Confidence Limits*
as-received	10	1.2605	0.7242	0.5245	0.922 and 1.600
pH 7.2 x 1	10	3.1150	2.9828	8.8969	1.719 and 4.511
pH 7.2 x 2	10	2.5451	1.6422	2.6967	1.777 and 3.134
pH 7.2 x 4	10	3.7680	1.6703	2.7900	2.986 and 4.550
pH 7.2 x 10	10	6.6760	1.6000	2.5599	5.927 and 7.425
pH 7.2 x 15	10	7.2495	2.3853	5.6896	6.133 and 8.366

Table 6-27 :- Cross-sectional porosity results for DGUN HA coatings aged under static loading at pH 7.2

Table 6-28 presents the significant test results from porosity data for the detonation gun sprayed coatings aged under static loading at pH 7.2, tested using a Student T-test at the 5 % significance level.

porosity	*as-received*	*1 week*	*2 weeks*	*4 weeks*	*10 weeks*	*15 weeks*
as-received		✓	✓	✓	✓	✓
1 week	✓		✖			
2 weeks	✓	✖		✓		
4 weeks	✓		✓		✓	
10 weeks	✓			✓		✖
15 weeks	✓				✖	

Table 6-28 :- Significant test results for DGUN HA coatings aged under static loading at pH 7.2

✓ = significantly different

✖ = not significantly different

= not tested

Therefore it was found that there was a significant difference in the porosities between the as-received coating and the aged coatings. There was also found to be a variable significance in the differences in porosity between coatings aged for different time periods.

6.4.8 Surface Roughness (Ra) Results

Table 6-29 presents the surface roughness results for the detonation gun sprayed hydroxyapatite coatings aged for various time periods under static loading in Ringer's solution buffered to pH 7.2.

Sample	*Scan Length (mm)*	*Ra (μm)*	*Rp (μm)*	*Rv (μm)*	*Rt (μm)*
as-received	11.4025	5.9837	30.1268	19.2205	49.3472
pH 7.2 x 1	11.3829	5.2991	23.0479	19.5471	42.5950
pH 7.2 x 2	11.4247	5.9655	24.9890	22.6834	47.6724
pH 7.2 x 4	11.3156	5.2932	22.0718	19.3512	41.4230
pH 7.2 x 10	11.1374	5.0528	28.7894	17.7288	46.5183
pH 7.2 x 15	11.2832	5.1501	25.2478	17.7199	42.9677

Table 6-29 :- Surface roughness results for DGUN HA coatings aged under static loading at pH 7.2

6.4.9 Residual Stress Results

Table 6-30 presents the residual stress analysis results for the detonation gun sprayed hydroxyapatite coatings aged for various time periods under static loading in Ringer's solution buffered to pH 7.2.

Sample	*d(c)*	*strain (c) %*	*E (Pa)*	*residual stress (MPa)*
DGUN HA powder	1.7172	0.003203	5.5^{09}	-
as-received	1.7220	0.002795	5.5^{09}	15.3739
pH 7.2 x 1	1.7215	0.002504	5.5^{09}	13.7724
pH 7.2 x 2	1.7227	0.003203	5.5^{09}	17.6159
pH 7.2 x 4	1.7212	-0.002330	5.5^{09}	-12.8116
pH 7.2 x 10	1.7094	0.001980	5.5^{09}	10.8898
pH 7.2 x 15	1.7182	0.000582	5.5^{09}	3.2029

Table 6-30 :- Residual stress results in 004 plane for DGUN HA coatings aged under static loading at pH 7.2

6.5 VPS HA Coatings Aged Under Static Loading at pH 4.5

6.5.1 X-Ray Diffraction Traces

Figure 6-17 presents sections from the x-ray diffraction traces for the vacuum plasma sprayed hydroxyapatite coatings aged for various time periods in Ringer's solution buffered to pH 4.5.

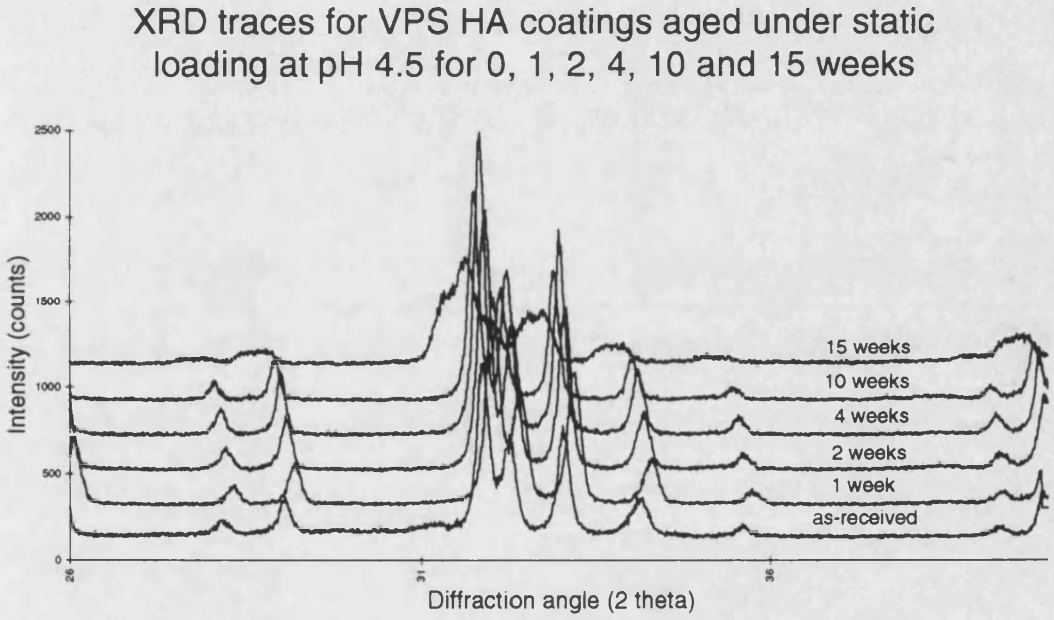

Figure 6-17 :- X-Ray diffraction traces for VPS HA coatings aged under static loading at pH 4.5

6.5.2 Crystallinity Results

Table 6-31 presents a summary of the crystallinity results for the vacuum plasma sprayed hydroxyapatite coatings aged for various time periods under static loading in Ringer's solution buffered to pH 4.5.

Sample	*No. of tests*	*Mean (%)*	*Standard Deviation*	*Variance*	*95% Confidence Limits*
as-received	10	60.9231	5.8287	33.9742	60.290 and 61.556
pH 4.5 x 1	10	75.0961	7.8249	61.2284	74.467 and 75.726
pH 4.5 x 2	10	79.6754	8.7791	77.0725	79.047 and 80.304
pH 4.5 x 4	10	76.1132	5.6623	32.0612	75.480 and 76.747
pH 4.5 x 10	10	73.5217	6.8422	46.8162	72.890 and 74.152
pH 4.5 x 15	10	56.8632	7.3175	53.5454	56.233 and 57.493

Table 6-31 :- Crystallinity results for VPS HA coatings aged under static loading at pH 4.5

Table 6-32 presents the significant test results from crystallinity data for the vacuum plasma sprayed coatings aged under static loading at pH 4.5, tested using a Student T-test at the 5 % significance level.

crystallinity	*as-received*	*1 week*	*2 weeks*	*4 weeks*	*10 weeks*	*15 weeks*
as-received		✓	✓	✓	✓	✖
1 week	✓		✖			
2 weeks	✓	✖		✖		
4 weeks	✓		✖		✖	
10 weeks	✓			✖		✓
15 weeks	✖				✓	

Table 6-32 :- Significant test results for VPS HA coatings aged under static loading at pH 4.5

✓ = significantly different

✖ = not significantly different

= not tested

Therefore it was found that all the aged coatings except those aged for fifteen weeks had significantly different crystallinities from that of the as-received coating. The was however no significant change in crystallinity between ageing times except between ten and fifteen weeks ageing.

6.5.3 X-Ray Plane Analysis

Table 6-33 presents a summary of the x-ray plane analysis results for the vacuum plasma sprayed hydroxyapatite coatings aged for various time periods under static loading in Ringer's solution buffered to pH 4.5.

Sample	*Major Compound*	*Significant Compounds*	*Trace Compounds*
as-received	HA	β-TCP	α-TCP, $Ca_4O(PO_4)_2$, $Ca_2P_2O_7$
pH 4.5 x 1	HA	-	β-TCP, $Ca_4O(PO_4)_2$, $Ca_2P_2O_7$
pH 4.5 x 2	HA	β-TCP, $Ca_4O(PO_4)_2$	-
pH 4.5 x 4	HA	-	β-TCP, $Ca_4O(PO_4)_2$
pH 4.5 x 10	HA	-	β-TCP, α-TCP, $Ca_2P_2O_7$
pH 4.5 x 15	HA	β-TCP, $Ca_4O(PO_4)_2$	α-TCP, $Ca_4O(PO_4)_2$

Table 6-33 :- X-Ray plane analysis results for VPS HA coatings aged under static loading at pH 4.5

6.5.4 Optical Microscopy

After ageing in solution for one week at pH 4.5 under static loading (Figure 6-18), the VPS HA coatings did not seem to be dramatically altered when compared with the as-received coatings. Cross-sectional analysis of the coatings showed no obvious changes in either thickness or porosity for these materials, nor did there seem to be any modification to the surface layers of the coatings when viewed in cross-section. A difference can still be observed between phases in the cross-section but the layered morphology of the coatings is not as clear as in the case of the as-received coating. This is an incongruous observation since the coatings aged with no load show considerable alteration even after this short exposure to the medium.

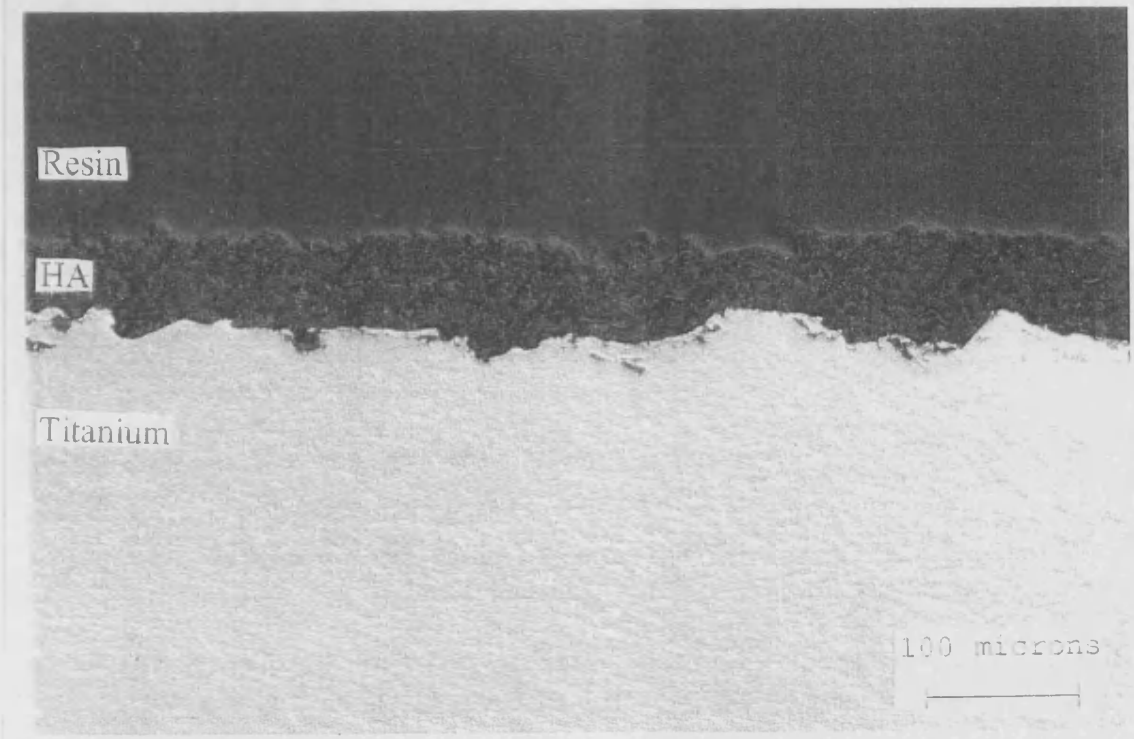

Figure 6-18 :- Optical micrograph showing cross-section through VPS HA coating aged under static loading at pH 4.5 for one week

A similar effect can be observed in the coating aged for two weeks at pH 4.5 under static loading (not shown). Again the coating shows no signs of thinning or of a surface modified layer although the coating does seem to have a higher porosity than the as-received coating. Again different phases can be observed in the coating but the layered morphology is not clear.

The coatings aged for four weeks and for ten weeks (not shown) show a progression of the effects observed in the coatings aged under static loading for shorter durations. The coatings show evidence for a progressive increase in porosity and the coatings aged for four weeks appear to have thinned considerably. Both coatings have a considerably rougher surface but still demonstrate no evidence for a modified surface layer. Both these coatings appear to have been considerably affected by the ageing medium.

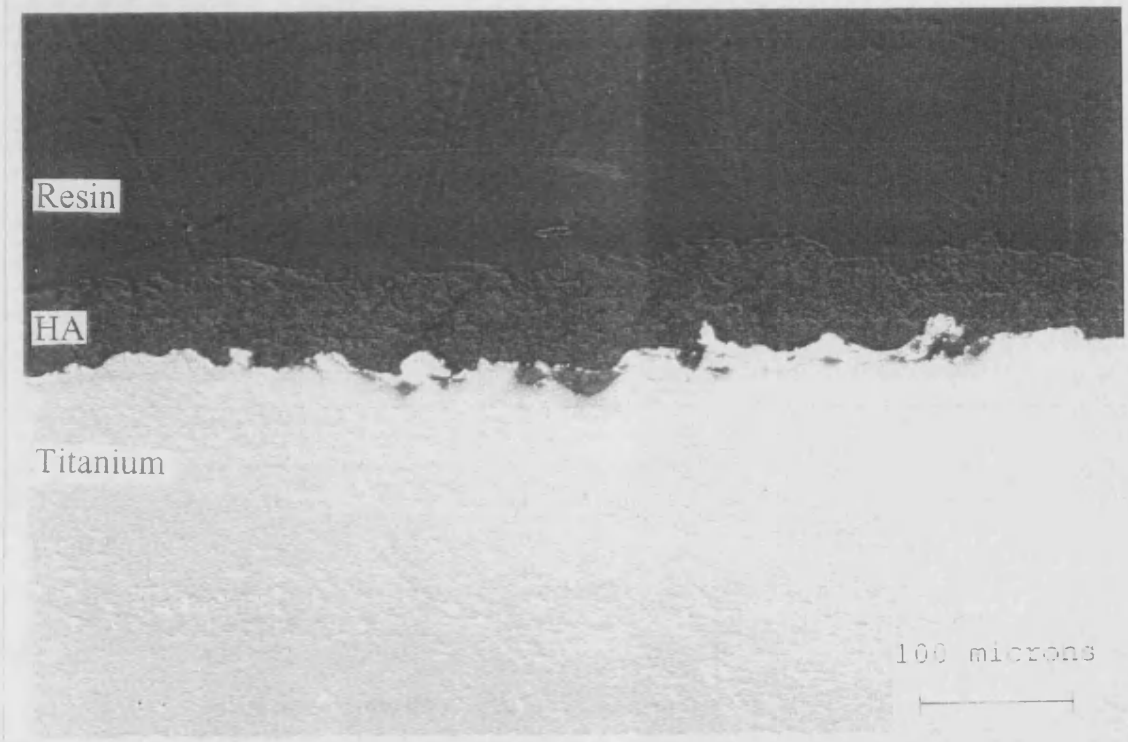

Figure 6-19 :- Optical micrograph showing cross-section through VPS HA coating aged under static loading at pH 4.5 for fifteen weeks

The coating aged for fifteen weeks at pH 4.5 under static loading (Figure 6-19) has an appearance which is remarkably similar to that of the coating aged for just one week. The coating still has an apparently unaffected thickness although a higher porosity than was determined for the as-received coating. There is again no evidence of gross dissolution of the coating surface (unlike in the coatings aged for shorter durations) and the layered morphology and substrate bond layer can still be seen.

Variations in the appearances of these coatings aged for different time periods make it difficult to appreciate a progressive effect of both ageing and static loading. Coatings aged for one and fifteen weeks appear to have survived the attack of the *in-vitro* medium but coatings aged for durations in between these show obvious signs of various degrees of damage.

6.5.5 Scanning Electron Microscopy

Looking at the surface of the vacuum plasma sprayed coatings which had been aged under static loading at pH 4.5 for one week (Figure 6-20) the damage caused to the coating as a result of the imposed environment can be seen. Although the coating still demonstrates the two phase morphology associated with this coating type, the flat, glassy regions show signs of etching and have a lace-like appearance at the region edges. Micro-cracks run along the amorphous regions but these crack do not appear to be more numerous or larger than those observed on the surface of the as-received coating.

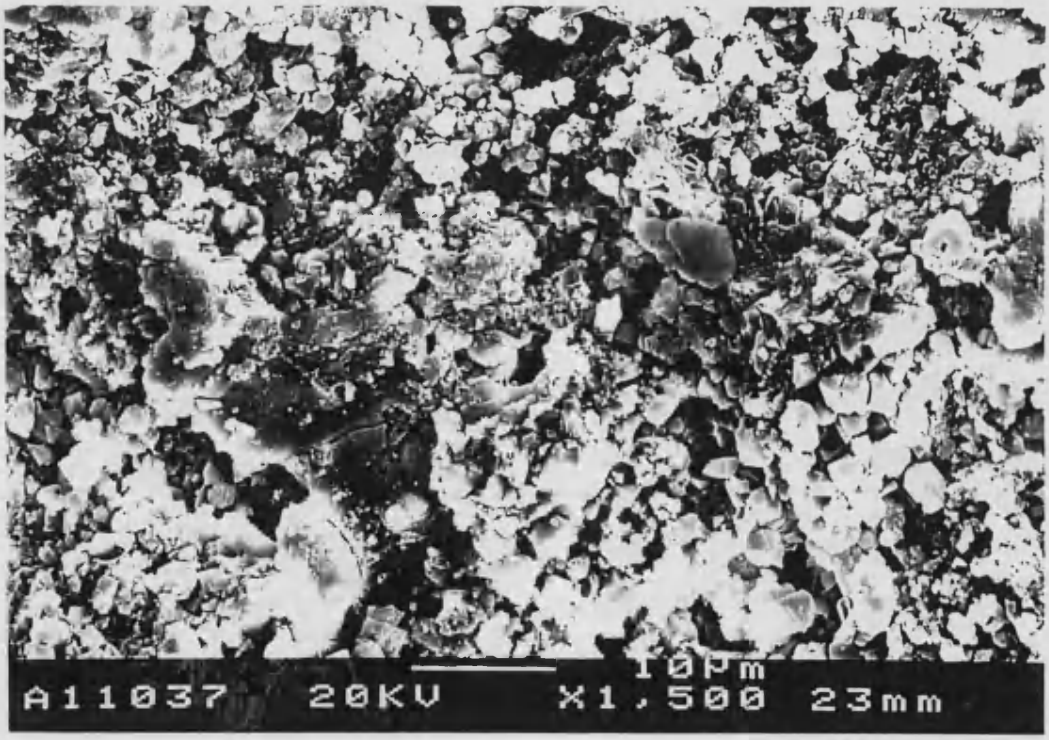

Figure 6-20 :- Scanning electron micrograph showing surface of VPS HA coating aged under static loading at pH 4.5 for one week

This slight dissolution appears to have been accentuated by continued exposure to the *in-vitro* solution. The coating aged for two weeks under static loading at pH 4.5 (not shown) still had areas of amorphous material but these have been more severely etched than those found on the surface of the coatings aged for a shorter duration. There is also evidence that some of the material has fallen away from the coating surface

leaving large, deep pores on the coating surface. This surface appears to be much rougher on a micro-scale that either the as-received coating or the coating aged for one week at pH 4.5.

The coating aged for four weeks (not shown) again shows a progression of the etching effect. In this sample, there is very little smooth amorphous material still to be seen on the coating surface. This etching gives the coating a very rough background microstructure although the overall surface appearance is not extremely rough itself. Again large pores can be seen in the surface which appear to have been formed by the loss of chunks of the coating. Micro-cracks can still be seen running over the areas which are covered by the badly etched glassy phase.

The surface of the coatings aged for ten weeks at pH 4.5 (not shown) show no signs of the smooth, glassy material characteristic of the as-received coating. The progressive etching of this amorphous material has resulted in its complete loss from the surface after this extended time. As seen in the coatings aged for shorter durations, there are large pores in the surface seeming to have resulted from the falling away of poorly cohered material in the surface layers. Micro-cracks present in the surface of this coating appear to be extremely large in nature, having a width of approximately 3 μm in places. It appears that the micro-cracks have been widened by the same dissolution processes attacking the rest of the coating.

The coating aged for fifteen weeks under static loading at pH 4.5 (Figure 6-21) has an appearance not unlike that of the coating aged with no applied load for eight weeks at the same pH. The regions which apparently used to be covered in amorphous material support a myriad of fine nodules. These have a appearance similar to a smaller version of the cauliflower-like protuberances seen in the coatings aged at pH 4.5 with no applied load and could correspond to the nucleation sites for these nodules. Large micro-cracks can still be seen running across the surface of the coating.

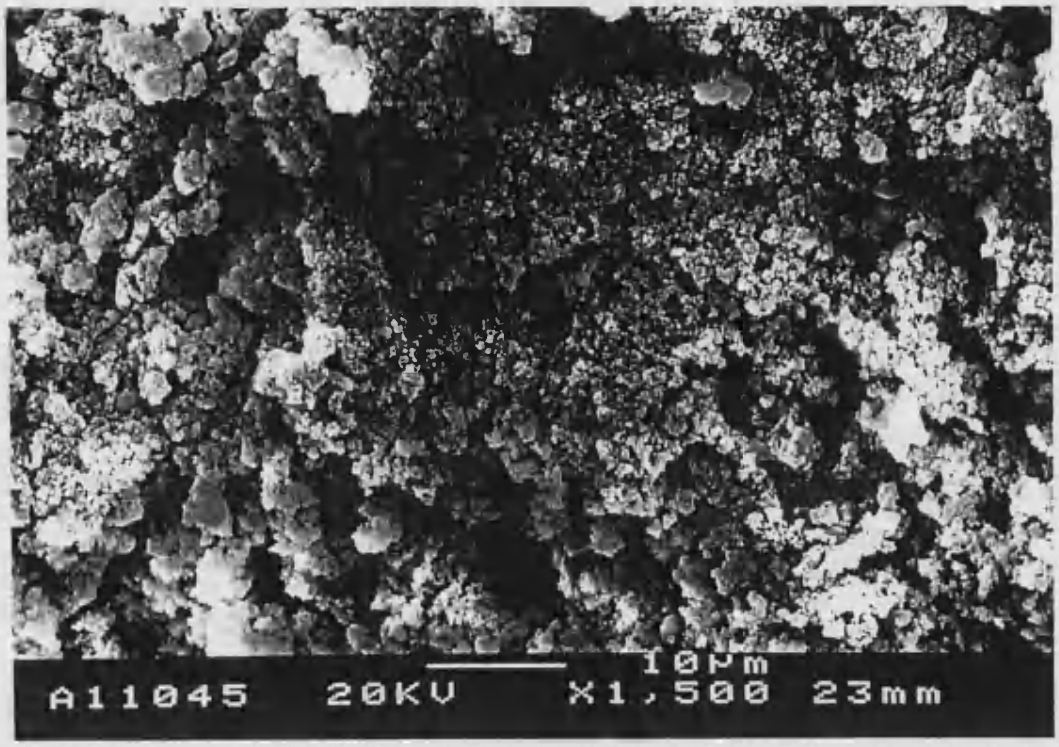

Figure 6-21 :- Scanning electron micrograph showing surface of VPS HA coating aged under static loading at pH 4.5 for fifteen weeks

In contrast to the observations made of the polished cross-sections through the vacuum plasma sprayed coatings aged under static loading at pH 4.5, a progressive surface modification process can be observed by scanning electron microscopy. Dissolution of the amorphous phases on the coating surface and the possible beginnings of the formation of the cauliflower like protuberances seen on the surfaces of coatings aged at pH 4.5 with no applied load can be observed to progress in magnitude with ageing time.

6.5.6 Coating Thickness Results

Table 6-34 presents a summary of the cross-sectional thickness results for the vacuum plasma sprayed hydroxyapatite coatings aged for various time periods under static loading in Ringer's solution buffered to pH 4.5.

Sample	*No. of tests*	*Mean (μm)*	*Standard Deviation*	*Variance*	*95% Confidence Limits*
as-received	10	57.443	10.621	112.813	56.545 and 58.341
pH 4.5 x 1	10	61.369	13.035	169.922	60.267 and 62.471
pH 4.5 x 2	10	57.408	11.412	130.230	56.444 and 58.373
pH 4.5 x 4	10	42.722	8.783	77.141	41.980 and 43.465
pH 4.5 x 10	10	59.507	9.476	89.174	58.706 and 60.308
pH 4.5 x 15	10	53.309	10.040	100.792	52.460 and 54.158

Table 6-34 :- Cross-sectional thickness results for VPS HA coatings aged under static loading at pH 4.5

Table 6-35 presents the significant test results from thickness data for the vacuum plasma sprayed coatings aged under static loading at pH 4.5, tested using a Student T-test at the 5 % significance level.

thickness	*as-received*	*1 week*	*2 weeks*	*4 weeks*	*10 weeks*	*15 weeks*
as-received		✖	✖	✓	✖	✖
1 week	✖		✖			
2 weeks	✖	✖		✓		
4 weeks	✓		✓		✓	
10 weeks	✖			✓		✖
15 weeks	✖				✖	

Table 6-35 :- Significant test results for VPS HA coatings aged under static loading at pH 4.5

✓ = significantly different

✖ = not significantly different

= not tested

Therefore, it was found that the aged coatings did not have a significantly different thickness to that of the as-received coating except in the case of the coatings aged at pH 4.5 for four weeks. The was a variable significance in the change in thickness between ageing periods.

6.5.7 Coating Porosity Results

Table 6-36 presents a summary of the cross-sectional porosity results for the vacuum plasma sprayed hydroxyapatite coatings aged for various time periods under static loading in Ringer's solution buffered to pH 4.5.

Sample	*No. of tests*	*Mean (%)*	*Standard Deviation*	*Variance*	*95% Confidence Limits*
as-received	10	4.680	1.817	3.301	3.830 and 5.530
pH 4.5 x 1	10	6.753	2.565	6.579	5.516 and 7.989
pH 4.5 x 2	10	8.870	3.166	10.008	7.389 and 10.350
pH 4.5 x 4	10	11.874	4.054	16.432	9.920 and 13.828
pH 4.5 x 10	10	13.952	4.118	16.961	11.967 and 15.937
pH 4.5 x 15	10	28.687	5.460	29.810	26.055 and 31.318

Table 6-36 :- Cross-sectional porosity results for VPS HA coatings aged under static loading at pH 4.5

Table 6-37 presents the significant test results from porosity data for the vacuum plasma sprayed coatings aged under static loading at pH 4.5, tested using a Student T-test at the 5 % significance level.

porosity	*as-received*	*1 week*	*2 weeks*	*4 weeks*	*10 weeks*	*15 weeks*
as-received		✓	✓	✓	✓	✓
1 week	✓		✓			
2 weeks	✓	✓		✓		
4 weeks	✓		✓		✓	
10 weeks	✓			✓		✓
15 weeks	✓				✓	

Table 6-37 :- Significant test results for VPS HA coatings aged under static loading at pH 4.5

✓ = significantly different

✖ = not significantly different

= not tested

Therefore it was found that there was a significant difference in the porosities between the as-received coating and the aged coatings. There was also found to be a significant difference in porosity levels between coatings aged for different time periods.

6.5.8 Surface Roughness (Ra) Results

Table 6-38 presents a summary of the surface roughness results for the vacuum plasma sprayed hydroxyapatite coatings aged for various time periods under static loading in Ringer's solution buffered to pH 4.5.

Sample	*Scan Length (mm)*	*Ra (μm)*	*Rp (μm)*	*Rv (μm)*	*Rt (μm)*
as-received	5.7931	5.5727	18.6202	22.0552	40.6753
pH 4.5 x 1	5.4192	4.9259	17.4863	14.9921	32.4783
pH 4.5 x 2	5.2988	4.6398	18.4209	14.9156	33.3365
pH 4.5 x 4	5.3557	5.4600	18.0792	17.5597	35.6389
pH 4.5 x 10	5.2696	4.3879	11.9518	15.8955	27.8472
pH 4.5 x 15	5.2506	4.7502	14.4931	13.0703	27.5634

Table 6-38 :- Surface roughness results for VPS HA coatings aged under static loading at pH 4.5

6.5.9 Residual Stress Results

Table 6-39 presents a summary of the residual stress analysis results for the vacuum plasma sprayed hydroxyapatite coatings aged for various time periods under static loading in Ringer's solution buffered to pH 4.5.

Sample	*d(c)*	*strain (c) %*	*E (Pa)*	*residual stress (MPa)*
VPS HA powder	1.7209	0.003777	5.5^{09}	-
as-received	1.7200	0.000523	5.5^{09}	2.8764
pH 4.5 x 1	1.7157	0.003022	5.5^{09}	16.6192
pH 4.5 x 2	1.7177	0.001859	5.5^{09}	10.2272
pH 4.5 x 4	1.7209	0	5.5^{09}	0
pH 4.5 x 10	1.7235	0.001511	5.5^{09}	8.3096
pH 4.5 x 15	1.7252	0.002499	5.5^{09}	13.7428

Table 6-39 :- Residual stress results in 004 plane for VPS HA coatings aged under static loading at pH 4.5

6.6 DGUN HA Coatings Aged Under Static Loading at pH 4.5

6.6.1 X-Ray Diffraction Traces

Figure 6-22 presents sections from the x-ray diffraction traces for the detonation gun sprayed hydroxyapatite coatings aged for various time periods under static loading in Ringer's solution buffered to pH 4.5.

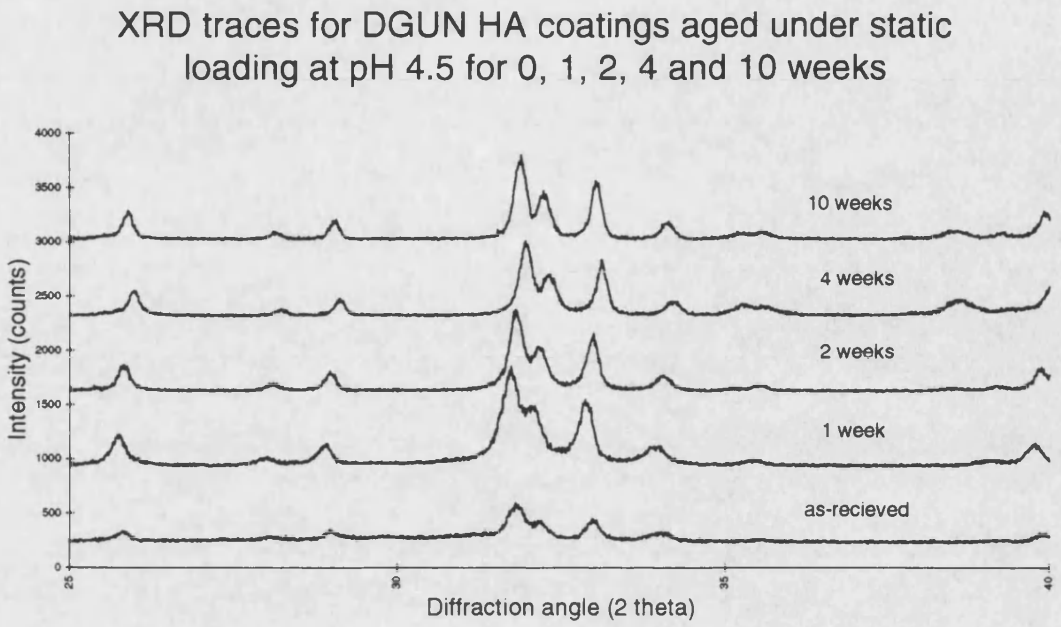

Figure 6-22 :- X-Ray diffraction traces for DGUN HA coatings aged under static loading at pH 4.5

6.6.2 Crystallinity Results

Table 6-40 presents a summary of the crystallinity results for the detonation gun sprayed hydroxyapatite coatings aged for various time periods under static loading in Ringer's solution buffered to pH 4.5.

Sample	*No. of tests*	*Mean (%)*	*Standard Deviation*	*Variance*	*95% Confidence Limits*
as-received	10	38.8604	1.2085	1.4604	37.996 and 39.725
pH 4.5 x 1	10	51.7558	1.8080	3.2688	50.463 and 53.049
pH 4.5 x 2	10	57.9780	1.4268	2.0357	56.957 and 58.999
pH 4.5 x 4	10	59.8613	1.9097	3.6468	58.495 and 61.227
pH 4.5 x 10	10	60.5370	0.9946	0.9892	59.826 and 61.249
pH 4.5 x 15	10	n / a *	n / a	n / a	n / a

Table 6-40 :- Crystallinity results for DGUN HA coatings aged under static loading at pH 4.5

* The coating aged at pH 4.5 for fifteen weeks disintegrated on removal from the tank and thus could not be analysed.

Table 6-41 presents the significant test results from crystallinity data for the detonation gun sprayed coatings aged under static loading at pH 4.5, tested using a Student T-test at the 5 % significance level.

crystallinity	*as-received*	*1 week*	*2 weeks*	*4 weeks*	*10 weeks*	*15 weeks*
as-received		✓	✓	✓	✓	
1 week	✓		✓			
2 weeks	✓	✓		✓		
4 weeks	✓		✓		✖	
10 weeks	✓			✖		
15 weeks						

Table 6-41 :- Significant test results for DGUN HA coatings aged under static loading at pH 4.5

✓ = significantly different

✖ = not significantly different

= not tested

Therefore it was found that all the aged coatings had significantly different crystallinities from that of the as-received coating. All the coatings also had crystallinities which varied significantly from ageing period to ageing period except in the case of the coatings aged between four and ten weeks.

6.6.3 X-Ray Plane Analysis

Table 6-42 presents a summary of the x-ray plane analysis results for the detonation gun sprayed hydroxyapatite coatings aged for various time periods under static loading in Ringer's solution buffered to pH 4.5.

Sample	*Major Compound*	*Significant Compounds*	*Trace Compounds*
as-received	HA	β-TCP	α-TCP
pH 4.5 x 1	HA	-	α-TCP, β-TCP, $Ca_4O(PO_4)_2$
pH 4.5 x 2	HA	β-TCP	α-TCP, $Ca_4O(PO_4)_2$
pH 4.5 x 4	HA	-	α-TCP, β-TCP, $Ca_4O(PO_4)_2$
pH 4.5 x 10	HA	β-TCP	α-TCP, $Ca_4O(PO_4)_2$
pH 4.5 x 15	n / a *	n / a	n / a

Table 6-42 :- X-Ray plane analysis results for DGUN HA coatings aged under static loading at pH 4.5

* The coating aged at pH 4.5 for fifteen weeks disintegrated on removal from the tank and thus could not be analysed.

6.6.4 Optical Microscopy

Optical micrographs showing polished cross-sections through DGUN HA coatings which have been aged for one week under static loading at pH 4.5 (Figure 6-23) show little perceivable change in overall cross-sectional thickness over the as-received sample but they do however show a considerable increase in porosity. This higher level of porosity is particularly prevalent in the surface 10 μm of the coating which demonstrates a considerable change in morphology. One can see the effect of attack by the *in-vitro* ageing medium after just one week of exposure by the increase in roughness and the apparent damage to the surface layers of the coating. Despite these attacks at the surface of the coating however, the ceramic still appears to be well adhered to the substrate along the cross-section.

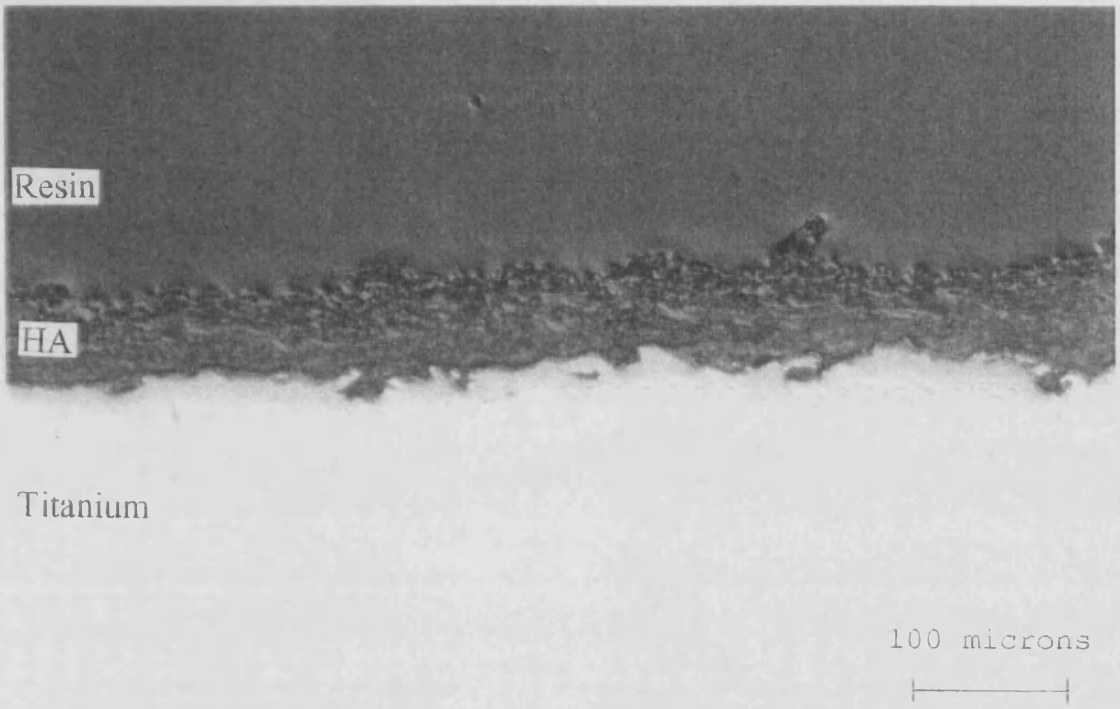

Figure 6-23 :- Optical micrograph showing cross-section through DGUN HA coating aged under static loading at pH 4.5 for one week

Coatings aged for two weeks (not shown) show a progression of this effect as the surface modified layer progresses into the coating itself. In this sample the change in morphology has consumed approximately half of the coating thickness, leaving the material extremely porous and visibly altered. The coating however doesn't appear to have changed in overall thickness and still remains well adhered to the substrate. Again these observations are found for the coating aged for four weeks at pH 4.5 under static loading (not shown). The morphologically altered coating seems to dominate the hydroxyapatite's cross-sectional thickness, leaving little evidence for unaltered material. The effects of the ageing medium on the HA coating seems progressive since the change in morphology is advancing from the coating surface through to the substrate. The coating again has a higher porosity than the as-received coating but shows little change in thickness. As noted earlier, the coating is still well adhered to the substrate and exhibits no signs of through thickness micro-cracking.

Figure 6-24 :- Optical micrograph showing cross-section through DGUN HA coating aged under static loading at pH 4.5 for ten weeks

Dramatic damage to the hydroxyapatite coating can been seen in the micrograph of the sample which has been aged for ten weeks under static loading at pH 4.5 (Figure 6-24). We can see that not only is the microstructure of the coating considerably modified over that of the as-received coating, through its entire thickness, but also much of the coating has been lost from the substrate. The progressive spalling of the coating from the substrate can be observed as layers of the coating are seen to be breaking away from the bulk of the material. In some regions along the coating length, so much of the coating has been lost that the substrate itself is exposed. What remains of the coating is however still well adhered to the substrate. The progressive nature of this attack on the coating by the *in-vitro* medium is apparent since it was not possible to section and mount coatings aged for longer durations than ten weeks. The coating aged for fifteen weeks had completely disintegrated during static ageing and could not be analysed.

6.6.5 Scanning Electron Microscopy

The DGUN HA coatings aged under static loading at pH 4.5 for one week (Figure 6-25) has a very different surface morphology to that of the as-received coating. There is a large increase in the number and size of micro-cracks crossing the coating surface, many of these having smaller cracking running off from them. The surface still bears a two phase morphology with rough agglomerated regions and smoother flat regions but these amorphous zones are pocked and etched in nature. The severe micro-cracking described above seems to be concentrated predominantly in the amorphous regions probably because crack propagation through these regions is easier than through the agglomerated areas. The coating no longer exhibits clear splat shapes on its surface, these having been either etched or broken up by micro-cracks. The whole appearance of the surface is one of considerable damage caused by a combination of the *in-vitro* medium and the applied load.

Figure 6-25 :- Scanning electron micrograph showing surface of DGUN HA coating aged under static loading at pH 4.5 for one week

The surface of the coating aged for two weeks under static loading at pH 4.5 (not shown) has a similar appearance to that of the one week aged sample. Here again we see a dramatic level of surface cracking and damage to the amorphous regions of the coating surface. The coating is still two phase in nature, still showing agglomerated regions and etched glassy regions but again these are broken up giving the surface the appearance of dry, cracked mud. The coating seems to have a higher surface porosity than the week aged coating and it is possible that parts of the surface have broken away from the bulk of the coating.

The coating aged for four weeks under static loading (not shown) again shows this morphology but in this case there is much less of the glassy, amorphous material visible. Large micro-cracks still criss-cross the surface but now the major effect on the coating seems to be one of dissolution. The coating shows a predominance of the agglomerated material on its surface and much less amorphous material, suggesting that this phase has been dissolved away from the surface.

This hypothesis is supported by looking at the coating aged for ten weeks under static loading at pH 4.5 (Figure 6-26). Here the roughness of the surface is apparently much greater than in the coatings aged for shorter durations, seeming to indicate that large areas of coating have broken away from the surface. The cracking of the surface due to the static loading, followed by subsequent dissolution of the amorphous phase seems to weaken the surface layers to such an extent that they can no longer remain attached to the bulk of the coating. In this micrograph one can see the large pores left by lost material and layers of freshly exposed amorphous material bearing micro-cracks at the bottom of these pores. This amorphous material in the pores of the coating does not appear to be as etched as the material nearer the coating surface supporting the suggestion that this deeper phase has been exposed more recently.

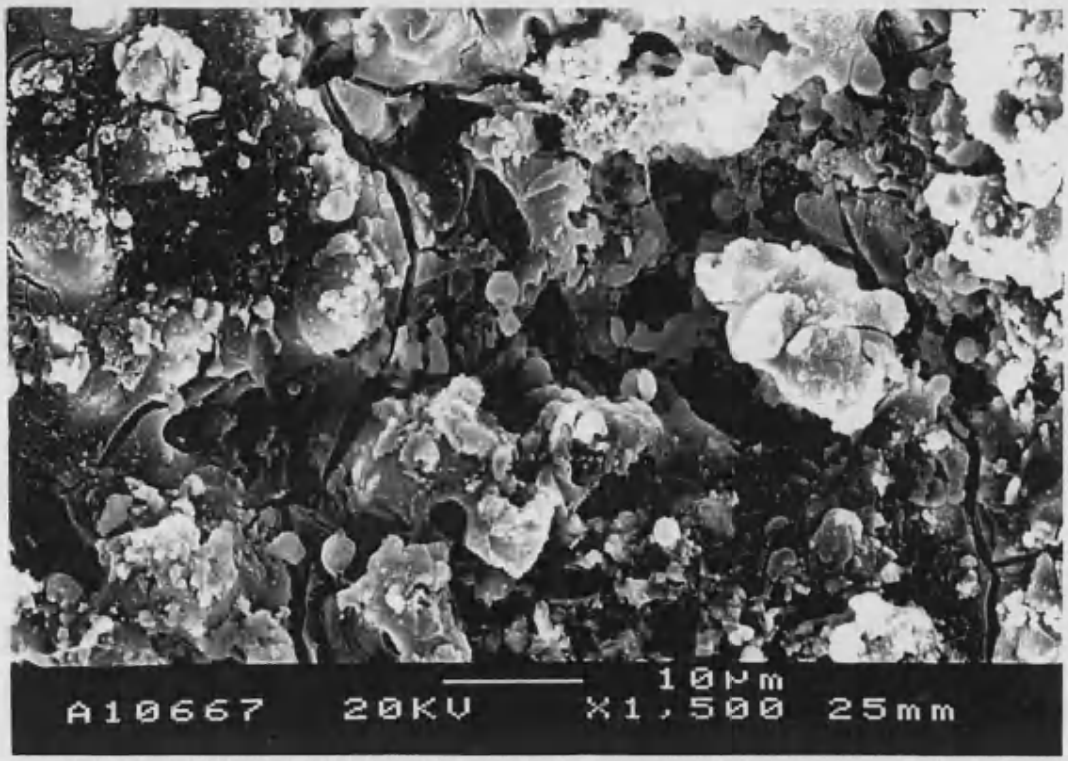

Figure 6-26 :- Scanning electron micrograph showing surface of DGUN HA coating aged under static loading at pH 4.5 for ten weeks

The coating aged for fifteen weeks under these conditions disintegrated on removal from the *in-vitro* tank and therefore could not be examined by scanning electron microscopy.

6.6.6 Coating Thickness Results

Table 6-43 presents a summary of the cross-sectional thickness results for the detonation gun sprayed hydroxyapatite coatings aged for various time periods under static loading in Ringer's solution buffered to pH 4.5.

Sample	*No. of tests*	*Mean (μm)*	*Standard Deviation*	*Variance*	*95% Confidence Limits*
as-received	10	71.2908	8.4365	71.1752	70.578 and 72.004
pH 4.5 x 1	10	49.5313	10.4783	109.7950	48.646 and 50.417
pH 4.5 x 2	10	55.1209	11.6909	136.6764	54.133 and 56.109
pH 4.5 x 4	10	60.7561	9.3086	86.6493	59.969 and 61.543
pH 4.5 x 10	10	61.9115	10.4807	109.8448	61.026 and 62.800
pH 4.5 x 15	10	n / a *	n / a	n / a	n / a

Table 6-43 :- Cross-sectional thickness results for DGUN HA coatings aged under static loading at pH 4.5

* The coating aged at pH 4.5 for fifteen weeks disintegrated on removal from the tank and thus could not be analysed.

Table 6-44 presents the significant test results from thickness data for the detonation gun sprayed coatings aged under static loading at pH 4.5, tested using a Student T-test at the 5 % significance level.

thickness	*as-received*	*1 week*	*2 weeks*	*4 weeks*	*10 weeks*	*15 weeks*
as-received		✓	✓	✓	✓	
1 week	✓		✖			
2 weeks	✓	✖		✓		
4 weeks	✓		✓		✖	
10 weeks	✓			✖		
15 weeks						

Table 6-44 :- Significant test results for DGUN HA coatings aged under static loading at pH 4.5

✓ = significantly different

✖ = not significantly different

= not tested

Therefore, it was found that the aged coatings had significantly different thicknesses to that of the as-received coating. There was however found to be no significant change in coating thickness with ageing time except between weeks two and four.

6.6.7 Coating Porosity Results

Table 6-45 presents a summary of the cross-sectional porosity results for the detonation gun sprayed hydroxyapatite coatings aged for various time periods under static loading in Ringer's solution buffered to pH 4.5.

Sample	*No. of tests*	*Mean (%)*	*Standard Deviation*	*Variance*	*95% Confidence Limits*
as-received	10	1.2605	0.7242	0.5245	0.922 and 1.600
pH 4.5 x 1	10	15.1470	5.1784	26.8158	12.723 and 17.571
pH 4.5 x 2	10	14.7310	7.2454	52.4959	11.340 and 18.122
pH 4.5 x 4	10	18.0741	8.6679	75.1332	14.017 and 22.394
pH 4.5 x 10	10	8.1523	2.6521	7.0039	6.911 and 9.394
pH 4.5 x 15	10	n / a *	n / a	n / a	n / a

Table 6-45 :- Cross-sectional porosity results for DGUN HA coatings aged under static loading at pH 4.5

* The coating aged at pH 4.5 for fifteen weeks disintegrated on removal from the tank and thus could not be analysed.

Table 6-46 presents the significant test results from porosity data for the detonation gun sprayed coatings aged under static loading at pH 4.5, tested using a Student T-test at the 5 % significance level.

porosity	*as-received*	*1 week*	*2 weeks*	*4 weeks*	*10 weeks*	*15 weeks*
as-received		✓	✓	✓	✓	
1 week	✓		✖			
2 weeks	✓	✖		✓		
4 weeks	✓		✓		✓	
10 weeks	✓			✓		
15 weeks						

Table 6-46 :- Significant test results for DGUN HA coatings aged under static loading at pH 4.5

✓ = significantly different

✖ = not significantly different

= not tested

Therefore it was found that there was a significant difference in the porosities between the as-received coating and the aged coatings. There was also found to be a significance in the differences in porosity between coatings aged for different time periods except for the coating aged between one and two weeks.

6.6.8 Surface Roughness (Ra) Results

Table 6-47 presents a summary of the surface roughness results for the detonation gun sprayed hydroxyapatite coatings aged for various time periods under static loading in Ringer's solution buffered to pH 4.5.

Sample	*Scan Length (mm)*	*Ra (µm)*	*Rp (µm)*	*Rv (µm)*	*Rt (µm)*
as-received	11.4025	5.9837	30.1268	19.2205	49.3472
pH 4.5 x 1	11.1456	6.6424	39.2420	22.9289	62.1709
pH 4.5 x 2	8.9214	7.2250	25.6682	27.7689	53.4370
pH 4.5 x 4	6.3216	6.6659	19.6030	22.2563	41.8593
pH 4.5 x 10	10.7985	7.9502	33.3987	28.2722	61.6709
pH 4.5 x 15	n / a *	n / a	n / a	n / a	n / a

Table 6-47 :- Surface roughness results for DGUN HA coatings aged under static loading at pH 4.5

* The coating aged at pH 4.5 for fifteen weeks disintegrated on removal from the tank and thus could not be analysed.

6.6.9 Residual Stress Results

Table 6-48 presents a summary of the residual stress analysis results for the detonation gun sprayed hydroxyapatite coatings aged for various time periods under static loading in Ringer's solution buffered to pH 4.5.

Sample	*d(c)*	*strain (c) %*	*E (Pa)*	*residual stress (MPa)*
DGUN HA powder	1.7172	0.003203	5.5^{09}	-
as-received	1.7220	0.002795	5.5^{09}	15.3739
pH 4.5 x 1	1.7280	0.006406	5.5^{09}	35.2318
pH 4.5 x 2	1.7256	0.004892	5.5^{09}	26.9043
pH 4.5 x 4	1.7197	0.001456	5.5^{09}	8.0072
pH 4.5 x 10	1.7196	0.001398	5.5^{09}	7.6869
pH 4.5 x 15	n / a *	n / a	n / a	n / a

Table 6-48 :- Residual stress results in 004 plane for DGUN HA coatings aged under static loading at pH 4.5

* The coating aged at pH 4.5 for fifteen weeks disintegrated on removal from the tank and thus could not be analysed.

7. Results - Fatigue Testing of HA Coatings

7.1 VPS HA Coatings Fatigued In Air and In Ringer's Solution

7.1.1 X-Ray Diffraction Traces

Figure 7-1 presents sections from the x-ray diffraction traces for the vacuum plasma sprayed hydroxyapatite coatings fatigued in air and in Ringer's solution for one and ten million cycles.

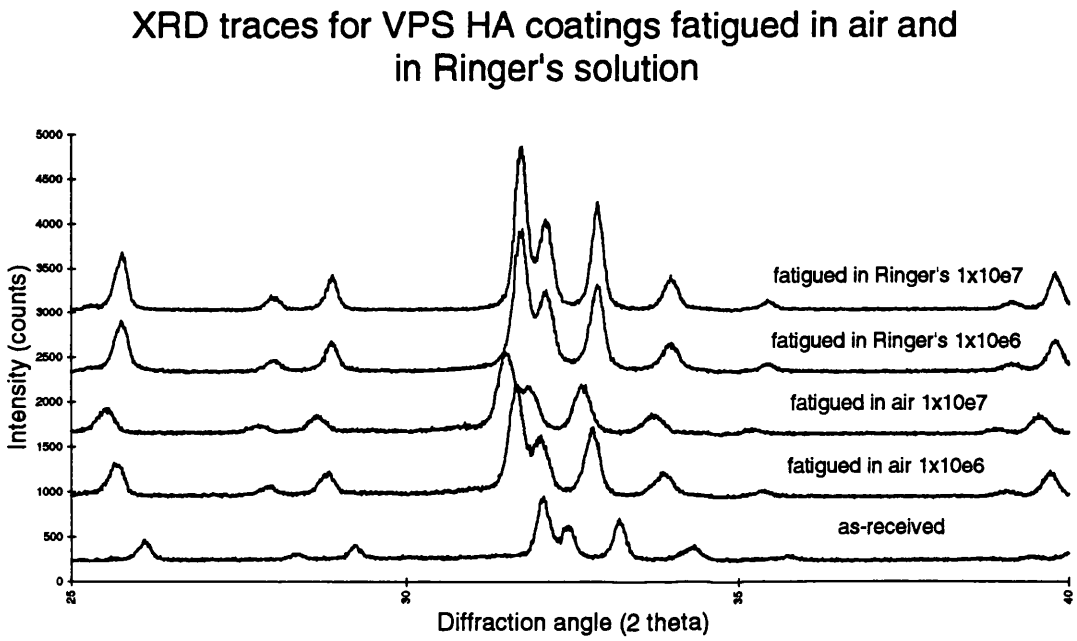

Figure 7-1 :- Amorphous hump region from X-Ray diffraction traces of VPS HA coatings fatigued in air and in Ringer's solution

7.1.2 Crystallinity Results

Table 7-1 presents a summary of the crystallinity results for the vacuum plasma sprayed hydroxyapatite coatings fatigued in air and in Ringer's solution for one and ten million cycles.

Sample	*No. of tests*	*Mean (%)*	*Standard Deviation*	*Variance*	*95% Confidence Limits*
as-received	10	60.3542	2.1942	4.8145	59.738 and 61.053
air 10^6	80	60.7260	3.5771	12.7957	60.002 and 61.450
air 10^7	10	59.2021	1.4268	2.0358	59.880 and 58.524
Ringer's 10^6	80	64.9611	2.6844	7.2059	64.096 and 65.827
Ringer's 10^7	10	73.9113	1.5172	2.3010	73.237 and 74.581

Table 7-1 :- Crystallinity results for VPS HA coatings fatigued in air and in Ringer's solution

Using a 2-tailed Student T-test the significance of these results was determined at the 5% level, revealing that :

The coating fatigued in air for 1x10e6 cycles did not have a significantly different crystallinity to the as-received coating.

The coating fatigued in air for 1x10e7 cycles did not have a significantly different crystallinity to the as-received coating nor from that of the coating fatigued in air for 1x10e6 cycles.

The coating fatigued in Ringer's solution for 1x10e6 cycles had a significantly different crystallinity from the as-received coating and also from the coating fatigued in air for 1x10e6 cycles.

The coating fatigued in Ringer's solution for 1x10e7 cycles was significantly different from the as-received coating and also from the coating fatigued for 1x10e6 cycles in Ringer's.

Therefore it was found that all the fatigued coatings had significantly different crystallinities from that of the as-received coating. All the fatigued coatings also had crystallinities which varied significantly between testing groups.

7.1.3 X-Ray Plane Analysis

Table 7-2 presents a summary of the x-ray plane analysis results for the vacuum plasma sprayed hydroxyapatite coatings fatigued in air and in Ringer's solution for one and ten million cycles.

Sample	*Major Compound*	*Significant Compounds*	*Trace Compounds*
as-received	HA	-	α-TCP, β-TCP, $Ca_4O(PO_4)_2$, $Ca_2P_2O_7$
air 10^6	HA	β-TCP	α-TCP, $Ca_4O(PO_4)_2$, $Ca_2P_2O_7$
air 10^7	HA	α-TCP, β-TCP	-
Ringer's 10^6	HA	-	β-TCP, α-TCP, $Ca_4O(PO_4)_2$
Ringer's 10^7	HA	β-TCP	α-TCP, $Ca_4O(PO_4)_2$

Table 7-2 :- X-Ray plane analysis results for VPS HA coatings fatigued in air and in Ringer's solution

7.1.4 Optical Microscopy

The polished cross-section through the VPS HA coating fatigued in air for one million cycles (Figure 7-2) has an appearance virtually identical to that of the as-received coating cross-section. The lamella nature of the coating and its variation in thickness along the cross-section are the same as the as-received coating as is the apparent surface roughness. The coating seems to be well adhered to the substrate showing no signs of delamination. The is also no evidence for surface to substrate cracking in this sample. The bond layer between the hydroxyapatite coating and the titanium alloy substrate is also still clearly visible. Fatigue testing the hydroxyapatite coating in air appears to have virtually no effect on the cross-sectional appearance of the coating.

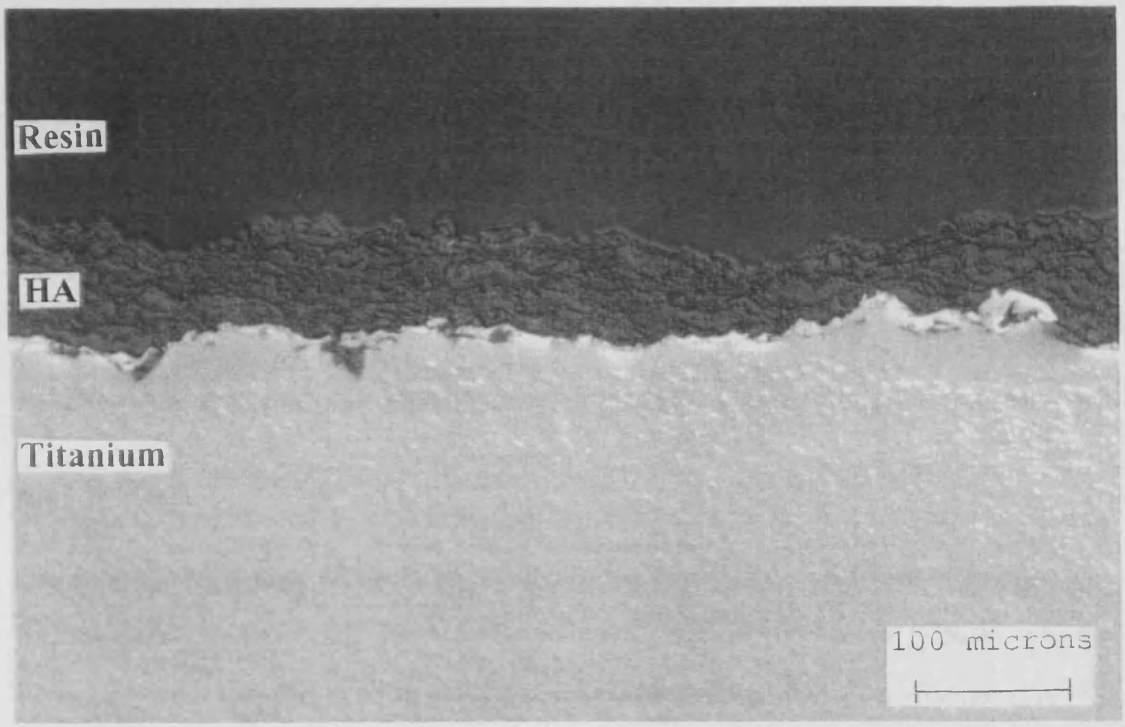

Figure 7-2 :- Optical micrograph showing cross-section through VPS HA coatings fatigued in air for one million cycles

The coating which was fatigued for ten million cycles (Figure 7-3) is again well adhered to the substrate and again shows no evidence for delamination or surface to substrate cracking. The layered nature of the coating, again imposed by the manufacturing process is still clearly visible, as is the pure titanium interlayer between the titanium alloy substrate and the hydroxyapatite coating. This coating does however show signs of damage occurring as a result of extensive fatigue testing. Here the cross-sectional view shows the much higher porosity in this coating over the as-received coating, or even that of the coating fatigued for just one million cycles. There is evidence that the surface of the coating has increased in roughness due predominantly to the higher level of porosity found throughout the coating cross-section.

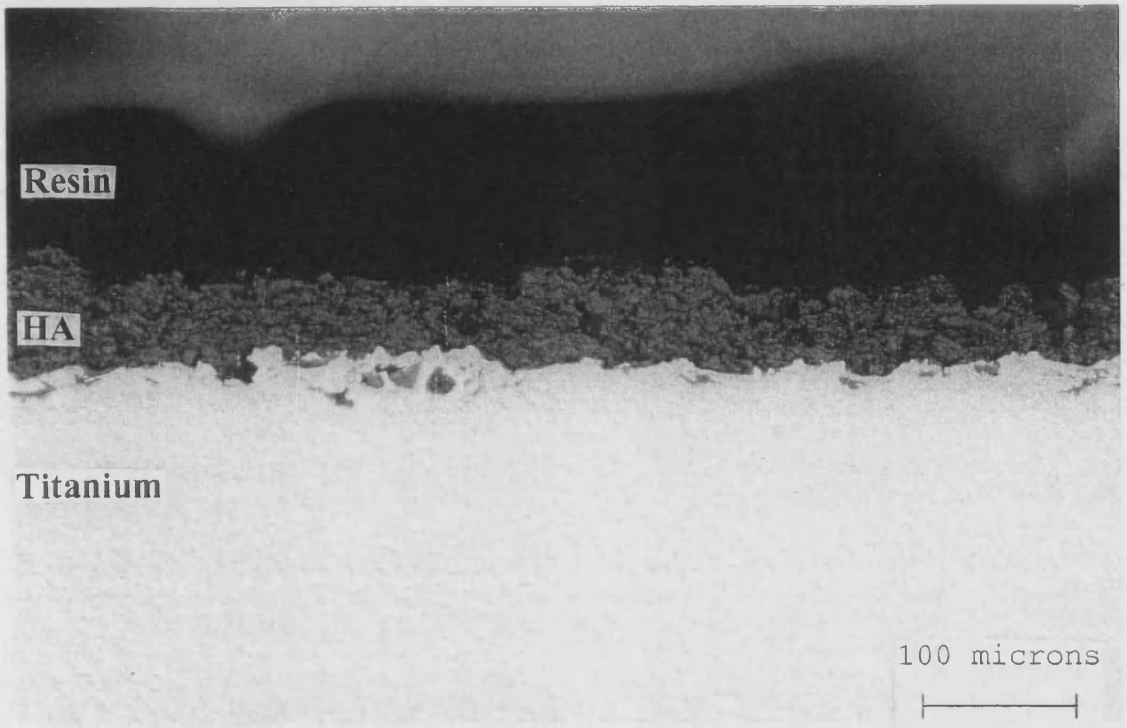

Figure 7-3 :- Optical micrograph showing cross-section through VPS HA coatings fatigued in air for ten million cycles

The coating fatigued in Ringer's solution for one million cycles (Figure 7-4) however shows a much greater degree of damage as a result of fatigue testing. Here although the coating itself appears to be coherent, the bulk of the coating has completely delaminated from the surface of the titanium substrate. The bulk of the coating shows no obvious change in thickness or porosity but contains a considerable number of surface to substrate cracks along its cross-sectional length and it is at these cracks that delamination failure has been initiated. The delamination failure is a mixed mode failure, the crack path not running cleanly along the interface between the coating and the substrate. In various areas along the cross-section there remains some coating affixed to the substrate despite bulk delamination. The crack path has obviously not always run directly along the interface but has on occasion deviated up into the coating itself.

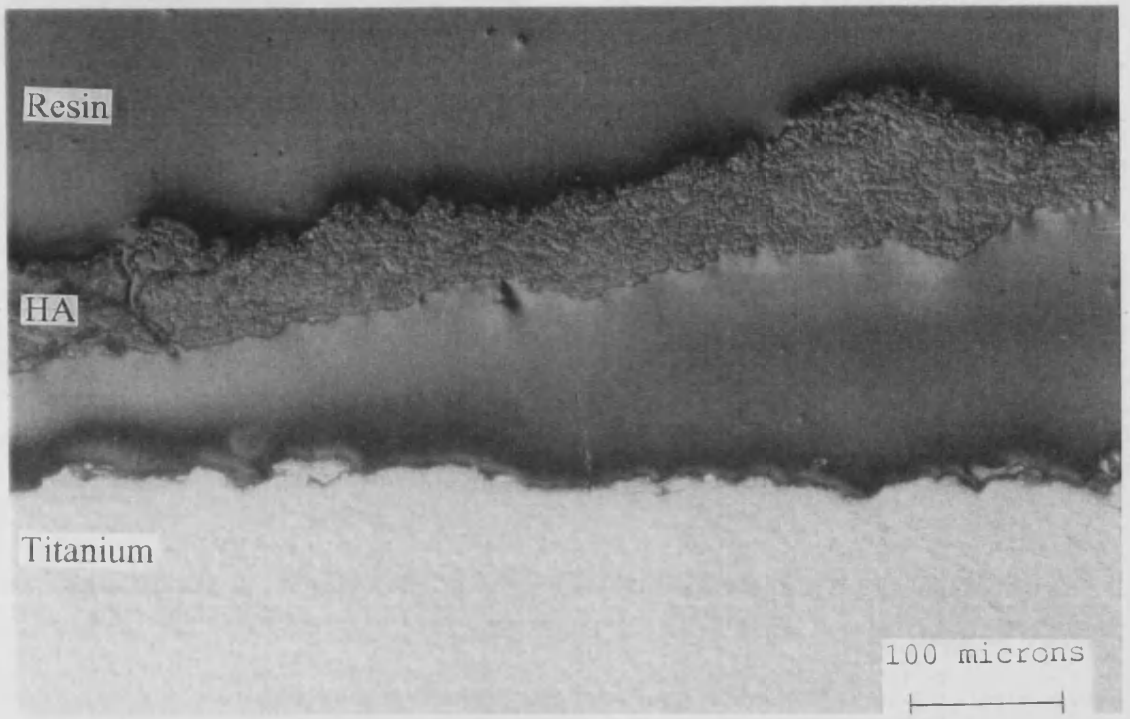

Figure 7-4 :- Optical micrograph showing cross-section through VPS HA coatings fatigued in Ringer's solution for one million cycles

The coating fatigued for ten million cycles in Ringer's solution disintegrated on removal from the ageing tank and therefore could not be prepared for optical microscopy.

7.1.5 Scanning Electron Microscopy

The surface of the VPS HA coating fatigued in air for one million cycles (Figure 7-5) has virtually an identical appearance to that of the as-received coating. The surface still consists of a dramatically two phase morphology with large areas of flat, glassy material in the obvious shapes of splats, and agglomerated crystalline debris. The amorphous material is still smooth in nature and shows no evidence for etching or pitting in any form. Small, fine micro-cracks can be seen running over the surface of the amorphous zones but these appear to be in the same numbers as were found in the as-

received surface. Basically it can be said that fatigue testing the coating in air for one million cycles appears to have had little or no apparent effect on the surface morphology.

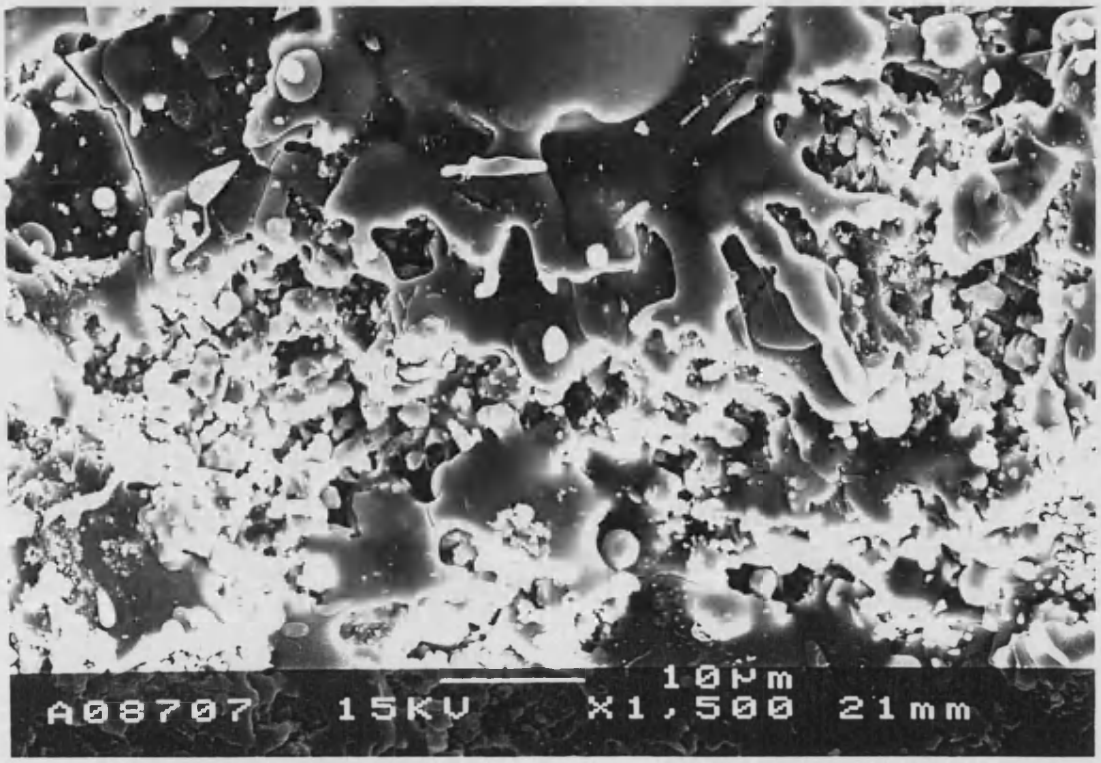

Figure 7-5 :- Scanning electron micrograph showing surface of VPS HA coatings fatigued in air for one million cycles

The surface of the coating fatigued in air for ten million cycles (Figure 7-6) does have a considerably different microstructure to the as-received coating however. Here one can see that the surface micro-cracks observed in the as-received coating have increased in size considerably. The cracks appear to have been opened up by the fatigue process and have smaller cracks running off from them, usually perpendicular to the original crack. In addition to the increase in crack size on the coating surface, there is evidence for the beginnings of surface dissolution of the amorphous phase. Although this effect is small in magnitude, fine scale etching of the glassy regions of the coating surface is apparent giving regions of the amorphous phase a lace-like morphology. The surface of the coating also appears to be more rough in nature than either the as-received coating or the coating fatigued for one million cycles. It is possible that this increase could be a result of the loss of clumps of material from the coating surface.

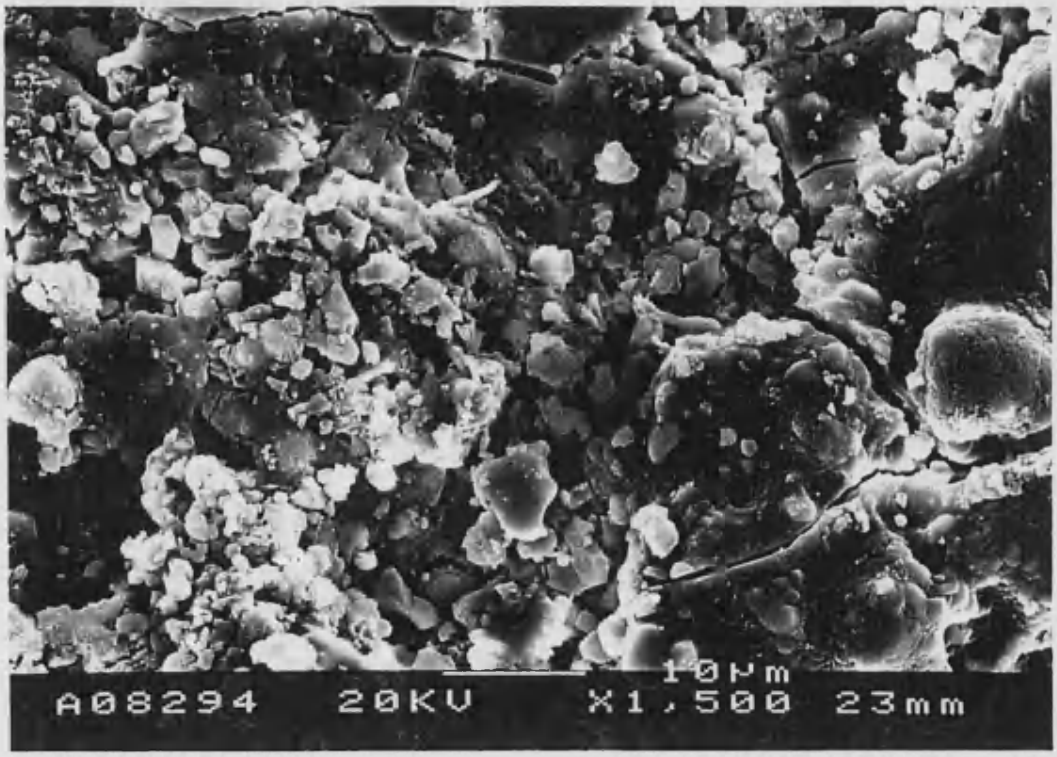

Figure 7-6 :- Scanning electron micrograph showing surface of VPS HA coatings fatigued in air for ten million cycles

The surface of the coating fatigued in Ringer's solution for one million cycles (Figure 7-7) has the usual appearance of a surface which has been exposed to the *in-vitro* medium. The amorphous regions appear to have become thinner in nature allowing the morphology of the material below these layers to show through. This glassy material also appears to have been etched by the ageing solution having a pocked appearance in some areas. The coating still shows signs of micro-cracks running through the amorphous regions of the surface but these cracks do not appear to have grown in width as a result of the fatigue process. The coating surface also appears to be rougher in nature than that of the as-received coating possibly as a result of the dissolution of some of the amorphous phase.

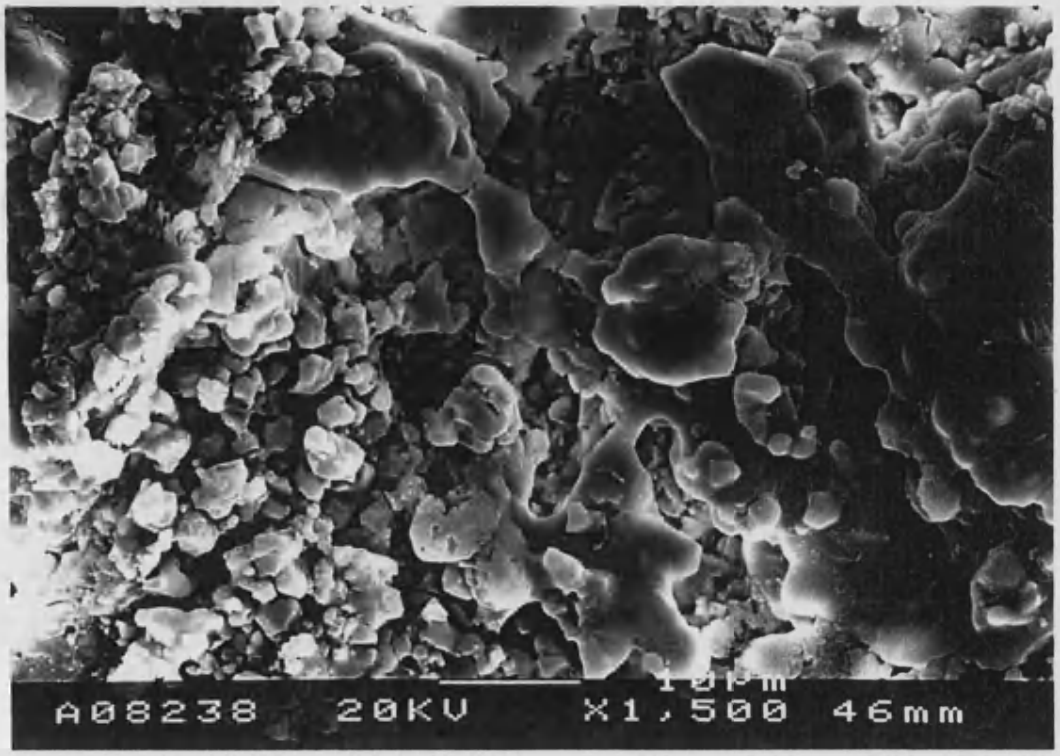

Figure 7-7 :- Scanning electron micrograph showing surface of VPS HA coatings fatigued in Ringer's solution for one million cycles

The coating fatigued for ten million cycles in Ringer's solution disintegrated on removal from the ageing tank and therefore could not be prepared for scanning electron microscopy.

7.1.6 Coating Thickness Results

Table 7-3 presents a summary of the cross-sectional thickness results for the vacuum plasma sprayed hydroxyapatite coatings fatigued in air and in Ringer's solution for one and ten million cycles.

Sample	*No. of tests*	*Mean (μm)*	*Standard Deviation*	*Variance*	*95% Confidence Limits*
as-received	10	42.4840	11.6308	135.2751	41.501 and 42.484
air 10^6	40	54.2456	12.6400	159.7677	53.869 and 54.623
air 10^7	10	61.5960	10.7230	114.9750	60.956 and 62.237
Ringer's 10^6	40	66.4104	10.8699	118.1545	39.408 and 98.413
Ringer's 10^7	n /a *	n / a	n / a	n / a	n / a

Table 7-3 :- Cross-sectional thickness results for VPS HA coatings fatigued in air and in Ringer's solution

* The coating fatigued in Ringer's solution for 1x10e7 cycles disintegrated on removal from the tank and thus could not be analysed.

Using a 2-tailed Student T-test the significance of these results was determined at the 5% level, revealing that :

The coating fatigued in air for 1x10e6 cycles had a thickness that was significantly different to that of the as-received coating.

The coating fatigued in air for 1x10e7 cycles had a thickness that was significantly different to that of the as-received coating and was also significantly different to the coating fatigued in air for 1x10e6 cycles.

The coating fatigued in Ringer's solution for 1x10e6 cycles had a thickness that was significantly different from that of the as-received coating and was also significantly different from that of the coating fatigued in air 1x10e6 cycles.

Therefore, it was found that all the fatigued coatings displayed significant differences in thickness from both the as-received coating and from each other.

7.1.7 Coating Porosity Results

Table 7-4 presents a summary of the cross-sectional porosity results for the vacuum plasma sprayed hydroxyapatite coatings fatigued in air and in Ringer's solution for one and ten million cycles.

Sample	*No. of tests*	*Mean (%)*	*Standard Deviation*	*Variance*	*95% Confidence Limits*
as-received	10	5.749	1.464	2.144	4.702 and 6.797
air 10^6	40	5.3743	1.8401	3.3860	4.965 and 5.784
air 10^7	10	23.9930	6.1900	38.3160	20.915 and 27.072
Ringer's 10^6	40	5.4037	3.7092	13.7583	4.446 and 6.362
Ringer's 10^7	n /a *	n / a	n / a	n / a	n / a

Table 7-4 :- Cross-sectional porosity results for VPS HA coatings fatigued in air and in Ringer's solution

* The coating fatigued in Ringer's solution for 1x10e7 cycles disintegrated on removal from the tank and thus could not be analysed.

Using a 2-tailed Student T-test the significance of these results was determined at the 5% level, revealing that :

The coating fatigued in air for 1x10e6 cycles did not have a porosity that was significantly different from that of the as-received coating.

The coating fatigued in air for 1x10e7 cycles had a porosity that was significantly different both from the as-received coating and from the coating fatigued in air for 1x10e6 cycles.

The coating fatigued in Ringer's solution for 1x10e6 cycles did not have a porosity that was significantly different from the as-received coating and was also not significantly different from the coating fatigued in air for 1x10e6 cycles.

Therefore it was found that there was a variable significance in the change in porosity between fatigued coatings and the as-received coating and between testing groups.

7.1.8 Surface Roughness (Ra) Results

Table 7-5 presents a summary of the surface roughness results for the vacuum plasma sprayed hydroxyapatite coatings fatigued in air and in Ringer's solution for one and ten million cycles.

Sample	*mean Ra (μm)*	*standard deviation*	*variance*	*95% conf. interval*
as-received	5.5727	-	-	-
air 10^6	6.1994	0.6315	0.3988	5.672 and 6.727
air 10^7	5.8855	-	-	-
Ringer's 10^6	5.5125	0.6531	0.4266	4.827 and 6.198
Ringer's 10^7	4.5083	-	-	-

Table 7-5 :- Surface roughness results for VPS HA coatings fatigued in air and in Ringer's solution

Using a 2-tailed Student T-test the significance of these results was determined at the 5% level, revealing that :

The coatings fatigued in air for 1x10e6 cycles had a surface roughness that was significantly different from the as-received coating.

The coatings fatigued in Ringer's solution for 1x10e6 cycles had a surface roughness that was not significantly different from the as-received coating but was significantly different from that of the coatings fatigued in air for 1x10e6 cycles.

7.1.9 Residual Stress Results

Table 7-6 presents a summary of the residual stress analysis results for the vacuum plasma sprayed hydroxyapatite coatings fatigued in air and in Ringer's solution for one and ten million cycles.

Sample	*residual stress (MPa)*	*standard deviation*	*variance*	*95% conf. interval*
VPS HA powder	-	-	-	-
as-received	2.8764	-	-	-
air 10^6	13.7428	11.4382	130.0323	4.180 and 23.305
air 10^7	27.1660	-	-	-
Ringer's 10^6	3.5689	4.7551	22.6113	-1.421 and 8.559
Ringer's 10^7	17.8374	-	-	-

Table 7-6 :- Residual stress results in 004 plane for VPS HA coatings fatigued in air and in Ringer's solution

Using a 2-tailed Student T-test the significance of these results was determined at the 5% level, revealing that :

The coatings fatigued in air for 1x10e6 cycles had a residual stress level that was significantly different from that of the as-received coating.

The coatings fatigued in Ringer's solution for 1x10e6 cycles had a residual stress level that was not significantly different from that of the as-received coating but was significantly different from that of the coatings fatigued in air for 1x10e6 cycles.

7.2 DGUN HA Coatings Fatigued In Air and In Ringer's Solution

7.2.1 X-Ray Diffraction Traces

Figure 7-8 presents sections from the x-ray diffraction traces for the detonation gun sprayed hydroxyapatite coatings fatigued in air and in Ringer's solution for one and ten million cycles.

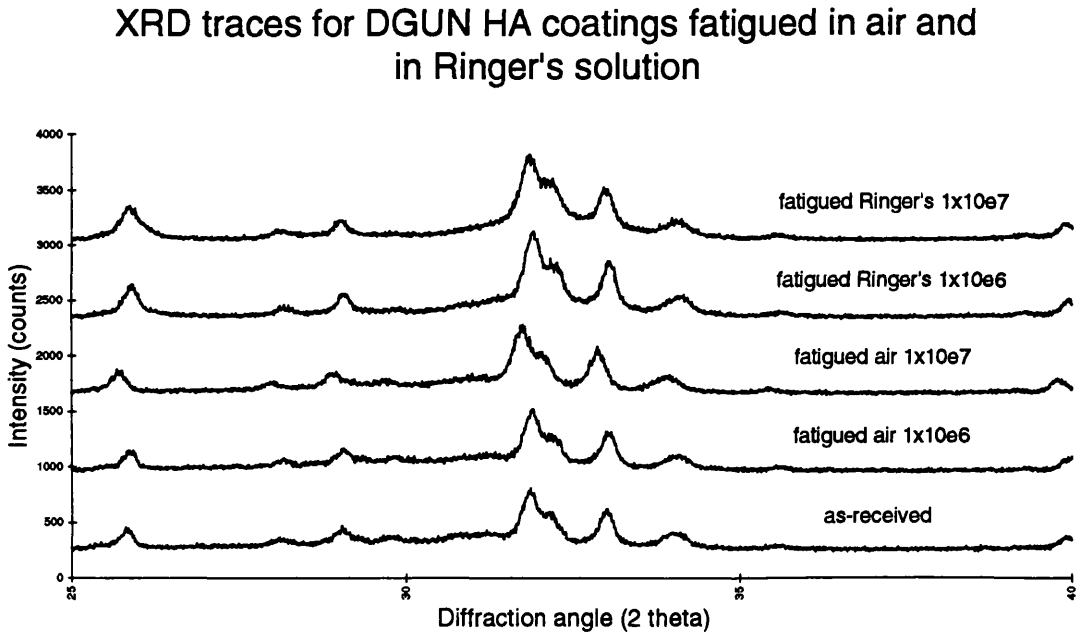

Figure 7-8 :- Amorphous hump region from X-Ray diffraction traces of DGUN HA coatings fatigued in air and in Ringer's solution

7.2.2 Crystallinity Results

Table 7-7 presents a summary of the crystallinity results for the detonation gun sprayed hydroxyapatite coatings fatigued in air and in Ringer's solution for one and ten million cycles.

Sample	*No. of tests*	*Mean (%)*	*Standard Deviation*	*Variance*	*95% Confidence Limits*
as-received	10	34.4223	0.9043	0.8183	33.7752 and 35.0694
air 10^6	80	33.7366	1.8098	3.2752	33.224 and 35.250
air 10^7	10	34.0888	0.6413	0.4112	33.630 and 34.548
Ringer's 10^6	80	38.5946	3.0871	9.5300	36.034 and 41.175
Ringer's 10^7	10	35.5361	1.0726	1.1504	34.769 and 36.303

Table 7-7 :- Crystallinity results for DGUN HA coatings fatigued in air and in Ringer's solution

Using a 2-tailed Student T-test the significance of these results was determined at the 5% level, revealing that :

The coating fatigued in air for 1x10e6 cycles did not have a significantly different crystallinity to the as-received coating.

The coating fatigued in air for 1x10e7 cycles did not have a significantly different crystallinity to the as-received coating and was also not significantly different from the that of the coating fatigued in air for 1x10e6 cycles.

The coating fatigued in Ringer's solution for 1x10e6 cycles had a significantly different crystallinity from the as-received coating and also from the coating fatigued in air for 1x10e6 cycles.

The coating fatigued in Ringer's solution for 1x10e7 cycles was significantly different from the as-received coating and also from the coating fatigued for 1x10e6 cycles in Ringer's.

Therefore it was found that all the air fatigued coatings did not have significantly different crystallinities from that of the as-received coating and were also not significantly different from each other. However, the Ringer's fatigued coatings had crystallinities which varied significantly both from the as-received coating and also from the other testing groups.

7.2.3 X-Ray Plane Analysis

Table 7-8 presents a summary of the x-ray plane analysis results for the vacuum plasma sprayed hydroxyapatite coatings fatigued in air and in Ringer's solution for one and ten million cycles.

Sample	*Major Compound*	*Significant Compounds*	*Trace Compounds*
as-received	HA	β-TCP, $Ca_4O(PO_4)_2$	α-TCP
air 10^6	HA	-	α-TCP, β-TCP, $Ca_4O(PO_4)_2$
air 10^7	HA	α-TCP, β-TCP	$Ca_4O(PO_4)_2$
Ringer's 10^6	HA	$Ca_4O(PO_4)_2$	α-TCP, β-TCP
Ringer's 10^7	HA	$Ca_4O(PO_4)_2$	α-TCP, β-TCP

Table 7-8 :- X-Ray plane analysis results for DGUN HA coatings fatigued in air and in Ringer's solution

7.2.4 Optical Microscopy

The polished cross-section through the DGUN HA coating fatigued in air for one million cycles (Figure 7-9), as for the VPS coating, looks remarkably similar to the as-received coating. There is no obvious change in porosity or thickness over the as-received coating and the characteristic nature of the detonation gun process can still be seen in the smaller size of the lamellae in this coating compared to the VPS sample. The coating seems to be well adhered to the substrate showing no signs of delamination. There is no sign of the dark line between the coating and substrate seen in some of the DGUN coatings tested by other means. The is also no evidence for surface to substrate cracking in this sample. Fatigue testing the hydroxyapatite coating in air appears to have virtually no effect on the cross-sectional appearance of the coating.

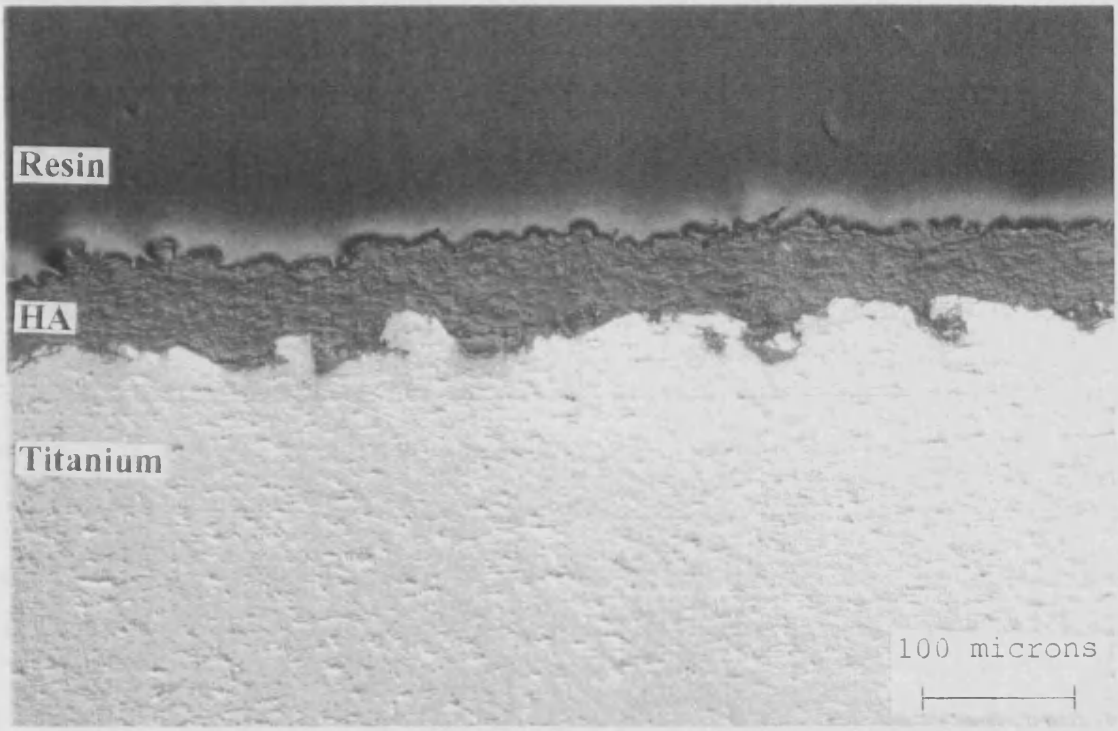

Figure 7-9 :- Optical micrograph showing cross-section through DGUN HA coatings fatigued in air for one million cycles

The coating which was fatigued for ten million cycles (Figure 7-10) is again well adhered to the substrate and again shows no evidence for large scale delamination or surface to substrate cracking. The dark line between substrate and coating seen in some other DGUN coatings is however visible in certain regions along the cross-sectional length. There is again no obvious change in cross-sectional thickness or porosity for this coating when compared with either the as-received coating or the coating fatigued in air for one million cycles. Yet again it can be said that there is no obvious effect on the cross-sectional morphology of the coating which has resulted from the air fatigue process.

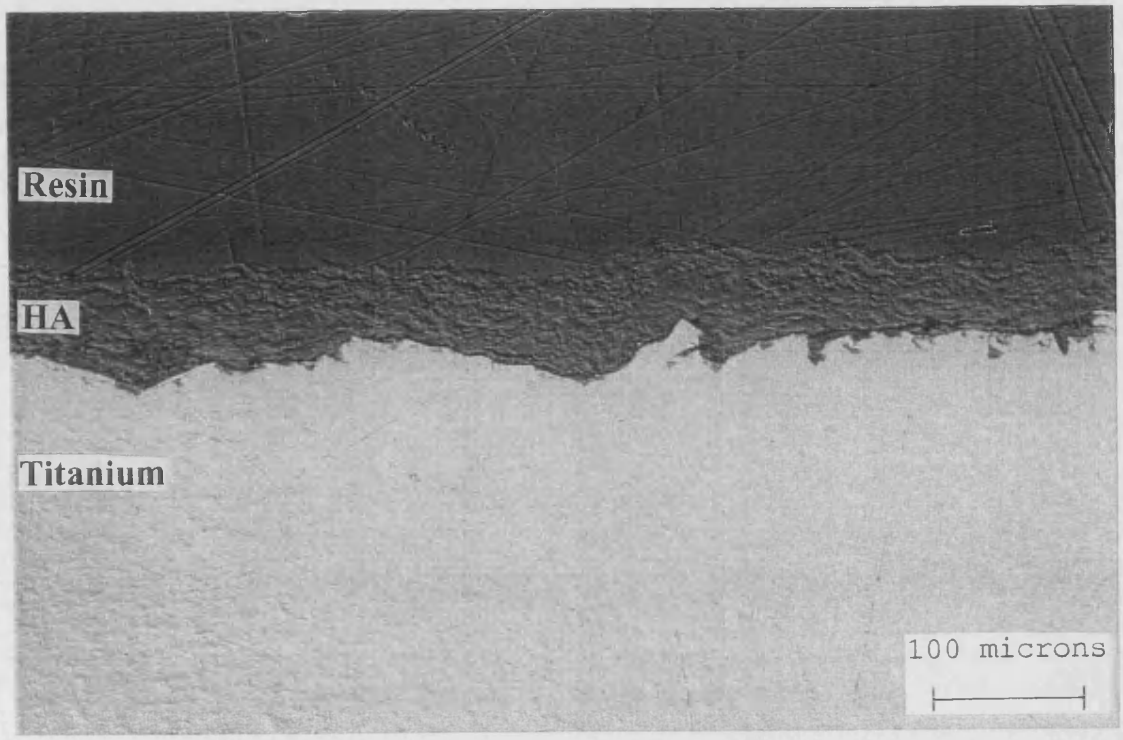

Figure 7-10 :- Optical micrograph showing cross-section through DGUN HA coatings fatigued in air for ten million cycles

The coating fatigued in Ringer's solution for one million cycles (

Figure 7-11) again, on the whole appears to be very similar to the as-received coating. The coating shows no signs of any modified surface layer which may have resulted from exposure to the *in-vitro* ageing medium and no obvious change in cross-sectional thickness or porosity. The coating also shows no evidence for an increase in surface roughness over that of the as-received coating. There is however a dark line running along most of the cross-sectional length of the sample which is thicker than that found for the air fatigued coatings and which could be an early indication of potential delamination failure.

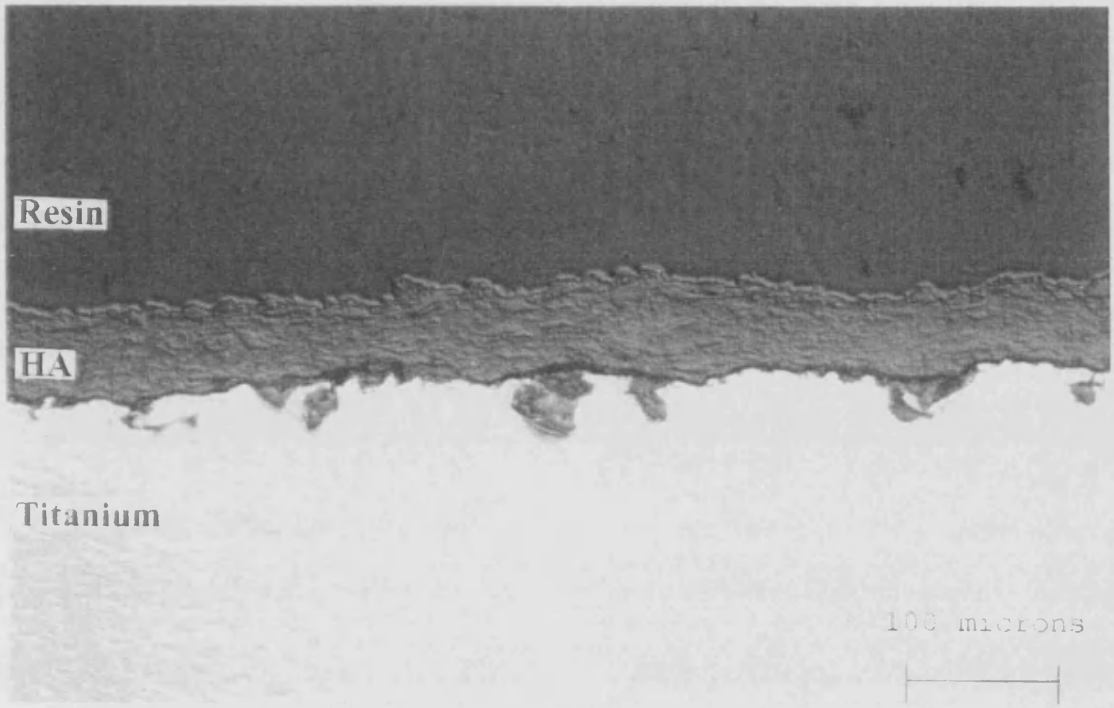

Figure 7-11 :- Optical micrograph showing cross-section through DGUN HA coatings fatigued in Ringer's solution for one million cycles

The coating fatigued in Ringer's solution for ten million cycles (Figure 7-12) however shows much more dramatically the damaging effect of the *in-vitro* fatigue environment. Here one can see several modifications to the appearance of the polished cross-section of the coating the most obvious being the modified surface layer to the coating and its apparent delamination from the substrate. The thickness of the bulk of the coating appears to be reduced on average along the cross-sectional length and its porosity is considerably higher than either the as-received coating or the coating fatigued for one million cycles in Ringer's solution. The modified surface layer appears to be approximately 5 - 10 μm thick and has brought about an apparent smoothing of the very surface of the coating. The black line seen in coatings fatigued in air and in Ringer's solution for only one million cycles seems to have grown to the extent that the coating is effectively completely delaminated from the substrate. The visible gap between the substrate and the coating itself varies between 10 and 20 μm although the coating was

apparently coherent enough with the substrate to allow sectioning and polishing of the material.

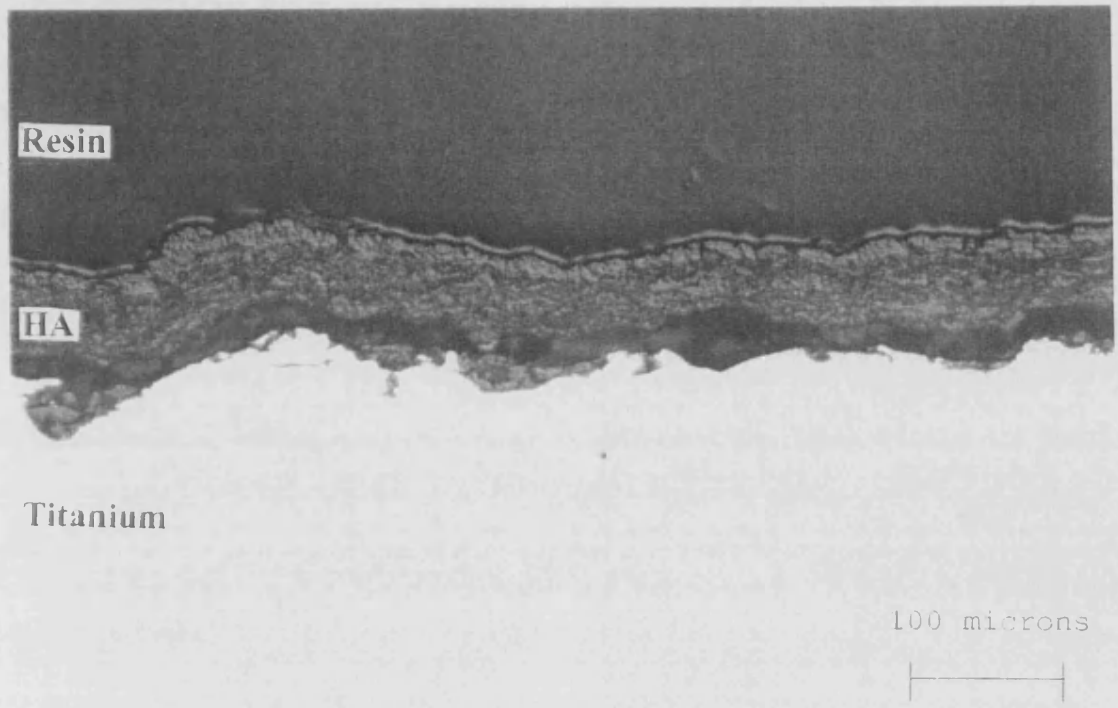

Figure 7-12 :- Optical micrograph showing cross-section through DGUN HA coatings fatigued in Ringer's solution for ten million cycles

7.2.5 Scanning Electron Microscopy

The surface of the coating fatigued for one million cycles in air (Figure 7-13) had a similar morphology to that of the as-received DGUN coating. The surface was still distinctly two phase in morphology with smooth, glassy amorphous regions as well as agglomerated, crystalline regions. The amorphous regions did not appear to be any different in morphology to those on the as-received coating surface. The coating surface again showed evidence of micro-cracking and although the difference may have been small it appeared that these cracks had grown during the fatigue process. The surface also appeared to be rougher in nature than that of the as-received coating with evidence or large pores in the coating possibly formed as a result of the fall-out of material from the coating surface.

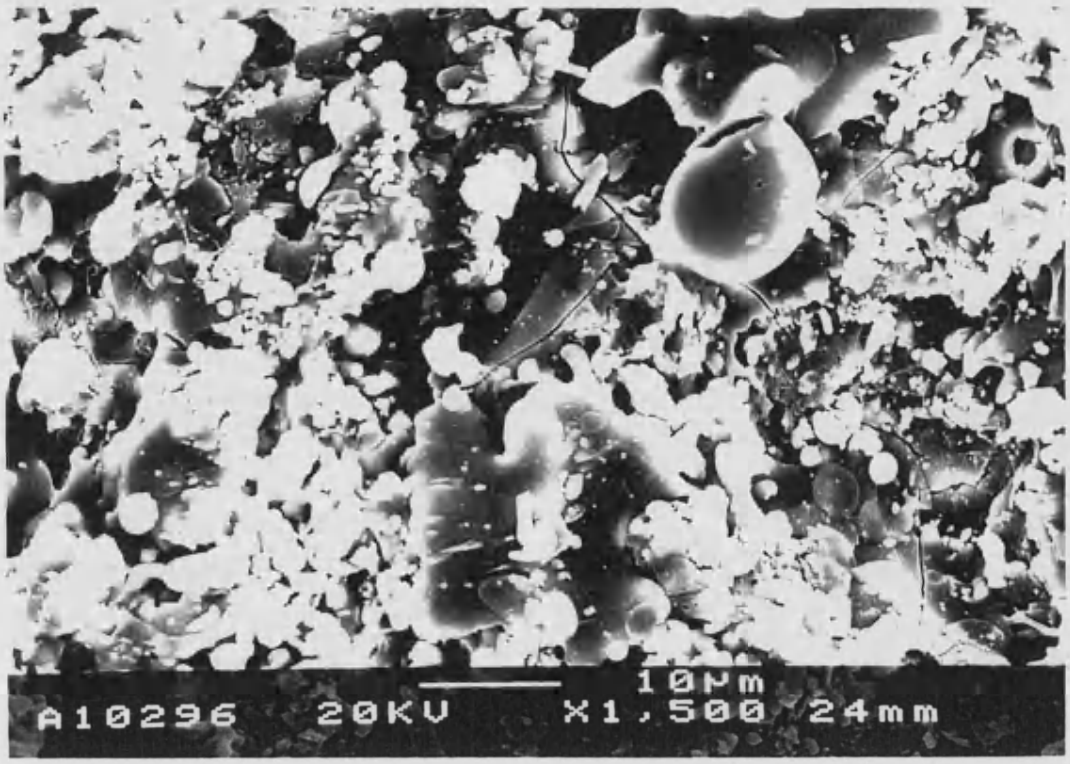

Figure 7-13 :- Scanning electron micrograph showing surface of DGUN HA coatings fatigued in air for one million cycles

This morphology was again observed in the coating fatigued for ten million cycles in air (Figure 7-14). The surface was still two phase in morphology although the amorphous phase showed some evidence for pitting or etching and had lost some of its smooth appearance. Again the enlarged micro-cracks were present and the depth of porosity in the surface seemed to indicate loss of material from the coating. As a whole however the effect of fatigue testing of the coatings in air appeared to be minimal and any loss in the integrity of the coating surface due to micro-crack enlargement seemed to be small.

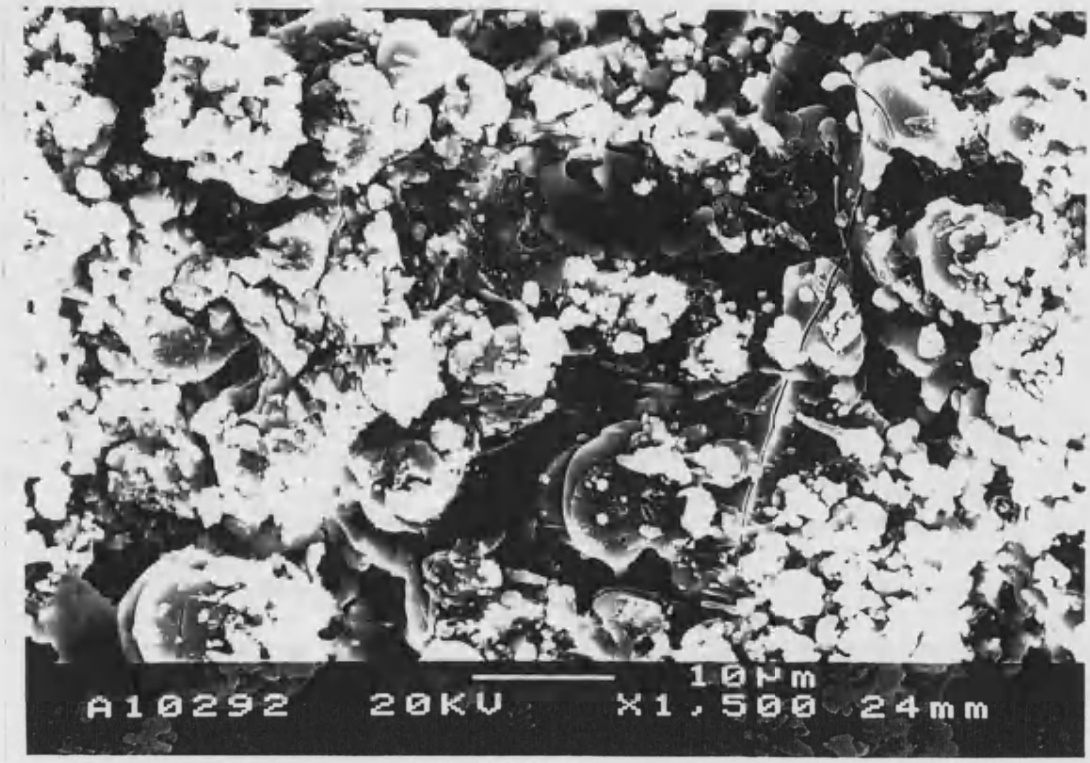

Figure 7-14 :- Scanning electron micrograph showing surface of DGUN HA coatings fatigued in air for ten million cycles

The coating fatigued in Ringer's solution for one million cycles (Figure 7-15) had a very different appearance to either the as-received coating or the coatings fatigued in air. Here the coating surface was criss-crossed by micro-cracks lending a crazed appearance to the coating surface. Apart from this cracking however the effect of the ageing medium on the surface of the coating was clearly visible. The surface morphology had dramatically changed loosing the two phase structure characteristic of HA coatings. Now the coating was covered in small, nodular growths and porosity. These nodules had a crystalline appearance and were assumed to be re-deposited hydroxyapatite laid down on a previously etched surface. Unlike in previous examples of these formations seen in aged coatings however, it is clear that in this case the formation of this phase has occurred before the extensive cracking of the surface has taken place. The growths do not spread over the edges of micro-cracks indicating that these have grown at a later time.

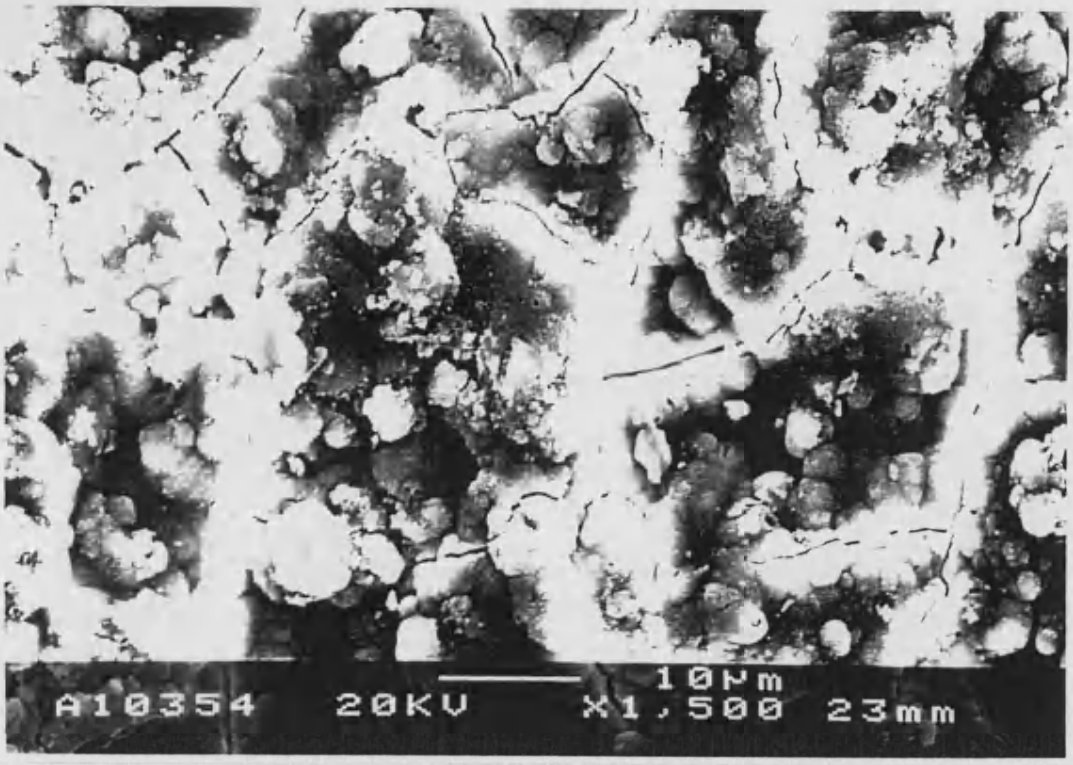

Figure 7-15 :- Scanning electron micrograph showing surface of DGUN HA coatings fatigued in Ringer's solution for one million cycles

The modified surface appearance is accentuated in the coating which has been fatigued for ten million cycles in Ringer's solution (Figure 7-16). Again here one can see evidence of these nodular surface growths but here they have a sintered appearance as if the crystallites have grown right up to one another to form a coherent layer. These formations themselves have however been subsequently attacked by the ageing medium and are pitted in nature. This newly formed layer on the coating surface seems to have had the effect of smoothing the surface roughness overall but it can clearly be seen that this is a temporary effect since in some areas this new layer has broken away from the surface revealing the rough surface beneath. The fragile nature of this layer probably results from the high degree of cracking of the surface. These cracks are larger and wider than on the surface of the coating fatigued for one million cycles and seem to boarder areas of the surface which have fallen away. The electron beam was seen to damage this fragile surface during scanning electron microscopy, again giving evidence for the delicate nature of the surface layer.

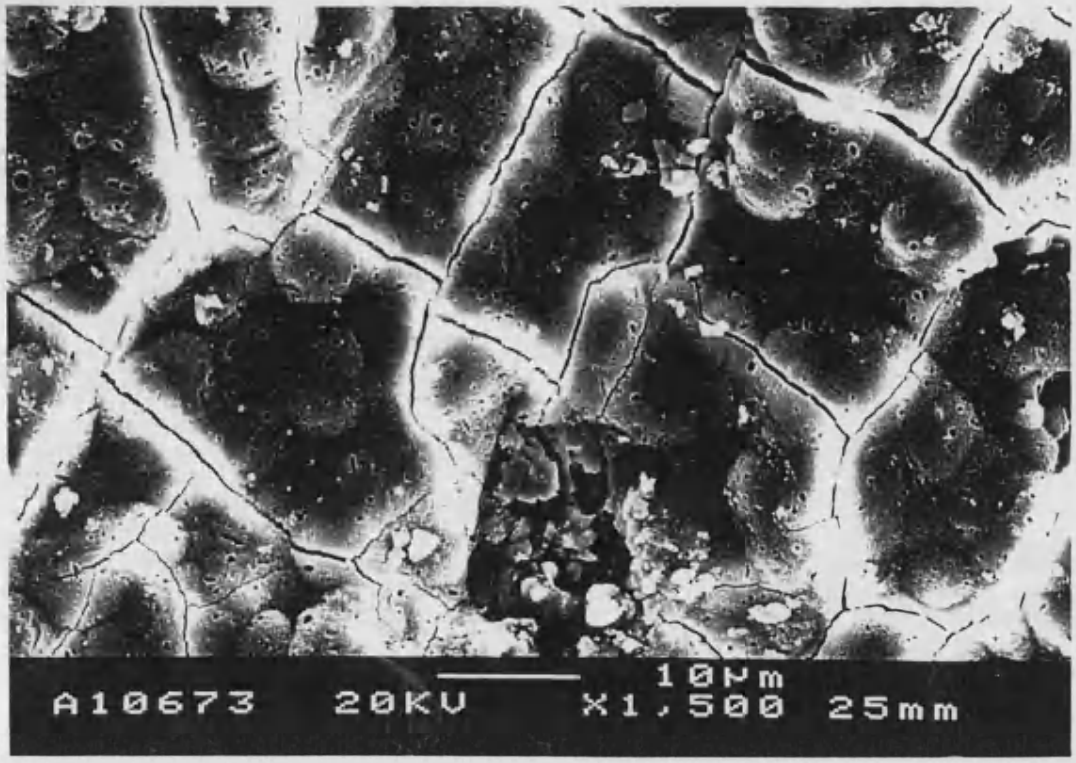

Figure 7-16 :- Scanning electron micrograph showing surface of DGUN HA coatings fatigued in Ringer's solution for ten million cycles

7.2.6 Coating Thickness Results

Table 7-9 presents a summary of the cross-sectional thickness results for the detonation gun hydroxyapatite coatings fatigued in air and in Ringer's solution for one and ten million cycles.

Sample	*No. of tests*	*Mean (μm)*	*Standard Deviation*	*Variance*	*95% Confidence Limits*
as-received	10	70.0840	9.5690	91.5653	69.275 and 70.893
air 10^6	40	59.7307	5.6375	31.7810	50.760 and 68.701
air 10^7	10	61.4273	9.4645	89.5772	60.627 and 62.227
Ringer's 10^6	40	61.1052	7.4864	56.0462	49.193 and 73.018
Ringer's 10^7	10	49.6867	8.9839	80.7106	48.927 and 50.446

Table 7-9 :- Cross-sectional thickness results for VPS HA coatings fatigued in air and in Ringer's solution

Using a 2-tailed Student T-test the significance of these results was determined at the 5% level, revealing that :

The coating fatigued in air for 1x10e6 cycles had a thickness that was significantly different to that of the as-received coating.

The coating fatigued in air for 1x10e7 cycles had a thickness that was significantly different to that of the as-received coating but was not significantly different to the coating fatigued in air for 1x10e6 cycles.

The coating fatigued in Ringer's solution for 1x10e6 cycles had a thickness that was significantly different from that of the as-received coating but was not significantly different from that of the coating fatigued in air 1x10e6 cycles.

The coating fatigued in Ringer's solution for 1x10e7 cycles had a thickness that was significantly different both from the as-received coating and also from that of the coating fatigued in Ringer's solution for 1x10e6 cycles.

Therefore, it was found that all the fatigued coatings displayed significant differences in thickness from the as-received coating. The coatings showed no significant differences between the thicknesses of different groups however except between the coatings fatigued in Ringer's solution.

7.2.7 Coating Porosity Results

Table 7-10 presents a summary of the cross-sectional porosity results for the detonation gun sprayed hydroxyapatite coatings fatigued in air and in Ringer's solution for one and ten million cycles.

Sample	No. of tests	Mean (%)	Standard Deviation	Variance	95% Confidence Limits
as-received	10	1.4485	0.7381	0.5448	1.103 and 1.794
air 10^6	40	6.5403	3.3349	11.1214	1.234 and 11.847
air 10^7	10	1.1298	0.6328	0.4005	0.834 and 1.426
Ringer's 10^6	40	5.8433	0.9623	0.9260	4.312 and 7.375
Ringer's 10^7	10	23.5333	3.1944	10.2361	22.036 and 25.031

Table 7-10 :- Cross-sectional porosity results for DGUN HA coatings fatigued in air and in Ringer's solution

Using a 2-tailed Student T-test the significance of these results was determined at the 5% level, revealing that :

The coatings fatigued in air for 1x10e6 cycles had a porosity that was significantly different from that of the as-received coating.

The coating fatigued in air for 1x10e7 cycles had a porosity that was not significantly different from the as-received coating but was significantly different from the coating fatigued in air for 1x10e6 cycles.

The coatings fatigued in Ringer's solution for 1x10e6 cycles had a porosity that was significantly different from the as-received coating and was also significantly different from the coating fatigued in air for 1x10e6 cycles.

The coating fatigued in Ringer's solution for 1x10e7 cycles had a porosity that was significantly different both from the as-received coating and from the coating fatigued in Ringer's solution for 1x10e6 cycles.

Therefore it was found that all the coatings except that fatigued in air for 1x10e7 cycles had porosity levels that varied significantly from the as-received coating. All the coatings also had significantly different porosity levels between testing groups.

7.2.8 Surface Roughness (Ra) Results

Table 7-11 presents a summary of the surface roughness results for the detonation gun sprayed hydroxyapatite coatings fatigued in air and in Ringer's solution for one and ten million cycles.

Sample	*mean Ra (μm)*	*standard deviation*	*variance*	*95% conf. interval*
as-received	5.5294	-	-	-
air 10^6	5.9074	0.6426	0.4130	5.370 and 6.445
air 10^7	6.2198	-	-	-
Ringer's 10^6	5.8256	0.4131	0.1706	5.480 and 6.171
Ringer's 10^7	6.6356	-	-	-

Table 7-11 :- Surface roughness results for DGUN HA coatings fatigued in air and in Ringer's solution

Using a 2-tailed Student T-test the significance of these results was determined at the 5% level, revealing that :

The coatings fatigued in air for 1x10e6 cycles had a surface roughness that was not significantly different from the as-received coating.

The coatings fatigued in Ringer's solution for 1x10e6 cycles had a surface roughness that was neither significantly different from the as-received value nor from that for the coatings fatigued in air for 1x10e6 cycles

7.2.9 Residual Stress Results

Table 7-12 presents a summary of the residual stress analysis results for the detonation gun sprayed hydroxyapatite coatings fatigued in air and in Ringer's solution for one and ten million cycles.

Sample	*residual stress (MPa)*	*standard deviation*	*variance*	*95% conf. interval*
DGUN HA powder	-	-	-	-
as-received	28.8260	-	-	-
air 10^6	14.6933	8.2185	67.5430	7.823 and 21.564
air 10^7	37.4738	-	-	-
Ringer's 10^6	14.1328	2.8413	8.0731	11.757 and 16.508
Ringer's 10^7	17.6159	-	-	-

Table 7-12 :- Residual stress results in 004 plane for DGUN HA coatings fatigued in air and in Ringer's solution

Using a 2-tailed Student T-test the significance of these results was determined at the 5% level, revealing that :

The coatings fatigued in air for 1x10e6 cycles had a residual stress that was significantly different from that of the as-received coating.

The coatings fatigued in Ringer's solution for 1x10e6 cycles had a residual stress level that was significantly different from that of the as-received coating but was not significantly different from that of the coatings fatigued in air for 1x10e6 cycles.

7.3 VPS HA Coatings Aged Then Fatigued In Ringer's Solution

7.3.1 X-Ray Diffraction Traces

Figure 7-17 presents sections from the x-ray diffraction traces for the vacuum plasma sprayed hydroxyapatite coatings aged for various time periods before fatigue testing in Ringer's solution for one million cycles.

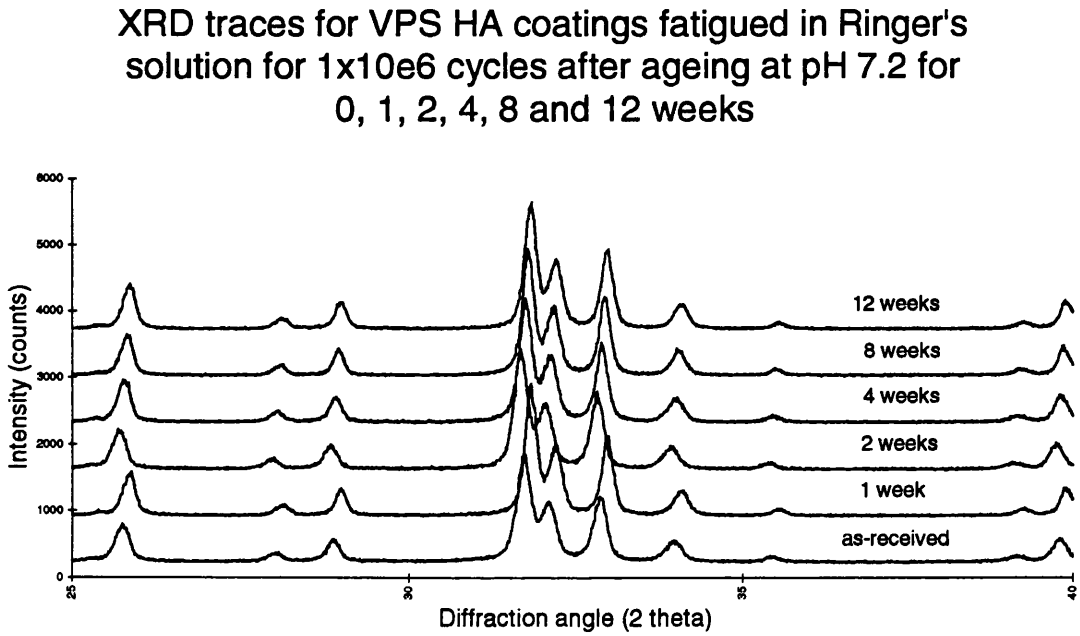

Figure 7-17 :- Amorphous hump region from X-Ray diffraction traces of VPS HA coatings aged then fatigued in Ringer's solution

7.3.2 Crystallinity Results

Table 7-13 presents a summary of the crystallinity results for the vacuum plasma sprayed hydroxyapatite coatings aged for various time periods before fatigue testing in Ringer's solution for one million cycles.

Sample	*No. of tests*	*Mean (%)*	*Standard Deviation*	*Variance*	*95% Confidence Limits*
as-received	10	60.3542	2.1942	4.8145	59.738 and 61.053
1 week	80	67.1530	1.1210	1.2560	66.338 and 67.969
2 weeks	80	68.6550	0.7732	0.5978	67.790 and 69.520
4 weeks	60	68.6882	0.4559	0.2079	67.886 and 69.491
8 weeks	60	68.1126	1.0211	1.0426	67.310 and 68.915
12 weeks	40	68.7733	2.5321	6.4116	67.789 and 69.758

Table 7-13 :- Crystallinity results for VPS HA coatings aged then fatigued in Ringer's solution

Table 7-14 presents the significance test results for the crystallinity data from vacuum plasma sprayed coatings aged for various time periods before fatigue testing in Ringer's solution for one million cycles.

crystallinity	*as-received*	*air fatigue*	*Ringer's fatigue*	*1 week*	*2 weeks*	*4 weeks*	*8 weeks*	*12 weeks*
as-received		✖	✓	✓	✓	✓	✓	✓
air fatigue	✖		✓	✓				
Ringer's fatigue	✓	✓		✓				
1 week	✓	✓	✓		✓			
2 weeks	✓			✓		✖		
4 weeks	✓				✖		✖	
8 weeks	✓					✖		✖
12 weeks	✓						✖	

Table 7-14 :- Significant test results for VPS HA coatings aged the fatigued in Ringer's solution

✓ = significantly different

✖ = not significantly different

= not tested

Therefore it was found that all the coatings which had been aged in Ringer's solution before fatigue testing in Ringer's solution for 1x10e6 cycles had significantly different crystallinities from that of the as-received coating. These coatings also showed

no significant change in crystallinity between testing groups except in the case of those coatings which had been aged for between one and two weeks.

7.3.3 X-Ray Plane Analysis

Table 7-15 presents a summary of the x-ray plane analysis for the vacuum plasma sprayed hydroxyapatite coatings aged for various time periods before fatigue testing in Ringer's solution for one million cycles.

Sample	*Major Compound*	*Significant Compounds*	*Trace Compounds*
as-received	HA	-	α-TCP, β-TCP, $Ca_4O(PO_4)_2$, $Ca_2P_2O_7$
1 week	HA	β-TCP	α-TCP
2 weeks	HA	β-TCP	α-TCP
4 weeks	HA	β-TCP	α-TCP, $Ca_4O(PO_4)_2$
8 weeks	HA	β-TCP	α-TCP
12 weeks	HA	-	α-TCP, $Ca_4O(PO_4)_2$

Table 7-15 :- X-Ray plane analysis results for VPS HA coatings aged then fatigued in Ringer's solution

7.3.4 Optical Microscopy

The polished cross-section through the VPS HA coating aged for one week in Ringer's solution before fatigue testing (Figure 7-18) has a morphology very similar to that of the as-received coating. The cross-sectional thickness and porosity levels for this coating seem to have remained the same after ageing and fatigue testing. The lamella nature of the coating imposed by the manufacturing technique is still clearly visible as is the pure titanium interlayer between the hydroxyapatite and the substrate. The surface of the coating also appears to have been unaffected by the testing regime and shows no obvious increase in roughness. The coating seems to be well adhered to the substrate although a thin dark line can be seen running along the interface between the coating and the titanium in some areas.

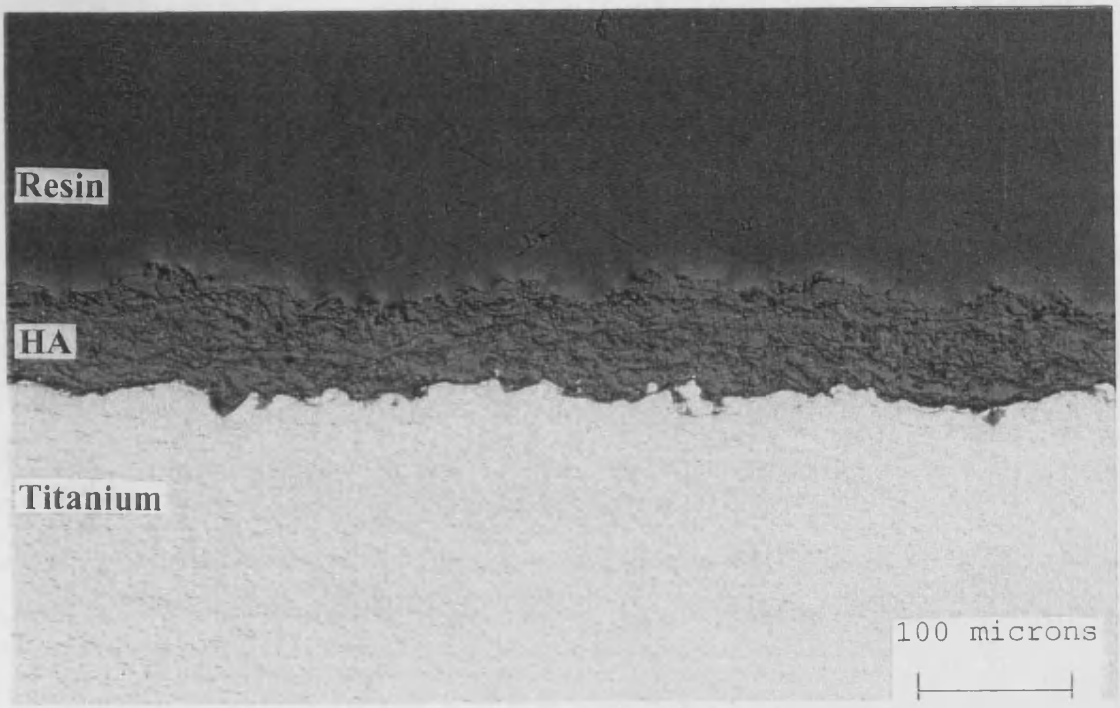

Figure 7-18 :- Optical micrograph showing cross-section through VPS HA coatings aged for one week then fatigued in Ringer's solution

The polished cross-section through the coating aged for two weeks before fatigue testing in Ringer's solution (not shown) again seems to be remarkably similar in morphology to the as-received coating. There is again no obvious change in the thickness of the coating in comparison to the as-received coating and also no apparent change in porosity. Again the coating is well adhered to the substrate and in this case there is no evidence for the dark line seen in the coating aged for one week. As reported for the coating aged for the shorter duration, there is no apparent morphological alteration occurring at the surface of the coating and no obvious change in surface roughness.

The coatings aged for four and eight weeks before fatigue testing in Ringer's solution (neither shown) again show no change in cross-sectional morphology resulting from the testing procedure. In both coatings, the layered nature imposed by vacuum plasma spraying and the titanium interlayer are still clearly visible. Both coatings are well adhered to the substrate and both show no evidence for the thin black line seen for the coating aged for just one week. Neither coating shows any obvious difference in

thickness compared to the as-received coating although it is possible that the variation in thickness along the cross-sectional length is greater for these coatings than for the coatings aged for shorter durations. The coatings also show no significant variation in porosity or surface roughness as a result of the ageing process and there is no evidence for a modification to the morphology of the coating surface layer.

This overall trend continues with the polished cross-section through the coating aged for twelve weeks before fatigue testing in Ringer's solution (Figure 7-19). Yet again here one can see no obvious changes in either thickness, porosity or surface roughness for this coating as opposed to the as-received coating. As described above for the other aged then fatigued coatings, this coating shows no signs of delamination from the substrate nor modification to the surface layers in the material. The layered morphology characteristic of the vacuum plasma sprayed coatings and the titanium bond layer between the coating and the Ti-6Al-4V substrate are also still visible.

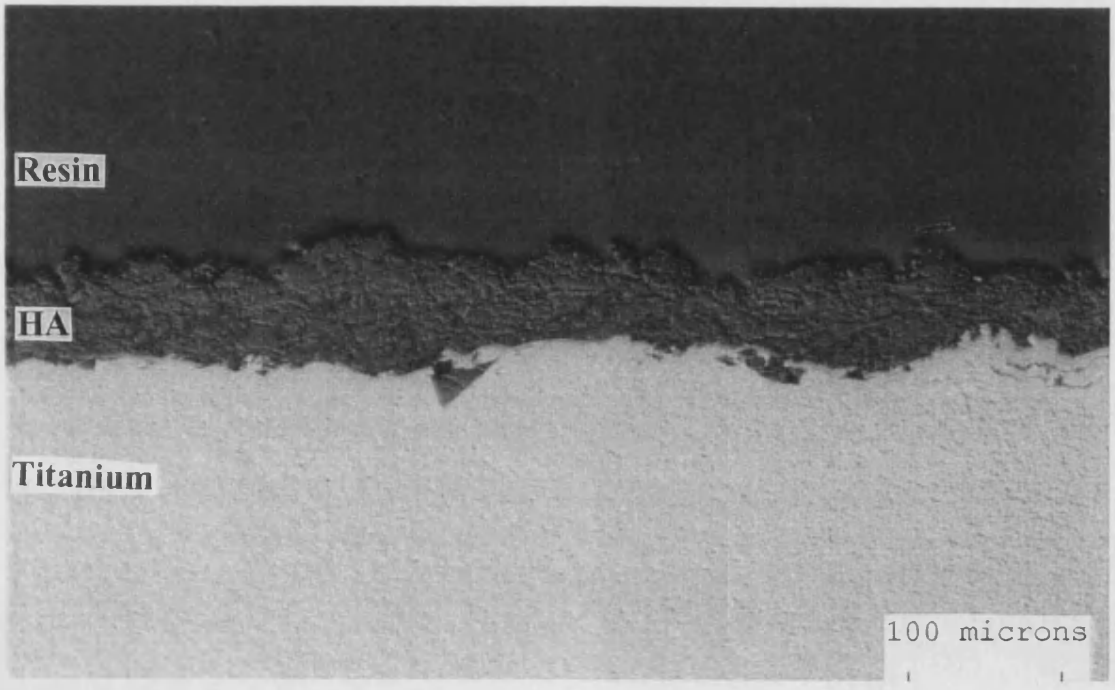

Figure 7-19 :- Optical micrograph showing cross-section through VPS HA coatings aged for twelve weeks then fatigued in Ringer's solution

Overall, the duration of ageing of the VPS HA coatings before fatigue testing in Ringer's solution seems to have no observable effect on the cross-sectional morphology of the coatings when prepared for optical microscopy. Looking at all the samples in fact no change in the samples seems to have been imposed by the combined effect of *in-vitro* ageing and fatigue.

7.3.5 Scanning Electron Microscopy

The coating which was aged in Ringer's solution for one week before fatigue testing for one million cycles in Ringer's solution (Figure 7-20) has a similar appearance to that of a coating which has just been aged in solution. The coating surface shows no signs of extensive micro-cracking which may have resulted from the fatigue process but does show evidence of attack by the ageing medium. The flat, glassy regions of amorphous material in the surface appear to have been slightly etched by the *in-vitro* solution giving them a lace-like appearance in some regions. In other regions the amorphous phase seems to have thinned allowing the morphology of the layer lying directly below it to be seen through the glassy phase. Micro-cracks are still present on the coating surface but these do not seem to have growth in width or length.

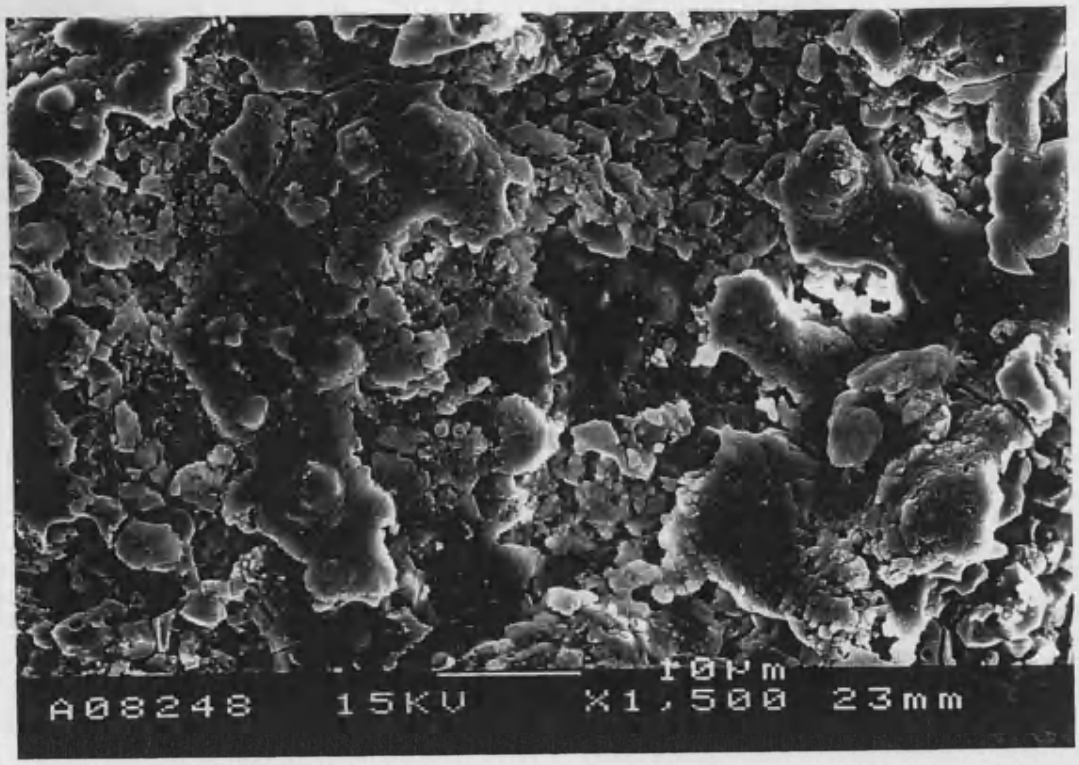

Figure 7-20 :- Scanning electron micrograph showing surface of VPS HA coatings aged for one week then fatigued in Ringer's solution

A very similar morphology can be seen for the surface of the coating aged for two weeks before fatigue testing (not shown). Here again one can see evidence for dissolution of the amorphous phase due to exposure to the ageing medium. Again the glassy phase shows some degree of pitting and reveals the morphology of the lower layers of the coating suggesting that it has become thinner as a result of attack by the *in-vitro* solution. In this surface however one can see some evidence for a propagation of the micro-cracks seen in earlier coatings. Here the cracks seem to be more numerous in nature and indeed show signs of branching and proliferation.

The coatings aged for four weeks before fatigue testing in Ringer's solution (not shown) however do not support this impression of growth in the number and magnitude of micro-cracks. This surface still shows large expanses of flat, amorphous material which, although showing signs of attack from the *in-vitro* medium is not excessively cracked. It has been observed that in other coatings, micro-cracking seems to propagate

through these glassy regions and large areas of un-cracked amorphous material seems to suggest that crack propagation is not occurring.

This view is supported by looking at the surface of coatings which have been fatigue tested after ageing for eight weeks *in-vitro* (not shown). Again here one can see large expanses of un-cracked amorphous material which although pitted by the ageing medium is otherwise undamaged. The dissolution process seems to have progressed in this surface however. Here one can see very small nodular formations lying in groups in some areas of the coating surface. These formations seem to be discrete in nature and may have formed as a result of reprecipitation of crystalline hydroxyapatite on the surface but are however considerably smaller than other cauliflower-like growths seen on other coatings.

The coating aged for twelve weeks before fatigue testing (Figure 7-21) again showed dissolution of amorphous material but no direct evidence for cracking of the surface as a result of cyclic loading. The surface shows both thinning and pitting of the glassy amorphous regions but also mineral-like regions composed of many tiny, regular sided crystallites. The clustering of these crystallites suggests that they are not a product of the original spraying process which would scatter them randomly across the coating surface, but that they have been deposited on the surface during the ageing process. It is possible that these crystallites have grown from the nodular structures seen on the surface of coatings aged for shorter durations.

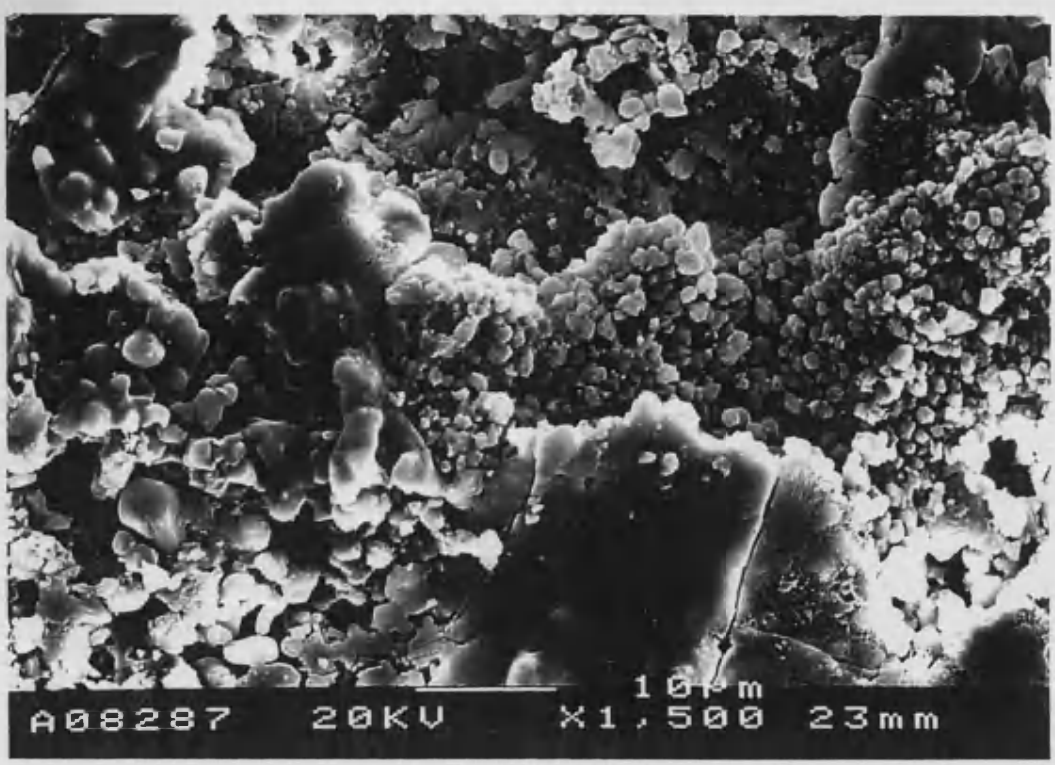

Figure 7-21 :- Scanning electron micrograph showing surface of VPS HA coatings aged for twelve weeks then fatigued in Ringer's solution

Looking at all the coatings which have been exposed to the *in-vitro* medium before fatigue testing is seems apparent that the effect of the ageing solution plays a much greater role in any modification of the coating surface than the process of cyclic loading.

7.3.6 Coating Thickness Results

Table 7-16 presents a summary of the cross-sectional thickness results for the vacuum plasma sprayed hydroxyapatite coatings aged for various time periods before fatigue testing in Ringer's solution for one million cycles.

Sample	*No. of tests*	*Mean (μm)*	*Standard Deviation*	*Variance*	*95% Confidence Limits*
as-received	10	42.4840	11.6308	135.2751	41.501 and 42.484
1 week	40	57.2374	15.2396	232.2464	32.988 and 81.487
2 weeks	40	59.9022	5.6261	31.6531	50.950 and 68.855
4 weeks	30	60.5231	13.9352	194.1890	25.906 and 95.140
8 weeks	30	70.1841	13.3536	178.3198	37.012 and 103.356
12 weeks	20	61.4658	2.5676	6.5927	38.397 and 84.535

Table 7-16 :- Cross-sectional thickness results for VPS HA coatings aged then fatigued in Ringer's solution

Table 7-17 presents the significance test results for the cross-sectional thickness data from vacuum plasma sprayed coatings aged for various time periods before fatigue testing in Ringer's solution for one million cycles.

thickness	*as-received*	*air fatigue*	*Ringer's fatigue*	*1 week*	*2 weeks*	*4 weeks*	*8 weeks*	*12 weeks*
as-received		✓	✓	✖	✖	✖	✖	✖
air fatigue	✓		✓	✖				
Ringer's fatigue	✓	✓		✖				
1 week	✖	✖	✖		✖			
2 weeks	✖			✖		✖		
4 weeks	✖				✖		✖	
8 weeks	✖					✖		✖
12 weeks	✖						✖	

Table 7-17 :- Significant test results for VPS HA coatings aged the fatigued in Ringer's solution

✓ = significantly different

✖ = not significantly different

= not tested

Therefore it was found that all the coatings which had been aged in Ringer's solution before fatigue testing in Ringer's solution for 1x10e6 cycles had thickness

values that did not vary significantly from that of the as-received coating. These coatings also showed no significant change in thickness between testing groups.

7.3.7 Coating Porosity Results

Table 7-18 presents a summary of the cross-sectional porosity results for the vacuum plasma sprayed hydroxyapatite coatings aged for various time periods before fatigue testing in Ringer's solution for one million cycles.

Sample	*No. of tests*	*Mean (%)*	*Standard Deviation*	*Variance*	*95% Confidence Limits*
as-received	10	5.749	1.464	2.144	4.702 and 6.797
1 week	40	4.2508	2.5630	6.5688	3.680 and 4.821
2 weeks	40	3.1845	2.9587	8.7537	2.526 and 3.843
4 weeks	30	2.7717	1.8967	3.5975	2.282 and 3.262
8 weeks	30	2.4167	1.8360	3.3710	1.942 and 2.891
12 weeks	20	1.7228	1.4218	2.0216	1.268 and 2.178

Table 7-18 :- Cross-sectional porosity results for VPS HA coatings aged then fatigued in Ringer's solution

Table 7-19 presents the significance test results for the cross-sectional porosity data from vacuum plasma sprayed coatings aged for various time periods before fatigue testing in Ringer's solution for one million cycles.

porosity	*as-received*	*air fatigue*	*Ringer's fatigue*	*1 week*	*2 weeks*	*4 weeks*	*8 weeks*	*12 weeks*
as-received		✖	✖	✖	✖	✖	✖	✖
air fatigue	✖		✖	✖				
Ringer's fatigue	✖	✖		✖				
1 week	✖	✖	✖		✖			
2 weeks	✖			✖		✖		
4 weeks	✖				✖		✖	
8 weeks	✖					✖		✖
12 weeks	✖						✖	

Table 7-19 :- Significant test results for VPS HA coatings aged the fatigued in Ringer's solution

✓ = significantly different

✖ = not significantly different

= not tested

Therefore it was found that all the coatings which had been aged in Ringer's solution before fatigue testing in Ringer's solution for 1x10e6 cycles had porosity values that did not vary significantly from that of the as-received coating. These coatings also showed no significant change in porosity between testing groups.

7.3.8 Surface Roughness (Ra) Results

Table 7-20 presents a summary of the surface roughness results for the vacuum plasma sprayed hydroxyapatite coatings aged for various time periods before fatigue testing in Ringer's solution for one million cycles.

Sample	mean Ra (μm)	standard deviation	variance	95% conf. interval
as-received	5.5727	-	-	-
1 week	5.6357	0.5059	0.2559	5.213 and 6.059
2 weeks	6.0558	0.3807	0.1449	5.736 and 6.374
4 weeks	5.9290	0.5160	0.2662	5.388 and 6.471
8 weeks	6.1026	0.4852	0.2354	5.593 and 6.612
12 weeks	5.4362	0.5009	0.2509	4.639 and 6.233

Table 7-20 :- Surface roughness results for VPS HA coatings aged then fatigued in Ringer's solution

Table 7-21 presents the significance test results for the surface roughness data from vacuum plasma sprayed coatings aged for various time periods before fatigue testing in Ringer's solution for one million cycles.

Ra (μm)	as-received	air fatigue	Ringer's fatigue	1 week	2 weeks	4 weeks	8 weeks	12 weeks
as-received		✖	✖	✓	✓	✓	✓	✖
air fatigue	✖		✓	✓				
Ringer's fatigue	✖	✓		✖				
1 week	✓	✓	✖		✓			
2 weeks	✓			✓		✖		
4 weeks	✓				✖		✖	
8 weeks	✓					✖		✖
12 weeks	✖						✖	

Table 7-21 :- Significant test results for VPS HA coatings aged the fatigued in Ringer's solution

✓ = significantly different

✖ = not significantly different

= not tested

Therefore it was found that all the coatings which had been aged in Ringer's solution before fatigue testing in Ringer's solution for 1x10e6 cycles had surface roughness values that varied significantly from that of the as-received coating. The exception to this was found in the case of those coatings which had been aged for twelve

weeks before fatigue testing. The aged and fatigued coatings however showed no significant change in surface roughness between testing groups again with the exception of one group. There was found to be a significant change in roughness between those coatings aged for between one and two weeks before fatigue testing.

7.3.9 Residual Stress Results

Table 7-22 presents a summary of the residual stress analysis results for the vacuum plasma sprayed hydroxyapatite coatings aged for various time periods before fatigue testing in Ringer's solution for one million cycles.

Sample	*residual stress (MPa)*	*standard deviation*	*variance*	*95% conf. interval*
VPS HA powder	-	-	-	-
as-received	2.8764	-	-	-
1 week	4.0350	3.1820	10.1251	1.375 and 6.695
2 weeks	3.7553	4.0164	16.1315	0.398 and 7.113
4 weeks	1.9709	1.7320	2.9996	0.153 and 3.788
8 weeks	1.7578	0.5252	0.2760	1.207 and 2.309
12 weeks	1.9975	1.9593	3.8389	-1.120 and 5.115

Table 7-22 :- Residual stress results in 004 plane for VPS HA coatings aged then fatigued in Ringer's solution

Table 7-23 presents the significance test results for the residual stress data from vacuum plasma sprayed coatings aged for various time periods before fatigue testing in Ringer's solution for one million cycles.

residual stress	*as-received*	*air fatigue*	*Ringer's fatigue*	*1 week*	*2 weeks*	*4 weeks*	*8 weeks*	*12 weeks*
as-received		✓	✖	✖	✖	✖	✖	✖
air fatigue	✓		✓	✓				
Ringer's fatigue	✖	✓		✖				
1 week	✖	✓	✖		✖			
2 weeks	✖			✖		✖		
4 weeks	✖				✖		✖	
8 weeks	✖					✖		✖
12 weeks	✖						✖	

Table 7-23 :- Significant test results for VPS HA coatings aged the fatigued in Ringer's solution

✓ = significantly different

✖ = not significantly different

= not tested

Therefore it was found that all the coatings which had been aged in Ringer's solution before fatigue testing in Ringer's solution for 1x10e6 cycles had residual stress values that did not vary significantly from that of the as-received coating. The aged and fatigued coatings also showed no significant change in residual stress between testing groups.

7.4 DGUN HA Coatings Aged Then Fatigued In Ringer's Solution

7.4.1 X-Ray Diffraction Traces

Figure 7-22 presents sections from the x-ray diffraction traces for the detonation gun sprayed hydroxyapatite coatings aged for various time periods before fatigue testing in Ringer's solution for one million cycles.

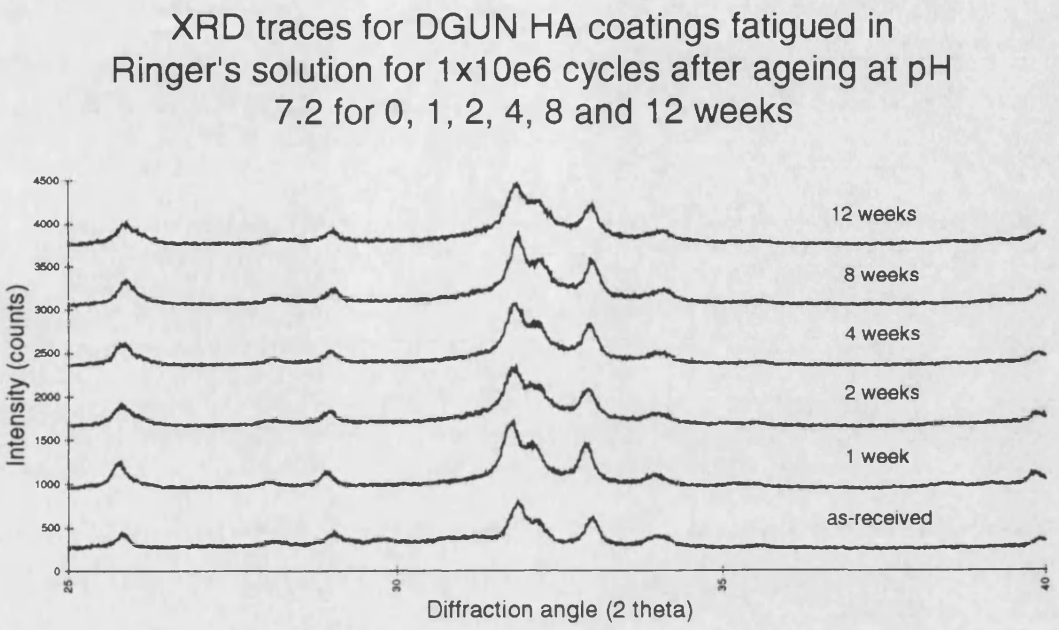

Figure 7-22 :- Amorphous hump region from X-Ray diffraction traces of DGUN HA coatings aged then fatigued in Ringer's solution

7.4.2 Crystallinity Results

Table 7-24 presents a summary of the crystallinity results for the detonation gun sprayed hydroxyapatite coatings aged for various time periods before fatigue testing in Ringer's solution for one million cycles.

Sample	*No. of tests*	*Mean (%)*	*Standard Deviation*	*Variance*	*95% Confidence Limits*
as-received	10	34.4223	0.9043	0.8183	33.7752 and 35.0694
1 week	80	40.3845	3.7728	14.2342	37.230 and 43.539
2 weeks	80	36.4294	3.7059	13.7336	33.331 and 39.528
4 weeks	80	34.6973	2.6359	6.9477	32.494 and 36.901
8 weeks	80	35.4215	2.4817	6.1589	33.347 and 37.496
12 weeks	80	35.4734	2.6762	7.1622	33.236 and 37.711

Table 7-24 :- Crystallinity results for DGUN HA coatings aged then fatigued in Ringer's solution

Table 7-25 presents the significance test results for the crystallinity data from detonation gun sprayed coatings aged for various time periods before fatigue testing in Ringer's solution for one million cycles.

crystallinity	*as-received*	*air fatigue*	*Ringer's fatigue*	*1 week*	*2 weeks*	*4 weeks*	*8 weeks*	*12 weeks*
as-received		✓	✓	✓	✓	✖	✓	✓
air fatigue	✓		✓	✓				
Ringer's fatigue	✓	✓		✓				
1 week	✓	✓	✓		✓			
2 weeks	✓			✓		✓		
4 weeks	✖				✓		✓	
8 weeks	✓					✓		✖
12 weeks	✓						✖	

Table 7-25 :- Significant test results for DGUN HA coatings aged the fatigued in Ringer's solution

✓ = significantly different

✖ = not significantly different

= not tested

Therefore it was found that all the coatings which had been aged in Ringer's solution before fatigue testing in Ringer's solution for 1x10e6 cycles had significantly different crystallinities from that of the as-received coating. The exception to this was the coating that was aged for four weeks in Ringer's solution before fatigue testing. The coatings also showed a significant change in crystallinity between testing groups except in the case of those coatings which had been aged for between eight and twelve weeks.

7.4.3 X-Ray Plane Analysis

Table 7-26 presents a summary of the x-ray plane analysis results for the detonation gun sprayed hydroxyapatite coatings aged for various time periods before fatigue testing in Ringer's solution for one million cycles.

Sample	*Major Compound*	*Significant Compounds*	*Trace Compounds*
as-received	HA	β-TCP, $Ca_4O(PO_4)_2$	α-TCP
1 week	HA	-	β-TCP, $Ca_4O(PO_4)_2$
2 weeks	HA	β-TCP	α-TCP, $Ca_4O(PO_4)_2$
4 weeks	HA	-	α-TCP, β-TCP, $Ca_4O(PO_4)_2$
8 weeks	HA	β-TCP	α-TCP, $Ca_4O(PO_4)_2$
12 weeks	HA	-	α-TCP, β-TCP, $Ca_4O(PO_4)_2$

Table 7-26 :- X-Ray plane analysis results for DGUN HA coatings aged then fatigued in Ringer's solution

7.4.4 Optical Microscopy

The polished cross-section through the DGUN HA coating aged for one week *in-vitro* before fatigue testing in Ringer's solution (Figure 7-23) has a very similar appearance to that of the as-received coating. The bulk of the coating still seems to display the characteristic morphology of detonation gun coatings but the coating itself is apparently thinner than the as-received coating. The coating also appears to have a higher porosity than the as-received coating and perhaps a higher surface roughness. The coating is still well adhered to the substrate but there is a thin black line running virtually continuously along the cross-sectional length of the coating and occasionally moving up into the coating itself.

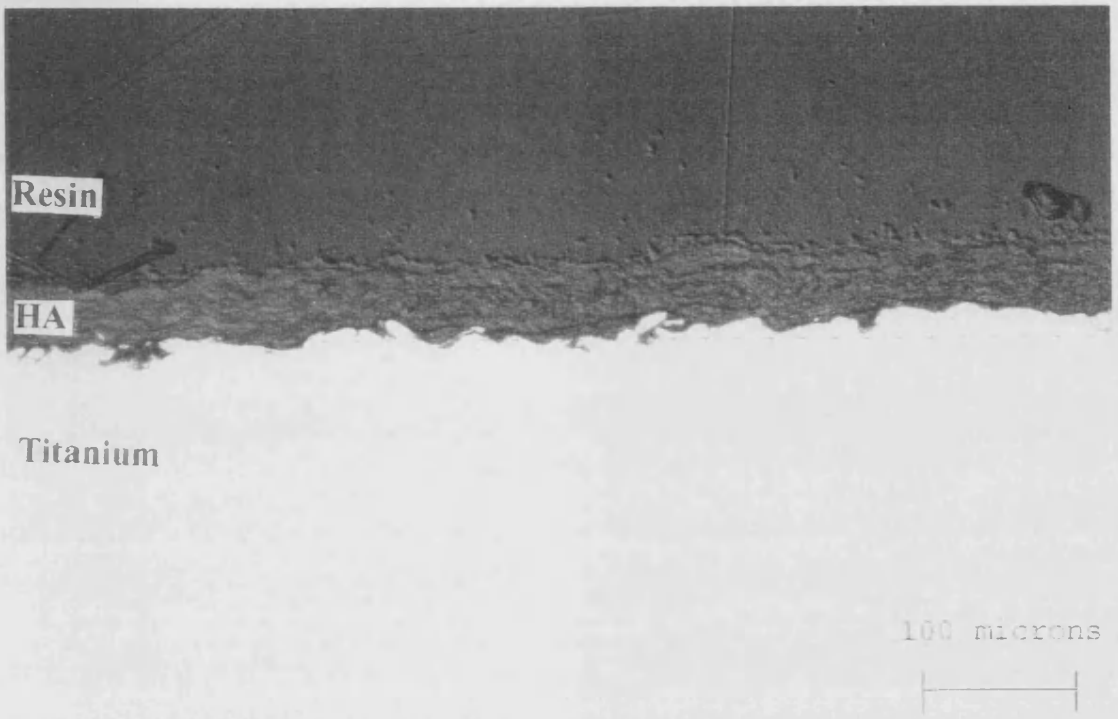

Figure 7-23 :- Optical micrograph showing cross-section through DGUN HA coatings aged for one week then fatigued in Ringer's solution

The coating aged for two weeks before fatigue testing in Ringer's solution (not shown) has a similar thickness to the coating aged for one week but the bulk of the coating appears to be more porous. The coating has a similar surface roughness to the one week aged sample but this coating shows a distinct modification to its surface layers. This modified surface morphology appears to be extremely dense in nature and lies over approximately 5 μm of the cross-sectional thickness of the coating. Again the coating appears to be well adhered to the substrate but the thin black line observed in the coating aged for one week is still present.

The coatings aged for four weeks and eight weeks before fatigue testing in Ringer's solution (neither shown) have very similar morphologies to the coating aged for two weeks. Again one can see little change in cross-sectional thickness, or in the porosity levels in the bulk of the coating but again the modification to the surface layer is present. This modified layer seems to get progressively thicker with increasing ageing time and is between 5 and 10 μm thick in the four week aged sample and approaching 20

μm in the coating aged for eight weeks. Again the coatings are well adhered to the substrates but still they demonstrate the fine black line which seems to be common to these coatings.

The coating aged for twelve weeks before fatigue testing (Figure 7-24) however shows no sign of the modified surface layer visible for coatings aged for shorter durations. The coating again shows no obvious change in thickness or porosity over the as-received coating and has a surface roughness also more like that of the as-received sample. The coating is again still well adhered to the substrate but still the black line between the substrate and hydroxyapatite is apparent. It is possible that the modified surface layer seen in coatings aged for shorter durations has spalled away from the coating surface in this sample but there is no obvious change in cross-sectional thickness which would be evidence for this hypothesis.

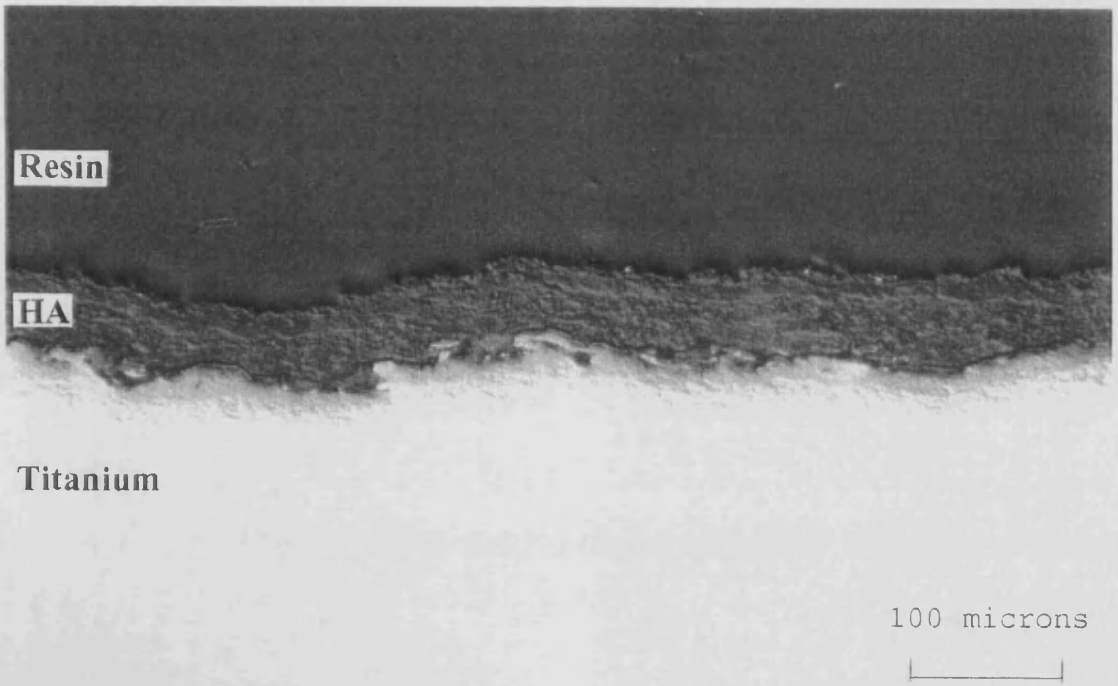

Figure 7-24 :- Optical micrograph showing cross-section through DGUN HA coatings aged for twelve weeks then fatigued in Ringer's solution

7.4.5 Scanning Electron Microscopy

The surface of the DGUN hydroxyapatite coating aged in Ringer's solution for one week before fatigue testing (Figure 7-25) shows characteristic signs of exposure to an *in-vitro* solution. Evidence of a two phase morphology still exists on the surface of the coating but the glassy, amorphous material has been extensively pitted by the dissolution effects of the solution. All the amorphous material is etched to some extent leaving no smooth regions surviving on the coating surface. The surface of the coating also supports a large number of micro-cracks many of which run into each other. These cracks however do not have clean edges and appear to have also been attacked by the ageing solution. This seems to imply that the cracks were present in the coating before the coating was exposed to the *in-vitro* medium. The amorphous regions seem to be showing the initial signs of the formation of a crystalline hydroxyapatite layer, this new material causing the alteration to the morphology of the micro-cracks.

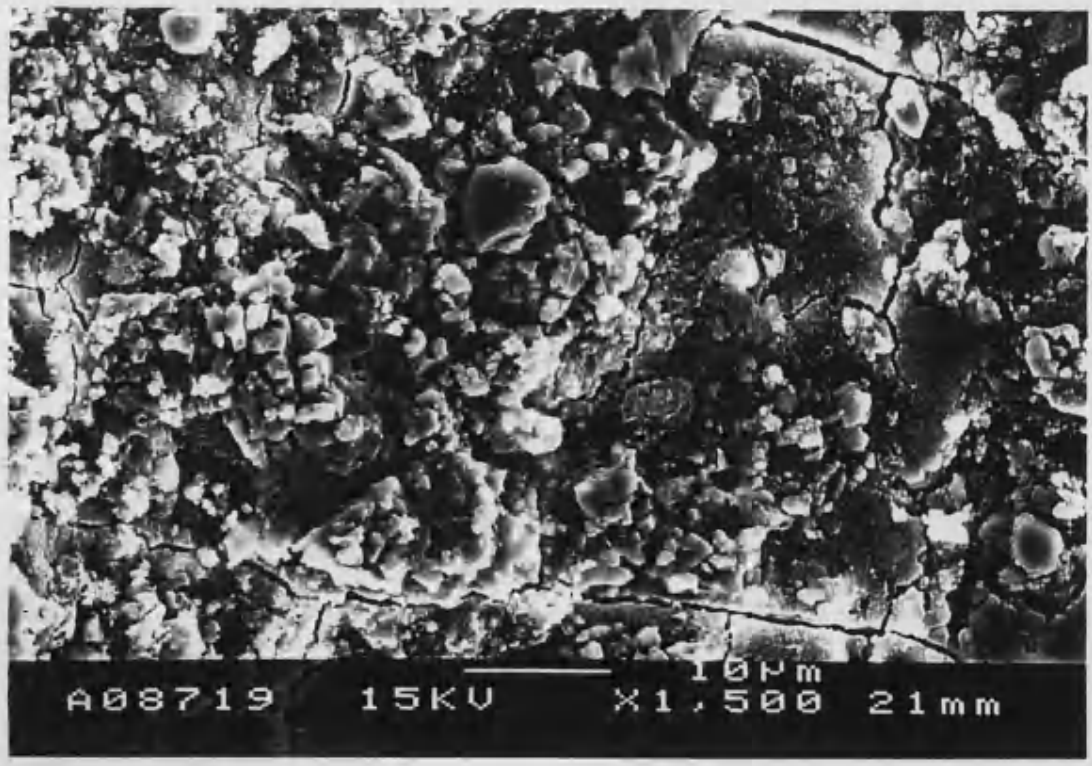

Figure 7-25 :- Scanning electron micrograph showing surface of DGUN HA coatings aged for one week then fatigued in Ringer's solution

Coatings which have been aged for two weeks before fatigue testing (not shown) show a progression in the growth of this crystalline phase on the coating surface. Here the crystallites have taken on the characteristic nodular appearance of re-deposited hydroxyapatite. These growths seem to be localised on what were regions of amorphous material since the rougher, agglomerated zones show no evidence of re-precipitated material. Micro-cracks are still clearly visible on the coating surface but these cracks do not appear to have multiplied or grown in size

The percentage of the overall coating surface covered by the re-precipitated crystalline hydroxyapatite seems to have increase in the coating which had been aged for four weeks before fatigue testing (not shown). The nodular growths seem to have spread outwards from just the amorphous regions over some of the agglomerated material too. The number of micro-cracks running over the coating surface is still high but not as extensive as has been seen in coatings fatigued in Ringer's solution with no ageing. There are several large pores which can be seen on the coating surface which seem to be evidence of loss of material. It is possible that the newly formed surface is less strongly adhered to the coating that the bulk of the material itself and has fallen away in some places.

The surface of the coating aged for eight weeks before fatigue testing (not shown) has a very similar appearance to that of the coating aged for four weeks. Again the surface is covered by a myriad of cauliflower-like protuberances which have spread up and over the remaining coating structure. There is little evidence for the original two phase morphology in this surface since virtually the whole coating is now covered in the re-precipitated phase. The micro-cracks seen in other coatings are still present but these have been bridged in some places by the growing crystalline phase.

The coating aged for twelve weeks before fatigue testing (Figure 7-26) has a morphology which appears to have reverted to that of the one week aged coating. Here we can again see the first stages of the dissolution effects of the *in-vitro* medium and the two phase nature of the original coating. As has been suggested before, it is possible that

the re-deposited, crystalline layer formed during shorter ageing times has become detached from the surface of the coating revealing a fresh surface which is seen here. The coating shows extensive signs of dissolution of the amorphous phase but no evidence of reprecipitation. Again micro-cracks are present running across the coating surface but these are not unusually numerous or large in size.

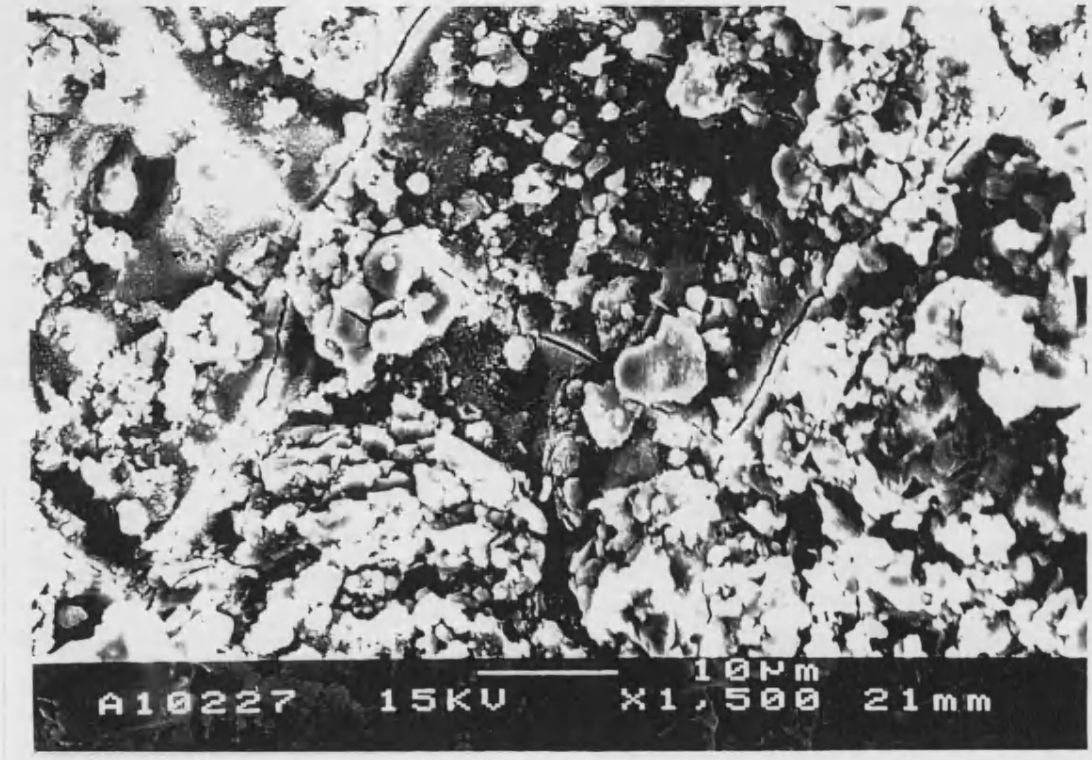

Figure 7-26 :- Scanning electron micrograph showing surface of DGUN HA coatings aged for twelve weeks then fatigued in Ringer's solution

As has been suggested before, the predominant factor effecting the morphology of these coatings which have been both aged and fatigued in Ringer's solution appears to be the ageing process itself. Fatigue testing does not seem to have caused excessive cracking of the coating surface although it may have hastened the loss of the re-precipitated layer from the coating surface. Any change to the morphology of the coatings is consistent with exposure to the *in-vitro* ageing medium only, it is difficult to differentiate between coatings which have been aged and fatigue tested and those which have only been aged.

7.4.6 Coating Thickness Results

Table 7-27 presents a summary of the cross-sectional thickness results for the detonation gun hydroxyapatite coatings aged for various time periods before fatigue testing in Ringer's solution for one million cycles.

Sample	*No. of tests*	*Mean (μm)*	*Standard Deviation*	*Variance*	*95% Confidence Limits*
as-received	10	70.0840	9.5690	91.5653	69.275 and 70.893
1 week	40	47.6600	6.9450	48.2333	36.609 and 58.711
2 weeks	40	47.8270	5.1203	26.2166	39.680 and 55.974
4 weeks	40	42.2785	2.8478	8.1010	37.747 and 46.810
8 weeks	40	39.2168	4.7721	22.7733	31.623 and 46.810
12 weeks	40	38.6750	6.4373	41.4387	28.432 and 48.918

Table 7-27 :- Cross-sectional thickness results for DGUN HA coatings aged then fatigued in Ringer's solution

Table 7-28 presents the significance test results for the cross-sectional thickness data from detonation gun sprayed coatings aged for various time periods before fatigue testing in Ringer's solution for one million cycles.

thickness	*as-received*	*air fatigue*	*Ringer's fatigue*	*1 week*	*2 weeks*	*4 weeks*	*8 weeks*	*12 weeks*
as-received		✓	✓	✓	✓	✓	✓	✓
air fatigue	✓		✖	✓				
Ringer's fatigue	✓	✖		✓				
1 week	✓	✓	✓		✖			
2 weeks	✓			✖		✓		
4 weeks	✓				✓		✓	
8 weeks	✓					✓		✖
12 weeks	✓						✖	

Table 7-28 :- Significant test results for DGUN HA coatings aged the fatigued in Ringer's solution

✓ = significantly different

✖ = not significantly different

= not tested

Therefore it was found that all the coatings which had been aged in Ringer's solution before fatigue testing in Ringer's solution for 1x10e6 cycles had thickness values that varied significantly from that of the as-received coating. These coatings showed a variability in significance in the change in thickness between testing groups.

7.4.7 Coating Porosity Results

Table 7-29 presents a summary of the cross-sectional porosity results for the detonation gun sprayed hydroxyapatite coatings aged for various time periods before fatigue testing in Ringer's solution for one million cycles.

Sample	*No. of tests*	*Mean (%)*	*Standard Deviation*	*Variance*	*95% Confidence Limits*
as-received	10	1.4485	0.7381	0.5448	1.103 and 1.794
1 week	40	4.6868	1.0788	1.1638	2.973 and 6.406
2 weeks	40	5.6896	1.0177	1.0356	4.070 and 7.309
4 weeks	40	5.4063	2.3493	5.5192	1.668 and 9.145
8 weeks	40	1.6679	0.3155	0.0995	1.166 and 2.170
12 weeks	40	3.0225	1.4378	2.0672	0.735 and 5.310

Table 7-29 :- Cross-sectional porosity results for DGUN HA coatings aged then fatigued in Ringer's solution

Table 7-30 presents the significance test results for the cross-sectional porosity data from detonation gun sprayed coatings aged for various time periods before fatigue testing in Ringer's solution for one million cycles.

porosity	*as-received*	*air fatigue*	*Ringer's fatigue*	*1 week*	*2 weeks*	*4 weeks*	*8 weeks*	*12 weeks*
as-received		✖	✖	✓	✓	✓	✓	✓
air fatigue	✖		✖	✓				
Ringer's fatigue	✖	✖		✓				
1 week	✓	✓	✓		✓			
2 weeks	✓			✓		✓		
4 weeks	✓				✓		✓	
8 weeks	✓					✓		✓
12 weeks	✓						✓	

Table 7-30 :- Significant test results for DGUN HA coatings aged the fatigued in Ringer's solution

✓ = significantly different

✖ = not significantly different

= not tested

Therefore it was found that all the coatings which had been aged in Ringer's solution before fatigue testing in Ringer's solution for 1x10e6 cycles had porosity values that varied significantly from that of the as-received coating. These coatings also showed significant changes in porosity between testing groups.

7.4.8 Surface Roughness (Ra) Results

Table 7-31 presents a summary of the surface roughness results for the detonation gun sprayed hydroxyapatite coatings aged for various time periods before fatigue testing in Ringer's solution for one million cycles.

Sample	mean Ra (μm)	standard deviation	variance	95% confidence. interval
as-received	5.5294	-	-	-
1 week	10.9399	3.7796	14.2857	7.780 and 14.100
2 weeks	10.4594	2.1720	4.7174	8.644 and 12.275
4 weeks	10.3816	2.4433	5.9695	8.339 and 12.424
8 weeks	12.1951	2.0408	4.1648	10.489 and 13.901
12 weeks	6.4047	3.0930	9.5667	3.819 and 8.991

Table 7-31 :- Surface roughness results for DGUN HA coatings aged then fatigued in Ringer's solution

Table 7-32 presents the significance test results for the surface roughness data from detonation gun sprayed coatings aged for various time periods before fatigue testing in Ringer's solution for one million cycles.

Ra (μm)	as-received	air fatigue	Ringer's fatigue	1 week	2 weeks	4 weeks	8 weeks	12 weeks
as-received		✖	✖	✓	✓	✓	✓	✖
air fatigue	✖		✖	✓				
Ringer's fatigue	✖	✖		✓				
1 week	✓	✓	✓		✖			
2 weeks	✓			✖		✖		
4 weeks	✓				✖		✓	
8 weeks	✓					✓		✓
12 weeks	✖						✓	

Table 7-32 :- Significant test results for DGUN HA coatings aged the fatigued in Ringer's solution

✓ = significantly different

✖ = not significantly different

= not tested

Therefore it was found that all the coatings which had been aged in Ringer's solution before fatigue testing in Ringer's solution for 1x10e6 cycles had surface roughness values that varied significantly from that of the as-received coating. The

exception to this was found in the case of those coatings which had been aged for twelve weeks before fatigue testing. The aged and fatigued coatings however showed no significant change in surface roughness between testing groups up until the eighth week of testing after which point significant differences were detected.

7.4.9 Residual Stress Results

Table 7-33 presents a summary of the residual stress analysis results for the detonation gun sprayed hydroxyapatite coatings aged for various time periods before fatigue testing in Ringer's solution for one million cycles.

Sample	*residual stress (MPa)*	*standard deviation*	*variance*	*95% conf. interval*
DGUN HA powder	-	-	-	-
as-received	28.8260	-	-	-
1 week	24.5822	6.2336	38.8577	19.371 and 29.794
2 weeks	18.8970	6.6834	44.6684	13.310 and 24.485
4 weeks	19.7778	8.2883	68.6953	12.849 and 26.707
8 weeks	14.6933	5.5001	30.2607	10.094 and 19.292
12 weeks	13.9326	5.8057	33.7065	9.079 and 18.786

Table 7-33 :- Residual stress results in 004 plane for DGUN HA coatings aged then fatigued in Ringer's solution

Table 7-34 presents the significance test results for the residual stress data from detonation gun sprayed coatings aged for various time periods before fatigue testing in Ringer's solution for one million cycles.

residual stress	*as-received*	*air fatigue*	*Ringer's fatigue*	*1 week*	*2 weeks*	*4 weeks*	*8 weeks*	*12 weeks*
as-received		✓	✓	✖	✓	✓	✓	✓
air fatigue	✓		✖	✓				
Ringer's fatigue	✓	✖		✓				
1 week	✖	✓	✓		✓			
2 weeks	✓			✓		✖		
4 weeks	✓				✖		✓	
8 weeks	✓					✓		✖
12 weeks	✓						✖	

Table 7-34 :- Significant test results for DGUN HA coatings aged the fatigued in Ringer's solution

✓ = significantly different

✖ = not significantly different

= not tested

Therefore it was found that all the coatings which had been aged in Ringer's solution before fatigue testing in Ringer's solution for 1x10e6 cycles had residual stress values that varied significantly from that of the as-received coating. The aged and fatigued coatings however showed a variability in the significance of changes in residual stress between testing groups.

8. Discussion

8.1 Effect of Spraying Technique on Coating Morphology

As has been reported [99, 101] powder particle size and shape will have a dramatic effect on the final structure of the hydroxyapatite coating. Maximum adhesion between impacting particles and the coating during manufacture will only be achieved if particles are completely molten and can flow into the surface. However, it was discussed earlier that since molten particles freeze rapidly on impaction and form a meta-stable amorphous phase [68] it may be considered to be undesirable, from a design perspective, to impose complete melting of material during coating manufacture. There is much debate in the literature regarding the ideal morphology of hydroxyapatite coatings [15, 53, 117] and a compromise should be drawn between adhesion of impacting particles to the coating and its in-service behaviour. Controlling the degree of melting of the powder during spraying can control the final levels of amorphous and crystalline phases in the coating. Particle size not only affects the degree of melting of particles during spraying but also their trajectory. Small particles melt more rapidly than larger ones, reach their maximum velocity faster and also freeze more rapidly on impaction with the substrate [104]. Therefore, the morphology of the powder particles used to manufacture the coating may have as large an effect on the structure of the final product as the manufacturing technique itself.

8.1.1 Vacuum Plasma Sprayed Hydroxyapatite Coatings

The particles used in the manufacture of the vacuum plasma sprayed coatings have a morphology which is extremely angular in nature. The particles have an average size of approximately 100 μm but a wide size distribution. The shape of the particles (Figure 4-2) suggests that they were manufactured by a process such as calcination and crushing [99]. Chen *et al* [72] reported the effects of spray powder particle size on the final

crystallinity of vacuum plasma sprayed hydroxyapatite coatings. Theye found that coatings produced from powders with an average particle size of 75 μm had crystallinities of 24 % while those produced from 125 μm powders were 30 % crystalline. Therefore, based on this work, it would be expected that the coatings produced from the spray powder used here would have an average crystallinity in the range of 24 - 40 %. In actual fact the coatings had a crystallinity of around 60%. The particles are not completely dense, showing regular porosity and an agglomerated, sintered morphology. The reasonably large size of the particles used to manufacture these coatings and the relatively low surface area of the powder as a whole suggests that only partial melting of the powder will take place during spraying. As was discussed earlier, this partial melting will not produce the maximum adhesion between impacting particles and the substrate since this can only be achieved by completely molten particles [101] . However, residual unmelted crystalline material may considerably increase the stability of the coatings upon exposure to the *in-vivo* environment. As was discussed earlier (section 2.7) it seems clear that any enhanced bond bonding and osseoconductive behaviour arising from the use of hydroxyapatite as a coating on biomedical prostheses is a product of its dissolution behaviour. It is commonly suggested in the literature [2, 15, 16, 17, 18] that new bone growth onto hydroxyapatite coatings is brought about by partial dissolution of the coating, and subsequent reprecipitation of the calcium phosphate back onto the coating as new natural bone. From these findings, it would seem that the performance of an hydroxyapatite coating will therefore depend on its dissolution behaviour. It has also been shown that amorphous HA is considerably more soluble in the body than crystalline HA [46, 48]. Highly amorphous coatings will therefore dissolve more rapidly in the body increasing the rate of availability of bone forming ions but will be far less stable than coatings with a high level of crystallinity. It can be postulated that highly amorphous coatings will dissolve away completely revealing the metallic substrate of the prosthesis which may allow enhanced metal ion release.

This hypothesis is supported when the morphology of the coating itself is investigated. Looking at the surface of the coating by scanning electron microscopy (Figure 4-6) a well defined two phase morphology in the material was seen. Considerable evidence for only partial melting of powder particles is seen in the agglomerated regions

of the surface which are probably composed of the unmelted cores of particles that have impacted on the coating surface and lesser splat debris. The rest of the surface is composed of flat, glassy regions which have arisen as a result of the instantaneous freezing of molten powder material as it impacts on the surface, forming a meta-stable amorphous phase. The surface morphology of the vacuum plasma sprayed hydroxyapatite coating has an appearance very similar to that of other coatings produced by the same technique seen in the literature [59, 68, 80, 118]. This combination of amorphous and crystalline material should allow the coatings to dissolve *in-vivo* while maintaining a good degree of structural integrity.

The polished cross-section through the vacuum plasma sprayed coating (Figure 4-5) again reveals a structure which is characteristic of the production process. The coating is clearly lamellar in morphology, each layer corresponding to a single pass of the plasma torch over the substrate during manufacture. The coating also contains porosity which will have been formed as a result of two processes. Impaction of powder particles on the coating surface can occur with such force that the impacting material damages the surface of the coating creating porosity. In addition to this, as described above, the powder particles become only partially molten during heating in the plasma flame, limiting the ability of the material to flow on impact with the coating. This low level of surface flow of material inhibits the filling of surface porosity as subsequent coating layers are put down, thus leaving closed pores in the bulk of the coating. The effects of these two processes are limited however and average porosity levels within the coating remain below 6 % (Table 4-6). This level of porosity is in agreement with that of 4.9 % reported by Wang *et al* for vacuum plasma sprayed hydroxyapatite coatings [59]. Low levels of porosity such as these may allow the lamellae in the coating a small degree of micro-motion in service while at the same time, not being of a level which may be detrimental to the strength or fatigue resistance of the composite system.

The average thickness of the coatings (Table 4-5) is approximately 40 μm, but the standard deviation in this value is around 12 μm. This value is in line with that of vacuum plasma sprayed coatings studied by other authors in the literature [54, 55, 58]. This large variation in thickness is a direct reflection of the irregular nature of the titanium

substrate itself. As the coating is laid down during spraying it takes on the approximate morphology of the material below it, this morphology becoming less and less recognisable with increasing thickness of the coating. However, in thin coatings such as these, the irregular nature of the substrate imposes large irregularities in the coating itself, reflected in the large variation in cross-sectional thickness seen here. As described in the literature [54] the substrate used in the manufacture of these coatings has been roughened by grit blasting with alumina (Figure 4-5) probably to increase the mechanical interlocking of the coating with the titanium. This roughening process will contribute to the irregular nature of the coating. A pure titanium interlayer can be seen between the hydroxyapatite and the Ti-6Al-4V. This has been applied to improve the mechanical strength of the interface either mechanically by roughening the substrate, or chemically, by promoting chemical bonding by inter-diffusion between the hydroxyapatite and the interlayer [110,111] . This bond coat may limit the extent of the loss of adhesion of substrate to coating caused by the incomplete melting of powder particles during vacuum plasma spraying.

The media used in the grit blasting stage of coating preparation has not been completely removed from the surface of the substrate by the subsequent cleaning process. Residual alumina grit can clearly be seen scattered along the interface between the substrate and the coating. These grit particles can be surprising large in size, on occasion, over 20 μm in length and are angular in nature. This residual grit has the potential to be extremely damaging to the performance of the hydroxyapatite coatings *in-vivo*. Not only may the grit prevent good adhesion between the coating and the substrate but any dissolution of the coating itself may release these alumina particles into the body system. These particles may subsequently cause extreme irritation and inflammation of tissues in close proximity to the implant which could be detrimental to the long-term performance of the prosthesis.

There is a large difference between the crystallinity of the hydroxyapatite in powder form and the material after it has been formed into the vacuum plasma sprayed coating. Not surprisingly, the crystallinity of the coating (Table 4-3) is lower than the original powder since some of the crystalline material in the powder has been frozen in a

meta-stable glassy phase in the coating. The crystallinity of the powder was determined to be approximately 80 % whereas the coating was only 60 % crystalline. This level of crystallinity is in line with that determined for other vacuum plasma sprayed hydroxyapatite coatings reported in the literature [55] but is in stark contrast to the level predicted by Chen *et al* [72] from the original powder particle size. There is also some evidence for a change in the composition of the material as a result of the spray process (Table 4-4). Before spraying the powder principally consists of hydroxyapatite with traces of beta-tri-calcium phosphate. The spraying process itself however causes a change in the composition of the material, transforming the tri-calcium phosphate phase back into hydroxyapatite, the coating itself appearing to be principally composed of pure hydroxyapatite. This result seems to be in contradiction with the work of other authors found in the literature [68, 110] who report that pure hydroxyapatite transforms into other phases (α-TCP, β-TCP, $Ca_4O(PO_4)_2$, $C_2P_2O_7$ etc.) during plasma spraying. It is however extremely difficult to determine the extent of the calcium phosphate phases present in hydroxyapatite coatings since calcium - phosphorous ratios for most of these phases were found to be indistinguishable using x-ray photoelectron spectroscopy. This difficulty makes suppositions about quantities of these minor phases in existence in a coating, beyond simple detection of their presence, unreliable.

The as-received vacuum plasma sprayed coating had a measured surface roughness which echoed the irregular appearance of its surface (Table 4-7). The average surface roughness Ra was found to be approximately 5 μm but the irregular nature of the surface is reflected in the Rt value of approximately 40 μm. These levels are very similar to those determined by other authors [54, 59] of between 0.4 and 14.7 μm measured for thin vacuum plasma sprayed hydroxyapatite coatings. The effect the surface roughness of these coatings will have on the clinical performance of the materials has been discussed by Wang *et al* [59] and Wilke *et al* [73] . These authors reported a linear increase of push-out failure load with increasing surface roughness for vacuum plasma sprayed hydroxyapatite coatings. These coatings have a comparably moderate roughness which should encourage coating dissolution due to the large surface area exposed to the body's environment and allow good mechanical interlocking with bone, without impairing the mechanical strength of the surface.

Residual stress levels (Table 4-8) for the as-received coating were determined by taking the lattice parameters for the spray powder as a zero point. The powder was assumed to be unstressed while the coating , having undergone thermal spraying was assumed to have had a stress imposed upon it. This assumption was based on the appearance of the surface of the as-received coating which showed evidence for the presence of these stresses in the form of micro-cracks. The difference in thermal expansion coefficient (Table 2-1) between the metallic substrate and the ceramic coating forces the ceramic to expand beyond its natural level causing it to become stressed. This stress will be observed as a distortion of the ceramic's crystal lattice which can be monitored by x-ray diffraction. The presence of micro-cracks on the coating surface (Figure 4-6) is evidence that some of these stresses have been relieved by the cracking mechanism. Assuming that any stress remaining in the coating after this cracking has taken place is unidirectional, for the as-received coating, residual stress levels were found to be around 21 MPa. This stress is only being measured in the surface layers of the coating since the x-ray beam only penetrates into the top few microns of the surface and can be assumed to be tensile in nature since the coating has undergone micro-cracking. It can also be assumed that the vacuum plasma spraying process imposed a far greater stress originally than was measured by x-ray diffraction since some degree of this stress has already been resolved by cracking before the measurement was undertaken. This 20 MPa level of residual stress is however apparently not great enough to cause spontaneous delamination of the coating from the substrate and is well below the elastic limit and Young's modulus of the coating itself (Table 2-1).

8.1.2 Detonation Gun Sprayed Coatings

The characterisation of detonation gun sprayed hydroxyapatite coatings reported here is unique to the literature. Hydroxyapatite coatings for biomedical applications have not been produced on any scale by this process before and the technique is still under development. These materials are therefore novel in nature.

The detonation gun spray technique is considerably different from the vacuum plasma spray process and this difference is reflected not only in the appearance of the final coatings but in the spray powders chosen for their manufacture. The powder particles used in the manufacture of the detonation gun coatings are much smaller and more uniform in size than the other particles and are spherical in nature, probably manufactured by a spray drying process [99] .The detonation technique is a higher velocity process involving the ignition of gas charges whose explosion heats the powder fed into the gas ball and accelerates it onto the substrate. The procedure requires more accurate control over the flow behaviour of both the carrier gas, combustion gases and the powder itself. This accounts for the use of the spherical powder chosen for detonation gun spraying since the particles will flow over one another in a more regular manner than would the angular particles used in vacuum plasma spraying. The particles, like the vacuum plasma spray material are not dense and have an agglomerated, sintered appearance (Figure 4-3).

The higher temperature which the powder particles reach during detonation spraying [107] should impose a higher degree of melting on the starting powder creating a more amorphous coating. As discussed earlier (section 8.1.1) this should allow better adhesion of the hydroxyapatite to the substrate. The different manufacturing process is also reflected in the morphology of the as-received detonation gun coating itself. The smaller powder particles and the higher surface area of the powder itself allows more extensive melting of the particles during spraying [98] . The higher velocity, higher energy detonation gun process imposes a greater degree of melting on the powder but this process may be counter-balanced by the extremely short dwell time of the particles in the plasma. These effects should combine to produce a more amorphous, more dense coating which, despite being better adhered to the substrate will undergo a more rapid dissolution *in-vitro* than the vacuum plasma sprayed coatings which will have an associated effect on the coating's behaviour *in-vivo* as discussed above (section 8.1.1).

The surface of the detonation gun coating (Figure 4-9) has a similar morphology to that of the vacuum plasma sprayed coating except that, as expected, there is apparently a far higher overall area of the surface covered with the flat, glassy phase. The

surface morphology is very similar to that of coatings produced by the high-velocity flame-spraying technique seen in the literature [92]. This would be expected if a higher degree of melting is taking place since more of the powder would be frozen in a meta-stable amorphous state in the coating. Regions of agglomerated splat debris and residual crystallites from the spray powder can however still be seen on the coating surface.

The crystallinity result for the as-received detonation gun coating reflects this supposition that the spray powder has undergone a higher degree of melting during spraying than was the case for the vacuum plasma sprayed powder. Although both spray powders had an initial crystallinity of approximately 80 % (Table 4-1), the as-received detonation gun coating had an average crystallinity of only 34 % (Table 4-9), much lower than that of the vacuum plasma sprayed coating (Table 4-3) and reflected by the higher proportion of amorphous material seen on the coating surface. This amorphous glassy phase can only have be formed as a result of rapid freezing of molten spray particles and its higher content in the coating suggests a higher content in the plasma and therefore a higher degree of powder melting during manufacture.

In line with reports in the literature [69, 110], the detonation process seems to have imposed a degradation of pure hydroxyapatite to beta-tri-calcium phosphate in some proportion in the final coating (Table 4-10). Although traces of this material were found in the detonation gun spray powder, it seems to be present in significant amounts in the final coating which suggests that the higher energy spray process has caused a phase change in the powder. Even if the detonation process is a higher energy technique this change in phase should not only be observed for this technique and not for the vacuum plasma spray process. The temperatures developed in the plasma during vacuum spraying [93] far exceed the temperature of the thermal transition of hydroxyapatite to beta tri-calcium phosphate which would occur in the temperature range of 800 - 1000 °C [71]. Therefore, such a transition should occur not only in the case of the detonation gun coatings but in the case of the vacuum plasma sprayed coatings as well. As described above it is possible that the difficulty in ascribing a significance level to phases other than hydroxyapatite in the x-ray diffraction data has led to an over or under-representation of other calcium phosphates in the analysis.

The high velocity of the manufacturing process is reflected in the thickness of the lamellae seen in the cross-section through the detonation gun coating (Figure 4-8). Here the coating has been laid down by a process of rapid deposition rather than by a layer on layer process and this is clearly reflected in the coating morphology. This coating also has an expectedly lower porosity than the vacuum plasma sprayed coating of around 1.5 % (Table 4-12). The higher degree of melting of the powder particles allows more flow of material on the coating surface causing the filling of porosity during spraying and a denser overall coating. The detonation coating has an extremely irregular thickness (Table 4-11), perhaps again a reflection of a shadowing in the coating of the irregular substrate, and a very similar surface roughness (Ra 5.5 μm) to the vacuum plasma sprayed coating (Table 4-13).

There is again a large amount of alumina present at the interface between the coating and the substrate (Figure 4-8) indicative once more of an inadequate cleaning operation after the titanium surface has been laid down. Again, this alumina grit has the potential to cause problems in the service life of the coating due to either loss of adhesion of the coating to the substrate or escape of the alumina into the body system and subsequent initiation of immune response. The coating does however show no evidence for the presence of a pure titanium bond layer between the hydroxyapatite and the Ti-6Al-4V. It is assumed that the coating manufacturers believe that the superior bonding of the detonation gun coatings to the substrate brought about by the higher degree of melting of the spray powder during this process precludes the need for the application of a bond coat here.

Taking the assumptions applied to the determination of residual stress levels in the vacuum plasma sprayed coatings as true for the detonation gun coatings (section 8.1.1), a stress level similar to that for the vacuum plasma sprayed material of approximately 30 MPa was recorded (Table 4-14). The same processes discussed for the other coating type, i.e. resulting from differences in the thermal expansion coefficients for the metal and the ceramic, would be assumed to have taken effect on the detonation gun coating. Again the presence of micro-cracks in the surface of the coating (Figure 4-9) supports the suggestion that these stresses are present and tensile in nature but again

imply that residual stress levels in the coating at the time of manufacture were considerably higher than those measured, since some of their magnitude has already been relieved. The higher values recorded for the detonation gun coatings may be directly linked to the denser nature of the coating, the lower porosity levels allowing less micro-motion within the coating on cooling. It is also possible that the exclusion of a pure titanium bond coating indeed increased the thermal mismatch between the hydroxyapatite and the Ti-6Al-4V as suggested by Ji *et al* [110] and Filliaggi *et al* [111] . This mismatch is reduced in the case of the vacuum plasma sprayed coatings where a bond layer has been used and this may account for the lower residual stress levels recorded for vacuum plasma sprayed hydroxyapatite coatings (Table 4-8).

8.1.3 Summary

The principal differences in the morphology of the two coatings therefore seems to lie in the crystallinity, thickness, porosity and residual stress levels in the coatings. The more amorphous detonation gun sprayed coatings should dissolve more rapidly *in-vitro* than the vacuum plasma sprayed coatings [46, 48] and would therefore be expected to encourage more rapid bone formation *in-vivo*. The mechanical stability of the coatings has been enhanced by the used of a bond coat [110, 111] in the case of vacuum plasma sprayed hydroxyapatite coatings which has reduced the potentially damaging levels of residual stress for these materials and may inhibit delamination during later testing. However the more amorphous, denser detonation gun coatings should also perform well due to their excellent expected mechanical bonding to the substrate [101].

8.2 Effect of *In-vitro* Ageing at pH 7.2

Both coating types were aged in the same tanks for the same time durations. The pH of the ageing solution was buffered to pH 7.2 using tri-hydroxymethylaminoethane and hydrochloric acid. Coatings were characterised in the same way as the as-received coatings after ageing for one, two, four and eight weeks. The coatings were placed in the

in-vitro ageing tanks so that the coating surface was facing away from the circulatory heater jet in an attempt to minimise damage due to turbulence effects.

8.2.1 Vacuum Plasma Sprayed Hydroxyapatite Coatings

Studying the change in the surface of the vacuum plasma sprayed coatings with ageing time (Figure 5-4 and Figure 5-5), it was reported that a reduction in the glassy, amorphous material was observed. This reduction is associated with the preferential dissolution of amorphous material from the surface of the hydroxyapatite coating, an effect reported widely in the literature [15, 16, 34] . This dissolution effect was not seen to increase in magnitude significantly with ageing time i.e. the appearance of the surface observed in the coatings aged for just one week was considerably different from that of the as-received coating but did not change dramatically with extended exposure to the medium. The magnitude of this dissolution is quantified in the thickness results for the samples (Table 5-4). There is no significant reduction in coating cross-sectional thickness with ageing time, clearly demonstrating that this dissolution effect is only taking place in the surface layers of the coating. There is also no change in porosity between ageing times for the vacuum plasma sprayed coatings (Table 5-6), which again confirms that the dissolution effect is not remarkably progressive. This minimal alteration to the cross-sectional morphology of the vacuum plasma sprayed coatings (Figure 5-2 and Figure 5-3) on exposure to ageing medium is in agreement with the work of Gross and Berndt [58] and Cook *et al* [50] in the literature. Gross and Berndt observed similar surface dissolution of vacuum plasma sprayed coatings exposed to Ringer's solution for various time periods.

That it is amorphous material which is dissolving from the surface is substantiated by the crystallinity data for the vacuum plasma sprayed samples (Table 5-1). It can be seen that the aged coatings have a significantly higher relative crystallinity than the as-received coating, indicating that it is amorphous material which is being lost from the surface. This is again in agreement with the work of Gross and Berndt [58] who reported an increase in crystallinity of vacuum plasma sprayed hydroxyapatite coatings aged for

upto twelve weeks *in-vitro*. Again, as observed by a visual inspection of the coating surfaces, there is no significant change between ageing times, only between the aged and unaged test groups.

It also seems apparent that exposure to the *in-vitro* ageing media does not bring about a change in the composition of the hydroxyapatite coatings (Table 5-3). Apart from in the case of the coating aged for the maximum duration, no change in composition is detected and the coating remains pure hydroxyapatite with only trace amounts of other calcium phosphate phases present. The coating aged for eight weeks seems to behave a little differently, showing a noticeable shift in the peaks of the x-ray trace and the appearance of significant quantities of beta tri-calcium phosphate in the phase composition of the material. It is entirely possible that, after this extended period, reactions which occur extremely slowly and are therefore not detected in the coating aged for shorter durations, are beginning to affect the hydroxyapatite.

This peak shift for the coating aged for eight weeks (Figure 5-1) will obviously also result in a change in the residual stress values for this sample. These values (Table 5-1) remain unchanged for the coatings exposed to the ageing medium for shorter durations, and are all around the 20 MPa level, very similar to the result for the as-received coating. The value however drops considerably to around 8 MPa for the coating aged for eight weeks. Looking at the composition change for this coating it is possible to hypothesise that the change in residual stress has come about as a result of a transformation in the crystal structure of some parts of the coating surface, corresponding to a change from pure hydroxyapatite to beta tri-calcium phosphate. This phase change which is observed in the x-ray diffraction data to have overtaken some of the hydroxyapatite in the surface of the coating aged for eight weeks would be associated with a transformation in crystal structure in these regions from a hexagonal unit lattice to an orthorhombic lattice in the case of beta tri-calcium phosphate. The reorganisation of the structure into the compact orthorhombic lattice morphology could result in a relief of the residual stresses set up in the material as a result of the manufacturing process.

The minimal nature of the disruption to the hydroxyapatite coatings is in contrast to the suppositions of many clinicians who claim significant dissolution of amorphous hydroxyapatite coatings upon implantation [58, 77]. The magnitude of loss of hydroxyapatite *in-vitro* measured here is well below those levels measured by these authors. Gross and Berndt [58] were however studying thicker coatings than those investigated in this research and it has already been discussed (sections 2.3, 2.5, 2.6 and 8.1.1) that coating thickness has a strong influence on the phase morphology and hence the stability of the coatings [70].

In-vivo work demonstrates that dissolution effects are greatly complicated by the presence of proteins and bacteria in the body situation. Bacteria [64] is seen to accelerate dissolution of hydroxyapatite while proteins in fetal calf serum inhibit this dissolution [65]. As reported here however, Cook *et al* [50] reported no evidence of disruption, mechanical failure or significant biological resorption of vacuum plasma sprayed hydroxyapatite coatings implanted in dogs for time periods between two and fifty two weeks. It can therefore be assumed that although the effects witnessed in *in-vitro* trials may be a good indication of what might occur *in-vivo*, the rate of such events may be controlled by other determinants. The effect of loading and implant positioning are crucial to such rates of dissolution and surface modification and will be discussed in conjunction with static test results subsequently.

8.2.2 Detonation Gun Sprayed Hydroxyapatite Coatings

As described above, detonation gun sprayed hydroxyapatite coatings have not been investigated before. Therefore it is only possible to compare the behaviour of these coatings with that of vacuum plasma sprayed materials which have been characterised previously.

As observed in the vacuum plasma sprayed coatings (Figure 5-4 and Figure 5-5), the detonation gun coatings also show signs of surface attack of the amorphous material by the *in-vitro* ageing medium (Figure 5-9 and Figure 5-10). This is seen in the surface of

the coatings when viewed by scanning electron microscopy as a reduction or complete loss of the flat, glassy regions from the coating surface. This effect however has a time dependency in the case of the detonation gun coatings not seen for the vacuum plasma sprayed materials. In the case of the detonation gun coatings, loss of the amorphous material is observed up until the four week ageing period has elapsed but after this, amorphous structures are once again seen on the coating surface (Figure 5-10). This seems to suggest that, since new amorphous material would not be deposited on the coating surface, whole layers must have been lost from the coating surface exposing fresh material which has not been so severely attacked by the *in-vitro* solution. It is also possible that the amorphous phase in the surface layers of the detonation gun coatings acts as a binder phase, holding the agglomerated and crystalline phases in place. Dissolution of this binder will therefore create poor interlocking of the second phase on the coating surface and potentially, loss of its cohesion to the surface.

Thickness data for the polished cross-sections through these aged detonation gun samples do appear to suggest that the coating thickness has been reduced with *in-vitro* ageing (Table 5-13). Unfortunately however, when standard deviations for this data are considered there is no significant trend in the thickness values to suggest that reduction in thickness is progressive with ageing time. The general trend in the data does appear to be towards a loss of material from the coatings and the measured thicknesses for the aged coatings are significantly lower than for the as-received material.

Again, in support of findings for the vacuum plasma sprayed coatings (Table 5-1), the loss of amorphous material from the surface of the detonation gun coatings is substantiated by the crystallinity measurements determined from x-ray diffraction data (Table 5-10). Here a significant increase in crystallinity levels in the aged coatings commensurate with loss of the amorphous phase from the coating surface can again be seen. The increase in crystallinity is of approximately the same scale as that observed for the vacuum plasma sprayed coatings but again is not progressive with increasing ageing time. Despite the observation that there is a physical change in the surface morphology of the coating between the ageing durations of four and eight weeks, this physical change is

not reflected in the crystallinity data, there being no apparent change in crystallinity for the coatings aged for four weeks and eight weeks.

This morphological change between the periods of four and eight weeks can been seen in the appearance of the x-ray diffraction traces for the detonation gun coatings (Figure 5-6). There is a distinctive shift in the position of the principal peaks for hydroxyapatite around the four week period. This peak shift is not associated with a change in the phase composition for the material (Table 5-12) (there is no additional compositional change with ageing time) but is reflected in residual stress values (Table 5-18). Residual stress levels in the coatings are seen to gradually decrease with ageing time up until the four week period where values undergo a dramatic increase. After this point, the coatings aged for eight weeks have residual stress levels very similar to the early aged coatings reflecting their similarity in surface appearance.

It seems that the process of layer loss from the surface of the hydroxyapatite coating is associated with a large fluctuation in the stress levels in the coating. Gradual reduction in stress levels with dissolution would be expected. Loss of the amorphous phase allows relaxation in the positioning of the other phase and thus stress relief. It has been discussed above (section 8.1.2) that the residual stress levels measured for the as-received coatings have been reduced by the process of micro-cracking on the coating surface. The measured values reported for the eight week aged coatings could therefore be a more realistic measurement of the real levels of residual stress inherent in the detonation gun coatings. After layer loss from the surface of the detonation gun coating a completely virgin surface is revealed and it is this unmodified material whose stress is recorded here. This clearly explains the higher value of stress determined for the aged coatings, it is entirely expected that after loss of the etched surface layer the lower layer would have a stress approaching that of the as-received coating and the higher levels recorded support the suggestion presented above.

Although, as described above, there was found to be no change in composition of the coatings with ageing (Table 5-12), there was a change between the as-received

coating and the aged coatings. A significant phase seen in the as-received coating was found to be beta tri-calcium phosphate. This phase however was not found to be present in any significant amounts in the aged coatings. It has been reported in the literature [15, 16, 41] that tri-calcium phosphate is considerably more soluble in aqueous solutions than pure hydroxyapatite. It seems clear therefore that not only is preferential dissolution of amorphous material from the coating surface being observed but also tri-calcium phosphate over hydroxyapatite itself. This would explain the apparent loss of this phase from coatings which have been exposed to the *in-vitro* medium.

Surface roughness (Ra) values (Table 5-17) fluctuate in accordance to the alteration in morphology occurring at the surface of the sample. Roughness values increase up to the four week limit then reduce again in association with material loss and exposure of virgin layers smoothed by amorphous phases. Coating porosity levels (Table 5-15) also fluctuate with ageing time although, with standard deviation taken into account there appears to be a general increase in porosity with ageing time. It has to be remembered however that the porosity levels being presented here are those measured overall in the bulk of the coating not just in the surface layers and so will not obey the same trends as surface roughness or crystallinity.

8.2.3 Summary

The *in-vitro* ageing solution buffered to a pH of 7.2 has several noticeable effects on the morphology and surface properties of both the vacuum plasma sprayed and detonation gun sprayed coatings.

As widely reported in the literature [15, 16, 34] exposure to the ageing medium brings about dissolution of amorphous material from the surface of the hydroxyapatite coatings. This dissolution was monitored visually by scanning electron microscopy (Figure 5-4, Figure 5-5, Figure 5-9 and Figure 5-10) and experimentally by determining the levels of crystalline material in the surface layers of the aged coatings (Table 5-1 and Table 5-10).

It was suggested that the dissolution process occurred in a cyclic manner. This process is more exaggerated in the case of the detonation gun sprayed coatings, an observation expected following characterisation of the two coating types in their as-received state. The detonation gun sprayed coatings had a higher percentage of amorphous material (Table 5-1 and Table 5-10) and also a higher level of residual stress (Table 5-9 and Table 5-18) in the coating surface than the vacuum plasma sprayed materials both of which would be expected to encourage a more rapid dissolution. Initially the amorphous material in the coating surface was attacked by the ageing medium, dissolving away. This amorphous phase acts as a binder phase for the crystalline and agglomerated material in the surface layer, and its loss causes loss of cohesion of this other material. This agglomerated material then spalls away from the surface of the coating to reveal a fresh surface layer below. The newly exposed surface would then again be attacked by the *in-vitro* solution giving the process a cyclic nature. Surface roughness data for the coating follows these trends, showing an increase in magnitude associated with a loss of the smooth glassy phase from the surface and a later reduction when new, smoother surface layers are exposed.

Dissolution of the amorphous material allows micro-movement of the remaining agglomerated material and hence a slight relief of the residual stresses measured in the surface layers of the coating. However, the period when incoherent, agglomerated material is spalling away from the coating surface is associated with a considerable increase in the residual stress levels in the coating associated with the emergence of the virgin surface.

The detonation gun coatings also show a phase change during exposure to the ageing solution which is not reported for the vacuum plasma sprayed coatings (Table 5-3 and Table 5-12). Again it is reported in the literature [48] that beta tri-calcium phosphate has a much higher solubility in aqueous solutions than hydroxyapatite. During exposure to the *in-vitro* environment, this beta tri-calcium phosphate phase is lost from the surface layers of the detonation gun coatings in accordance with the work of other authors.

8.3 Effect of *In-vitro* Ageing at pH 4.5

8.3.1 Vacuum Plasma Sprayed Hydroxyapatite Coatings

A general trend observed for both types of coatings exposed to the *in-vitro* ageing solution is that they undergo dissolution of the amorphous phase from the coating surface. This effect is however not reflected by any significant change in the crystallinity data (Table 5-19) for the vacuum plasma sprayed coatings aged at pH 4.5. Here no observable change in crystallinity levels in the aged coatings is seen. The reasoning for this lack of change is discussed below. The exception to this rule occurs in the case of the coating aged for eight weeks. This coating however had disintegrated on removal from the *in-vitro* ageing tank and was analysed in the form of a very small amount of powder on a glass slide. It is thought that the x-ray diffraction trace for this sample shows imposition of amorphous broadening in the x-ray data as a result of shadowing from the glass slide. Since the powder clearly cannot have increased in amorphous content with ageing this is one possible explanation for its erratic x-ray result.

Looking at the polished cross-sections through the coatings aged at pH 4.5 (Figure 5-12 and Figure 5-13) a gradual alteration in the surface layers of the coatings with ageing time is observed. This effect continues until the surface layers are seen to spall away from the bulk of the coating after four weeks. Comparing this with images obtained using scanning electron microscopy (Figure 5-14 and Figure 5-15) the reason for this modified surface layer becomes clear. The surfaces of the coatings aged for various time periods at pH 4.5 show evidence for a complete modification of the surface morphology corresponding to the alteration seen in the polished cross-sections. Here a new phase has formed on the surface of the coatings, with a crystalline, cauliflower like appearance not dissimilar to that observed by Bagambisa *et al* [16] for plasma sprayed coatings exposed to an electrolyte solution. This material is almost certainly crystalline hydroxyapatite which has been re-deposited on the surface following surface attack by the *in-vitro* medium. Other authors have also reported this reprecipitation of apatite

crystals onto the surface of hydroxyapatite following dissolution of material [4, 5, 6, 7, 43] and it has been suggested [2, 3] that it is this reprecipitated material which is responsible for the supposed osseoconductive properties of these materials.

As discussed above (section 8.2.2), loss of the amorphous binder phase from the coating surface leads to loss in cohesion of the surface layers and ultimately loss of these layers. That these layers have been lost is evident in micrographs taken from the coatings aged for four weeks (Figure 5-13). Here the cyclic nature of the dissolution / reprecipitation process can be seen. The coating surface has dissolved and crystalline hydroxyapatite has been deposited on the damaged surface. This new layer however is not well adhered by the amorphous binder phase and is soon lost from the surface to expose a fresh layer which has in turn been partially dissolved by the ageing solution initiating the formation of a new precipitated layer.

It would be expected that this newly formed crystalline layer on the surface of the vacuum plasma sprayed coatings aged at pH 4.5 would increase the crystallinity levels detected in the coatings, but this does not appear to be the case (Table 5-19). In fact the crystallinity values determined for coatings aged at pH 4.5 were found to be lower than those of the coatings aged at pH 7.2 (Table 5-1) but in the former case the standard deviation in results was considerably greater. However it is known that very small crystallites have a similar effect on the appearance of x-ray diffraction traces as an amorphous phase, causing scattering of the incident beam and hence broadening of the x-ray peaks. Consequently, this micro-crystalline broadening of the diffraction traces would result in an apparent increase in the relative ratio of amorphous to crystalline phase for these coatings.

Looking again at the cross-sectional analysis of the vacuum plasma sprayed coatings aged at pH 4.5 the variation in cross-sectional thickness with ageing time can be seen (Table 5-22). The thickness results vary considerably from ageing time to ageing time which is again a reflection of the dramatic alterations in the coating's morphology. Spalling of the coating from the surface of the material is occurring in the material aged

for extended durations and this process is also embodied by the large scatter of thickness results.

As seen previously, the surface roughness data shows variation in agreement with morphological alterations occurring at the surface of the samples (Table 5-24). The surface roughness increases with the formation of the irregular crystalline nodules on the coating surface (Figure 5-14) and decreases again around the four week ageing period (Figure 5-15) as the surface layers spall off the coating and fresh, less irregular material is exposed.

The validity of examining the residual stress values for all these coatings is demonstrated in examination of the change in these values for the vacuum plasma sprayed coatings aged at pH 4.5 (Table 5-27). Here a gradual decrease in the residual stress levels associated with slight remodelling of the coating surface due to dissolution and reprecipitation of hydroxyapatite is observed. The increase in stress levels during spalling of surface layers is again recorded for the coatings aged for four weeks at this pH. The logic of the measurement system is however most demonstrated by looking at the results for the coatings aged for eight weeks. As described above this material was only obtained in the form of a powder since the coating had virtually completely disintegrated. As would be expected, the results for this sample show virtually no residual stress still remaining in the material - the coating is no longer in a form in which the material is being strained and therefore the measured residual stress drops to close to zero.

The severe nature of the attack of amorphous vacuum plasma sprayed hydroxyapatite at pH 4.5 may have a dramatic effect on the behaviour of these coatings *in-vivo*. It is commonly suggested [15, 16, 17, 18] that hydroxyapatite's early bone bonding properties arise as a direct result of its dissolution behaviour and the reason behind this appears to be apparent here. Immediately following the total hip replacement operation the pH in the traumatised tissues will drop to a lower level as cellular repair processes begin. It has been shown here that at this lower pH, dissolution and reprecipitation of

calcium phosphate phases occurs at an accelerated pace. It is suggested that this effect may be responsible for the rapid post-operative fixation of HA coated prostheses.

8.3.2 Detonation Gun Sprayed Hydroxyapatite Coatings

Crystallinity measurements for the detonation gun coatings aged at pH 4.5 show a distinct and progressive increase in value (Table 5-28). Here a significant increase in the crystallinity levels for the coatings is seen, associated with a relative reduction in the amount of amorphous material in the surface layers of the coatings. The x-ray diffraction data (Table 5-30) for the detonation coatings again show a loss of significant amounts of beta tri-calcium phosphate from the composition of the coatings exposed to the *in-vitro* ageing medium. As discussed above (section 8.2.2), it is widely reported that beta tri-calcium phosphate has a higher solubility *in-vitro* than hydroxyapatite and so its loss along with loss of amorphous material is expected.

Looking at the optical (Figure 5-17 and Figure 5-18) and scanning electron (Figure 5-19 and Figure 5-20) images of the coatings, more evidence for the cyclic nature of the dissolution process is seen. With time, a morphologically altered layer can be observed to be forming at the surface, which initially increases in depth before it spalls completely away from the bulk of the material. Looking at the sample surface by scanning electron microscopy this process is seen in more detail. Initial dissolution of amorphous material is observed in coatings aged for one week (Figure 5-19). After two and four weeks however the freshly exposed surface of the coatings is revealed following loss of the damaged layer. The subsequent attack of these newly exposed layers is documented in the micrographs of the coatings aged for eight weeks (Figure 5-20).

Porosity (Table 5-33) and thickness (Table 5-31) data for the detonation gun samples follow trends which mirror the dissolution and surface loss cycle described above. Thickness values can be seen to be gradually reducing with increasing ageing time although the large deviation in this data limit the statistical significance of these

results. Porosity levels are also seen to be high when the coating has large altered layers present. These levels fluctuate with formation and loss of damage layers again supporting suggestions that the dissolution process is cyclic in nature.

Further support for this hypothesis comes with analysis of the residual stress data obtained for these coatings (Table 5-36). As reported above, during spallation and loss of coating material from the surface of the sample, the residual stress levels measured in the coating layers increase. This is clearly seen in the results for the detonation gun samples aged at pH 4.5 with residual stress levels dropping during the dissolution phase of the attack by the *in-vitro* medium as a result of surface morphological alteration, then increasing again as the damaged surface layers are lost from the coating exposing fresh material.

That the detonation gun coatings show no evidence for reprecipitation of crystalline material must be a reflection of the rate of surface modification occurring for these materials. As discussed above (section 8.1.2) the detonation gun coatings would be expected to undergo a more rapid dissolution *in-vitro* as a direct result of their higher amorphous content and levels of residual stress than vacuum plasma sprayed coatings. It was seen (section 8.3.1) that the vacuum plasma sprayed coatings show accelerated degradation at pH 4.5 and a similar effect would be expected for the detonation gun coatings. In fact, the surface modification occurs so rapidly on detonation gun coatings that the re-precipitation of crystalline hydroxyapatite layers cannot be maintained. If a similar process were to be observed *in-vivo* as *in-vitro* it is possible to suppose that the detonation gun coatings will not have the same effective osseoconductive properties as the vacuum plasma sprayed coatings since the surface layer loss mechanism seems to dominate over that of re-precipitation.

8.3.3 Summary

The effects observed for exposure of hydroxyapatite coatings to an *in-vitro* ageing solution at pH 4.5 obey the same trends as those reported for the coatings aged at pH 7.2. In addition to cyclic dissolution processes which are seen to occur at a much faster rate and in a more dramatic manner for the coatings aged at the lower pH, there is also evidence for re-precipitation of crystalline hydroxyapatite on the surface of the vacuum plasma sprayed coatings (Figure 5-14 and Figure 5-15). As described above (section 8.3.1), this process is thought to occur in cycles of dissolution of amorphous material, loss of cohesion of remaining agglomerated material in the surface layer, subsequent loss of the damaged surface layer and exposure of fresh material by that surface loss. The cyclic nature of the process was observed in changes in crystallinity (Table 5-19), porosity (Table 5-24), thickness (Table 5-22) and surface roughness (Table 5-26). As the surface layer was attacked by the medium, there was an associated increase in crystallinity and porosity levels in the coating and also an increase in surface roughness. When the damage layers spalled away from the surface these levels returned to lower values and the coating cross-sectional thickness reduced. Residual stress was again observed to decrease gradually in accordance with slight micro-motion at the sample surface during the dissolution phase and increase during surface spallation to return to levels around the initial stress shortly after the fresh surface was exposed.

In the case of the vacuum plasma sprayed coatings, the dissolution of amorphous material from the coating surface was followed by re-precipitation of this material in the form of crystalline hydroxyapatite. This material covered the coating surface with a myriad of cauliflower like crystalline nodules. This modified surface layer was however subject to the same poor cohesion constraints as the *in-vitro* attacked surface and underwent cyclic spallation ultimately resulting in the exposure of a new surface. The increase in surface roughness associated with the formation of these nodular protuberances and the smoothing of the surface as this layer spalled off was recorded by Talysurf analysis.

It was suggested (section 8.3.1) that the severe nature of the attack of amorphous vacuum plasma sprayed hydroxyapatite at pH 4.5 may have a dramatic effect on the behaviour of these coatings *in-vivo*. Since dissolution and re-precipitation of crystalline hydroxyapatite was seen to occur at a more rapid rate at this lower pH which may be present immediately post operatively, it was suggested that it may be this effect which causes the rapid post-operative fixation of vacuum plasma sprayed hydroxyapatite coated prostheses.

That the detonation gun coatings show no evidence for re-precipitation of crystalline material was also considered to be a reflection of the rate of surface modification occurring for these materials. It was suggested that in the case of these coatings, the surface modification occurred so rapidly on detonation gun coatings that the re-precipitation of crystalline hydroxyapatite layers could not be maintained. It was postulated that if a similar process were to be observed *in-vivo* as *in-vitro* it is possible that the detonation gun coatings will not have the same effective osseoconductive properties as the vacuum plasma sprayed coatings since the surface layer loss mechanism may dominate over the re-precipitation mechanism inhibiting new bone growth.

8.4 Effect of Static Loading in Air at 37°C

Vacuum plasma sprayed and detonation gun sprayed hydroxyapatite coatings were aged under static loading in air in an environment chamber held at 37°C. Analysis of the effect of this imposed regime on the coatings enabled the effect of static loading alone to be distinguished from the effect of the ageing medium in later static *in-vitro* testing.

8.4.1 Vacuum Plasma Sprayed Hydroxyapatite Coatings

Exposing the vacuum plasma sprayed coatings to air held at 37°C for extended durations has a minimal effect on the morphology and properties of the coatings. Even

after fifteen weeks exposure to this environment the surfaces of the coatings (Figure 6-3) show no discernible change in appearance over the as-received coating. When the large standard deviations in value are taken into account the aged coatings show no real change in thickness (Table 6-3) or crystallinity (Table 6-1) and no change in composition (Table 6-2). The surface of the coating shows no signs of damage to the amorphous phases, a result supported by the unchanging crystallinity and surface roughness data (Table 6-5). The polished cross-sections through the vacuum plasma sprayed coatings (Figure 6-2) also show no visually apparent change in thickness.

The only measured changes occurring to these coatings lies in analysis of porosity levels (Table 6-4) in the polished cross-sections and in the residual stress data (Table 6-6) for the material. Porosity levels in the bulk of the coatings show measurable increases in value. This is probably due to the appearance of a small number of large pores in the aged coatings. The residual stress values for aged coatings fluctuate considerably between ageing durations. The residual stress measured in the surface layers of both the aged coatings is considerably higher than that reported for the as-received sample. This increase in stress is not associated with any observable change in the morphology or the composition of the material at the coating surface. It is possible that the act of imposing the three point bending strain on the coating during ageing has in some way built up stress levels in the coating which were not released when the coating was removed from the bending jig at the end of the test. The coatings were bent in a manner that imposed a tensile strain in the surface layers of the coating and the lack of evidence for relief of this strain, for example by increased micro-cracking at the surface (Figure 6-3) may suggest that the strain is being stored in the coatings during testing. This increase in the stress levels detected in the coating is really the only sign that the static loading is having any effect on this material.

8.4.2 Detonation Gun Sprayed Hydroxyapatite Coatings

As with the vacuum plasma sprayed coatings (section 8.4.1) there appears to be virtually no effect on the morphology and composition resulting from ageing of the

detonation gun coatings in air at 37°C. Full characterisation of the coatings reveals no significant changes in the crystallinity (Table 6-7), thickness (Table 6-9) or surface roughness (Table 6-11). These results are supported by visual examination of the coating surfaces (Figure 6-6) and polished cross-sections (Figure 6-5). There is no apparent change in the surface morphology of the coatings - no evidence of any kind for attack of the vulnerable meta-stable glassy phases on the coating surface and no increase in the degree of surface micro-cracking even after exposure to the environment for fifteen weeks.

In contrast to the results presented for the vacuum plasma sprayed coatings however, ageing the detonation gun coatings in air for one and fifteen weeks produces no measurable change in the residual stress levels in the coatings (Table 6-12). These coatings do not apparently store any of the strain imposed by three point static bending as the vacuum plasma sprayed coating seem to. The polished cross-sections through the detonation gun samples do however show a considerable increase in porosity (Table 6-10) with ageing time under static loading and it is possible that the imposed strain is causing an increase in the size of pores in the coating and it is this process which relieves any increased strain built up by bending. As discussed above, it is only this increase in bulk porosity in the detonation gun coatings that reveals that the coatings have been tested.

8.4.3 Summary

Static loading of coatings in air for one and fifteen weeks seemed to produce virtually no change in the surface morphology of the coatings. Both the vacuum plasma sprayed coatings (section 8.4.1) and the detonation gun coatings (section 8.4.2) showed no significant changes in thickness (Table 6-3 and Table 6-9), crystallinity (Table 6-1 and Table 6-7), surface roughness (Table 6-5 and Table 6-11) or appearance (Figure 6-2 and Figure 6-5) with ageing in air. There was no evidence that dissolution of the amorphous phase was occurring in these coatings which confirms that this effect is associated with exposure to aqueous solutions rather than being a time dependent degradation.

Both coating types however did show an increase in porosity associated with ageing in air under static loading (Table 6-4 and Table 6-10). It is suggested that this increase in porosity results from an enlargement of existing pores in the bulk of the coating as a consequence of the application of the static bending stress.

Investigation of the effect of ageing under static loading in air held at 37°C has demonstrated that the effect of an imposed static load alone on the hydroxyapatite coatings is negligible.

8.5 Effect of Static Loading at pH 7.2

8.5.1 Vacuum Plasma Sprayed Hydroxyapatite Coatings

Vacuum plasma sprayed coatings aged under static loading at pH 7.2 for various time periods show little change in morphology when compared to the as-received coating. Examination of polished cross-sections through the aged coatings shows no observable change in morphology with ageing (Figure 6-9) with the exception of an increase in bulk porosity (Table 6-18). This increase occurs on exposure to the *in-vitro* medium but does not progressively increase with ageing time. Coating porosity increases from approximately 5 % to over 12 % with static loading in the solution. This increase is not observed in the coatings which were aged with no applied load (Table 5-6) but a similar magnitude of porosity increase was observed in the coatings aged under static loading in air (Table 6-4). It therefore seems to be evident that this increase results from the static loading regime rather that exposure to the ageing environment.

The cross-sections (Figure 6-9) show the appearance of a semi-continuous or continuous black line running along the interface between the coating and the substrate in the aged coatings. This line may be an indication of the initiation of delamination failure, however even after fifteen weeks exposure to the testing regime the coatings still seem to

be well adhered to the substrate. Looking at measurements of cross-sectional thickness (Table 6-16) taken from the polished coatings, no change in thickness either between the aged coatings and the as-received coating or between coatings aged for different time periods was observed, indicating that no quantifiable dissolution of the coating surface was underway.

This suggestion is supported by examination of the surfaces of the aged coatings (Figure 6-10 and Figure 6-11). As reported above (section 8.2.1), exposure of the coatings to the *in-vitro* environment in the unloaded state brings about slight dissolution of the amorphous glassy regions on the coating surface. This effect is again seen for the coatings aged at pH 7.2 under static loading conditions. The magnitude of the dissolution is again seen to be progressive with the attack increasing in severity with longer exposure to the ageing medium. The coating aged for the maximum duration, fifteen weeks also shows some signs of re-precipitation of a crystalline phase in some regions of the surface, in particular where dissolution of the amorphous material has taken place. This effect was not observed in the coatings aged at pH 7.2 without an applied load but then the coatings aged for fifteen weeks under static loading were exposed for a much longer duration than any of the unloaded samples. The re-precipitated phase can therefore be considered to be a natural progression of the earlier cumulative dissolution effects. As discussed earlier (section 8.3.1) ageing at pH 4.5 offers an accelerated indication of the effects of the dissolution and in this latter case, re-precipitation has been observed. This seems to substantiate the supposition that with time, re-precipitation would have occurred in the coatings aged with no applied load.

The vacuum plasma sprayed coatings aged under static loading also presented evidence for the formation of new micro-cracks on their surfaces (Figure 6-11). Coatings aged for four and ten weeks clearly supported new, sharp edged cracks which showed no evidence of dissolution by the ageing medium and therefore were considered to be newly formed. Examination of these cracks also allowed the age of the coral-like deposits on the coating aged for fifteen weeks to be judged since they showed signs of bridging these new micro-cracks and therefore must have been formed after the cracks themselves. The formation of the new cracks on the coating surface however does suggest that static

loading of the coatings is responsible for this surface damage since an increase in crack density in the unloaded, aged samples was not observed (Figure 5-4 and Figure 5-5).

Relief of built up residual stress by this process of micro-cracking is however not supported by examination of stress data (Table 6-21). The stress levels in the statically loaded vacuum plasma sprayed coatings are considerably higher than the levels in the as-received coating and are also seen to fluctuate quite considerably. However, these fluctuations are not associated with the new crack formations seen for four and ten week aged coatings and can also not be attributed to the loss of material from the coating surface since this effect was not observed in these samples (Table 6-16). The modification of the surface morphology associated with the formation of crystallites on the coating surface is however reflected in the residual stress data, the new phase clearly causing some stress relief since the data for the coatings aged for fifteen weeks suggests a return to the very low, as-received stress level.

Preferential dissolution of the beta tri-calcium phosphate phase found in the as-received coating (section 8.2.1) was again observed in the vacuum plasma sprayed coatings aged under static loading. Evidence of this phase was not found in coatings exposed to the *in-vitro* environment (Table 6-15). In addition to this compositional change however, a new phase was detected in the coating surface in significant quantities. This change in a small proportion of the hexagonal hydroxyapatite phase or indeed the orthorhombic beta tri-calcium phosphate phase to the monoclinic calcium oxide phosphate phase could be responsible for some of the changes in residual stress observed in the coatings. However this suggestion is difficult to support thermodynamically since phase changes would usually be expected to reduce, not raise residual stress levels.

Crystallinity results for the vacuum plasma sprayed coatings (Table 6-13) follow the same trends as those obtained for the coatings aged with no applied load (Table 5-1). An increase in the relative crystallinity levels for coatings which have been exposed to the *in-vitro* ageing environment, associated with preferential dissolution of amorphous

material from the coating surface is observed. The results obtained for the coating aged for fifteen weeks under static loading seem to be incongruously low in comparison to the other data. It would be expected that the combination of dissolution of amorphous material and the formation of new crystallites on the coating surface would give an overall increase to the levels of crystallinity measured for this sample, however, the mean value is surprising low. This low value may however be artificial. Looking at the standard deviation in measurements for this material, over three times higher than for the other samples, it is entirely possible that the coating could have a real crystallinity much closer and possibly higher than the other aged coatings.

No apparent change was detected in surface roughness values for these coatings aged under static loading (Table 6-20), reflecting the minimal change in surface morphology which has resulted from the exposure to this testing regime.

Very little work has been found in the literature offering a discussion of the effect of an applied load on the rate of dissolution of hydroxyapatite coatings. Reis *et al* [80] aged air plasma sprayed hydroxyapatite under four point bending in buffered Hank's solution. These authors reported a measurable thinning of the coatings and a smoothing of their surfaces. These results seem to be an exaggeration of those reported here for vacuum plasma sprayed hydroxyapatite coatings. It is entirely possible that the defective structural morphologies of the air plasma sprayed coatings undergo dissolution by the ageing medium more rapidly than would vacuum plasma sprayed coatings. It is also possible that the ageing medium used by Reis *et al* was more aggressive than that investigated here. It is not however illogical to suggest that this earlier work offers an indication of an effect which may have become increasingly apparent in the vacuum plasma sprayed coatings had they been aged for a longer duration under an applied static load. However, since no apparent thinning had occurred after fifteen weeks exposure to the *in-vitro* ageing medium it seems sensible to assume that the coatings would survive long enough *in-vivo* to perform their suggested role in encouraging early bone apposition.

8.5.2 Detonation Gun Sprayed Hydroxyapatite Coatings

As reported for all the other coatings which have been exposed to an *in-vitro* environment (section 8.2.2), the detonation gun coatings aged under static loading at pH 7.2 show an increase in the relative percentage of crystalline material on the coating surface (Table 6-22). As suggested above, this is thought to be associated with progressive and preferential dissolution of amorphous material from the coating surface. Again, as reported above, the crystallinity levels do not seem to change in a progressive manner with increased ageing time but simply show a distinctive difference between the unaged and aged values.

Again as reported above (section 8.2.2), loss of beta tri-calcium phosphate from the coatings with ageing is also reported for the detonation gun coatings aged at pH 7.2 under static loading (Table 6-24). This is thought to correspond to the preferential dissolution of this phase over hydroxyapatite itself. Dissolution of material from the surface of the coating is however not occurring in quantities large enough to be detected by image analysis. Measurement of cross-sectional thickness (Table 6-25) for these coatings reveal no change in thickness over the as-received coating with exposure to the testing environment.

Again, as in the case of the vacuum plasma sprayed coatings (section 8.4.1), examination of the polished cross-sections through the detonation gun coatings reveal an increase in the porosity levels in the coatings with ageing time (Table 6-27). This increase in porosity could be associated with the growth of pores already present in the coating allowing accommodation of the stresses imposed by the static loading regime.

Looking at the surfaces of these coating using scanning electron microscopy (Figure 6-15 and Figure 6-16) the effects of this gradual dissolution process can be observed. A progressive dissolution of the glassy, amorphous phase from the coating surface is seen in the coatings aged for one to ten weeks *in-vitro*. Micro-cracks seen on the coating surface become smoothed with etching by the ageing media and large pores

begin to develop associated with fall out of damaged surface material. This fall out is again evidence that the amorphous phase in the coatings acts as a binder, holding the agglomerated material *in-situ* on the coating surface. The dissolution of this phase creates weaknesses in the surface bonding and eventual loss of the particulate phases from the outermost coating layers.

After ten weeks ageing however, a distinctive change occurs in the coating morphology. Here the coating has an appearance much more like that of the coatings aged for only short durations. Amorphous material can again been seen on the coating surface, although it shows signs of etching. As suggested before (section 8.3.2), it seems that the dissolution process is cyclic in nature with progressive dissolution causing eventual loss of the surface coating layer to reveal a new un-etched surface to the environment. The coatings aged for ten and fifteen weeks also show clean, sharp micro-cracks running along the coating surfaces. These cracks may appear to be newly formed for one of two reasons. Either, as suggested, they belong to a newly exposed surface layer which has not effectively been attacked by the ageing medium, or they have been newly formed on the surface as a result of the static loading regime.

These changes in the surface morphology of the coatings are not of a magnitude large enough to be detected by Talysurf analysis (Table 6-29). Surface roughness data for these coatings aged under static loading at pH 7.2 shows no apparent trend associated with the observed changes in surface appearance. Results show virtually no change in surface roughness for any of the statically loaded samples over the as-received coating.

Residual stress values (Table 6-30) for these coatings do not give a clear indication of which of these processes is occurring. Both the loss of surface material and the formation of micro-cracks is expected to result in a reduction in the residual stress levels in the coatings. Since this trend is observed in residual stress data it is still not obvious which effect is occurring. It is of course equally possible that both effects are underway simultaneously. In contrast to the values reported for the vacuum plasma

sprayed coatings (Table 6-21), the detonation gun coatings do not show an increase in residual stress on exposure to the testing environment. Here the trend is much more satisfactory, with the dissolution process, possibly in conjunction with the formation of new micro-cracks, resulting in a progressive relief on stresses imposed by the manufacturing process. This effect may again be a direct result of the initially high amorphous content of the detonation gun coatings. As described previously (section 8.1.2), the higher degree of amorphous material in the detonation gun coatings is expected to cause more rapid modification of the coating surface than would be the case for vacuum plasma sprayed coatings. It is possible that it is the rate of this surface alteration which is allowing stress relief in the detonation gun coatings but not in the vacuum plasma sprayed materials.

8.5.3 Summary

Static loading at pH 7.2 seems to have very little additional effects on the coatings that exposure to the *in-vitro* environment alone did not produce. Both coating types showed small amounts of progressive dissolution of amorphous material from the coating surface (Figure 6-10, Figure 6-11, Figure 6-15 and Figure 6-16), which in the case of the detonation gun coatings was followed by loss of cohesion of the etched surface and material loss. Both coating types showed an increase in crystallinity associated with loss of amorphous material from the coating surface (Table 6-13 and Table 6-22) but no significant change in coating thickness which would indicate the loss of large quantities of the coating (Table 6-16 and Table 6-25). Loss of the beta tri-calcium phosphate phase was also detected for both the vacuum plasma sprayed coatings and the detonation gun sprayed coatings (Table 6-15 and Table 6-24). It is possible that this phase was transformed to calcium oxide phosphate in the case of the vacuum plasma sprayed coatings.

The major effects on coating morphology associated purely with the effects of static loading were found in an increase in bulk porosity in the coatings (Table 6-18 and Table 6-27). This may have resulted from an enlargement of existing pores in the coating

due to the application of a tensile bending stress. It is also postulated that the static loading regime caused the formation of new micro-cracks in the surface of the coatings under some circumstances (Figure 6-10, Figure 6-11, Figure 6-15 and Figure 6-16).

Static loading of both detonation gun and vacuum plasma sprayed hydroxyapatite coatings, even for extended durations, therefore seems to have no major detrimental effects on the integrity of the coatings. Other than the effect of exposure to the ageing medium therefore, the coatings show no evidence for large scale modification as a result of the applied testing regime. This suggests that were the coatings stressed upon initial insertion in a patient, providing that the surrounding tissue pH remained high, the coatings would remain coherent.

8.6 Effect of Static Loading at pH 4.5

8.6.1 Vacuum Plasma Sprayed Hydroxyapatite Coatings

The effects of the *in-vitro* ageing solution are again observed in the vacuum plasma sprayed coatings which have been aged at pH 4.5 under static loading. However, the effects of the ageing medium on the coatings aged under static loading do not seem to be as severe as those which occurred to the unloaded materials (section 8.3.1).

As discussed above, exposure to the *in-vitro* solution brings about preferential dissolution of the amorphous phases in the surface of the hydroxyapatite coatings (section 8.2.1). This loss of amorphous material results in a relative increase in the percentage of crystalline material in the surface layers of the coating. This effect is once again observed in the vacuum plasma sprayed coatings which have been aged under static loading at pH 4.5 (Table 6-31). In addition to this, the much higher solubility of the beta tri-calcium phosphate phase over pure hydroxyapatite is demonstrated in the compositional change occurring in the surface layers of the material after exposure to the

ageing environment (Table 6-33). In the majority of the coatings, a loss of beta tri-calcium phosphate from the composition of the coatings with ageing was observed.

The dissolution of amorphous material from the surface of the vacuum plasma sprayed coatings is not easily observed by examination of the polished cross-sections through the coatings (Figure 6-18 and Figure 6-19). No obvious modification to the surface layers of the coatings exposed to the testing regime could be detected by cross-sectional analysis and no significant change in thickness was measured to indicate gross loss of material from the bulk of the coatings (Table 6-34). No detectable change in surface roughness was recorded for any of the coatings either (Table 6-38). There was however seen to be a gradual increase in the cross-sectional porosity of the coatings which appeared to increase with increased exposure to the testing environment (Table 6-36), i.e. porosity increased with increased static ageing. This porosity increase was thought to be attributed to an increase in the size of existing porosity resulting from growth of pores under the action of the applied static load (section 8.5.1).

Evidence for this applied load could be detected in the residual stress levels measured in the surface layers of the coatings (Table 6-39). The coatings which had been exposed to *in-vitro* static loading showed increased levels of residual stress over those found in the as-received coating. This implies that the application of the static load causes stress to be stored in the coating and it could be the increase in this stored stress that causes porosity growth (section 8.5.1).

Examination of the surface of the vacuum plasma sprayed coatings reveals the damage which has occurred to the samples as a result of exposure to the *in-vitro* environment (Figure 6-20 and Figure 6-21). Here a gradual and progressive etching of the amorphous, glassy regions of the coating surface with extended exposure to the ageing solution can be seen. This dissolution also causes the formation of large pores in the coating surface which have probably resulted from the fall out of poorly adhered agglomerates from the surface. As discussed above (section 8.2.2), it is suggested that the amorphous phase in the coating acts like a binder for small crystallites and

agglomerates on the surface of the coating. Dissolution of this binder phase therefore could result in loss of cohesion of areas of the coating and their loss, leaving large pores of the type seen in surface micrographs of these coatings. After ten weeks exposure to the ageing medium there is no evidence for surviving amorphous material on the coating surface and microcracks which have been observed on all the coating surfaces are seen to have widened considerably. The coating aged for fifteen weeks shows some evidence for the nucleation of crystalline nodules on the material surface. These nodules are much smaller in size that those seen on other coatings (section 8.3.1) which suggests that they are only in the initial stages of growth.

Even after exposure to the testing regime for fifteen weeks these vacuum plasma sprayed coating do not show the degree of surface damage and cross-sectional modification observed for the same coatings aged at pH 4.5 with no applied load (Figure 5-14 and Figure 5-15). The surface of the coating aged for fifteen weeks did look very similar to that of the unloaded vacuum plasma sprayed coating aged for eight weeks (Figure 5-5) but this latter surface had resulted from the spalling off of a much more highly modified surface layer. In fact it was suggested that the surface seen in the latter case was one which had been newly exposed to the environment. It therefore must be concluded that the combined effects of static loading and *in-vitro* ageing have a less damaging effect on the vacuum plasma sprayed coatings than ageing alone.

No obvious explanation for this inhibition of damage can easily be presented based on the morphological characterisations performed on these coatings during this research. The only major differences between the two coating groups seems to lie in the levels of residual stresses measured in the surface layers of the coatings (Table 6-39) and in their cross-sectional porosity (Table 6-36). In contrast to the result expected for these two groups, the coatings which were aged with no applied load have much higher average residual stresses than those aged under static loading. It is therefore possible that the process of internal porosity growth which was observed in the statically loaded samples but not in the unloaded samples allows sufficient relief of residual stress in the coating that gross surface damage in inhibited. Although this explanation for the morphological differences in the coatings after exposure to the medium is not very

satisfactory, others are not readily suggested by the data obtained for the coatings. Whatever the cause of this effect, it does suggest that the coatings will perform differently *in-vivo* if initially inserted in a manner which leaves them under a constant applied stress than under no stress. Dissolution has been found to occur much more rapidly when the coatings are unstressed. Since, as described previously (section 8.1.3) it is this dissolution which is supposed to encourage early bone growth into the hydroxyapatite coatings, it would seem logical to suggest that a clinician should try to ensure minimal stressing of the prosthesis on insertion into the patient. This is however not recommended in practice since the long term stability of an implant demands that it is securely positioned initially. Although hydroxyapatite coatings may effectively lock a well fitted prosthesis in place, the rate of surface re-modification from an unstressed implant would not be rapid enough to secure a loosely positioned device. Consequently, despite the inhibition of surface remodelling brought about by stressing of the hydroxyapatite coated surface, it is recommended that the tightest fit possible is achieved to ensure the best long-term fixation of the prosthesis.

8.6.2 Detonation Gun Sprayed Hydroxyapatite Coatings

As has been reported for hydroxyapatite coatings above (section 8.2.2, 8.3.2, 8.5.2), exposure to the *in-vitro* environment brings about an increase in the relative crystallinity of the detonation gun coatings aged under static loading at pH 4.5 (Table 6-40). For these coatings, the crystallinity increases gradually with ageing time from approximately 40 % in the as-received case to over 60 % measured after ten weeks exposure to the ageing medium.

Again as suggested before, this increase in crystallinity is associated with a dissolution of amorphous material from the surface of the detonation gun coatings. This effect can be seen in the scanning electron micrographs taken of the coating surfaces after various ageing times (Figure 6-25 and Figure 6-26). Even after exposure to the ageing regime for just one week (Figure 6-25), the coatings show an extensive dissolution of the amorphous phase, the glassy regions are pocked and etched over the

majority of their area, and large pores have developed in some places. This effect is progressive in nature, the coatings exposed for longer durations demonstrating a progressive degree of damage to the amorphous region and an increase in the size and depth of pores (Figure 6-26). It has been suggested earlier (section 8.2.2) that the amorphous material acts as a binder for the crystalline, agglomerated phase and this appears to be the case here. Loss of the amorphous material has allowed large lumps of coating to fall away revealing fresh, un-etched material below. The coating which had been aged for fifteen weeks disintegrated completely on removal from the *in-vitro* ageing tank and thus could not be examined by any of the analysis methods used to characterise the other coatings.

The coating surfaces are also criss-crossed with a myriad of microcracks which appear to be sharply edged and thus newly formed. These cracks do not appear in the surface of coatings aged at pH 4.5 with no applied load (Figure 5-19 and Figure 5-20) and therefore seem to have formed directly as a result of the static loading regime.

The cyclic nature of the dissolution process is again supported by visual inspection of the polished cross-sections through the detonation gun coatings (Figure 6-23 and Figure 6-24). Initially a morphologically modified highly porous surface layer is seen in the coatings aged for the shortest durations. This layer is then seen to grow and progress in depth through the coating. At the same time the coating itself is visibly thinning, although this effect is obscured by the variance in results in thickness data (Table 6-43). As described above, the coatings aged for fifteen weeks showed the extreme nature of the cyclic dissolution process. The dissolution followed by loss of layers from the coating surface had progressed to such an extent that no coating remained intact on the substrate after fifteen weeks.

The measured porosity seen in polished cross-sections was also found to increase as a result of exposure to the testing environment (Table 6-45). Values were magnified by the highly porous modified surface layer in which a large majority of the measured porosity existed. In the coating aged for ten weeks the modified surface layer has fallen

away and the relative porosity in the remaining portion of the coating therefore appears to be lower. Bulk porosity levels for these coatings aged under static loading are approximately 30 % higher than those determined for the unloaded aged coatings (Table 5-33) suggesting that the static loading effect causes an increase in the porosity levels in the coatings.

The modifications occurring at the coating surface are detected by surface roughness analysis (Table 6-47). This data shows a gradual increase in surface roughness associated with the dissolution of amorphous material from the outer layers of the coating and the breaking away of agglomerated hydroxyapatite. As described above (section 8.5.1) Reis *et al* [80] observed gradual thinning of air plasma sprayed coatings aged under static loading in Hank's solution. However, these authors reported a decrease rather than an increase in the surface roughness of the hydroxyapatite with ageing time. The results presented here seem more realistic since dissolution of the smooth, amorphous material in the coating surface leads to an increase in roughness with ageing time as only the rough agglomerated material is left behind. However, Reis *et al* were working with a different coating type (air plasma sprayed) and ageing medium (Hank's solution) which may have played an influential role in altering the dissolution process, hence altering their data.

Residual stress data for the coatings (Table 6-48) also obeys the expected trend, following an initial increase in stress associated with the imposition of the three point bending load to the sample. The levels then gradually decrease with ageing time. As describe above this relaxation is due to the loss of amorphous material from the coating surface allowing slight micro-motion in the bulk of the coating itself. In addition to this effect it is clear that stress is being relieved in these coatings by a dramatic increase in the number of micro-cracks crossing the coating surface (Figure 6-25 and Figure 6-26). In this instance, spalling off of the coating from the substrate is not associated with a detectable increase in residual stress (corresponding to levels in the newly exposed surface layer). Rather, stress obeys a steady and sustainable downwards trend towards

relief of stress with increased ageing time which again indicated the high rate of surface dissolution.

Again, the fundamentally different behaviour of the vacuum plasma sprayed coatings to those produced by detonation gun spraying is exposed in the results of characterisation of the detonation gun coatings aged under static loading at pH 4.5. Here, unlike in the case of the vacuum plasma sprayed coatings (section 8.6.1) dissolution of amorphous hydroxyapatite is not inhibited by the application of a constant stress. The reason for this difference in behaviour must lie in the manner in which each coating type dissipates residual stress. It was reported earlier (section 8.5.1) that vacuum plasma sprayed hydroxyapatite coatings store the applied static stresses whilst detonation gun coatings do not. It was suggested that this ability to dissipate stress was stabilising the detonation gun sprayed coatings, but this may now be seen not to be the case. It is possible that the detonation gun hydroxyapatite coatings have undergone a partial loss of coherence the result of which is a drop in residual stress. Under less severe circumstances, this destabilisation produced no visible alteration to the morphology or structure of the coatings but under the low pH, loaded environment, the harsher regime demonstrates the, previously unnoticed, increased fragility of the coatings.

8.6.3 Summary

In agreement with results discussed earlier for the coatings aged under static loading at pH 7.2 (section 8.5), both the vacuum plasma sprayed coatings and the detonation gun sprayed coatings show only minor alteration resulting directly from the application of static three point bending stress and not from the effects of the ageing solution. As in the case of the coatings aged with no applied load at pH 4.5 (Figure 5-14, Figure 5-15, Figure 5-19 and Figure 5-20), both coating types show the effects of surface attack by the *in-vitro* medium (Figure 6-20, Figure 6-21, Figure 6-25 and Figure 6-26). Dissolution of amorphous material in general (Table 6-31 and Table 6-40) and associated preferential dissolution of beta tri-calcium phosphate (Table 6-33 and Table 6-42) are reported for both sets of coatings. Both coating types show increased levels of

micro-cracking on the coating surface (Figure 6-20, Figure 6-21, Figure 6-25 and Figure 6-26), particularly in the case of the detonation gun coatings. Reprecipitation of crystalline hydroxyapatite is reported in particular for the vacuum plasma sprayed coatings aged for the maximum duration although this effect is far less pronounced than that seen for the unloaded aged coatings. As concluded for the unloaded samples, exposure to the lower pH ageing medium has a much more devastating effect on the surface morphology of the coatings than ageing at pH 7.2.

Again as discussed above for the coatings aged under static loading at pH 7.2, the coatings behave quite differently in terms of their resolution of the residual stresses both inherent in the coatings as a result of the manufacturing processes and imposed by the testing regime. Detonation gun coatings seem to be able to allow relief of residual stresses by surface micro-cracking and modification, resulting in a gradual reduction in stress with exposure to the testing environment. The vacuum plasma sprayed coatings however show no apparent change in residual stress levels over the testing period. In contrast, the detonation gun coatings show a much more marked surface modification than is observed for the vacuum plasma sprayed coatings, which, as discussed (section 8.6.2), negatively influences coatings stability. The benefits and drawbacks of coating stability have been described at length elsewhere (sections 8.1.3, 8.2.3, 8.3.3 and 8.5.3), it is sufficient to say here that the coatings demonstrate a considerable difference in their responses to applied load *in-vitro*. While the stability of vacuum plasma sprayed hydroxyapatite coatings seems to be increased by the application of the static load, the reverse is observed for the detonation gun coatings.

The only other difference reported for coatings aged under an applied static load over those aged with no applied load lies in the porosity levels measured for the samples (Table 6-36 and Table 6-45). Both vacuum plasma sprayed and detonation gun sprayed coatings have increased levels of porosity over the unloaded aged samples. It is suggested that some relief in residual stress is achieved in the statically loaded samples by the action of porosity growth during the test.

8.7 Effect of Fatigue Testing in Air and in Ringer's Solution

8.7.1 Vacuum Plasma Sprayed Hydroxyapatite Coatings

A considerable difference exists in the behaviour and morphology of coatings which have been fatigued in air as opposed to those which have been fatigued in Ringer's solution. The coatings which have been fatigue tested in air for one and ten million cycles show no apparent change in crystallinity levels associated with the dissolution of amorphous material from their surfaces (Table 7-1). The coatings fatigued in Ringer's solution however show the expected increase in crystallinity associated with exposure to the *in-vitro* ageing solution. The crystallinity of these coatings increases with increasing fatigue duration, which is not surprising since the increased number of fatigue cycles also requires an extended duration of exposure to the ageing medium. Coatings fatigue tested for one million cycles were exposed for approximately three days whilst those fatigued for ten million cycles were of course exposed for thirty days. It is therefore expected that the coatings will have crystallinities that correspond to those of coatings exposed for similar times (Table 5-1), and this was found to be the case.

Looking at the surfaces of the vacuum plasma sprayed coatings, the dramatic physical differences imposed on the materials by the testing regime were again seen. The coatings fatigued in air show no obvious change in surface morphology after the one million cycles test (Figure 7-5). However after ten million cycles (Figure 7-6) the samples show small amounts of etching of the flat glassy regions probably associated with dissolution due to exposure to moisture in the atmosphere, and a considerable increase in the number of surface micro-cracks. The coatings exposed to Ringer's solution during the fatigue test show the expected effects of the *in-vitro* environment on their surface appearance. The coatings fatigued for one million cycles (Figure 7-7) show slight dissolution of the amorphous material from the coating surface, as described above (section 8.2.1), resulting from preferential attack of the amorphous material by the medium. However the coating fatigue tested for ten million cycles had completely spalled

off the substrate during testing and thus could not be investigated. Such spallation of vacuum plasma sprayed hydroxyapatite coatings away from metallic substrates appear to have only been reported by two other authors in the literature [150, 151]. Both these authors reported some delamination of hydroxyapatite coatings away from titanium substrates under cyclic loading conditions in sheep. However, both models allowed a two month unloaded ageing of the implanted prostheses prior to load bearing to allow implant stabilisation and bone ingrowth.

The reason for this failure can be investigated by looking at the polished cross-sections through the fatigued vacuum plasma sprayed samples. Coatings fatigued in air for one million cycles (Figure 7-2) appear to be virtually identical to the as-received coatings (Figure 4-5) as do those fatigued in air for ten million cycles in general (Figure 7-3). However, the coatings fatigued for ten million cycles show a large increase in bulk porosity over the as-received coatings (Table 7-4). This effect was observed in the coatings aged in air under static loading (Table 6-4) and therefore should be attributed again to the action of the applied stress on the coating causing enlargement of existing porosity.

As described above however, the coatings fatigued in Ringer's solution show a much more dramatic reaction to the testing regime. The coating fatigued for one million cycles in Ringer's solution has completely delaminated from the substrate in many areas (Figure 7-4). Although the bulk of the coating remained intact large areas are separated completely from the titanium leaving large expanses of substrate exposed. The delamination failures in these coatings are initiated from the point of small micro-cracks which run through the thickness of the coating from surface to substrate. The delamination obviously occurs at the coating - substrate interface but initiates at these cracks which have probably resulted from fatigue damage to the coating. It has been reported in the literature [148] that through-thickness cracks develop in coatings predominantly during the loading cycle of fatigue testing, while delamination cracks are formed during the unloading cycle. Such micro-cracks and interface delamination has been reported previously for alumina air plasma sprayed coatings which have undergone cyclic indentation loading [149]. However the only other reference to fatigue of

hydroxyapatite coatings *in-vitro* is by Reis *et al* [80] who imposed four point bending fatigue for one million cycles on 50 μm thick air plasma sprayed hydroxyapatite coatings in buffered Hank's solution. Despite reporting significant thinning of the coatings and smoothing of their surfaces, no delamination failures were reported. These surface to substrate cracks have not been observed in the polished cross-sections through other vacuum plasma sprayed coatings and therefore must be assumed to be a product of the *in-vitro* fatigue process.

Residual stress values for all these coatings (Table 7-6) do not demonstrate relief of inherent stress by the formation of the observed micro-cracks (Figure 7-4) or by the dissolution processes occurring to the coatings fatigue tested in Ringer's solution. Rather, the imposed stress resulting from the fatigue test seems to be being built up in the surface layers of the coating resulting in an increasing magnitude of this stress with increasing number of fatigue cycles. For example, the coatings fatigued in air for one million cycles have a residual stress which is only half that of the coatings fatigued in air for ten million cycles. Samples submitted for x-ray analysis were usually taken from the only surviving region of coating still attached to the substrate and the magnitude of the stresses built up in these regions is noteworthy. Even the processes of delamination of the bulk of the cross-sectional length of the coating has not relieved the levels of residual stress in the small areas of intact coating remaining after fatigue testing in Ringer's solution.

There is no observable change in the roughness of the surfaces of either the coatings fatigue tested in air or the coatings fatigued in Ringer's solution (Table 7-5). This result supports the evidence from surface examination of the coatings by scanning electron microscopy (Figure 7-5, Figure 7-6 and Figure 7-7). Although the coatings become riddled with micro-cracks following long-term fatigue testing, the roughness of the surface changes very little.

Delamination of vacuum plasma sprayed hydroxyapatite coatings in the manner described here upon fatigue testing *in-vitro* would be extremely undesirable *in-vivo*. Not

only will a coating which has spalled away from its substrate not be able to perform its function in encouraging new bone growth into the surface of the implant, but it will also offer no shielding of the body from metal-ion release from its substrate. The latter problem is not an issue in implants which are only partially coated, however loss of the coating will in all cases allow release of the residual alumina grit seen at the Ti-6Al-4V / hydroxyapatite interface (Figure 4-5) into the body. This particulate debris will not easily be tolerated by the body and could lead to extreme tissue irritation and ultimately failure of the implant.

8.7.2 Detonation Gun Sprayed Hydroxyapatite Coatings

The detonation gun coatings fatigue tested in air and in Ringer's solution, like the vacuum plasma sprayed coatings, demonstrate the considerable difference the testing environment imposes in the morphology of the coatings (section 8.7.1). Examination of polished cross-sections through the detonation gun coatings begins to reveal the differences between fatigue testing in air and in Ringer's solution. Coatings fatigued in air for either one or ten million cycles (Figure 7-9 and Figure 7-10) show no apparent change in morphology over the as-received coatings (Figure 4-8), no obvious changes in cross-sectional thickness (Table 7-9) nor porosity (Table 7-10). The coatings fatigued in Ringer's solution are very differently affected by the testing environment. Although the coating fatigued for just one million cycles shows little change over the as-received coating in cross-sectional view (Figure 7-11) the ten million cycle tested sample (Figure 7-12) shows not only a measurable thinning of the coating thickness (Table 7-9) but also evidence for a large degree of modification to the surface layers of the coating. This modified layer is extremely porous in nature and imposes a large increase in the overall porosity measurement for the coating (Table 7-10).

Examining the surfaces of the coatings by scanning electron microscopy reveals more about the modifications occurring to the Ringer's fatigued samples. The coatings fatigued in Ringer's solution for one million cycles (Figure 7-15) show surfaces which have been dramatically altered by the combined effects of the *in-vitro* environment and

the cyclic loading. The coatings are covered in nodular cauliflower-like growths which are found to be centred upon regions which were obviously once covered with amorphous material. These growths are assumed to be the result of re-precipitation of the dissolved amorphous phase, in a crystalline form and are very similar in morphology to those seen on vacuum plasma sprayed hydroxyapatite coatings described earlier (section 8.3.1). Not only has the surface been modified in this way however, like the vacuum plasma sprayed coatings which were fatigue tested in Ringer's solution (Figure 7-7), here the surface is covered with micro-cracks. These cracks have obviously formed after the new surface phase since they criss-cross the crystalline precipitate and judging by their sharp edges, are newly formed.

The coating fatigued for ten million cycles in Ringer's solution (Figure 7-16) shows a progression of this effect. Here the crystalline growths seem to have fused together and cover the entire surface of the coating, not just being confined to what were once the amorphous regions. This re-precipitated phase also appears to have been attacked by the *in-vitro* ageing medium. There are several regions over the new surface where the nodules are themselves pitted and in fact areas where the whole new surface has broken away leaving large regions of porosity within which the etched original surface can be seen. Again the surface is criss-crossed with micro-cracks which have obviously weakened the modified surface layer to such an extent that it has begun to break away. As recorded for other aged coatings (section 8.2.2) it is suggested the process of attack by the *in-vitro* medium is cyclic in nature proceeding according to a process of surface dissolution, loss of cohesion and spalling off of the coating, or dissolution, re-precipitation, then loss of cohesion and spalling. The crazing of the surface by micro-cracks formed by the process of fatigue loading of the coating have accelerated the degree of damage and loss occurring to the hydroxyapatite.

Coatings fatigued in air for one million cycles (Figure 7-13) have a very similar appearance to the as-received material (Figure 4-9) except that it appears that the micro-cracks seen on the coating surfaces have grown in size. This effect has been accentuated in the coating fatigued for ten million cycles in air (Figure 7-14) where the size of the surface cracks are considerably larger than in the as-received coating. As suggested for

the coatings aged in air under static loading (section 8.4.2), this crack broadening process must be a direct effect caused by the process of load application.

The effect of the surface dissolution taking place in the coatings fatigued in Ringer's solution has also altered the composition of the material in its surface layers (Table 7-8). Although the material is still principally hydroxyapatite, the other significant phase has transformed, as before, from beta tri-calcium phosphate to calcium oxide phosphate. It seems that the re-precipitated phase has a different composition to the original coating and this is clearly reflected in its morphology when examined by scanning electron microscopy (Figure 7-15 and Figure 7-16).

In contrast to the vacuum plasma sprayed coatings (sections 8.5.1, 8.6.1 and 8.7.1), as reported for the statically loaded detonation gun coatings (sections 8.5.2 and 8.6.2), fatigue testing of these coatings principally results in a reduction in the residual stress levels measured in the surface layers of the material (Table 7-12). This implies that the detonation gun coatings do not store up the applied cyclic stresses in the same manner as do the vacuum plasma sprayed coatings. Rather, the actions of surface micro-cracking and morphological alteration allow overall relief of the residual stresses left in the coating by the manufacturing process. Alternatively of course it is possible that, like the vacuum plasma sprayed coatings, the detonation gun coatings do absorb stresses from the fatigue test but that the process of stress relief underway in these coatings is more effective than that occurring in the case of the vacuum plasma sprayed samples.

As was discussed earlier (sections 8.6.2 and 8.6.3), the detonation gun hydroxyapatite coatings do not store any applied stress nor use it to inhibit surface dissolution, and that this is not necessarily a phenomenon which would be detrimental to the coatings performance *in-vivo*. If the detonation gun coatings are more soluble than the vacuum plasma sprayed coatings this may allow them to encourage more rapid osseoconduction when implanted. The detonation gun coatings seem to be more rapidly attacked by the ageing medium under *in-vitro* fatigue conditions but this may in fact be beneficial to the performance of the coating *in-vivo* provided that it remains adhered to

the substrate. It was discussed earlier (section 8.7.1) that the vacuum plasma sprayed hydroxyapatite coatings fatigued in Ringer's solution seem to show a propensity to delaminate from their substrates. If this effect is not occurring with the detonation gun coatings then they will offer superior performance *in-vivo* since they will not present the possibility of the problems discussed for delaminated vacuum plasma sprayed coatings, i.e. enhanced metal ion release or release of free alumina grit. However, evidence from optical micrographs taken from detonation gun hydroxyapatite coatings fatigued in Ringer's solution for extended durations, i.e. ten million cycles (Figure 7-12), seems to imply that delamination is beginning to occur. Even if this is the case however, the detonation gun coatings have survived for much longer under the imposed testing environment than the vacuum plasma sprayed hydroxyapatite coatings which demonstrated gross delamination after just one million cycles fatigue.

8.7.3 Summary

As was reported for the coatings tested in static loading, in these fatigued samples the principal effect which causes damage to the material seems to be exposure to the *in-vitro* environment. Although both the detonation gun and vacuum plasma sprayed coatings clearly show signs of surface damage in the form of increased numbers or size of micro-cracks (Figure 7-5 to Figure 7-16), which has resulted from the fatigue process, it is the combined effects of the fatigue and the *in-vitro* environment which are most damaging to the coatings.

All the coatings fatigued in air seem to be little damaged by the process, even after ten million cycles of fatigue. As described above, there is an increase in surface micro-cracking in both coating types and a large increase in bulk porosity (Table 7-4) for the vacuum plasma sprayed coatings. Overall however, the coatings are well adhered to their substrates and show little or no change in crystallinity (Table 7-1 and Table 7-7) or cross-sectional thickness (Table 7-3 and Table 7-9). However fatigue in Ringer's solution proved to cause catastrophic failure of vacuum plasma sprayed coatings, even after just one million cycles (Figure 7-4), and a dramatic alteration to the morphology

(Figure 7-11 and Figure 7-12) and composition of detonation gun coatings (Table 7-8). Although the detonation gun coatings were still coherent enough to allow cutting and mounting of the samples after testing, the coatings were considerably thinned after ten million cycles and it was suggested that there was evidence that the coatings were actually beginning to delaminate from the substrate.

The effect of this delamination has been discussed above (sections 8.7.1 and 8.7.2). If either coating were to delaminate from the substrate *in-vivo* this will remove any benefits gained from its used to encourage early bone ingrowth into the substrate and may also invoke additional problems associated with the release of alumina grit from the Ti-6Al-4V / hydroxyapatite interface. Out of the two coating types, the detonation gun coatings seem to offer the best expected performance *in-vivo* based on the results of *in-vitro* fatigue testing. Although there was some evidence that delamination had begun after ten million cycles fatigue for these coatings (Figure 7-12), they had long outlasted the vacuum plasma sprayed coatings which had delaminated after just one million cycles (Figure 7-4). This, combined with the more rapid expected dissolution of the detonation gun coatings *in-vivo* discussed elsewhere (sections 8.1.3, 8.2.3, 8.3.3 and 8.5.3) suggest that the detonation gun coatings may be superior to the vacuum plasma sprayed alternatives.

8.8 Effect of Simulated Physiological Environment

8.8.1 Vacuum Plasma Sprayed Hydroxyapatite Coatings

Ageing the vacuum plasma sprayed coatings in buffered Ringer's solution prior to *in-vitro* ageing makes a considerable difference to their behaviour during the fatigue test. Some process apparently takes place during the unloaded ageing of the samples prior to fatigue testing that stabilises the coatings, minimising the effects of the cyclic loading.

Looking at the polished cross-sections through the vacuum plasma sprayed coatings which have been aged for various durations before fatigue testing (Figure 7-18 and Figure 7-19), it is extremely difficult to detect any change in the coating morphology when compared with the as-received coatings (Figure 4-5). Even after eight or twelve weeks in the ageing medium before fatigue testing, there is no evidence to suggest the morphology has been altered either by the action of the ageing medium or by the fatigue test. None of the coatings show significant evidence for a change in thickness (Table 7-16) or porosity (Table 7-18) as a result of the imposed testing regime and no modifications to the surface layers of the material was apparent. This lack of change was substantiated by the unchanging values for surface roughness (Table 7-20) measured by Talysurf analysis for all the coatings.

This examination of the aged and fatigued coatings produces observations which are very different to those reported for the vacuum plasma sprayed coatings which were fatigue tested in Ringer's solution with no prior ageing (section 8.7.1). In the latter case, substantial damage and even catastrophic delamination failure was seen for coatings fatigued for one million cycles (Figure 7-4) in the simulated physiological solutions. The coatings which were aged before fatigue testing show no signs of delamination failure or cross-sectional morphological alteration of any kind (Figure 7-18 and Figure 7-19).

Looking at the surfaces of the coatings which have been aged before fatigue testing (Figure 7-20 and Figure 7-21), the minimal effect of the testing regime can be seen. As was reported previously (section 8.2.1), exposure to the *in-vitro* environment brings about a progressive dissolution of the amorphous phase in the coating surface. This dissolution is reflected in the increase in crystallinity (Table 7-13) for the coatings which have been exposed to the *in-vitro* medium over the as-received coating. This effect, as reported above (section 8.2.1) is not progressive in nature. There is no increase in crystallinity with ageing time, purely a simple increase in the coatings which have been aged over those which have not.

However, unlike the coatings which were fatigue tested during initial exposure to the ageing medium, the coatings aged prior to fatigue testing show no evidence for an increase in the levels or size of surface micro-cracks (Figure 7-20 and Figure 7-21). The coatings show surface modification which corresponds to that which was observed for the unloaded aged material, i.e. preferential and progressive dissolution of the glassy amorphous regions on the coating surface (Figure 5-4 and Figure 5-5) and, after extended durations, the formation of a re-deposited crystalline hydroxyapatite phase (Figure 6-11). It would in fact be extremely difficult to distinguish between the morphologies of the coatings which have undergone fatigue testing after ageing in buffered Ringer's solution and those coatings which had only been exposed to the solution. Some process is occurring during ageing of the coatings which actively inhibits damage to the coatings by cyclic loading. This is in contrast to the findings of David *et al* [150] and Shen *et al* [151] discussed earlier (section 8.7.1) who reported delamination of vacuum plasma sprayed HA coatings implanted in sheep femora and stabilised for two months with no load bearing before the sheep were allowed full normal movement.

A clue to the behaviour of these coatings may be found in examination of the residual stress values for these aged and fatigued coatings (Table 7-22). It was found that extended ageing of vacuum plasma sprayed coatings induces a considerable reduction in the residual stress levels measured in the surface layers of the coatings. It was also reported previously that vacuum plasma sprayed coatings appear to store stress imposed by an external force. However these coatings which have been exposed to the *in-vitro* ageing medium before fatigue testing show no signs of this stress build up resulting from the application of cyclic loading. The residual stress levels measured for these coatings are all extremely low. Some process has occurred which has reduced the propensity of these coatings to either delaminate from their substrates or crack excessively at their surface. It must be the ageing process itself which has brought about sufficient relief of the stresses left in the coatings after manufacture to allow the material to transfer those stresses imposed during testing rather than store them. Storing the stress ultimately requires the coating to seek stress relief by, for example, surface cracking. The nature of this change in the coating has not been determined by the characterisation techniques employed here.

It was seen in the unloaded coatings which were aged in the simulated physiological solutions (section 8.2.1), that relief of inherent residual stress occurred after extended exposure to the medium. In the coatings which were both aged and fatigued however this relief process has occurred within one week of ageing. This suggests that a different process is occurring which combines the relief effects of the medium with some other process which is induced by the cyclic loading regime. Unfortunately evidence for the nature of this process was not provided by the range of morphological examinations conducted for this research.

The remarkable alteration in the properties of the vacuum plasma sprayed hydroxyapatite coatings as a result of ageing prior to fatigue testing is puzzling. Despite a possible link between changes in residual stress and the behaviour of the coatings under fatigue, no obvious explanation for this phenomenon presents itself. Whatever the cause of this effect however, it will have a considerable significance in terms of the expected behaviour of the coatings *in-vivo* and indeed on any recommendations for their use. If, by ageing the vacuum plasma sprayed hydroxyapatite coatings prior to fatigue loading them, an inhibiting of their propensity to delaminate is achieved, the usefulness of the coatings is once again established. Since a patient will be immobilised immediately after the insertion of an hydroxyapatite coated prosthesis this should allow time for the stabilisation of the coating described above to take place. Therefore, in actuality the vacuum plasma sprayed hydroxyapatite coatings should behave in an expected manner *in-vivo* and not demonstrate the delamination failure predicted by unaged fatigue experiments alone.

8.8.2 Detonation Gun Sprayed Hydroxyapatite Coatings

The marked effect the difference in manufacturing technique has on the morphological behaviour of hydroxyapatite coatings becomes clear when the effect of *in-vitro* ageing prior to fatigue testing on the detonation gun coatings is examined. Whilst the vacuum plasma sprayed coatings became stabilised by the process of ageing prior to

fatigue testing the detonation gun coatings are extremely adversely affected by the combined effects of ageing and fatigue.

Looking at the polished cross-sections through the detonation gun coatings, although initially the coatings seemed to be withstanding effects of the testing regime (Figure 7-23), the effects of degradation soon became apparent. After exposure to the *in-vitro* ageing medium for two weeks prior to fatigue testing the final coating showed evidence for a high porosity morphologically modified surface layer with an approximate depth of 5 μm. The depth of this layer increases with subsequent samples which have been aged for longer durations before fatigue testing. The coatings aged for four weeks had a 5 - 10 μm deep modified surface layer while the coatings aged for eight weeks had layers which extended upto 20 μm into the bulk of the coating. However, the coating which was exposed to the ageing medium for fifteen weeks before fatigue testing showed no evidence for this modified layer (Figure 7-24).

The surfaces of the coatings viewed using scanning electron microscopy showed considerable evidence for the attack of the *in-vitro* medium (Figure 7-25 and Figure 7-26). The coatings showed progressive levels of etching of the amorphous phase with increased ageing time. This corresponds to preferential dissolution of the meta-stable amorphous phase discussed above (section 8.2.1). In addition to this etching, crystalline protuberances began to form on the coating surfaces even after just one weeks ageing before fatigue testing (Figure 7-25). These growths spread out over the surface of the coating in the samples aged for longer durations, emanating from the regions of the surface which appeared to have been covered with the glassy phase originally and covering the surface entirely by the time the coatings had been aged for eight weeks. The coating aged for twelve weeks before fatigue testing showed a surface morphology which more closely resembled the initial stages of surface damage (Figure 7-26). This is again taken as evidence for the cyclic nature of the dissolution process as described previously (section 8.2.2).

There was found to be no dramatic increase in the size or number of microcracks seen on the surfaces of the detonation gun coatings after exposure to the testing regime (Figure 7-25 and Figure 7-26). In fact, although microcracks were still seen on the surfaces of the coatings aged for long durations prior to fatigue testing, these cracks had an etched appearance suggesting that they had been formed before the coatings were held for extended periods in the *in-vitro* ageing solutions. This suggests that, unlike the coatings which had not been aged before fatigue testing in Ringer's solution, these coatings showed no propensity for prolific surface cracking. The coating surfaces showed the dramatic effects of exposure to the ageing medium but did not demonstrate the characteristic surface cracking associated with the unaged fatigue test.

As was suggested for the vacuum plasma sprayed coatings tested in this way (section 8.8.1), the lack of propensity for these coatings to develop extensive networks of surface micro-cracks cannot simply be explained in terms of relief of residual stresses by the process of surface modification. Although the residual stress levels measured for these detonation gun coatings were seen to decrease gradually with increasing exposure time in the *in-vitro* ageing medium (Table 7-33), the levels had not dropped below those measured for the detonation gun coatings fatigued in solution with no prior ageing (Table 7-12). These latter coatings showed considerable surface cracking damage at the residual stress levels recorded for the aged then fatigued coatings which demonstrated no increased propensity to crack. As was discussed for the vacuum plasma sprayed coatings (section 8.8.1), the detonation gun coatings seem to have been stabilised by the action of *in-vitro* ageing prior to fatigue testing and again, the mechanism for this stabilisation process has not been revealed by the morphological characterisations carried out in this research.

As expected, the porosity levels (Table 7-29) measured for the coatings which had undergone ageing prior to dynamic loading appeared to increase with increased exposure to the testing regime. Values fluctuated in a manner which suggested the growth and loss of the highly porous modified surface layer seen in the polished cross-sections through the coatings (Figure 7-23 and Figure 7-24). The coatings were also seen to show progressive thinning with increased exposure to the *in-vitro* environment

(Table 7-27), an indication that the spalling off of damaged surface layers from the coatings was taking place. The surface roughness values (Table 7-31) also fluctuated in accordance with the formation of the crystalline agglomerates and their spalling off from the surface causing the removal of this deposited phase. The roughness values for the samples aged for one to eight weeks, were higher than those for the as-received coating, the values then dropped to around the as-received coating value for the sample aged for twelve weeks. This drop in surface roughness corresponds to the exposure of a fresh surface layer following the spalling off of the irregular surface covered with crystalline nodules.

As with the vacuum plasma sprayed hydroxyapatite coatings (section 8.8.1), the act of ageing the detonation gun hydroxyapatite coatings prior to fatigue testing seems to cause some kind of morphological stabilisation, although the mechanism for this process is not understood. Again there was little evidence (Figure 7-25 and Figure 7-26) with the aged and fatigued coatings for the surface microcracking observed with coatings which were not aged prior to fatigue testing (Figure 7-15 and Figure 7-16). As was again the case for the vacuum plasma sprayed coatings, there was no evidence for delamination failure at all in the aged and fatigued detonation gun coatings. The more rapid rate of dissolution of detonation gun hydroxyapatite coatings over vacuum plasma sprayed coatings, linked to the differences in initial morphology and described elsewhere (section 8.1.2) was once more seen during this testing. Modification of the coating surface (Figure 7-23 and Figure 7-24) leading to loss of material and thinning of the coatings (Table 7-27) is again reported. As discussed above (section 8.7.3) if both coatings remain coherent *in-vivo* and shown no propensity for delamination, then the coating which encourages the most rapid formation of new bone on its surface will be considered superior. If the coatings examined here behave in the same manner in the body as they have done *in-vitro*, then the detonation gun coatings would be considered to be the more effective coating type.

8.8.3 Summary

Exposure to the *in-vitro* solution prior to fatigue testing is the most thorough simulation used in this research of the processes which would actually occur in practice to a coating implanted in the body. This section of the testing reveals the benefits obtained by allowing the coatings to stabilise *in-vitro* prior to application of a force. This final testing group once again demonstrates the considerable differences in behaviour of the coatings manufactured by different techniques.

Both coating types appeared to benefit from ageing before being exposed to dynamic loading. The vacuum plasma sprayed coatings appeared to withstand the rigours of this test extremely well. The catastrophic delaminations (Figure 7-4) observed in the coatings fatigued in Ringer's solution but not aged prior to this fatigue (section 8.7.1) appeared to have been eliminated by the ageing process. Although the coatings showed signs of the characteristic damage caused to the surface layers of the material as a result of exposure to the *in-vitro* solution (Figure 7-20 and Figure 7-21), the dramatic cracking of the surface observed in the unaged fatigued coatings was inhibited. It was very difficult to differentiate between coatings which had been both aged and fatigued and those which had simply undergone ageing in the *in-vitro* medium.

Although, on the whole, the detonation gun coatings did not seem to withstand the simulated physiological environment as well as the vacuum plasma sprayed coatings, the advantages of ageing these samples before fatigue testing were again apparent. As observed in the vacuum plasma sprayed coatings, there was no evidence for the formation of fatigue cracks in the surface layers of these coatings (Figure 7-25 and Figure 7-26) although surface modification resulting from exposure the ageing medium continued. Provided the coatings remain attached to the substrates, dissolution of the surface layers should not be considered to be a negative effect. As discussed (section 8.8.2), it is suggested that, since it is dissolution of amorphous material from the coating surface which stimulates the formation of new bone, a coating which remains attached to the substrate yet dissolves, should perform well *in-vivo*. If more rapid dissolution creates

more rapid proliferation of new bone, all other things being equal, the more amorphous detonation gun coatings may be expected to perform in a superior manner in the patient.

The mechanism which is causing this stabilisation of both types of hydroxyapatite coatings and minimising the effects of the fatigue test has not been determined here. However it is clear that the process is not solely an effect which occurs during exposure to the *in-vitro* solution alone, since morphological changes occurring in the aged and fatigued samples (section 8.8) are different to those found in samples which have only exposed to *in-vitro* solutions.

9. Conclusions

The two thermal spray techniques studied in this work produce different structural morphologies in the final coatings. The detonation gun spraying process is a higher temperature, higher velocity technique which is thought to impose a higher degree of melting on the ceramic feedstock. It has been suggested that optimum adhesion between powder particles and substrate is attained when the spray powder is completely molten [101]. Therefore, the use of the detonation gun should produce a coating which is more amorphous in nature than the vacuum plasma sprayed coatings and is more strongly adhered to its substrate. It is interesting to note that this assumed higher adhesion has been taken into account in the manufacture of the two coating types. The detonation gun coatings show no evidence for an interfacial bond layer which is believed to increase the mechanical strength of the join between the hydroxyapatite and Ti-6Al-4V substrate by a combination of increased mechanical interlocking and chemical bonding [110, 111]. This bond layer is seen in the vacuum plasma sprayed system but has been omitted in the case of the detonation gun coatings, the manufacturers obviously believing that the enhanced adhesion of the powder particles during spraying renders its use unnecessary.

As expected, there is a considerable difference in the crystallinity of the two coating types, the detonation gun process, as suggested, producing a coating which has a higher proportion of the amorphous phase. This is due to the higher degree of melting of the spray powder which leaves a lower percentage of residual crystalline material in the coating surface. This higher temperature process has also induced a degree of phase change in the detonation gun coatings with some evidence for the appearance of beta tri-calcium phosphate being observed by x-ray diffraction. The molten particles flow to some degree on impaction of the surface (giving rise to a coating with a lower porosity) then freeze rapidly to form an amorphous glass. The two phase morphology of thermally sprayed hydroxyapatite coatings consisting of an amorphous glass and agglomerates of

residual crystallites from the spray powder can clearly be seen in examination of the coating surfaces by scanning electron microscopy.

It has been widely reported in the literature [46, 48] that amorphous hydroxyapatite dissolves more rapidly *in-vitro* than crystalline hydroxyapatite. It has also been suggested that the early bone formation properties ascribed to hydroxyapatite results from this dissolution behaviour [2, 15, 16, 17, 18]. It seems that hydroxyapatite is dissolved in the body and re-precipitated in the form of new natural bone tissue. This process can therefore be assumed to be most rapid when amorphous hydroxyapatite materials are used since these dissolve more rapidly. For this reason, the more highly amorphous detonation gun coatings are being developed since their higher expected dissolution rate *in-vivo* is expected to induce superior early bone growth properties than those found for other coating types [116]. However, the dissolution rate of hydroxyapatite coatings should be carefully controlled since, if the coating should dissolve away completely, residual alumina grit seen at the hydroxyapatite / Ti-6Al-4V interface in both types of coating may be released into the surrounding tissues causing extreme irritation.

Both types of thermally sprayed coatings have extremely irregular cross-sectional thicknesses. This makes statistical analysis of the rate of dissolution of the coatings difficult since the standard deviations from thickness data preclude trend observation. For this reason coating behaviour must be characterised using other techniques, principally microscopy.

Residual stress levels were monitored in the coatings during all stages of experimentation by x-ray diffraction. It was found initially that the vacuum plasma sprayed coatings had lower levels of residual stress in the as-received condition than the detonation gun coatings. The higher levels of stress in the detonation gun coatings was assumed to be another factor which would cause a more rapid dissolution of the material *in-vitro*.

The dissolution behaviour of the coatings was studied by exposing them to an *in-vitro* ageing media consisting of Ringer's solution buffered to pH 7.2 or pH 4.5. As was expected, the lower pH medium produced a more dramatic dissolution than the pH 7.2 solution. As suggested above, morphological examination of the coatings aged in the solutions produced results which were in agreement with those of previous authors in the literature [15, 16, 34]. Preferential dissolution of the glassy amorphous material from the coating surfaces was reported, this effect being more pronounced in the case of the highly amorphous detonation gun coatings. Re-precipitation of crystalline material, assumed to be crystalline hydroxyapatite was also seen in the case of coatings aged at the lower pH, in agreement with observations from the literature [4, 5, 6, 7, 43]. It has been suggested that it is this re-precipitated material which is responsible for the bone bonding properties of hydroxyapatite [2, 3].

A cyclic nature was ascribed to the dissolution behaviour of hydroxyapatite coatings and it was suggested that the amorphous materials in the coating surface acts as a binder phase for the agglomerated crystalline phase. Dissolution of this amorphous binder therefore disrupts the cohesion of the surface layer of the coating, leading to its loss. The loss of the surface layer then exposes a new layer to the ageing medium and the process is repeated. In cases where dissolution is followed by re-precipitation (such as at low pH), the same process occurs with the addition of the re-precipitation stage prior to surface layer loss.

The difference in composition of the detonation gun coatings over the vacuum plasma sprayed coatings was described above. It is known that different calcium phosphate phases, like different morphologies of hydroxyapatite, have different solubilities *in-vitro*. It has been reported [48] that beta tri-calcium phosphate has a higher solubility than amorphous hydroxyaptate and this was also displayed here. A loss of the beta tri-calcium phosphate peaks from the x-ray diffraction data for the aged detonation gun coatings was reported. Therefore, in the case of these materials, not only is amorphous hydroxyapatite being dissolved in preference to crystalline hydroxyapatite but

additionally, beta tri-calcium phosphate is being lost in preference to the amorphous phase.

Some authors have found that the application of a load to hydroxyapatite coatings increases the rate of surface dissolution *in-vitro* [80]. This effect was not reported here. In fact the application of a static load to the coatings during *in-vitro* ageing produced virtually the same response in the materials to ageing with no applied load. There was some evidence that, apart from the effects of exposure to the ageing medium, static loading produced and increase in the number and size of surface micro-cracks and an increase in the levels of cross-sectional porosity. Both these effects were attributed to stress relief processes evoked as a result of the increase in applied stress experienced by the coatings under this environment.

Having been able to isolate the effects of an applied static load from the effects of exposure to the *in-vitro* ageing medium in this way progressive testing was undertaken which involved application of a dynamic load to the coatings. Again in order to distinguish between the effects of fatigue alone over the effect of exposure to the ageing medium, coatings were fatigued in air as well as in Ringer's solution.

Fatigue testing of the coatings in air produced little change to their morphology. As was found to be the case with the application of a static load, fatigue testing in air alone produce only an increase in surface micro-cracking and bulk porosity in both the detonation and vacuum plasma sprayed coatings. However, when this process was combined with exposure to the *in-vitro* environment dramatic damage was seen to occur to both coating types. After just one million cycles of fatigue in Ringer's solution, the vacuum plasma sprayed hydroxyapatite coatings had completely delaminated from their substrates. Had this effect occurred *in-vivo* it would have had a considerable influence on the performance of the prosthetic system. Not only would the early bone bonding properties to the substrate have been lost completely along with loss of the coating, but removal of the hydroxyapatite may have allowed release of the alumina grit seen at the hydroxyapatite / Ti-6Al-4V interlayer. This alumina grit would cause extreme irritation

to the surrounding tissues and possibly gross inflammation and implant loosening. Such an effect would necessitate revision surgery. Although the detonation gun coating was still present after fatigue testing for ten million cycles, it too was beginning to show signs of delamination with the same implications to its performance *in-vivo*. These results seemed to preclude the use of these coatings in orthopaedic surgery. However, another *in-vitro* fatigue test of vacuum plasma sprayed hydroxyapatite coatings found no delamination of coatings during testing upto five million cycles [152]. Here Ashroff *et al* performed biaxial fatigue testing on cylindrical hydroxyapatite coated bars with a 50 μm thick coating. The authors reported no mechanical failure of the coatings and no change in mechanical strength of the coatings following fatigue testing.

The necessity of attempting to make the most extensive and realistic simulation of the in-service situation the coatings would experience was clearly demonstrated here. Had research been halted after the results of *in-vitro* fatigue had been obtained, the usefulness of applying hydroxyapatite coatings to implants would have been questioned. However, a further modification to the testing regime was developed thought to be a more accurate simulation of the service environment the coatings would experience.

The process of ageing before fatigue testing was considered the most comprehensive simulation of the service conditions an hydroxyapatite coating would experience if used in total hip replacement surgery. Immediately following insertion of the implant into the patient, he or she is immobilised for a short duration before being encouraged to use the new prosthesis. This period of stabilisation was simulated by ageing the coatings *in-vitro* prior to fatigue testing. It seems that this stabilisation period is in fact crucial to the performance of these coatings under a simulated physiological environment. Both coating types benefited considerably from this unloaded ageing prior to testing. Characterisation of the materials following this final testing regime producing surprising results. It seems that, provided the coatings experience this period of unloaded ageing before they are subjected to fatigue, the effects of this dynamic loading are eradicated. Some process occurs during this ageing process which inhibits the propensity of both coating types to delaminate. In fact it was extremely difficult to distinguish

between coatings which had only been aged before characterisation and those which had been both aged and fatigued. As described above Ashroff *et al* [152] performed *in-vitro* fatigue testing on vacuum plasma sprayed hydroxyapatite coated cylindrical components. In agreement with results presented here, these authors observed that the rate of coating degradation appears to be less in aged and fatigued coatings than in those which are aged with no applied load. Again, the authors could find no apparent reason for this behaviour. What the process causing this phenomenon in actuality is, could not be determined by the experimental techniques employed here but it is clear that this process restores the ability of both the vacuum plasma sprayed and the detonation gun sprayed coatings to perform their function as materials for use in total hip replacement surgery.

In summary therefore, the following may be concluded from the research carried out here. Full characterisation of a novel coating type has been carried out supporting the suggestion that detonation gun sprayed hydroxyapatite coatings may be useful materials for use in total hip replacement applications. In addition to this, unique research into the *in-vitro* fatigue properties of both this new type of thermally sprayed coating and the more familiar vacuum plasma sprayed material was undertaken. The ability of both coating morphologies to withstand the rigors of fatigue testing in a simulated physiological environment was documented and the irrefutable necessity to stabilise the materials before imposing dynamic loading highlighted. The processes occurring during this *in-vitro* fatigue could be attributed to either an effect of loading or an effect of exposure to the ageing medium since each had been studied in isolation. Both the vacuum plasma sprayed and the detonation gun sprayed hydroxyapatite coatings ultimately performed well under the simulated physiological testing. It was suggested that the morphology of the latter, in particular its higher dissolution rate *in-vitro* would render it a superior choice for application in hip arthroplasty. Alternatively, altering the morphology of the vacuum plasma sprayed coatings to reduce their crystallinity, e.g. by altering the spray parameters, could improve their expected early post operative effectiveness.

Finally, the necessity of attempting to create a full simulation of the actual regime a material would be expected to experience was demonstrated. Had testing been limited to an *in-vitro* fatigue test, the prognosis for the use of hydroxyapatite coatings in total

hip replacement surgery would have been poor. The advanced simulation attempted here reversed this finding entirely. However, it must be accepted that even this simulation was not exhaustive. Other factors such as the influence of proteins or bacteria on coating dissolution rate [64] should also be taken into consideration before recommendations for the use of these coatings are made.

10. Further Work

- Further microscopical analysis of the surface of hydroxyapatite coatings is recommended both in the as-received state and following *in-vitro* testing. Suggested techniques for this work may include transmission electron microscopy, auger microscopy and atomic force microscopy. Understanding the processes underway at the surface of hydroxyapatite coatings during dissolution would be extremely helpful in the design of these materials.
- Ideally, some kind of in-situ study of the dissolution behaviour as it actually occurs would be desirable in improving understanding of this phenomenon. Techniques such as *in-situ* atomic force microscopy or time-of-flight mass spectroscopy may enable such an achievement and could be investigated.
- The nature of the interface between the hydroxyapatite coating and the metallic substrate should be more fully characterised by higher resolution microscopy such as transmission electron microscopy.
- This understanding of the nature of join between ceramic and metal may be improved by reliable mechanical investigation of the adhesion strength of the coating to the substrate. The area of adhesion testing of coatings is fraught with difficulty but if a comprehensive technique were developed, the mechanical test data for hydroxyapatite coatings both before and after *in-vitro* testing would be invaluable.
- It was discussed that coating thickness will have an effect on the dissolution rate of hydroxyapatite coatings, in part due to the change in residual stress with thickness. Investigation into the dissolution behaviour of hydroxyapatite coatings with varying thicknesses may end the debate in the literature regarding the ideal coating thickness.
- As above, comprehensive consideration of the rate of dissolution of hydroxyapatite coatings with changing crystallinities would enhance the knowledge of the ideal nature of hydroxyapatite coatings for biomedical applications. During this research, coatings with different crystallinities were manufactured using different process. Careful control of the spray parameters of either the vacuum plasma spraying or the

detonation gun spraying techniques should allow manufacture of a range of coatings with different crystallinities for further analysis.

- It was suggested earlier that spectroscopical analysis of hydroxyapatite coatings would provide a useful further characterisation methodology for monitoring the change in phase of coatings with exposure to the *in-vitro* environment. It is know that different calcium phosphate phases have different solubilities and that this may affect the bone forming properties of the coatings. A reliable method of characterising the quantity of such phases in the surface layers of coatings would therefore allow more accurate prediction of their behaviour *in-vivo* and should be developed.

11. Appendix One - X-Ray Diffractometer Calibration

Calibration carried out April 1997.

	Silicon standard, 26629			*ICDD 27 - 1402 Silicon, synthetic*		
h k l	*2-theta (degrees)*	*d-spacing (Angstroms)*	*Relative Intensity*	*2-theta (degrees)*	*d-spacing (Angstroms)*	*Relative Intensity*
1 1 0	*25.615 (β)*	*3.140*	*1*			
	28.440	3.136	100	28.443	3.1355	100
2 2 0	*42.455 (β)*	*1.923*	*1*			
	47.295	1.920	61	47.304	1.9201	55
3 1 1	*50.320 (β)*	*1.637*	*1*			
	56.105	1.638	45	56.122	1.6375	30
4 0 0	69.135	1.3577	10	69.132	1.3577	6
	69.345 (α_2)	1.3574	5			
3 3 1	76.375	1.2460	13	73.380	1.2459	11
	76.610 (α_2)	1.2458	7			
4 2 2	88.050	1.1084	29	88.029	1.0086	12
	88.330 (α_2)	1.1083	15			
5 1 1	94.265	1.0451	10	94.951	1.0452	6
	95.265 (α_2)	1.0451	5			
4 4 0	106.720	0.9300	6	106.719	0.9600	3
	107.095 (α_2)	0.9300	3			
5 3 1	114.095	0.9180	11	114.092	0.9180	7
	114.535 (α_2)	0.9180	5			
6 2 0	127.530	0.8588	8	127.547	0.8587	8
	128.100 (α_2)	0.8588	4			
5 3 3	136.870	0.8283	4	136.897	0.8282	3
	137.600 (α_2)	0.8282	2			

Table 11-1 :- X-ray diffraction results for silicon test sample versus documented silicon standard

X-Ray intensities, NIST calibration					
Reflection	***Standard reference material***		***26630 (NIST)***		
(h k l)	***2 - theta (degrees)***	***Relative area***	***ICDD 43 - 1484***	***Measured area***	***Relative area***
0 1 2	25.6	32.3	25.577_{72}	3201	26.0
1 0 4	35.1	100	35.151_{98}	12311	100
1 1 3	43.4	51.1	43.341_{100}	6409	52.1
0 2 4	52.6	26.7	52.549_{48}	3554	28.9
1 1 6	57.5	92.1	57.500_{96}	12282	99.8
3 0 0	68.2	19.1	68.204_{57}	2550	20.7
1 0 10 & 1 1 9	*Double*	*55.6*		*7208*	*58.5*
0 2 10	89.0	11.8	89.000_{8}	1528	12.4
2 2 6	95.2	10.1	95.239_{19}	1377	11.2
2 1 10	101.1	16.1	101.067_{14}	2205	17.9
3 2 4 & 0 1 14	*Double*	*20.9*		*2892*	*23.5*
1 3 0	127.7	15.58	-	2208	17.9
1 4 6	136.2	15.5	-	2098	17.0
4 0 10		11.3	-	-	-

Table 11-2 :- X-ray diffraction results for calibration with standard reference material

12. Appendix Two - Residual Stress Technique

In order to validate the use of the residual stress technique in monitoring changes in the behaviour of thermally sprayed coatings under different environments it was necessary to demonstrate that the process could detect changes in stress in the coatings. To show this, the residual stress levels in a detonation gun coating were measured by x-ray diffraction before and after various strains were imposed that material. The table below shows the determined residual stresses measured in the detonation gun coating strained in three point bending to 0, 2, 4 and 10 %.

strain (%)	*d(c)*	*strain (c)*	*E (Pa)*	*residual stress, c (GPa)*
0	1.7178	0	5.5^{9}	0
2	1.7182	0.000233	5.5^{9}	1.2707
4	1.7178	0	5.5^{9}	0
10	1.7174	-0.000230	5.5^{9}	-1.2807

Table 12-1 :- Residual stress data for DGUN HA coating following the imposition of various strains

Although a direct correlation between imposed strain and measured residual stress is not apparent, the data clearly shows a change of stress with changing strain. Therefore it can be assumed that this technique can be used to monitor changes in the residual stress levels of coatings following testing.

13. Experimental Errors

When considering the validity of results presented in this text, certain points should be observed regarding the accuracy of data, in particular with respect to certain test methodologies.

Crystallinity Measurement

The determination of crystallinity by this technique is a subjective. Since the technique is manually intensive and requires a subjective appraisal of x-ray trace shape, its accuracy should not be considered beyond the first decimal place. Other considerations such as the degree of background noise in x-ray traces and the scattering effects of very small crystallites will also contribute to trace distortion. However, despite such problems, it can be seen in this work that standard deviations in crystallinity results are extremely small, hence the validity of direct comparison of data between testing groups is proven. In the body of the text, crystallinity values are presented to three decimal places of accuracy for the purpose of statistical calculations.

Residual Stress Measurements

Measurement of lattice distortion via an x-ray diffraction technique will again be prone to experimental error. Peak positioning will be affected by scattering from amorphous material in the sample, small crystallites and interference from other plane peaks. Sample positioning in the diffractometer, i.e. sample height and angle relative to the incident x-ray beam, will also cause variations in lattice calculations. For these reasons, residual stress results should only be considered to two significant figures. As above, for the purpose of statistical calculations, figures presented in the body of the text are given to a higher assumed accuracy than would normally be considered for such data.

Porosity Measurement

As was the case for crystallinity measurement, the determination of cross-sectional porosity using an image analysis technique should be considered to be operator dependent. The experimenter should be able to identify areas of porosity within the coating reliably and consistently. This may be facilitated by examination of cross-sections by SEM analysis prior to optical microscopy. Since a single operator performed all porosity measurements quoted in this text, and an average of ten measurements for each tested sample was determined, comparison of results between sample test groups can be considered reliable. As above, several decimal places of accuracy are presented for the purpose of statistical calculations, but the real porosity values should not be considered as accurate beyond the first decimal place.

Surface Profilometry

The size of the spherical sapphire tip stylus used with the profilometer does not allow the measurement of narrow or over-hanging features, thus the main morphology of the surface is recorded rather than very fine detail. However the measurable range of the instrument used here was considered to have a resolution of 500 nm. Therefore, although the true shape of the sample surface cannot be assumed to have been measured by profilometry, the accuracy of surface roughness values presented here should be considered to be valid certainly upto the third decimal place. As above, figures quoted in the body of the text are presented to higher supposed accuracy for the purpose of statistical calculations.

14. Appendix Three - References

[1] Kokubo, T., Ito, S., Sakka, S., Yamamuro, T., "Mechanical properties of a new type of apatite-containing glass ceramic for prosthetic application", Journal of Materials Science, 1985, Vol. 20, p. 2001

[2] Osborne, J.F., Newesley, H., "Dynamic aspects of the implant - bone interface" Dental Implants, Ed. Heimke, G., Carl Hansen Verlag, Muchen, 1980

[3] Orly, I., Gregoire, M., Menaneau, J., Heughebaert, M., Kerebel, B., "Chemical changes in hydroxyapatite biomaterial under *in-vivo* and *in-vitro* biological conditions", Calcified Tissue International, 1989, 45, p. 20

[4] Ducheyne, P., "Bioceramics: Material characteristics versus *in-vivo* behaviour", Journal of Biomedical Materials Research, 1987, 21, (A2), p. 219

[5] Fujiu, T., Ogino, M., "Difference of bone bonding behaviour among surface active glasses and sintered apatite", Journal of Biomedical Materials Research, 1984, 18, p. 845

[6] Daculsi, G., LeGeros, R.Z., Nevy, E., Lynch, K., Kerebel, B., "Transformation of biphasic calcium phosphate ceramics *in-vivo*: Ultrastructural and physico-chemical characterisation", Journal of Biomedical Materials Research, 1989, 23, p. 883

[7] Tracy, B.M., Doremus, R.H., "Direct electron microscopy studies of the bone - hydroxyapatite interface", Journal of Biomedical Materials Research, 1984, 18, p. 719

[8] Gross, K.A., Berndt, C.C., "*In-vitro* testing of plasma-sprayed hydroxyapatite coatings", Journal of Materials Science: Materials in Medicine, 1994, 5, p. 219

[9] Gustavson, L.J., "Evaluation of materials for porous coated implants", Total Hip Arthroplasty - A New Approach, Ed. D.S. Hungerford, 1984, University Park Press

[10] Bourne, R.B., Roraceck, C.H., Burkart, B.C., Kirk, P.G., "Ingrowth surfaces - plasma spray coating to titanium alloy hip replacements", Clinical Orthopaedics and Related Research, 1994, 298, p. 37

[11] Ducheyne, P., Radin, S., Heughebaert, M., Heughebaert, J.C., "Calcium phosphate ceramic coatings on porous titanium : Effect of structure and composition on electrophoretic deposition, vacuum sintering and *in-vitro* dissolution", Biomaterials, 1990, 11, p. 244

[12] Thorpe, R.J., Thorpe, M.L., "High pressure HVOF - An update", Proceedings of the 1993 National Thermal Spray Conference, Anaheim, CA, 1993, June, p. 199

[13] English, T.A., Kilvington, M., "*In-vivo* records of hip loads using a femoral implant with telemetric output (a preliminary report)", Journal of Biomedical Engineering, 1979, Vol. 1, No. 2, p. 111

[14] Smith, R., Oliver, C., Williams, D.F., "The enzymatic degradation of polymers *in-vitro*", Journal of Biomedical Materials Research, 1987, 21, 8, p. 991

[15] de Bruijn, J.D., Klein, C.P.A.T., de Groot, K., van Blitterswijk, C.A., "The ultrastructure of the bone - hydroxyapatite interface *in-vitro*", Journal of Biomedical Materials Research, 1992, Vol. 26, p. 1365

[16] Bagambisa, F.B., Joos, U., Schilli, W., "Mechanisms and structure of the bond between bone and hydroxyapatite ceramics", Journal of Biomedical Materials Research, 1993, Vol. 27, p. 1047

[17] Hench, L.L., Paschall, H.A., "Direct chemical bond of bioactive glass-ceramic materials to bone and muscles", Journal of Biomedical Materials Research Symposia, 1973, Vol. 4, p. 25

[18] Ban, S., Maruno, S., Iwata, H., Itoh, H., "Calcium phosphate precipitation on the surface of HA-G-Ti composite under physiologic conditions", Journal of Biomedical Materials Research, 1994, Vol. 28, p. 65

[19] Galletti, P.K., Boretos, J.W., "Report on the Consensus Development Conference on Clinical Applications of Biomaterials 1-3 November 1983", Journal of Biomedical Materials Research, 1983, Vol. 17, p. 539

[20] Greenfield, E.J., "Mounting for artificial teeth", Serial No. 478360, 1909, Washington D.C., United States Patent Office, Dec. 14,

[21] Williams, D.F., "Review tissue-biomaterial interactions", Journal of Materials Science, 1987, 22, p. 3421

[22] Heimke, G., Griss, P., Jentschura, G., Werner, E., "Bioinert and bioactive ceramics in orthopaedic surgery", Mechanical Properties of Biomaterials, Eds. G.W. Hastings and D.F. Williams, John Wiley and Sons Ltd., 1980

[23] Scales, J.T., "Arthroplasty of the hip using foreign materials: A history", Proceedings of the Institute of Mechanical Engineers, 1966, 181, 37, p. 63

[24] Charnley, J., "The long-term results of low-friction arthroplasty of the hip performed ASA primary intervention", Journal of Bone and Joint Surgery, 1972, 54 B, p. 61

[25] Bonfield, W., "Materials for the replacement of osteoarthritic hip joints", Metals and Materials, 1987, December, p. 712

[26] Feith, R., "Side-effects of acrylic cement implanted into bone", Acta Orthopaedica Scandinavica, 1975, 56, p. 161

[27] Boss, J.H., Sharjrawi, I., Mendes, D.G., "The nature of the bone - implant interface", Medical Progress Through Technology, 1994, 20, p. 119

[28] Chappard, D., Alexandre, C., Montheard, J.P., "Polymerisation of methacrylates - bubble-hole artefact reconsidered with bone morphology", Journal of Histotechnology, 1992, 15, 1, p. 51

[29] Hirschhorn, J.S., Reynolds, J.T., "Powder metallurgy fabrication of cobalt alloy surgical implant materials", Research into Dental and Medical Materials, Ed. E. Korostoff, 1979, New York Plenum Press, p. 137

[30] Spector, M., "Historical review of porous coated implants", Journal of Arthroplasty, 1991, Vol. 6, p. 51

[31] Klatwitter, J.J., Hulbert, S.F., "Application of porous ceramics for the attachment of load bearing internal orthopaedic applications", Journal of Biomedical Materials Research, 1971, Vol. 2, p. 161

[32] Pillar, R.M., Weatherly, G.C., "Critical reviews in biocompatibility", CRC Press, 1985, Boca Raton, Fl,

[33] Callaghan, J.J., "The clinical results and basic science of total hip arthroplasty with porous-coated prostheses", Journal of Bone and Joint Surgery, 1993, Vol. 73-A, No. 2, p. 299

[34] Hench, L.L., "Cementless fixation", Biomaterials and Clinical Applications, Eds. A. Pizzoferrato, P.G. Marchetti, A. Ravaglioli and A.J.C. Lee, 1987, Elsevier Science Publishers B.V., Amsterdam

[35] Nordin, M., Frankel, V.H., "Biomechanics of the hip", from Biomechanics of Tissues and Structures of the Musculoskeletal System, pub. Lea and Febiger, Philadelphia, London, 1989

[36] Fallon, M.D., "Alterations in the pH of osteoclast resorbing fluid reflects changes in bone degradative activity", Calcified Tissue International, 1984, 36, p. 458

[37] Kaplan, S.S., "Biomaterial-host interactions: consequences, determined by implant retrieval analysis", Medical Progress Through Technology, 1994, 20, p. 209

[38] Goldring, S.R., Jasty, M., Roelke, M.S., Bringhurst, F.R., Jarros, W.H., "Formation of a synovial like membrane at the bone-cement interface: Its role in bone resorption and implant loosening after total hip replacement", Journal of Arthritis and Rheumatism, 1986, 29, p. 836

[39] Driskell, T.D., "Significance of resorbable bioceramics in the repair of bone defects", 1973, Proceedings of the Annual Conference of Biomedical Engineering, 15, p.199

[40] Klein, C.P.A.T., de Blieck-Hogervorst, J.M.A., Wolke, J.G.C., de Groot, K., "Studies of the solubility of different calcium phosphate ceramic particles *in-vitro*", Biomaterials, 1990, 11, p. 509

[41] Kohri, M., Miki, K., Waite, D.E., Nakajima, H., Okabe, T., "*In-vitro* stability of bi-phasic calcium phosphate ceramics", Biomaterials, 1993, 14, 3, p. 225

[42] Knowles, J.C., Gross, K., Berndt, C.C., Bonfield, W., "Structural changes of thermally sprayed hydroxyapatite investigated by Rietveld analysis", Biomaterials, 1996, 17, p. 639

[43] Ducheyne, P., Beight, J., Cuckler, J., Evans, B., Radin , S., "Effect of calcium phosphate coating characteristics on early postoperative bone tissue ingrowth", Biomaterials, 1990, 11, p. 531

[44] Hench, L.L., "Stability of ceramics in the physiological environment", Fundamental Aspects of Biocompatibility, CRC Press, Boca Raton, 1981, 1, p. 67

[45] Kitsugi, T., Yamauro, T., "Bone bonding behaviour of apatite containing glass-ceramics", Journal of Biomedical Materials Research, 1986, 20, p. 1295

[46] Radin, S.R., Ducheyne, P., King, L., "The effect of phase composition on the *in-vitro* dissolution of calcium phosphate ceramics", Abstracts of the Third International Symposium on Ceramics in Medicine, NE., Rose-Hulman Institute of Technology, Terre Haute, IN., 1990, p. 263

[47] Best, S., Sim, B., Kayser, M., Downes, S., "The dependence of osteoblastic response on variations in the chemical composition and physical properties of hydroxyapatite", Journal of Materials Science: Materials in Medicine, 1997, 8, p. 97

[48] Daculsi, G., le Geros, R.Z., Nary, E., Lynch, K., Kerebel, B., "Transformation of biphasic calcium phosphate ceramics *in-vivo* - ultrastructure and physico-chemical characterisation", Journal of Biomedical Materials Research, 1989, 23, p. 883

[49] Cook, S.D., Kay, J.F., Thomas, K.A., Jarcho, M., "Interface mechanics and histology of titanium and hydroxylapatite coated titanium for dental implant applications", International Journal of Oral Maxillofacial Implants, 1987, 2, 1, p. 15

[50] Cook, S.D., Thomas, K.A., Dalton, J.E., Volkman, T.K., Whitecloud III, T.S., Kay, J.F., "Hydroxylapatite coating of porous implants improved bone ingrowth and interface attachment strength", Journal of Biomedical Materials Research, 1992, 26, p. 989

[51] Oonishi, H., Kushitani, S., Aono, M., Ukon, Y., Yamamoto, M., Ishimaru, H., Tsuji, E., "The effect of hydroxyapatite coating on bone growth into porous titanium alloy implants", Journal of Bone and Joint Surgery, 1989, 71B, p. 213

[52] Hayashi, K., Uenoyama, K., Mashima, T., Sugioka, Y., "Remodelling of bone around hydroxyapatite and titanium in experimental osteoporosis", Biomaterials, 1994, 15, 1, p. 11

[53] Moroni, A., Caja, V.L., Sabato, C., Egger, E.L., Gottsauner-Wolf, F., Chae, EYS, "Bone ingrowth analysis and interface evaluation of hydroxyapatite coated versus uncoated titanium porous bone implants", Journal of Materials Science: Materials in Medicine, 1994, 5, p. 411

[54] Yankee, S.J., Pletka, B.J., Salsbury, R.L., "Quality control of hydroxylapatite coatings: The surface preparation stage", Proceedings of the 4th National Thermal Spray Conference, Pittsburgh, PA, USA, 4-10 May, 1991, p. 475

[55] Maxian, S.H., Zawadsky, J.P., Dunn, M.G., "Mechanical and histological evaluation of amorphous calcium phosphate and poorly crystallised hydroxyapatite coatings on titanium implants", Journal of Biomedical Materials Research, 1993, 27, p. 717

[56] Klein, C.P.A.T., Patka, P., Wolke, J.G.C., de Blieck-Hogervorst, J.M.A., de Groot, K., "Long-term *in-vivo* study of plasma-sprayed coatings on titanium alloys of tetra-calcium phosphate, hydroxyapatite and α-tri-calcium phosphate", Biomaterials, 1994, 15, 2, p. 146

[57] Wong, M., Eulenberger, J., Schenk, R., Hunziker, E., "Effect of surface topology on the osseointegration of implant materials in trabecular bone" Journal of Biomedical Materials Research, 1995, 29, p. 1567

[58] Gross, K.A., Berndt, C.C., "*In-vitro* testing of plasma-sprayed hydroxyapatite coatings", Journal of Materials Science: Materials in Medicine, 1994, 5, p. 219

[59] Wang, B.C., Change, E., Lee, T.M., Yang, C.Y., "Changes in phases and crystallinity of plasma-sprayed hydroxyapatite coatings under heat treatment: A quantitative study", Journal of Biomedical Materials Research, 1995, 29, p. 1483

[60] Geesink, R.G.T., de Groot K., Klein, C.P.A.T., "Chemical implant fixation using hydroxyl-apatite coatings", Clinical Orthopaedics and Related Research, 1987, 225, p. 147

[61] Poser, R.D., Magee, F.P., Kay, J.F., Toal, T.R., Hedley, A.K., "Biomechanical and histologic assessment of HA enhanced long-term fixation in a unique loaded canine implant", Transactions of the 4th World Biomaterials Congress, 1992, p. 252

[62] Thomas, K.A., Cook, S.D., Haddad, R.J., Kay, J.F., Jarcho, M., "Biologic response to hydroxylapatite-coated titanium hips - a preliminary study in dogs", Journal of Arthroplasty, 1989, 4, 1, p. 43

[63] Cook, S.D., Thomas, K.AA., Kay, J.F., "Experimental coating defects in hydroxyapatite - coated defects", Clinical Orthopaedics and Related Research, 1991, 265, p. 280

[64] Verheyen, C.C.P.M., Dhert, W.J.A., Petit, P.L.C., Rozing, P.M., de Groot, K., "*In-vitro* study on the integrity of a hydroxylapatite coating when challenged with staphylococci", Journal of Biomedical Materials Research, 1993, 27, p. 775

[65] Shelton, R.M., Mei, J., Marquis, P.M., "Surface development of bioglass exposed to culture medium in the presence or absence of proteins and bone derived cells", Transactions of the Fifth World Biomaterials Congress, Toronto, 1996, 2, p.57

[66] Yang, C.Y., Wang, B.C., Chang, E., Wu, B.C., "Bond degradation at the plasma-sprayed HA coating / Ti-6Al-4V alloy interface: an *in-vitro* study", Journal of Materials Science: Materials in Medicine, 1995, 6, p. 258

[67] Reber, R., Ha, S.W., Baerloacher, C., Wintermantel ,E., Gruner, H., "X-ray diffraction studies of vacuum plasma sprayed hydroxyapatite coatings after immersion in simulated body fluid and fetal calf serum", Transactions of the Fifth World Biomaterials Congress, Toronto, 1996, 2, p.832

[68] Zyman, Z., Weng, J., Liu, X., Zhang, X., Ma, Z., "Amorphous phase and morphological structure of hydroxyapatite plasma coatings", Biomaterials, 1993, 14, 3, p. 225 ..

[69] Zyman, Z., Weng, J., Liu, X., Li, X., Zhang, X., "Phase and structural changes in hydroxyapatite coatings under heat treatment", Biomaterials, 1994, 15, 2, p. 151

[70] Zyman, Z., Cao, Y., Zhang, X., "Periodic crystallisation effect in the surface layers of coatings during plasma spraying of hydroxyapatite", Biomaterials, 1993, 14, 15, p. 1140

[71] American Ceramic Society, "Phase diagrams for ceramists", pub. American Ceramic Society, Washington DC, 1983, 5, p. 320

[72] Chen, J., Wolke, J.G.C., de Groot, K., "Microstructure and crystallinity in hydroxyapatite coatings", Biomaterials, 1994, 15, 5, p. 396

[73] Wilke, H.J., Claes, L., Steinemann, S., "The influence of various titanium surfaces on the interface shear strength between implants and bone", Advances in Biomaterials, 1990, 9, p. 309

[74] Berndt, C.C., Lin, C.K., "Measurement of adhesion for thermally sprayed materials", Journal of Adhesion Science and Technology, 1993, 7, 12, p. 1235

[75] Wolke, J.G.C., de Groot, K., Kraak, T.G., Herlaar, W., de Blieck-Hogervorst, J.M.A., "The characterisation of hydroxylapatite coatings sprayed with VPS, APS and DJ systems", Proceeding of the 4th National Thermal Spray Conference, Pittsburgh, PA, USA, 1991, 4-10 May

[76] Iida, K., Otsuka, A., Danjo, K., Sunada, H., "Measurement of the adhesive force between particles and a substrate by means of the impact separation method. Effect of surface roughness and type of material of the substrate", Chemical Pharmacy Bulletin, 1993, 41, 9, p. 1621

[77] Chern Lin, J.H., Liu, M.L., Ju, C.P., "Morphologic variation in plasma - sprayed hydroxyapatite - bioactive glass composite coatings in Hank's solution", Journal of Biomedical Materials Research, 1994, 28, p. 723

[78] Evans, S.L., Gregson, P.J., "The effect of a plasma-sprayed hydroxyapatite coating on the fatigue properties of Ti-6Al-4V", Materials Letters, 1993, 16, p. 270

[79] Curtiss-Wright, "The effect of plasma spray coatings on the fatigue properties of titanium 6Al-4V and MSI 9310 steel", Metallurgical Report B-725, Curtiss-Wright Corporation, Wood-Ridge, New Jersey, 1971, March 31

[80] Reis, R.L., Monteiro, F.J., Hastings, G.W., "Stability of hydroxylapatite plasma sprayed coated Ti-6Al-4V under cyclic bending in simulated physiological solutions", Journal of Materials Science: Materials in Medicine, 1994, 5, p. 457

[81] Urist, M.R., Nilsson, O., Rasmussen, J., Hirota, W., Lovell, T., Schmalzreid, T., Finerman, G.A., "Bone regeneration under the influence of a bone morphogenetic protein (BMP) beta tri-calcium phosphate (TCP) composite in skull trephine defects in dogs", Clinical Orthopaedics and Related Research, 1987, 214, p. 295

[82] Downes, S., Di Silvio, L., Klein, C.P.A.T., Kayser, M.V., "Growth hormone loaded bioactive ceramics", Journal of Materials Science: Materials in Medicine, 1991, 2, p. 176

[83] Mohan, S., Baylink, D.J., "Bone growth factors", Clinical Orthopaedics and Related Research, 1990, 252, p. 294

[84] Downes, S., Clifford, C.J., Scotchford, C., Klein, C.P.A.T., "Comparison of the release of growth hormone from hydroxyapatite, heat-treated hydroxyapatite, and fluoroapatite coatings on titanium", Journal of Biomedical Materials Research, 1995, 29, p. 1053

[85] Geesink, R.G.T., "Experimental and clinical experience with hydroxyapatite - coated hip implants", Clinical Orthopaedics and Related Research, 1989, 12, p. 1239

[86] Tonino, A.J., Romanini, L., Rossi, P., Borroni, M., Greco, F., Garcia-Araujo, C., Garcia-Dihinx, L., Murcia-Mazon, A., Hein, W., Anderson, J. "Hydroxyapatite - coated hip prostheses", Clinical Orthopaedics and Related Research, 1995, 312, p. 211

[87] Therin, M., Tonino, A.J., "Retrospective analysis of a HA coated ABG hip prosthesis", Report No. 130C501, Howmedica International, Pfizer Hospital Products Limited, Ash House, Fairfield Avenue, Staines, Middlesex, September 15th 1995

[88] D'Antonio, J.A., Capello, W.N., Jaffe, W.L., "Early clinical experience with hydroxyapatite - coated femoral implants", Journal of Bone and Joint Surgery, 1992, 74, 7, p. 995

[89] Geesink, R.G.T., "Hydroxyapatite - coated total hip prostheses. Two-year clinical and roentgenographic results of 100 cases", Clinical Orthopaedics and Related Research, 1990, 261, p. 39

[90] Gross, K.A., Berndt, C.C., "Thermal spraying of hydroxyapatite for bioceramic applications", Key Engineering Materials, 1991, 53 - 55, p. 124

[91] Ong, J.L., Lucas, L.C., Raikar, G.N., Weimer, J.J., Gregory, J.C., "Surface characterisation of ion-beam sputter-deposited Ca-P coatings after *in-vitro* immersion", Colloids and Surfaces A: Physicochemical and Engineering Aspects, 1994, 87, p. 151

[92] Oguchi, H., Ishikawa, K., Ojima, S., Hirayama, Y., Seto, K., Eguchi, G., "Evaluation of a high velocity flame spraying technique for hydroxyapatite", Biomaterials, 1992, 13, 7, p. 471

[93] Herman, H., "Plasma sprayed coatings", Scientific American, 1988, September, p. 78

[94] Williams, C.A., Jones, H., "The effect of melt superheat and impact velocity on splat thickness", Materials Science and Engineering, 1975, 19, p. 293

[95] McPherson, R., "The relationship between the mechanism of formation, microstructure and properties of plasma sprayed coatings", Thin Solid Films, 1981, 83, p. 297

[96] McPherson, R., "On the formation of thermally sprayed alumina coatings", Journal of Materials Science, 1980, 15, p. 3141

[97] Yang, C.Y., Wang, B.C., Chang, E., Wu, J.D., "The influence of plasma spraying parameters on the characteristics of hydroxyapatite coatings: a quantitative study", Journal of Materials Science: Materials in Medicine, 1995, 6, p. 249

[98] Cheang, P., Khor, K.A., "Influence of Powder Characteristics on Plasma Sprayed Hydroxyapatite Coatings", Journal of Thermal Spray Technology", 1996, 5, 3, p. 310

[99] Kushner, B.A., Rangaswamy, S., Rotolico, A.J., "Thermal spray powders - manufacturing methods and quality control procedures", 1st Plasma-Technik-Symposium, Lucerne, Switzerland, 1988, 2, p. 191

[100] Khor, K.A., Cheang, P., "Plasma sprayed hydroxyapatite (HA) coatings produced with flame spheroidised powders", Journal of Materials Processing Technology, 1997, 63, p. 271

[101] Tsui, Y.C., "Adhesion of plasma sprayed coatings", PhD Thesis, Department of Materials Science and Metallurgy, University of Cambridge, February 1996.

[102] Apelian, D., Paliwal, M., Smith, R.W., Schilling, W.F., "Melting and solidification in plasma deposition - phenomenological review", International Metallurgical Review, 1983, 28, 5, p. 271

[103] Houben, J.M., "Relation of the adhesion of plasma sprayed coatings to the process parameters size, velocity and heat content of the spray particles", PhD Thesis, Submitted December 1988, University of Eindhoven, Holland

[104] Pfender, E., "Fundamental studies associated with the plasma spray technique", Surface Coating Technology, 1988, 34, p. 1

[105] Vardelle, M., Vardelle, A., Fauchais, P., Boulas, M., "Plasma-particle momentum and heat-transfer modelling and measurement", Journal of the American Institute of Chemical Engineering, 1983, 29, 2, p. 236

[106] "Engineering coatings - design and application", Ed. Stan Grainger, 1989, Abingdon Publishing, Cambridge, England, p. 87

[107] Ahmed, R., Hadfield, M., "Rolling contact fatigue performance of detonation gun coated elements", Tribology International, 1997, 30, 2, p. 129

[108] Barabasi, A.L., Stanley, H.E., "Fractal concepts in surface growth", Cambridge University Press, 1995

[109] Fischer, W., Gruhn, H., Mallener, W., "Residual stresses in plasma sprayed ceramic coatings", Materials Science Forum, 1996, 228 - 231, p. 481

[110] Ji, H., Ponton, C.B., Marquis, P.M., "Microstructural characterisation of hydroxyapatite coating on titanium", Journal of Materials Science - Materials in Medicine, 1992, 3, p. 283

[111] Filliaggi, M.J., Coombs, N.A., Pilliar, R.M., "Characterisation of the interface in the plasma sprayed HA coating / Ti-6Al-4V implant system", Journal of Biomedical Materials Research, 1991, 25, p. 1211

[112] Hobbs, M.K., Reiter, H., "Residual stresses in ZrO_2-8%Y_2O_3 plasma sprayed thermal barrier coatings", Surface and Coatings Technology, 1988, 34, p. 33

[113] Gill, S.C., Clyne, T.W., "The effect of substrate temperature and thickness on residual stresses in plasma sprayed deposits", Proceedings of the 2nd European Conference on Advanced Materials and Processes, 1992, 1, p. 298

[114] Kuroda, S., Clyne, T.W., "The quenching stress in thermally sprayed coatings", Thin Solid Films, 1991, 200, p. 49

[115] Suzuki, K., Kageyama, Y., Yokoyama, Y., Harada, Y., Kokubo, T., "Structural change of hydroxyapatite coated on polymers implanted in soft tissue", Bioceramics, Vol. 7, Eds. Andersson, O.H., Yli-Urpo, A., Butterworth-Heinemann Ltd., Turku, Finland, 1994, p. 113

[116] Nagano, M., Nakamura, T., Kokubo, T., Tanahashi, M., Ogawa, M., "Differences of bone bonding ability and degradation behaviour *in-vivo* between amorphous calcium phosphate and highly crystalline hydroxyapatite coating", Biomaterials, 1996, 17, p. 1771

[117] Brossa, F., Cigada, A., Chiesa, R., Paracchini, L., Consonni, C., "Post deposition heat treatment effects on hydroxyapatite vacuum plasma spray coatings", Journal of Materials Science: Materials in Medicine, 1994, Vol. 5, p. 855

[118] de Bruijn, J.D., Bovell, Y.P., van Blitterswijk, C.A., "Structural arrangements at the interface between plasma sprayed calcium phosphates and bone" , Biomaterials, 1994, Vol. 15, No. 7, p. 543

[119] Head, W.C., Bauk, D.J., Emerson, R.H., "Titanium as the material of choice for cementless femoral components in total hip arthroplasty", Clinical Orthopaedics and Related Research, 1995, 311, p. 85

[120] Bannom, B.P., Mild, E.E., "Titanium alloys in surgical implants", ASTM Special Technical Publication 796, Philadelphia, 1983, p. 3

[121] Dittmar, C.B., Bauer, G.W., Evers, D., "Titanium and titanium alloys", Ed. Zwicker, U., Springer Verlag, Berlin, 1974, p. 330

[122] Imam, M.A., Fraker, A.C., Gilmore, C.M., "Corrosion and degradation of implant materials", ASTM Special Technical Publication 684, Philadelphia, 1979, p. 330

[123] Viceconti, M., Toni, A., Giunti, A., "Effects of some technological aspects on the fatigue strength of a cementless hip stem", Journal of Biomedical Materials Research, 1995, 29, p. 875

[124] Smith, T., "The effect of plasma sprayed coatings on the fatigue of titanium alloy implants", Journal of the Minerals and Metals Society, 1994, 46, 2, p. 54

[125] Kohn, D.H., Ducheyne, P., Awerbuch, J., "Acoustic emission during fatigue of porous coated Ti-6Al-4V implant alloy", Journal of Biomedical Materials Research, 1992, 26, p. 19

[126] Noort, R., "Review titanium: the implant materials of today", Journal of Materials Science, 1987, p. 3801

[127] Cook, S.D., Thongpreda, N., Anderson, R.C., Haddad, R.J., "The effect of post sintering heat-treatments on the fatigue properties of porous coated Ti-6Al-4V alloy", Journal of Biomedical Materials Research, 1988, 22, p. 287

[128] Manero, J.M., Gil, F.J., Planell, J.A., "Effect of saline solution environment on the cyclic deformation of Ti-6Al-4V alloy", Journal of Materials Science: Materials in Medicine, 1996, 7, p. 131

[129] Skoog, D.A., Leary, J.J., "Principles of instrumental analysis", Saunders College Publishing, 1971

[130] Farrahi, G.H., Markho, P.H., Maeder, G., "A study of fretting wear with particular reference to measurement of residual stresses by x-ray diffraction", Wear, 1991, 18, 2, p. 249

[131] Jarcho, M., Bolen, C.H., Thomas, M.B., Bobick, J., Kay, J.F., Doremus, R.H., "Hydroxylapatite synthesis and characterisation in dense polycrystalline form", Journal of Materials Science, 1976, 11, p. 2027

[132] Akae, M., Aoki, H., Kato, K., "Mechanical properties of sintered hydroxyapatite for prosthetic applications", Journal of Materials Science, 1981, 16, p. 809

[133] Cullity, B.D., "Elements of X-Ray diffraction", Addison-Wesley Publishing Company Inc., 1978

[134] Lee, J.D., Ra, H.Y., Hong, K.T., Hur, S.K., "The effect of residual stress on martensitic transformation on plasma sprayed ZrO_2 (8wt.% Y_2O_3) coatings", Surface Coatings Technology, 1992, 54 / 55. p. 64

[135] Scardi, P., Leoni, M., Bertamini, L., "Influence of phase stability on the residual stress in partially stabilised zirconia TBC produced by plasma spraying", Surface Coating Technology, 1995, 76 / 77, p. 106

[136] Brown, S.R., Turner, I.G., Reiter, H., "Residual stress measurement in thermal sprayed hydroxyapatite coatings", Journal of Materials Science : Materials in Medicine, 1994, 5, p. 756

[137] Cohen, J.B., "Stresses in thin films", Advances in X-Ray Analysis, 1990, 33, p. 25

[138] Sergo, V., Sbaizero, O., Clarke, D.R., "Mechanical and chemical consequences of the residual stresses in plasma sprayed hydroxyapatite coatings", Biomaterials, 1997, 18, p. 477

[139] Berglund, T., "Grain size charts for ferritic and austenitic structures", Jernkontorets Ann., BISI no. 1171, 1953, 137, 11, p. 767

[140] Walker, G.W., "Rating of inclusions ('Dirt Chart')", Metallographic Progress, 1939, 35, p. 167

[141] Ryntz, E.F., "Reference microstructures for visual estimation of iron carbide content in nodular iron", Transactions of the American Foundrymen's Society, 1974, 82, p. 551

[142] Voort, V, "Metallography principles and practice", McGraw-Hill Book Company, 1984, p. 410

[143] "Image analysis - principles and practice", Joyce - Loebl, 1985, Great Britain

[144] Wolke, J.C.G., Klein, C.P.A.T., de Blieck-Hogervorst, J.M.A., de Groot, K., "The biological and physical properties of apatite coatings", Proceedings of the 1993 National Thermal Spray Conference, Anaheim, CA, 1993, June, p. 619

[145] de Bruijn, J.D., van Blitterswijk, C.A., Davies, J.E., "Initial bone matrix formation at the hydroxyapatite interface *in-vivo*", Journal of Biomedical Materials Research, 1995, 29, p. 89

[146] Siperko, L.M., Landis, W.J., "Atomic force microscopic determination of substrate effects on the structure of deposited biomineral phosphate", Analyst, 1994, 119, p. 1935

[147] Haman, J.D., Lucas, L.C., Crawmer, D., "Characterisation of high velocity oxy-fuel combustion sprayed hydroxyapatite", Biomaterials, 1995, 16, 3, p. 229

[148] Fischer-Cripps, A.C., Lawn, B.R., Pajares, A., Wei, L., "Stress analysis of elastic-plastic contact damage in ceramic coatings on metal substrates", Journal of the American Ceramics Society, 1996, 79, 10, p. 2619

[149] Pajares, A., Wei, L., Lawn, B.R., "Contact damage in plasma sprayed alumina-based coatings", Journal of the American Ceramics Society, 1996, 79, 7, p. 1907

[150] David, A., Eitenmuller, J., Muhr, G., Pommer, A., Bar, H.F., Ostermann, P.A.W., Schildhauer, T.A., "Mechanical and histological evaluation of hydroxyapatite coated titanium coated and grit blasted surfaces under weight bearing conditions", Archives of Orthopaedic and Trauma Surgery, 1995, 114, p. 112

[151] Shen, W.J., Chung, K.C., Wang, G.J., "Mechanical failure of hydroxyapatite- and polysulphone-coated titanium rods in a weight bearing canine model", Journal of Arthroplasty, 1992, 7, p. 43

[152] Ashroff, S., Napper, S.A., Hale, P.N., Siriwardane, U., Mukherjee, D.P., "Cyclic fatigue of hydroxyapatite coated titanium alloy implant material - effect of crystallinity", Journal of Long-Term Effects of Medical Implants", 1996, 6, p. 143